Synthetic Analogues of Marine Bisindole Alkaloids as Potent Selective Inhibitors of MRSA Pyruvate Kinase

A thesis submitted in fulfilment of the

requirements for the degree of

Doctor of Philosophy

of

Rhodes University

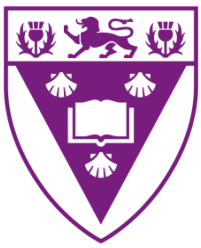

by

Clinton Gareth Lancaster Veale

January 2014

Abstract

Globally, methicillin resistant *Staphylococcus aureus* (MRSA) has become increasingly difficult to manage in the clinic and new antibiotics are required. The structure activity relationship (SAR) study presented in this thesis forms part of an international collaborative effort to identify potent and selective inhibitors of an MRSA pyruvate kinase (PK) enzyme target. In earlier work the known marine natural product bromodeoxytopsentin (**1.6**), isolated from a South African marine sponge *Topsentia pachastrelloides*, exhibited selective and significant inhibition of MRSA PK (IC_{50} 60 nM). Accordingly bromodeoxytopsentin provided the initial chemical scaffold around which our SAR study was developed.

Following a comprehensive introduction, providing the necessary background to the research described in subsequent Chapters, this thesis has been divided into three major parts. Part one (Chapter 2) documents the synthesis of two natural imidazole containing topsentin analogues **1.40, 1.46**, five new synthetic analogues **1.58—1.61, 2.104.**

In the process we developed a new method for the synthesis of topsentin derivatives via selenium dioxide mediated oxidation of *N*-Boc protected 3-acetylindoles to yield glyoxal intermediates which were subsequently cyclized and deprotected to yield the desired products. Interestingly we were able to demonstrate a delicate relationship between the relative equivalents of selenium dioxide and water used during the oxidation step, careful manipulation of which was required to prevent the uncontrolled formation of side products.

Synthetic compounds **1.40, 1.46, 1.58—1.61** were found to be potent inhibitors of MRSA PK (IC_{50} 238, 2.1, 23, 1.4, 6.3 and 3.2 nM respectively) with 1000-10000 fold selectivity for MRSA PK over four human orthologs.

In the second part of this thesis (Chapter 3) we report the successful synthesis of a cohort of previously unknown thiazole containing bisindole topsentin analogues **1.62—1.68** via a Hantzsch thiazole synthesis. Bioassay results revealed that these compounds were only moderate inhibitors of MRSA PK (IC_{50} 5.1—20 μM) which suggested that inhibitory activity was significantly reduced upon substitution of the central imidazole ring of topsentin type analogues with a thiazole type ring.

In addition in Chapter 3 we describe unsuccessful attempts to regiospecifically synthesize oxazole and imidazole topsentin analogues through a similar Hantzsch method.

As a consequence of our efforts in this regard we investigated three key reactions in depth, namely the synthesis of **2.2, 3.38, 3.40, 3.41** via α-bromination of 3-acetylindole and the synthesis of indolyl-3-carbonylnitriles **2.13, 3.45—3.47** and α-oxo-1*H*-indole-3-thioacetamides **3.48—3.51**. The investigation of the latter led to the isolation and elucidation of two anomalous *N*,*N*-dimethyl-1*H*-indole-3-carboxamides **3.52** and **3.53**.

Finally the third part of this thesis (Chapter 4) deals with *in silico* assessment of the binding of both the imidazole and thiazole containing bisindole alkaloids to the MRSA PK protein which initially guided our SAR studies. In this chapter we reveal that there appears to be no correlation between *in silico* binding predictions and *in vitro* MRSA PK inhibitory bioassay data. Superficially it seems that binding energy as determined by the docking program used for these studies correlated with the size of the indole substituents and did not reflect IC_{50} MRSA PK inhibitory data. Although this led us to computationally explore possible alternative binding sites no clear alternative has been identified.

Table of Contents

List of Figures

List of Schemes

List of Tables

List of Abbreviations

Å	angstrom
2D	two dimensional
3D	three dimensional
µg	microgram
µl	microlitre
µM	micromolar
Ac	acetyl
ACN/MeCN	acetonitrile
AcOH	acetic acid
Ac_2O	acetic anhydride
ADP	adenosine diphosphate
AIDS	acquired immunodeficiency syndrome
aq.	aqueous
ATP	adenosine triphosphate
BF_3OEt	boron trifluoride diethyl etherate
Boc	*tert*-butyl dicarbonate
Boc_2O	di-*tert*-butyl dicarbonate
BOM	benzyloxymethyl acetal
br	broad
calcd	calculated
conc.	concentrated
CCDC	Cambridge Crystallographic Data Centre
COSY	^1H-^1H homonuclear correlation spectroscopy
d	doublet
DCE	dichloroethane
DCM	dichloromethane

D-CSA	D-(+)-camphorsulfonic acid
DDQ	2,3-dichloro-5,6-dicyano-1,4-benzoquinone
decomp.	decompose
DMA	dimethyl acetamide
DMAP	4-dimethylamminopyridine
DMF	*N,N*-dimethyl formamide
DMSO	dimethyl sulfoxide
eq.	molar equivalents
ESMS	electrospray mass spectrometry
Et_2O	diethyl ether
EtOAc	ethyl acetate
EtOH	ethanol
EXSY	exchange spectroscopy
g	gram
h	hour
Hz	hertz
HMBC	heteronuclear multiple bond correlation
HPLC	high performance liquid chromatography
HRMS	high resolution mass spectrometry
HRESMS	high resolution electrospray mass spectrometry
HSQC	heteronuclear single quantum coherence
HTS	high throughput screening
IBX	2-iodoxybenzoic acid
IC_{50}	median inhibitory concentration
IR	infrared
K	Kelvin
kcal	kilocalorie
KDa	kilodalton
lit	literature

LTMP	lithium tetramethylpiperidide
m	metre/multiplet
Me	methyl
MeI	methyliodide
$MeNO_2$	nitromethane
MeOH	methanol
MeOD	methanol-d_4
mg	milligram
MHz	megahertz
MIC	minimum inhibitory concentration
min	minute
ml	millilitre
mol	moles
mmol	millimole
MRSA	methicillin resistant *Staphylococcus aureus*
MS	mass spectrometry
mp	melting point
MW	molecular weight
MWI	microwave irradiation
n-Bu_3SnH	tributyltin hydride
NaOMe	sodium methoxide
NCE	new chemical entity
NH_4OAc	ammonium acetate
nM	nanomolar
nm	nanometre
NMA	*N*-methylacetamide
NMO	*N*-morpholine oxide
NMR	nuclear magnetic resonance
No.	number

NO_2BF_4	nitronium tetrafluoroborate
NOE	nuclear Overhauser effect
NOESY	nuclear Overhauser effect spectroscopy
NP	normal phase
OBn	benzyl ether
ORTEP	Oak Ridge thermal ellipsoid plot
PBP	penicillin binding protein
PDB	protein database
PEP	phosphoenol pyruvate
Ph	phenyl
PIN	protein interaction network
ppm	parts per million
$PyHBr_3$	pyridinium hydrobromide perbromide
PK	pyruvate kinase
PMe_3	trimethylphosphine
q	quartet
quant	quantitative
R	specified or unspecified functional group
r.t.	room temperature
rel. int.	Relative intensity
RMSD	root mean square distance
RNA	ribonucleic acid
RP	reversed phase
s	singlet
SAR	structure activity relationship
sat	saturated
SDS	sodium dodecyl sulfate
SEM	[2-(trimethylsilyl)ethoxy]methyl
SO_2Ph	phenylsulfone

SrtA	sortase A
t	triplet
TBAF	tetra-*N*-butylammonium fluoride
TBDMS/TBS	*tert*-butyldimethylsilyl ether
TBHP	*tert*-butyl hydroperoxide
TFA	trifluoroacetic acid
t-BuLi	*tert*-butyllithium
t-BuOK	potassium *tert*-butoxide
TEA/Et_3N	triethylamine
tert	tertiary
THF	tetrahydrofuran
TLC	thin layer chromatography
TMEDA	tetramethylethylenediamine
TMS	trimethylsilyl
TMSCN	trimethylsilyl cyanide
TPAP	tetrapropylammonium perruthenate
UV	ultraviolet
W	Watts

“Nothing in life is to be feared, it is only to be understood.”

-Marie Curie-

Dedicated to my dad Colin Veale, for his imagination

and my Grandpa, Ted Ashby, who had forgotten more than I know.

Acknowledgements

I would firstly like to extend my special thanks and gratitude to my two supervisors, Professor Michael Davies-Coleman and Dr. Kevin Lobb, for their guidance, endless encouragement and vast knowledge. Both have unique approaches and have managed to mould me into a chemist. I never imagined the depth of the journey when I started.

Staff and students of the Chemistry and Pharmacy departments particularly Dr. Denzil Beukes, Dr. Rosa Klein and Prof. Perry Kaye for invaluable advice, wisdom and support

I would like to acknowledge the members of my lab past and present for the rich culture of scholarship, excellence and teamwork and in particular I would like to thank Dr. Sunny Sunassee for being an excellent leader and patient teacher and Dr. Ryan Young for his massive contribution to the direction of this project and his super optimism. A special thank you is due to Candice Bromley, who is not only a close friend who listens to me talk endlessly about mainly science and cricket, but I am certain that without her support and advice through numerous challenges, I could not have completed this thesis.

I would like to thank Dr. Roya Zoraghi and Prof. Raymond Andersen for inviting us onto this project and assisting in biological assay.

I gratefully thank Nancy and David Gass as well as Roy Archibald whose immense generosity and kindness put me on this path

My sincere love and appreciation must go to my mom, Lesley Veale my sister Kirsty Veale, the rest of my family and 'The News Team' for encouragement and belief throughout my PhD.

Finally, the financial support provided by the National Research Foundation, the Medical Research Foundation and by Rhodes University is gratefully acknowledged.

Chapter One

General Introduction

1.1 *Staphylococcus aureus* and antibiotic resistance

The approval for clinical use of the β-lactam penicillin antibiotics in the early 1940's for the first time allowed *Staphylococcus aureus* (*S. aureus*) infections to be effectively treated, ushering in the antibiotic era,[1] which for more than half a century, in conjunction with other antibiotics, saved millions of lives. The well established targets of β-lactam antibiotics are a series of transpeptidases aptly named penicillin binding proteins (PBPs), which are responsible for peptidoglycan cross linking during bacterial cell wall biosynthesis.[2,3] Peptidoglycan is an essential component of *S. aureus* cell walls, enabling the bacterium to resist high environmental osmotic pressures, as well as playing a role in pathogenesis.[4] β-Lactams irreversibly acylate a serine residue located in the active site of PBPs, thereby rendering them inactive.[2] This class of antibiotics were found to be potently antibacterial toward both gram-positive and gram-negative pathogens, with low toxicity toward eukaryotic cells, therefore giving them widespread clinical applicability.[3] β-Lactam antibiotics account for roughly 50% of all antibiotics used globally.[5] However, after only a few years, universal efficacy of penicillin was already on the decline, and by 1946, an estimated 60% of clinically isolated *S. aureus* displayed penicillin resistance, via the production of β-lactamase, an enzyme responsible for hydrolysis of the β-lactam ring.[1,5] The problem of β-lactamase sensitivity was partially solved with the introduction of β-lactamase inhibitor clavulanic acid[5] as well as semi-synthetic β-lactamase resistant penicillin derivatives such as methicillin (**1.1**).[1] This success was short lived, with the emergence of methicillin resistant *S. aureus* (MRSA) which imparts resistance via the production of a cohort of mutated PBPs with low affinity for β-lactam binding, referred to as PBP2', PBP2a or MRSA-PBP.[2,3,6]

Despite the widespread emergence of *S. aureus* resistance to methicillin, up until recently many hospital physicians did not consider MRSA to be a major threat, since glycopeptides antibiotics such as the reference standard vancomycin (**1.2**), have for two decades remained active against serious MRSA infections, despite intensive clinical usage of this compound.[7,8]

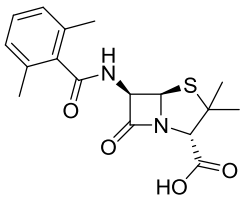

1.1 methicillin

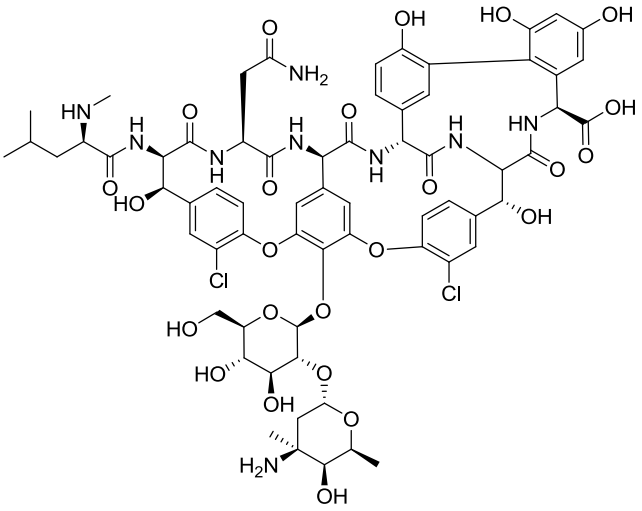

1.2 vancomycin

The mechanism of action of vancomycin also involves inhibition of bacterial cell wall synthesis, however, **1.2** does not interact with cell wall biosynthetic enzymes, but rather complexes with the terminal D-ala-D-ala portion of the *N*-acetylglucosamine-(β-1,4)-*N*-acerylmuramic acid pentapeptide (NAGNAM) peptidoglycan precursor,[4,9] therefore preventing cross linking without relying on enzyme affinity.[10] Unfortunately, as a result of limited distribution throughout tissues, and sub optimal dosing regimens, vancomycin-intermediate *Staphylococcus aureus* (VISA) and vancomycin resistant *Staphylococcus aureus* (VRSA) strains have been identified across the globe.[7,8,11] Resistance is mediated by modification of the peptidoglycan precursor, resulting in a target with lowered affinity to vancomycin.[10]

1.2 Identification of pyruvate kinase as a potential MRSA antibacterial drug target

This rapid emergence of VRSA and MRSA coupled with limited development of new antibacterials over the preceding three decades, has created a crisis in public health care systems.[12–14] This crisis has been compounded by the spread of these infections from the clinic into the general

community,[13] for example in the USA the mortality rate attributed to MRSA now exceeds that of AIDS in that country.[15] Therefore, the identification of new antibacterials with novel mechanisms of action is urgently required.[12,16] The current commercially available antibiotics were originally identified almost exclusively from the screening of libraries of natural products and small molecules against whole cells.[12] Advanced techniques in genomics, proteomics, target identification and assay development have greatly improved target based approaches toward drug discovery.[17] However, the strategy for target selection has focused almost exclusively on unique bacterial targets, due to concerns about selectivity and subsequent toxicity.[12,14] Contemporary thinking has raised concerns that targeting pathogen specific proteins will exert selective pressures on the pathogen as seen in the cases of β-lactams and vancomycin, with the inevitable emergence of resistance.[12,14] Modern integrative knowledge of bacterial pathogenesis and cellular processes is beginning to influence target selection in an effort to minimize the rapid emergence of resistance.[12,14] Large scale, genome wide investigation of bacterial protein interaction networks (PIN), also referred to as the bacterial interactome, provides invaluable insight into cellular pathways and networks, and identify highly connected hub proteins as possible drug targets.[12,14]

Intuitively, arising from the high level of hub protein connectivity, deletion or inhibition of a hub protein is more likely to be lethal to a given organism than when similar actions are applied to a non hub protein.[14] Hub proteins are also generally essential for network integrity and stability, therefore they are less prone to mutation, thereby limiting resistance.[12,14] Additionally PIN analysis often identifies evolutionary conserved proteins, meaning that structural differences between prokaryotes and eukaryotes can be exploited to introduce selectivity between the bacterial and host protein isoforms.[14]

This strategy was exploited by Zoraghi *et al.*[12,15] who mapped the PIN or interactome of 608 proteins of a hospital acquired strain of MRSA-252.[12,15] Pyruvate kinase (PK) was identified as a highly connected evolutionary conserved hub protein[12,15,16] that was determined by gene disruption

experiments to be essential for bacterial viability, due to its high enzymatic activity during the exponential phase of the bacterial life cycle.[12] Additionally, MRSA PK was found to have several structural features distinct from mammalian orthologs of the protein, reflected in part by differing molecular weights (**Figure 1.1,** left). X-ray crystallography has revealed PKs exist as homotetramers, with each subunit being identical, and consisting of between three and four domains, namely the A, B and C domains and the N-terminal domain, which is notably absent in prokaryotic bacterial PKs.[12,18] The tetramer forms through interaction of the A and C subunits of adjacent monomers, revealing a quaternary structure with bordering A domains, and C domains to form an A—A and an A—C interface referred to as the large and small interface respectively.[16,12] The active site for kinase activity is situated at the interface of the A and B domains, while the allosteric effector site is located in the C domain (**Figure 1.1,** right).[16,12,18]

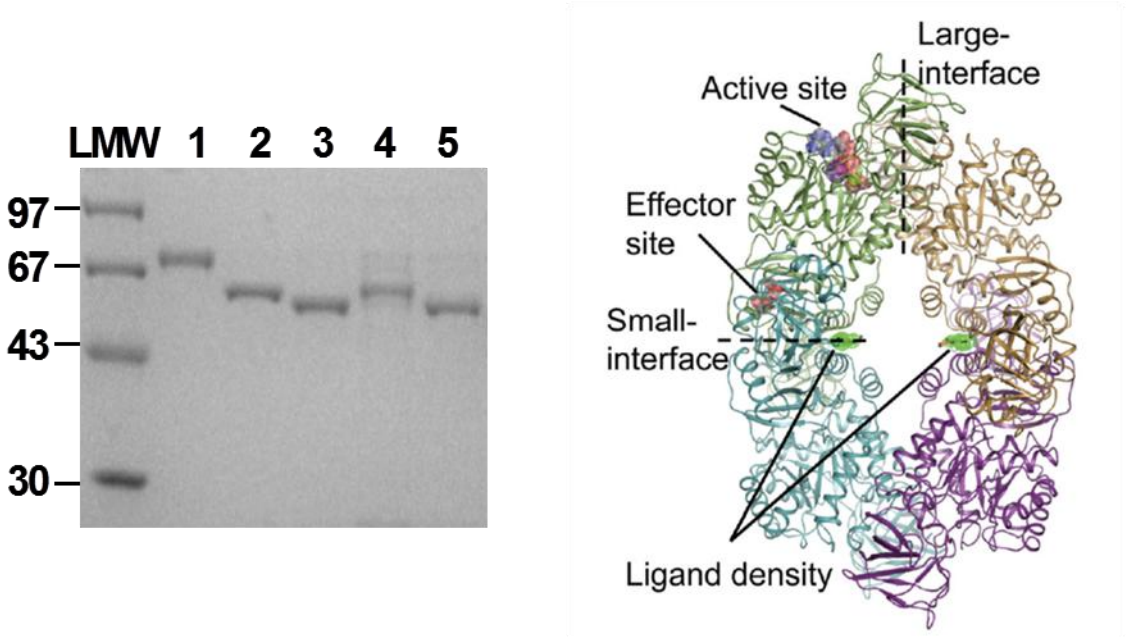

Figure 1.1 SDS page gel (LMW = lower molecular weight in kDa) of *S. aureus* pyruvate kinase (**1**) and four human pyruvate kinase orthologs M1 (**2**), M2 (**3**), R (**4**), and L (**5**) (left). Quaternary structure of MRSA pyruvate kinase comprising of four identical subunits. Important features to note are the large and small interface, the active and effector/allosteric site as well as the area of high ligand density indicating the bisindole binding pocket (right). Images reproduced with permission from Zoraghi *et al*..[16]

PK catalyses the rate limiting final step in glycolysis with the irreversible conversion of phosphoenolpyruvate (PEP) into pyruvate with subsequent phosphorylation of ADP into ATP.[12,16] Both the products and substrates of PK are involved in a number of additional biological pathways, therefore providing a critical intervention point to disrupt wholesale bacterial metabolism. Not surprisingly Zoraghi *et al*. have identified MRSA PK as a novel drug target with promising potential.[12,16]

1.3 Marine natural products as selective inhibitors of MRSA PK

In a study to identify marine natural products that potently inhibit MRSA PK with high selectivity, a library of 968 crude extracts from marine invertebrates and microbes collected from seven countries across the globe (**Figure 1.2** left) were screened as part of a collaboration between Professor Raymond Andersen at the Department of Chemistry, University of British Columbia (UBC) in Vancouver Canada, his colleagues in the Centre for Disease Control and the Departments of Medicine, Biochemistry and Molecular Biology, and Microbiology and Immunology at UBC and the marine natural product research groups around the world including ours at Rhodes University.[16] Only one of the 968 extracts *viz.* our methanolic our extract of the sponge *Topsentia pachastrelloides* (**Figure 1.2** right) collected on the Aliwal Shoal off the South African east coast in 1994, and submitted by our research group to the screening program, was active in the MRSA PK screen.

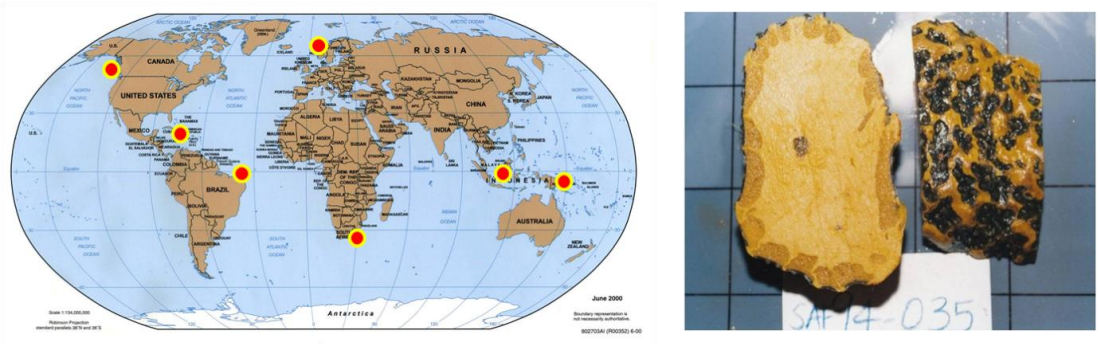

Figure 1.2 Countries of origin for the marine invertebrate and microbial extracts screened against MRSA PK in Vancouver (left) The South African sponge *Topsentia pachastrelloides* photographed shortly after collection (right. Photo: M. Davies-Coleman 1994).

Further purification of the methanolic extract of *T. pachastrelloides* yielded four known bisindole alkaloids, spongotine A (**1.3**), bromotopsentin (**1.4**), *cis*-3,4-dihydrohamacanthin B (**1.5**), and bromodeoxytopsentin (**1.6**).[16] Of these four compounds, **1.5** and **1.6** potently inhibited MRSA PK at an IC_{50} of 16 and 60 nM respectively, while additionally displaying 166—600 fold selectivity for the bacterial PK over four human PK isoforms (M1,M2,R and L) (**Figure 1.3**). [16]

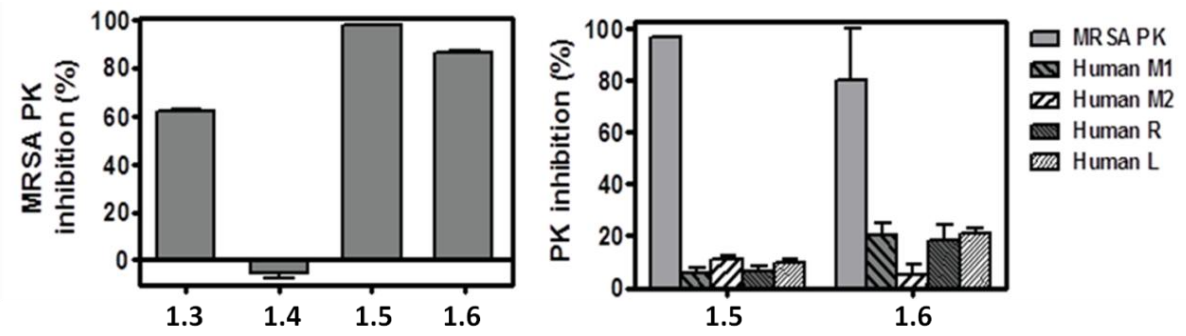

Figure 1.3 MRSA PK % inhibition data of compounds **1.3—1.6** at a concentration of 10 µM (left). Selectivity of **1.5** and **1.6** over four human PK orthologs (right). Images reproduced with permission from Zoraghi *et al.*.[16]

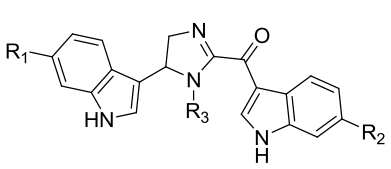

1.3 R_1 = Br, R_2 = R_3 = H spongotine A (4,5-dihydro-6"-deoxybromotopsentin)
1.48 R_1 = R_3 = H, R_2 = Br spongotine B
1.49 R_1 = R_2 = Br, R_3 = H spongotine C
1.50 R_1 = R_2 = Br, R_3 = Me topsentin C
1.51 R_1 = R_2 = R_3 = H topsentin D

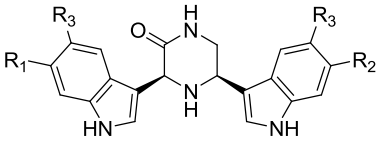

1.5 R_1 = R_2 = Br, R_3 = H *cis*-3,4-dihydrohamacanthin B
1.7 R_1 = R_2 = Cl, R_3 = H
1.8 R_1 = R_2 = F, R_3 = H
1.9 R_1 = R_2 = R_3 = H
1.10 R_1 = R_2 = H, R_3 = Br
1.11 R_1 = R_2 = Me, R_3 = H
1.12 R_1 = R_3 = H, R_2 = Br

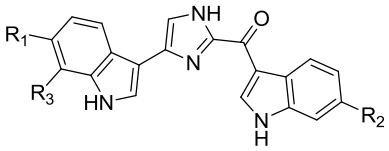

1.4 R_1 = Br, R_2 = OH, R_3 = H bromotopsentin (topsentin B2)
1.6 R_1 = Br, R_2 = R_3 = H bromodeoxytopsentin
1.40 R_1 = R_2 = R_3 = H deoxytopsentin (topsentin A)
1.41 R_1 = R_3 = H, R_2 = OH topsentin (topsentin B1)
1.45 R_1 = H, R_2 = Br, R_3 = OH isobromotopsentin
1.46 R_1 = R_2 = Br, R_3 = H dibromodeoxytopsentin
1.47 R_1= R_3 = H, R_2 = Br isobromodeoxytopsentin

Following successful co-crystallization of the most active compound, **1.5**, with the MRSA PK tetramer (PDB ID 3T07), X-ray analysis revealed that **1.5** did not bind at either the active or effector site as expected, but rather was bound at the small interface, a region crucial in determining tetramer rigidity and efficient catalytic activity (**Figure 1.1** right).[16] Sequence alignment between MRSA and human PK isoforms revealed sequence divergence in the C domain[13,16] which implied that the entrance to the hamacanthin binding site is partially obstructed by six amino acid residues in human PK orthologs e.g. M2 (**Figure 1.4**).[13] These six amino acid residues are not present in the hamacanthin binding site of MRSA PK which may explain the significant selectivity of **1.5** over human PK orthologs.[13]

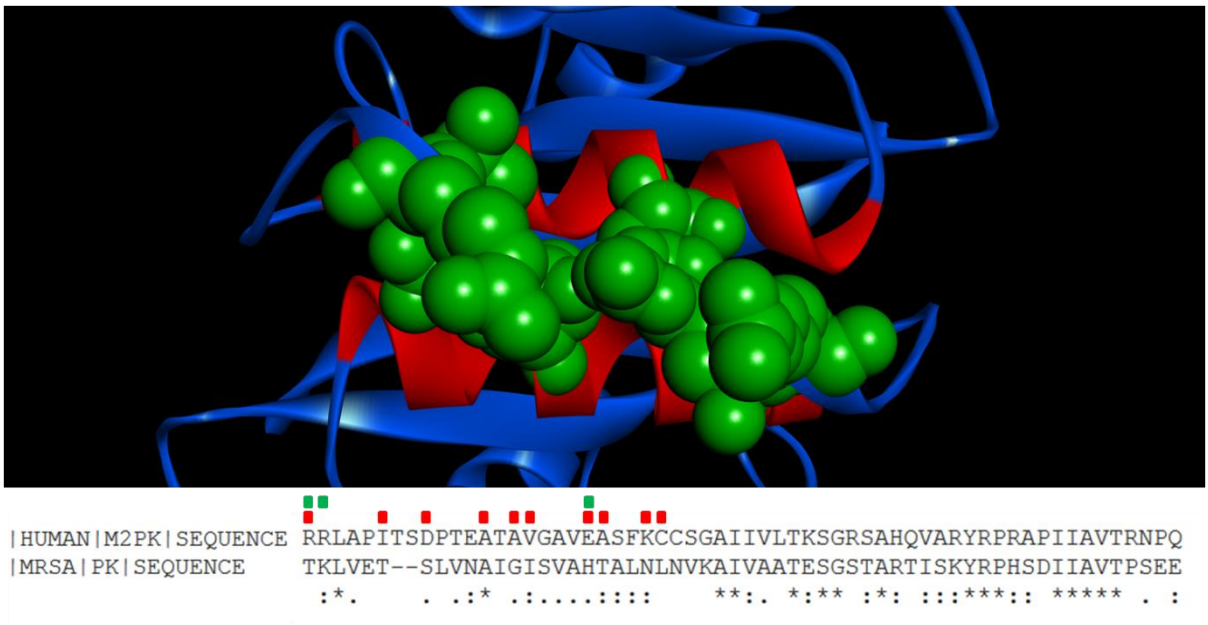

Figure 1.4 Above, a portion of the X-ray crystal structure of human M2 PK (PDB ID 4FXF)[19] highlighting the hamacanthin binding pocket (red), obstructed by two arginine residues (R 399 and 400) and one glutamic acid (E 418) highlighted in green, from each of the two protein subunits. Below a Clustal Omega sequence alignment[20] between the hamacanthin binding sites of 4FXF and 3T07 revealing distinct sequence divergence. Red squares indicate binding site residues, while green indicates blocking residues. '*' denotes identical residue, ':' indicates very similar residue, '.' denotes somewhat similar and 'space' denotes different residue. Protein image modeled using Discover Studio Visulaizer.[21]

The small hydrophobic binding pocket is formed from the anti-parallel interaction of two identical α-helices 357—370 from the respective subunits.[16] This results in a symmetrical hydrophobic binding pocket, lined with 10 amino acid residues, namely Thr348, Thr353, Ser354, Ala358, Ile361, Ser362, His365, Thr366, Asn369 and Leu370 with identical residues opposite each other, therefore mirroring the pseudo-symmetrical nature of ligands like *cis*-3,4-dihydrohamacanthin B (**Figure 1.5**). Zoraghi *et al.* also noted that the prominent histidine residues undergo side chain rearrangement in the presence of the ligand, thus anchoring the piperazine moiety to the binding site, while the respective serine residues form a hydrogen bond with the indole NH. The ligand indole moieties were also proposed to interact hydrophobically with the relevant amino acid residues, while the two bromine residues appear to each occupy a hydrophobic pocket at either end of the binding site.[16]

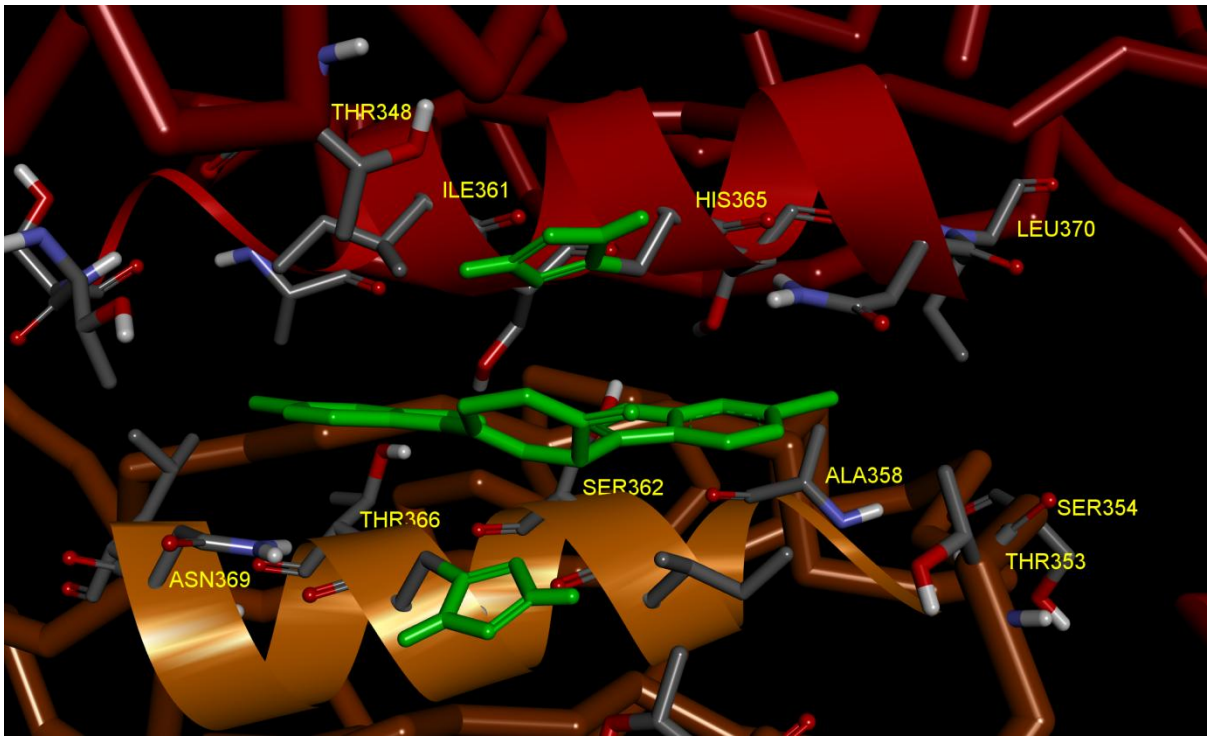

Figure 1.5 X-ray co-crystal structure of **1.5** bound to the hydrophobic binding pocket located at the small interface (PDB ID 3T07). Highlighted in green are **1.5** (centre) and the prominent aromatic histidine residues (above and below **1.5**). The binding site is constructed from the anti-parallel arrangement of two identical α-helices from individual subunits coloured in brown and red respectively. This therefore generates a symmetrical binding pocket with identical resides located opposite each other. Protein image modeled using Discover Studio Visulaizer.[21]

Provided with the details of the binding site from X-ray analysis of **1.5** bound to MRSA PK. Professors Andersen and Davies-Coleman agreed to explore the structure activity relationship (SAR) of **1.5** and **1.6** respectively as a parallel endeavour to synthesize compounds with even greater activity against MRSA PK while simultaneously increasing selectivity for MRSA PK over a group of four human PK orthologs. This thesis initially describes the synthesis of six analogues of **1.6** and reports the activity and selectivity of these compounds. Further exploration of the centrality of the imidazole ring to the activity of **1.6** and related analogues through the synthesis of a similar cohort of seven thiazole analogues is also presented. A brief rationale for our SAR strategy is presented here and will be elaborated further elsewhere in this thesis.

While the chemical structures of both inhibitors (**1.5** and **1.6**) consist of two indole moieties bonded to a central heterocyclic ring, the two obvious structural differences that caught our attention were firstly, the levels of bromination (dibromination in **1.5** as opposed to monobromination in the less active **1.6**) and secondly, the structure of the central heterocyclic ring (the aromatic imidazole of **1.6** compared to the non-aromatic piperazine-2-one of **1.5**). We hypothesized that given the potential for π-stacking opportunities between the aromatic imidazole and the prominent histidine residues located in the binding site (**Figure 1.5**) the MRSA PK inhibitory activity observed for **1.6** (60 nM) and **1.5** (16 nM) may be a direct result of the degree of halogenation of the two indole rings and not the difference in structure of the central heterocyclic ring.

Our hypothesis was tentatively supported by SAR studies on *cis*-3,4-dihydrohamacanthin B conducted at the University of British Colombia[22] which revealed an interesting trend where activity was seemingly related to the size, nature and position of the halogen substituent (**Figure 1.6**). Analogues substituted with smaller more electronegative chlorine (**1.7**) and fluorine (**1.8**) respectively, were less active than the natural product **1.5** while the non halogenated analogue (**1.9**) was completely inactive as was a C-5 dibrominated analogue (**1.10**).[22] C-6 Methyl substitution on both indole rings (**1.11**) resulted in a dramatic loss of activity, opening the possibility that bromine

does not interact simply as a hydrophobic residue, and may in fact be involved in halogen bonding (see Chapter 4).[23] A similar loss of activity was observed for a singly brominated derivative (**1.12**) of **1.5**.[22] To the best of our knowledge the diiodo analogue of **1.5** had not been synthesized which would have possibly provided further useful information about halogen bonding of this series of compounds to MRSA PK.

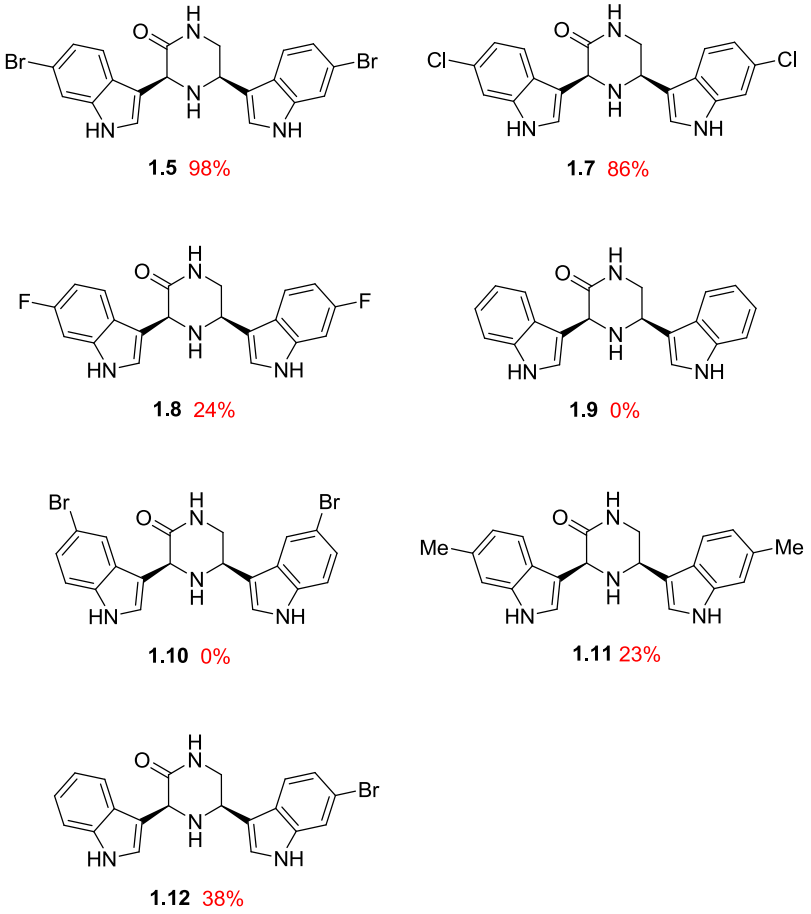

Figure 1.6 SAR studies on *cis*-3,4-dihydrohamacanthin D conducted at the University of British Columbia. Percentage inhibition of MRSA PK at 10 µM presented in red.

1.4 Natural products as sources of drugs

Natural products have traditionally provided either the source or the inspiration for new drugs, with many successful drugs synthesized to mimic nature's compounds.[24] An analysis by Cragg and

Newman[25] of the source of new drugs in the period between 1981 and 2010 found that of the 1073 new chemical entities (NCEs) only 36% can be classified as truly synthetic, with the majority of drugs identified as being of natural origin, or inspired by natural products (**Figure 1.7**).[25] Equally as impressive is the natural product-derived drugs developed during the period between 2000 and 2006, where 26 plant natural products were in one of the phases of drug development. Of note is the fact that plant derived drugs accounted for $18 billion worth of commercial sales in 2005 alone.[26] The impact of natural products is particularly significant in discovery of anti-infectives and anticancer drugs, where according to Cragg and Newman, natural product inspiration accounts for 69% and 75% of NCEs in this period respectively.[25]

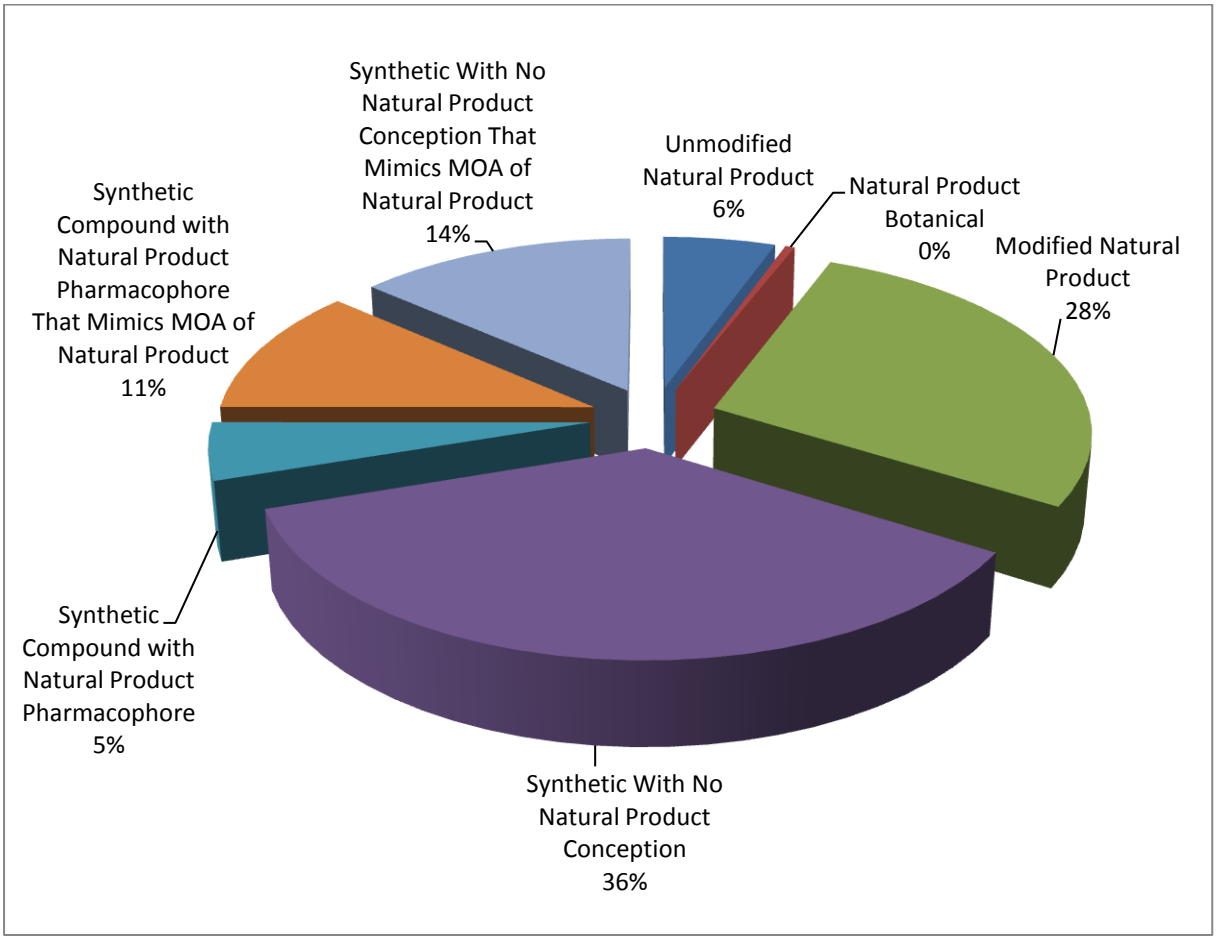

Figure 1.7 Distribution of NCEs in the period between 01/1981 and 12/2010.[25] Of the 1073 NCEs in this period, 64% are unmodified natural products, inspired by a natural product or mimic a natural product mechanism of action. Image reproduced with permission from David Newman.

The marine environment provides a rich source of chemical diversity, where selective pressure on the reef coupled to sedentary life styles of many soft-bodied marine invertebrates e.g. sponges, requires protection from predators via potent chemical defenses which maintain efficacy even when rapidly diluted by the surrounding ocean.[27,28] These naturally occurring compounds can either be synthesized by the host invertebrate (e.g. sponges, ascidians, soft corals etc.) or sequestered (e.g. nudibranchs) from their invertebrate diet, or by symbiotic marine microorganisms that inhabit the interstitial spaces in many filter feeding marine invertebrates (e.g. sponges). The overwhelming diversity of marine microorganisms coupled to the fact that over 70% of the earth's surface is ocean with an estimated biological diversity greater than in tropical rain forests,[27] underpins the potential for drug discovery from the ocean.

Natural products are a heterogeneous class of compounds with distinct molecular properties and structural features, differentiated by source organism, host biosphere and biological role.[26] Almost all biosynthetic compounds have receptor binding capacity,[24] and have been optimized for interaction with biomacromolecules (e.g. proteins) through evolutionary selection[17,29] and biosynthetic pathways requiring sequential binding of chemical intermediates to protein enzymes and receptors, each providing a plethora of unique chemical environments for biogenesis.[26]

1.5 Natural products and chemical space

Over the last two decades combinatorial chemistry was anticipated to become the major source of NCEs in drug discovery, with a concomitant decline in interest in natural products as a source of new drugs. The limitations of combinatorial chemistry in providing the next generation of pharmaceuticals is evident in the decline in the output of new drugs from the pharmaceutical industry over recent years.[24,25] While no single reason for the relative failure of combinatorial chemistry is clear, it is thought that the attempts to improve efficiency of combinatorial approaches

has limited the chemical diversity in combinatorial libraries. Natural products, however, are known to occupy a large component of biologically relevant space as supported by principal component analysis.[24,29] A principal component analysis of randomly selected combinatorial compounds, natural products and drugs was conducted by Feher *et al*..[24] Their plot of the first two principle components (**Figure 1.8**) showed that the products of combinatorial chemistry occupy a well defined area not completely coincident with the same relative space occupied by known pharmaceuticals. Conversely, natural products and drug compounds display similar coverage to each other, jointly occupying a much larger area, including that occupied by a significant portion of the combinatorial compounds.[24] The principle component analysis of Feher *et al.* thus adds weight to the argument that the chemical diversity more readily associated with natural products than combinatorial chemistry products is important in driving new drug discovery. The enhanced chemical complexity of natural products also has a role to play in expanding the range of known druggable targets.[17] Currently the array of drugs commonly available address a limited range of biological targets.[17] Overington *et al*. estimate that there are only 324 molecular targets for currently approved drugs.[30] Natural products therefore provide additional opportunities to identify new ligands which occupy regions of currently underrepresented biologically relevant space. The large binding surfaces and unique multiple array of chiral centres, functional groups and charge states found in natural products are often absent from libraries of randomly synthesized 'drug like' molecules.[17]

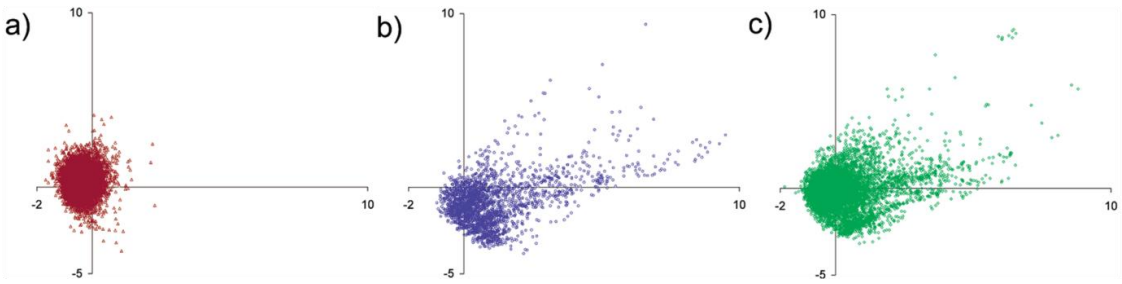

Figure 1.8 Plot of the first two principle components randomly selected combinatorial compounds (a), natural products (b), and drug compounds (c). The area occupied in a is a very dense well defined area, while the area in b and c is far more diffuse occupying a greater area of chemical space, highlighting the drug like nature of natural products. Image reproduced with permission from Miklos Feher.

1.6 New pharmaceuticals from marine organisms and the problem of supply

Currently the pharmaceutical industry drug discovery pipeline favours high throughput screening (HTS) of massive libraries of 'screen friendly' synthetic compounds, which are easy to produce and modify, and require relatively short timelines in order to examine a large number of compounds, while evading the high risk associated with natural products, and in particular those from the marine environment.[31,32,33] The main risk to the pharmaceutical industry associated with natural product drug discovery is the issue of limited access to sources of natural products diversity coupled to intellectual property rights ownership.[32,34] The Rio Convention on Biodiversity enshrines the sovereign rights of countries to benefit from bioactive natural products originating from their country.[32,34] When coupled to the heavy investment required from pharmaceutical companies to deliver a lead compound to market, the included financial burden of devolving intellectual property rights to a third party with unequal financial risk, often means that natural product based drug discovery becomes an unappealing prospect to the risk adverse pharmaceutical industry.

Additionally, there are several chemistry related issues associated with natural product drug discovery, including a high probability re-isolating known natural products as well as access to, and supply of, compounds in industry scale quantities[32,34] i.e. the supply of 1 g of trabectedin (Yondelis®)(**1.13**) requires one metric ton of the ascidian *Ecteinascidia turbinate*.[35] The issue of supply can realistically be tackled by three main approaches namely aquaculture, microbial fermentation and synthesis.[36] The laboratory synthesis of natural products, while appealing, is not considered viable for many natural products on an industrial scale, usually due to the challenges of synthesizing complex chemical scaffold with numerous stereocentres.[36] Aquaculture of marine organisms is an attractive method of acquiring sufficient amounts of the desired secondary metabolites, especially in cases where the organism is rare or grows in extreme conditions.[36] However, this approach is not without its challenges, since the host organism is being removed from the environment which likely stimulates the production of the secondary metabolite(s). This is

exemplified by the New Zealand sponge *Lissodendoryx* sp. which produces the antimitotic agent halichondrin B (**1.14**). Aquaculture feasibility studies[36] conducted on *Lissodendoryx* sp. found that seasonal factors played a role in sponge's survival with a summertime mortality rate of 95% compared to 15% in winter, while the rate of halichondrin B biosynthesis in aquacultured *Lissodendoryx* sp. reduced to 30—60% of that observed in wild type *Lissodendoryx* sp.[36] Similarly, in the case of the colonial ascidian *Ecteinascidia turbinate* (which produces **1.13**), aquaculture was found to be a non viable option due the high costs of transporting and deep freezing large masses of biological material coupled to the expense of a complex extraction and purification process.[37]

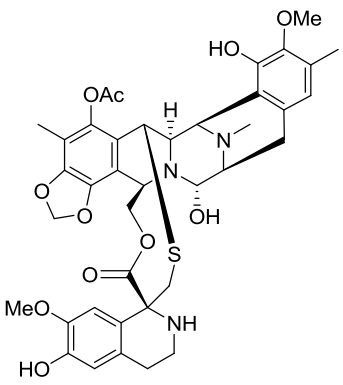

1.13 trabectedin (Yondelis®)

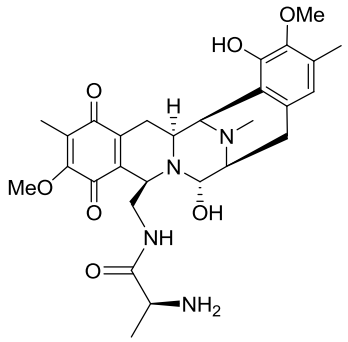

1.15 cyanosafracin B

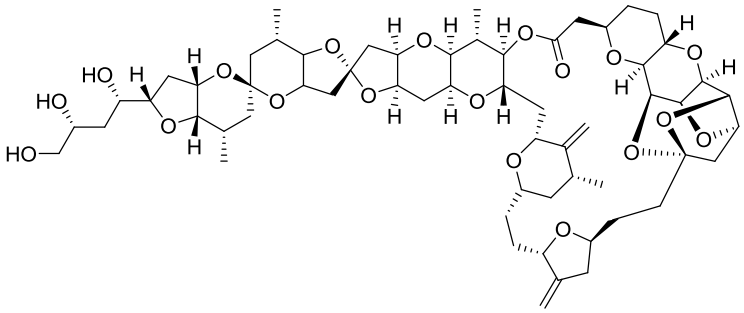

1.14 halichondrin B

The relatively recent interest in the large biomass of marine microbes including cyanobacteria, fungi and eubacteria isolated from marine sediments as well as marine invertebrates associated with

symbiotic microbial colonies,[35,33] have yielded a rich source of new natural products.[33] With high selectivity to culture medium, isolation and cultivation of these putative producers of bioactive natural products remains a challenge for lab scale culture as well as large scale fermentation.[35,38] Modern molecular biology techniques at the interface of marine natural products have allowed discovery and exploration of biosynthetic gene clusters.[33] Cloning and heterologous gene expression in easily culturable microbial strains, have given researchers access to marine natural products that would normally be difficult to obtain,[38,39] and in large enough scale for potential industrial application.[38] Related to this are cases where, terrestrial microbes that are generally easier to culture, produce chemical scaffolds similar to marine natural products, which can be used as synthetic precursors. A classic example of a possible role for microorganisms to solve the marine drug supply challenge is *Pseudomonas fluorescens* which produces the antibiotic cyanosafrican B (**1.15**). Cyanosafrican B contains the majority of the chemical structure and five of the seven stereocentres of **1.13** intact and was a logical precursor for a multigram semi synthesis to yield sufficient trabectedin for the market place.[37]

While supply of material and intellectual property rights remain challenges that hamper drug discovery from marine natural products, modern approaches integrating molecular biology techniques, and improvements in dereplication and high throughput screening is beginning to harness the potential of marine natural products.[33]

Finally, seven commercially available therapeutic agents from marine sources are currently available with a further 13 in phase I, II or III trials.[33] These seven marine drugs are either purely marine natural products i.e. trabectedin **1.13** (soft tissue sarcoma and ovarian carcinoma) and ziconotide (**1.16** for severe chronic pain) or are derived from marine natural products, i.e. cytarabine (**1.17** cancer), vidarabine (**1.18** antiviral), eribulin mesylate (**1.19**, metastatic breast cancer, derived from halichondrin), brentuximab (Hodgkin's lymphoma) and omega-3-acid ethyl esters (hypertriglyceridemia).[33] These compounds represent the significant contribution that marine

natural products have made to modern medicine, in a field that is only beginning to reach its potential.

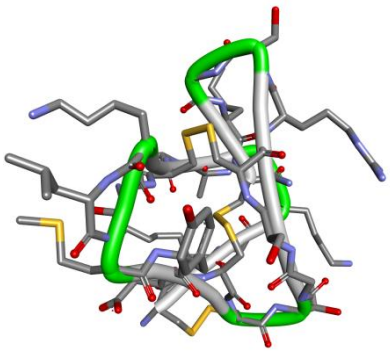

1.16 ziconotide (Prialt®) modeled on Discovery Studio Visualizer.[21]

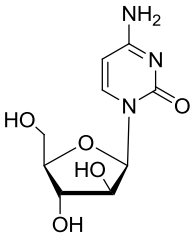

1.17 cytarabine

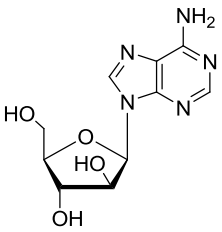

1.18 vidarabine

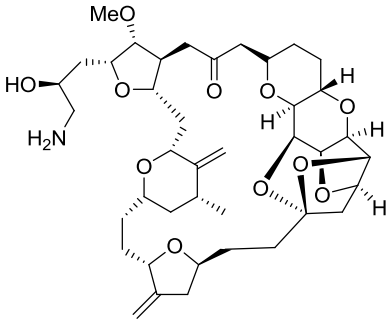

1.19 eribulin mesylate (Halaven®)

1.7 An overview of selected naturally occurring marine bi- and bisindole alkaloids

Before embarking on a description of our approach to the synthesis of analogues of the marine bis-indole imidazole alkaloid **1.6** it is important to contextualize the marine origin of **1.6** by briefly over viewing the distribution and diversity of naturally occurring alkaloids containing two and occasionally three, indole rings that have been isolated from marine organisms over the past four decades. In a recent review we identified 130 naturally occurring marine bi-, bis- and trisindole alkaloids[40] where either two or three indole moieties are bonded directly to each other (biindoles) or the indole rings (bis and trisindoles) are separated by a limited number of functionalities that are usually but not exclusively a heterocyclic ring. While experimental confirmation of the details of the biosynthetic pathways that generate these bi-, bis- and trisindole alkaloids remain elusive, tryptophan and tyramine are regularly suggested as suitable precursors for their biogenesis.

Metabolic nitrogen for incorporation into the biosynthetic pathways of marine organisms is generated via the complex oceanic nitrogen cycle that controls productivity in the oceans and is often limited relative to other nutrients.[41] As a result, bioactive marine alkaloids like the bisindole alkaloids that form the subject of this thesis are generally isolated in low concentrations. Despite the general paucity of marine alkaloids available for bioassays, these compounds continue to show interesting activity in targeted screening programmes[16] as we have found in our investigation of MRSA PK inhibitors. Unlike secondary metabolites produced by terrestrial organisms, marine natural products often incorporate halogens, the most common of which is bromine, which can have a profound influence on biological activity.[28] Not surprisingly, many bioactive marine bi- and bisindole alkaloids are often brominated as indicated in the following carefully selected bi-and bisindole alkaloid representative examples from this interesting group of naturally occurring compounds. There are only approximately 11 known trisindole marine alkaloids and representative members of this class are not included here.[40]

1.7.1 Marine biindole alkaloids

The first examples of biindoles from the marine environment (**1.20—1.25**) were isolated from marine blue-green alga *Rivularia firma*, collected at Westernpoint, Victoria, Australia.[42] While in the context of bi- and bisindoles, these compounds are relatively simple, they feature tri-, tetra- and hexabromination patterns in addition to 3,3'- 3,1'- 4,1'- and 4,3'-indole-indole linkages.[42]

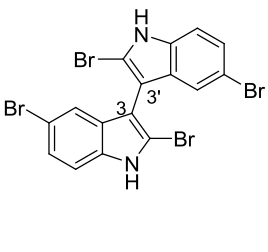

1.20

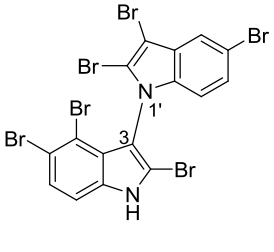

1.21

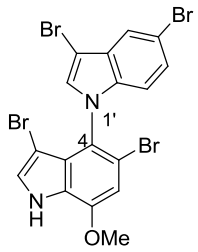

1.22

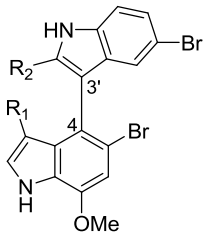

1.23 R_1 = Br, R_2 = Br
1.24 R_1 = Br, R_2 = H
1.25 R_1 = H, R_2 = Br

1.7.2 Marine bisindole alkaloids

An increase in chemical complexity is observed in the class of bisindole enamides typified by chondriamide A and B (**1.26, 1.27**) isolated from the red alga, *Chondria* sp., collected off the rocky shores near Buenos Aires, Argentina.[43] These compounds, displayed the versatile biological activity often associated with marine bisindoles, *viz*. cytotoxicity, antiviral activity, antihelminthic and antifungal activity [43,44]

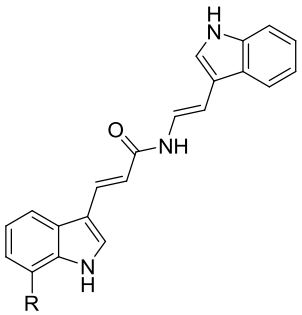

1.26 R = H chondriamide A
1.27 R = OH chondriamide B

The piperazine and pyrazinone containing bisindoles with the trivial names dragmacidins, dragmacidons and hamacanthins are joined by a central six-membered heterocyclic ring formed by a head to tail tryptamine assembly. This interesting alkaloid class is often isolated in conjunction with topsentin analogues,[45] and includes *cis*-3,4-dihydrohamacanthin B **1.5** discussed above. The first reported member of this class dragmacidin (**1.28**), isolated from the Bahaman deep water marine sponge *Dragmacidon* sp. was the first known example of a marine natural product possessing an unoxidised piperazine ring.[46]

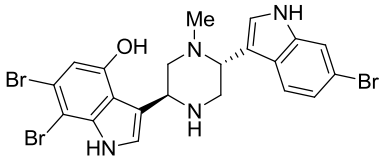

1.28 dragmacidin

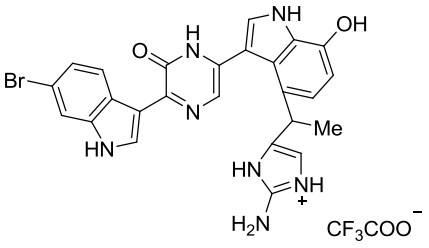

1.29 dragmacidin D

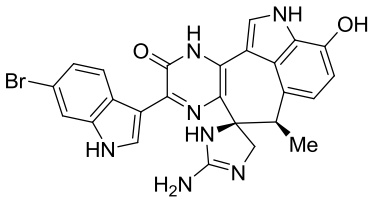

1.30 dragmacidin E

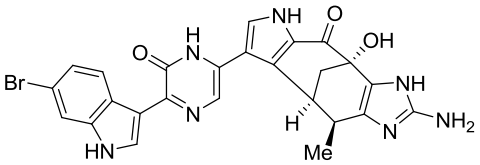

1.31 (–)-dragmacidin F

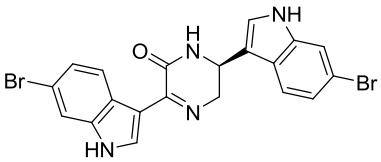

1.32 (+)-hamacanthin A

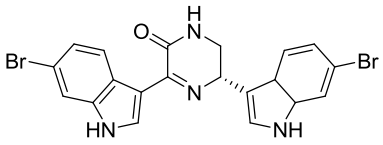

1.33 (+)-hamacanthin B

The piperazine and pyrazinone bisindole class encompasses the greatest structural diversity of any of the bisindole classes (**1.29—1.33** are presented here as selected examples),[47–50] and as such display broad bioactivity in a number of assays including cytotoxicity against various cancer cell lines,[45,51,52,53] as well as antifungal,[49,53] antimalarial[54] and significant antibacterial activity,[16,49,51,52,53,55] in both whole cell and target specific assays.

Extending the range of heterocyclic rings known to separate the two indole rings in marine bisindole alkaloids is the cytotoxic pyrimidine ring containing Okinawan *Hyritos* sp. sponge metabolite hyrtinadine A (**1.34**).[56,57] The chemical complexity of bis-indoles is further typified by the eusynstyelamides (eusynstyelamide E, **1.35** is selected example), featuring several functionalities in addition to three chiral centres.[58,59] These compounds have exhibited moderate activity against *S. aureus*[59,60] and have shown potential as neuronal nitric oxide synthase inhibitors. Neuronal nitric oxide synthase is an enzyme implicated in neuronal disorders including Alzheimer's and Parkinson's disease.[59]

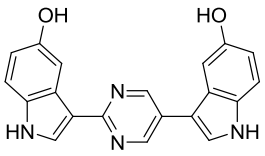

1.34 hyrtinadine A

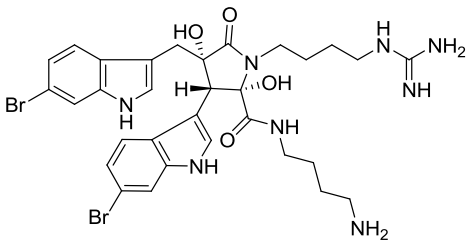

1.35 eusynstyelamide E

Fused ring bisindoles are commonly found in the marine environment and include the plant growth regulating caulerpin (**1.36**) from the green alga *Caulerpa* sp.,[61,62] the aplysinopsin dimers cycloaplysinopsin B (**1.37**) from the Philippine *Tubastraea* sp. hard coral[63] and dictazoline A (**1.38**),[64] as well as the dictazoline ring contraction constitutional isomer dictazole A (**1.39**)[65] from the marine sponge *Smenospongia cerebriformis*.

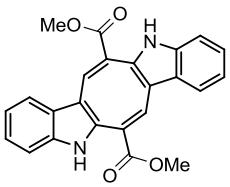

1.36 caulerpin

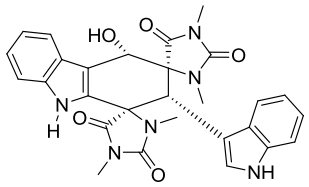

1.37 cycloaplysinopsin B

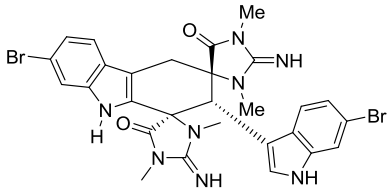

1.38 dictazoline A

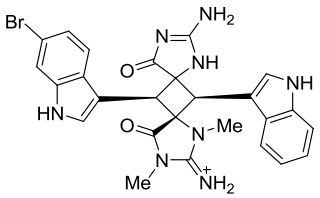

1.39 dictazole A

1.8 Isolation of marine bisindole imidazole, imidazoline and 1*H*-imidazole-5(4*H*)-ones.

The most relevant class of marine bisindole alkaloids, to the work presented in this thesis are the imidazole, imidazoline and 1*H*-imidazole-5(4*H*)-one containing bisindole compounds, typified by compounds given the trivial names topsentins, spongotines and rhopaladins. The isolation and diverse bioactivities of this group of compounds is described in detail here. A detailed discussion of synthetic approaches to the topsentins is presented in Chapter two.

The topsentin class of bisindole alkaloids, which characteristically feature an 2-acylimidazole moiety connecting two indole rings, were first isolated from the sponge *Topsentia genitrix*, collected in the Mediterranean near Banylus in France.[66] The crude methanolic extract of *T. genitrix* displayed varying degrees of toxicity towards the fish *Lebistres fluviatilis* and the freshwater sponge *Ephydatia fluviatilis* while additionally displaying general antibacterial properties.[66] Further purification of the crude extract yielded three major bisindole imidazole metabolites, originally named topsentin A, (**1.40**) B1 (**1.41**), and B2 (**1.4**).[66] These names were later changed to deoxytopsentin, (**1.40**) topsentin (**1.41**) and bromotopsentin (**1.4**) respectively.[67] Bartik *et al.* also recognized a doubling of resonances in the ^{1}H and ^{13}C NMR spectra of these compounds in neutral solution which he rationalized as slowly interconverting imidazole tautomers.[66] Compounds **1.40** **1.41** and **1.4** were again isolated

alongside 4,5-dihydro-6”-deoxybromotopsentin (**1.3**) (later renamed spongotine A) from a series of four related sponges of the genus *Spongosorites* collected in the Caribbean.[67]

The trivial name spongotine has generally been reserved for dihydro-topsentin analogues which are mostly, but not exclusively, isolated from the genus *Spongosorites* where an acylimidazoline moiety replaces the acylimidazole moiety characteristic of topsentins. Additionally, the name nortopsentin has been reserved for bisindole imidazoles in which the ketone functionality common to both topsentins and spongotines is absent. Interestingly, no nor-spongotines have been reported thus far from marine sources. Over the last quarter of a century topsentin, nortopsentin and spongotine analogues, featuring variably substituted indole rings, have regularly been isolated from a number of sponge genera collected across the globe at depths ranging from —15 m to —630 m[55,68] including: *Spongosorites* spp. collected from the Bahamas (**1.4**, **1.41, 1.42**, **1.43**, **1.44**)[68], Australia (**1.45**),[47,69] and Korea (**1.3, 1.4, 1.6, 1.40, 1.41, 1.46, 1.47, 1.48, 1.49**),[51,52,53,55,70] *Hexadella* sp. from Canada (**1.40**, **1.50**),[71,72] *Rhaphisia* spp. from the Mediterranean (**1.3**, **1.4, 1.6**, **1.40, 1.41, 1.51**),[73] Korean *Discodermia* (**1.6**, **1.40**, **1.46**),[74] and *Topsentia sp.* from South Africa (**1.3**, **1.4**, **1.6**)[16]and the Mediterranean (**1.51**).[75]

Topsentin C (**1.50**)**,** (more correctly referred to as a spongotine analogue) isolated from a Canadian *Hexadella* sp.,[72] was the first metabolite in this class to feature an *N*-methyl substituted imidazoline ring. The confusion surrounding the use of either topsentin or spongotine trivial names when naming imidazole or imidazoline containing bisindoles was further exacerbated when the bisindole 2-acylimidazoline **1.48** isolated from a *Spongosorites* sp was named as a hamacanthin.[51] Conventionally, hamacanthins possess either a dihydro or tetrahydro pyrazinone ring connecting the two indole moieties and are occasionally isolated together with topsentins and spongotines.[16] This oversight[51] was corrected in a follow-up publication where **1.48** was designated the trivial name spongotine B.[52] While optical rotation data was reported by Bao *et al.* in their later paper the absolute configuration of **1.48** had not been established.[51,52]

Nortopsentin A, B and C (**1.42—1.44**), were first reported in 1991 by Sakami *et al.*,[76] together with known compounds **1.4** and **1.41** from the same Caribbean *Spongosorites* investigated by Tsujii *et al.*.[67,76] Interestingly, the doubling of NMR signals was not reported, suggesting either a rapid proton transfer reaction relative to the topsentins, or alternatively, none at all. It was postulated by Sakami *et al.* that the *N*-1 proton on the imidazole ring in topsentins and spongotines undergoes hydrogen bonding with the 2-acyl functionality, hence slowing down proton exchange and possibly rotation, resulting in NMR signal duplication. The absence of a carbonyl functionality in the nortopsentins would therefore not allow this process to occur. In an earlier patent Sakemi and co-workers reported the same nortopsentins together with the synthetic nortopsentin D (**1.52**), prepared by catalytic hydrogenation and concomitant reductive elimination of bromine in presence of the Pd catalyst of **1.42—1.44**.[77]

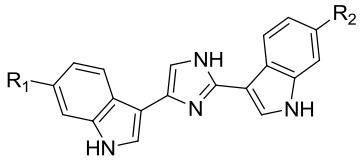

1.42 $R_1 = R_2 = Br$ nortopsentin A
1.43 $R_1 = H$, $R_2 = Br$ nortopsentin B
1.44 $R_1 = Br$, $R_2 = H$ nortopsentin C
1.52 $R_1 = R_2 = H$ nortopsentin D

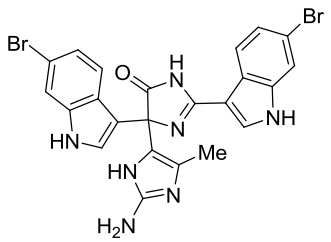

1.53 nortopsentin E

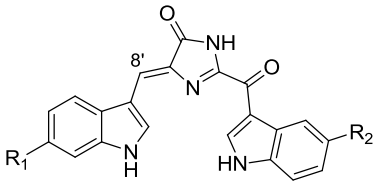

1.54 $R_1 = OH$, $R_2 = Br$ rhopaladin A
1.55 $R_1 = OH$, $R_2 = H$ rhopaladin B
1.56 $R_1 = H$, $R_2 = Br$ rhopaladin C
1.57 $R_1 = R_2 = H$ rhopaladin D

An unusual nortopsentin variant **1.53** featuring a central 1*H*-imidazol-5(4*H*)-one nucleus with a 2-amino-methyl imidazole and two 6-bromoindole substituents, was isolated from a *Dragamacidon* sp. collected off the south coast of New Caledonia.[78] Presumably Mancini *et al.* were unaware of the patent describing the preparation of the synthetic nortopsentin D[77] and gave the same name to

1.53. This was later rectified by Yang *et al.* in which **1.53** was renamed nortopsentin E.[45] Nortopsentin D was most recently reported to have been isolated from the New Caledonian sponge *Agelas dendromorpha* in which this compound was the only bisindole alkaloid in amongst a series of pyrrole-2-aminoimidazole alkaloids also isolated from the sponge.[79] In their manuscript, the authors stated that they had isolated nortopsentin D (no spectral data for this compound was provided) and cited the work of Mancini *et al.* suggesting that they incorrectly named the metabolite isolated from *Agelas dendromorpha* which is most likely nortopsentin E.

The Okinawan ascidian *Rhopalaea* sp. yielded a series of imidazolinone bisindoles, rhopaladins A—D (**1.54—1.57**) possessing an "extra" olefinic methine moiety (C-8') between the indole and the imidazolinone ring.[80] NOE experiments revealed that these compounds exist as rotational isomers, around the C-3'-C-8' bond.[80] These are the only examples of this class of bisindole alkaloids isolated thus far from ascidians (tunicates).

1.9 Biological activity of topsentin and related compounds

The wide range of biological activity exhibited by the topsentins, spongotines and nortopsentins appears to be influenced by substitution patterns on the indole and relative saturation of the imidazole ring. A substantial body of work has been dedicated to exploring the role of these compounds as potential cytotoxic agents and as a result many topsentin and nortopsentin compounds have been tested against various cancer cell lines of both human and non-human origin, including, but not limited to: colon, lung [51,52,81] and bromcopulmonary cancer cell lines,[73] KB tumoral cells,[78] adenocarcinoma, breast, hepatoma,[53] ovarian, skin and CNS cancer cell lines,[51,52] and various leukemia cell lines.[53,67,70,72,81] The diverse biological role of this class of alkaloids is also expressed through their respective antiviral,[67] antifungal,[76] antibacterial,[80] adrenal ligand displacement[68] together with anti-inflammatory and neural nitric oxide synthase activities.[45] While the most

recently reported cytotoxicity data have shown that compounds **1.3**, **1.47** and **1.47** exhibit moderate activity against five solid tumor lines, while **1.4**, **1.6**, **1.40**, **1.46**, **1.41** and **1.48** were virtually inactive in the same assay.[52,51]

Of greatest interest to us is the antibacterial activity displayed by this class of compounds. A thorough screen of the antibacterial properties of compounds **1.3**, **1.4**, **1.40** and **1.41** was conducted by Oh *et al.*[53] against a variety of gram positive and negative bacteria including *Bacillus subtilis, Micrococcus leuteus,* three strains each of *S. aureus* and MRSA, *Escherichia coli* strains*, Proteus vulgaris* and *Salmonella typhimurium*. Deoxytopsentin (**1.40**) exhibited activity (MIC 3.12—12.5 μg/ml) against all strains except *E. coli* where it was inactive as were all the other compounds tested.[53] Most promising of all was the fact that **1.40** proved to be equally or more active than oxacillin against all three strains of MRSA tested.[53] Additional indole substituents in **1.4** and **1.41** resulted in reduced activity while the 2-acylimidazoline containing **1.3** was inactive against all tested strains.[53]

In addition to the MRSA PK inhibition assays,[16] topsentin as well as spongotine compounds have been identified as inhibitors of *S. aureus* sortase A (SrtA).[55] The pathogenesis of *S. aureus* is partly dependent on proteins that impart surface adhesion and virulence to the bacteria which enable them to adhere to host tissue and subsequently infect these tissues. This process is mediated by SrtA which covalently anchors the virulence associated proteins to the cell wall peptidoglycan of the bacterium.[55] Inhibition of SrtA results in infection impedance, while not affecting microbial viability.[55] With the exception of **1.3**, which was inactive in the assay, the remaining three compounds screened in the SrtA enzyme assay (**1.40, 1.4** and **1.6**), exhibited IC_{50} inhibition values of 15.7, 16.7 and 19.4 μg/ml respectively, a result comparable to the known SrtA inhibitor β-sitosterol-3-*O*-glucopyranoside (18.3 μg/ml).[55] Oh *et al.*[55] further demonstrated that **1.6** dose dependently inhibited the adhesion of wild type *S. aureus* to a plate coated in fibronectin comparable to an isogenic knockout mutant, unable to produce SrtA.[55] MIC values for bacterial growth inhibition

revealed that the order of antimicrobial activity for **1.3**, **1.4**, **1.6** and **1.40** mirrored the SrtA inhibition.[53,55]

1.10 Aims of the thesis

The versatile biological activity of bisindole alkaloids with particular reference to antibacterial activity[53,55,80] was supported by the selective, low nanomolar MRSA PK inhibitory activity exhibited by marine bisindoles **1.5** and **1.6**.[16] The preparation of analogues of **1.5** in which the position and number of halogen substituents was varied as well as replaced with other substituents (**1.7—1.12**) was found to have a profound effect on the activity observed for the natural product **1.5**.[22] Inspection of the binding site revealed two features, namely the symmetrical nature of the binding pocket and the prominent histidine residues with π-stacking capability, which we hoped to exploit in our design of analogues of **1.6** with greater affinity and selectivity for MRSA PK over human PK orthologs. Computational analysis of the binding site and ligand binding (Chapter 4) informed our design and synthesis of a series of pseudo symmetrical analogues of **1.6** in Chapter 2 (**1.40, 1.46, 1.58—1.61**) and Chapter 3 (**1.62—1.68**) with improved activity and selectivity over the original marine natural product.

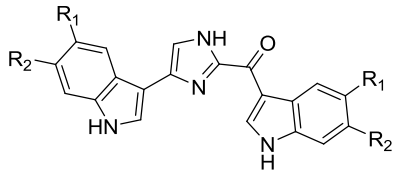

1.40 R_1 = R_2 = H deoxytopsentin (topsentin A)
1.46 R_1 = H, R_2 = Br dibromodeoxytopsentin
1.58 R_1 = H, R_2 = F
1.59 R_1 = H, R_2 = Cl
1.60 R_1 = Br, R_2 = H
1.61 R_1 = H, R_2 = **I**

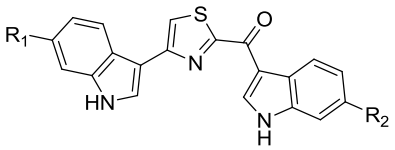

1.62 R_1 = R_2 = H
1.63 R_1 = R_2 = F
1.64 R_1 = R_2 = Cl
1.65 R_1 = R_2 = Br
1.66 R_1 = Br, R_2 = F
1.67 R_1 = F, R_2 = Br
1.68 R_1 = F, R_2 = Cl

Chapter Two

Synthesis and Biological Activity of Bromodeoxytopsentin Analogues

2.1 An overview of the synthesis of topsentin and related compounds

Deoxytopsentin (**1.40**) is the simplest of the topsentin class of marine bisindole alkaloids. First isolated in 1987 by Bartik *et al.*[66] **1.40** also became the first topsentin type compound to be synthesized as reported by Braekman *et al.*.[82] Allylic bromination of 3-acetylindole (**2.1**) gave the α-bromoketone **2.2** which on treatment with dimethylhydrazine, followed by subsequent rearrangement and imidazole ring condensation afforded **1.40** (**Scheme 2.1**)[82]

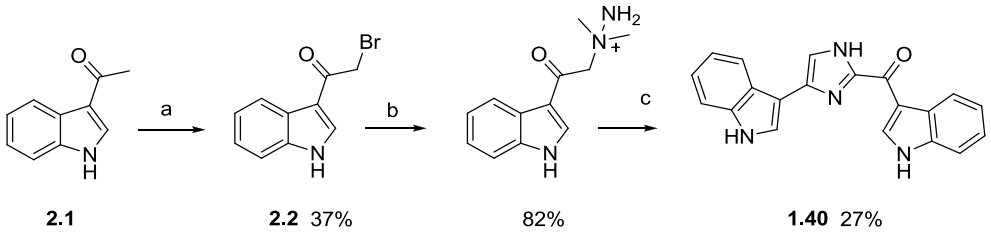

2.1 **2.2** 37% 82% **1.40** 27%

Scheme 2.1 Braekman *et al.*'s synthesis of **1.40**[82]

a) $CuBr_2$, $CHCl_3$/EtOAc; b) 1,1-dimethylhydrazine, EtOH, −15 °C; c) *n*-propanol reflux

Using a similar synthetic strategy, Tsujii *et al.*[67] reported two methods to synthesize several topsentin analogues (**Scheme 2.2**). Hydrolysis of the respective 3-(chloroacetyl)indole starting materials into the corresponding 3-(hydroxyacetyl)indoles was achieved by heating the chlorinated precursors in a 10:1 mixture of formamide and water. Subsequent oxidation of the 3-(hydroxyacetyl)indoles with copper (II) acetate monohydrate yielded the corresponding indolyl-3-glyoxal (**2.3**) and 6-benzoyloxyindolyl-3-glyoxal (**2.4**). Glyoxals **2.3** and **2.4** were separately condensed in the presence of ammonia to afford deoxytopsentin from **2.3** and a mixture of four variously substituted bisindole imidazoles **1.40**, **2.5**, **2.6** and **2.7**. Removal of the benzyl ether protecting group from **2.5—2.7** with 10% palladium/charcoal afforded topsentin **1.41**, isotopsentin **2.8** and dihydroxytopsentin **2.9** respectively.

Alternatively, the extra oxidation step to produce the glyoxals was made redundant by a one pot oxidation and cyclization in which copper (II) acetate monohydrate in aq. ammonia solution was added dropwise to a refluxing ethanol solution of the intermediate 3-(hydroxyacetyl)indoles.[67] While this synthesis was the first to yield hydroxylated topsentin products, and like the Braekman synthesis, it involved a simple condensation reaction, it was low yielding and non regiospecific, resulting in a mixture of products.

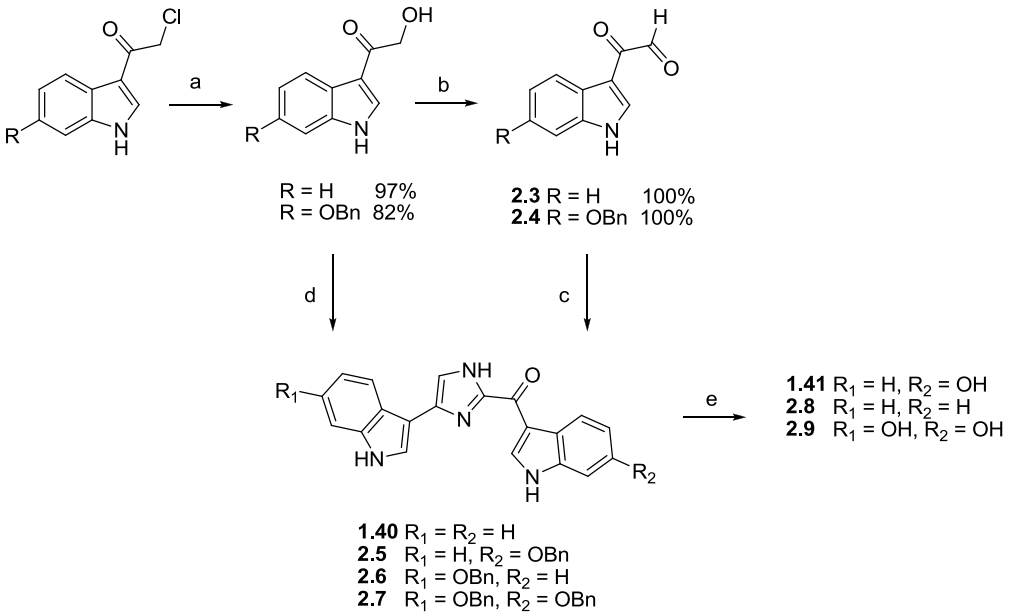

Scheme 2.2 Tsujii *et al*.'s synthesis of **1.40, 1.41, 2.8** and **2.9**[67]

a) $H_2O/HCONH_2$, 110 °C; b) $Cu(OAc)_2$; c) NH_4OH aq. EtOH, d) $Cu(OAc)_2$; NH_4OH aq. EtOH; e) 10% Pd/C, N_2.

The first example of the use of a Suzuki type cross coupling and not a condensation and cyclization strategy to access the imidazole ring, was the synthesis of the non-naturally occurring nordeoxytopsentin (**1.52**) by Kawasaki *et al.*[83] via successive regioselective arylation reactions (**Scheme 2.3**). 2,4,5-Tribromoimidazole (**2.10**), followed by 2-indolyl-4,5-dibromoimidazole (**2.11**)

were sequentially coupled with *N*-silyl protected 3-indolylboronic acids in a Suzuki type reaction, followed by debromination and deprotection to yield **1.52**.[83]

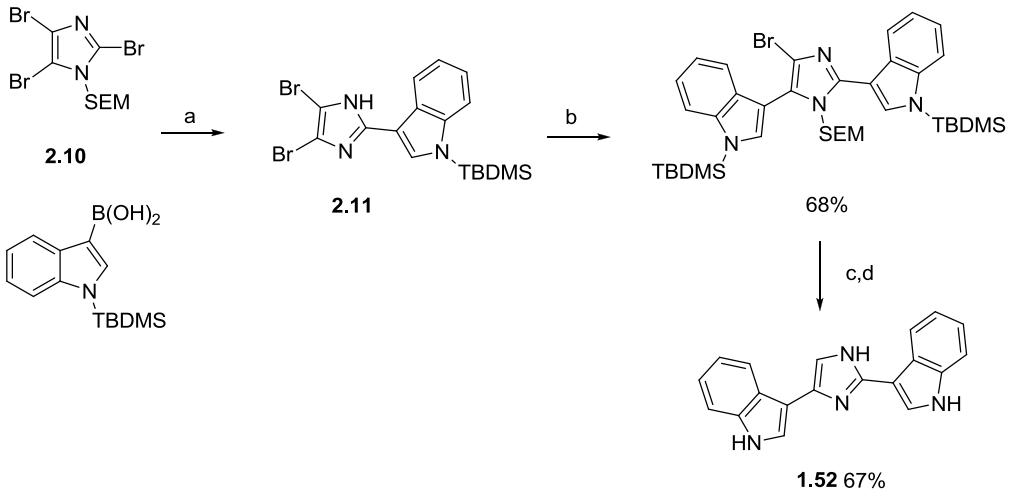

Scheme 2.3 Kawasaki *et al*.'s synthesis of **1.52**[83]

a) $Pd(PPh_3)_4$; b) $Pd(PPh_3)_4$, Na_2CO_3; c) *t*-BuLi, H_2O; d) TBAF

The coupling of aryl boronic acids with aryl bromides, in the presence of $Pd^{(0)}$ using Kawasaki *et al.*'s synthesis imposes restrictions on the use of brominated nortopsentin and topsentin analogues, because of the possibility of bromine removal during the reduction step as reported by Tsujii *et al.*.[67] Accordingly, Kawasaki *et al.*[84] subsequently utilized the greater affinity of $Pd^{(0)}$ for iodine and coupled iodinated imidazoles to brominated indole boronic acids to overcome this problem. Therefore 2,5-diiodoimidazole (**2.12**) was reacted with two equivalents of 6-bromo-3-indolylboronic acid followed by deprotection to yield nortopsentin A (**1.42**) (**Scheme 2.4**). Kawaski *et al.* adapted this general strategy outlined in **Scheme 2.4** to synthesize nortopsentins B (**1.43**) and C (**1.44**).[84]

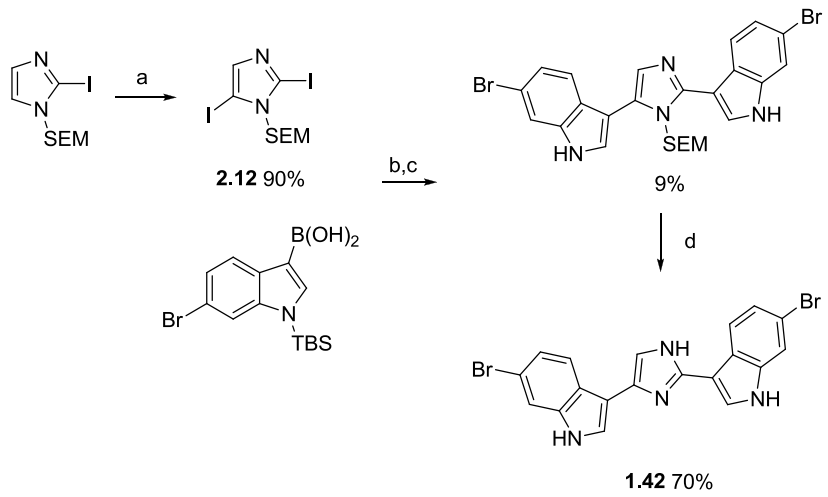

Scheme 2.4 Kawasaki *et al*.'s synthesis of **1.42**[84]

a) LTMP, I_2; b) $Pd(PPh_3)_4$, Na_2CO_3; c) TBAF; d) 20% HCl.

The metal coupling approach was then applied by Achab[85] to the synthesis of topsentins in which a Stille coupling was used in the penultimate step in the synthesis of four analogues **1.4, 1.6, 1.40** and **1.41**. Importantly this cohort of products included brominated 'non-symmetrical' analogues and were synthesized via two different methods (**Scheme 2.5** and **2.6**). Both involving a palladium catalyzed coupling of the functionalized iodoimidazole with a 3-stannylindole.[85] Achab's initial synthetic communication was followed 12 years later with a full publication in which greater detail of the experimental methodology was provided.[86]

Both of these metal coupling based methodologies for the first time allowed for differently substituted indole moieties to be introduced into the topsentin scaffold, without the random distribution of substituted indole products seen with the condensation approach of Braekman *et al.*[82] and Tsujii *et al.*.[67] In addition the use of iodinated precursors and the established order of reactivity of iodine vs. bromine protected the 6-bromoindoles from involvement in unwanted side reactions.

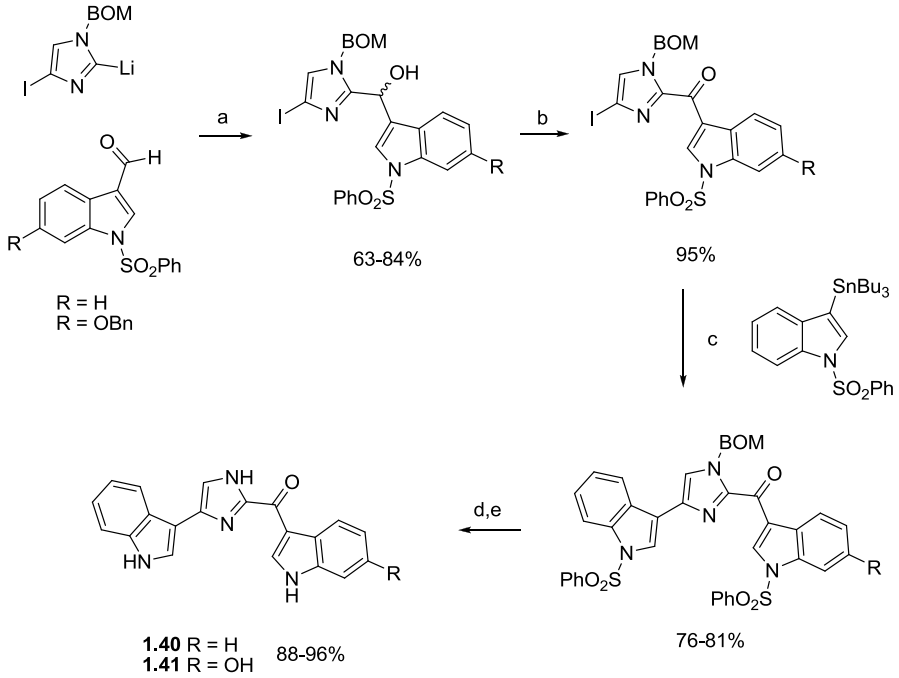

Scheme 2.5 Achab *et al*.'s synthesis of **1.40** and **1.41**[85]

a) THF, −78 - 0 °C; b) MnO_2, CH_2Cl_2, r.t. 5h; c) $PdCl_2(PPh_3)_2$, CuI, DMF, 100 °C, 2h; d) 10% KOH, EtOH/THF, reflux, 2h; e) EtOH, HCO_2NH_4, 10% Pd/C, reflux, 4h.

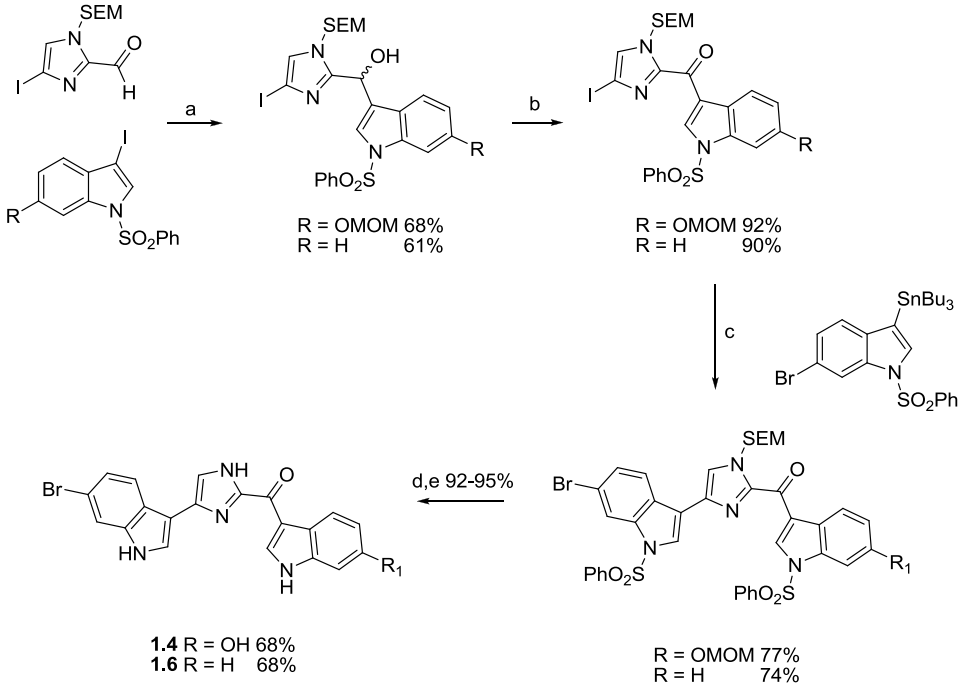

Scheme 2.6 Achab *et al*.'s synthesis of **1.4** and **1.6**[85]

a) *t*-BuLi, THF, −90 - 0 °C, 4h; b) MnO_2, CH_2Cl_2, r.t. 4h; c) $PdCl_2(PPh_3)_2$, CuI, DMF, 100 °C, 2h; d) 10% KOH, EtOH/THF, reflux, 2h; e) 5M HCl, EtOH 3h.

Miyake *et al.* established a novel regioselective method for synthesizing 'non symmetrical' nortopsentin B (**1.43**) as well as 'pseudo symmetrical' nortopsentin D (**1.52**),[87] which did not involve the intricate coupling of three separate ring systems, but rather the separate preparation of differently functionalized indoles, that could ultimately be coupled and cyclized. Their approach involved the initial synthesis of indolyl-3-carbonylnitrile (**2.13**) from indole in a previously reported two step, single pot procedure.[88] The indolyl-3-carbonylnitrile was then subsequently hydrogenated over 10% Pd/C in acetic acid to yield the versatile oxotryptamine (**2.14**) as the acetate salt. Condensation of **2.14** with 6-bromo-3-cyanoindole (**2.15**) or 3-cyanoindole (**2.16**) afforded **1.43** and **1.52** respectively (**Scheme 2.7**).[87]

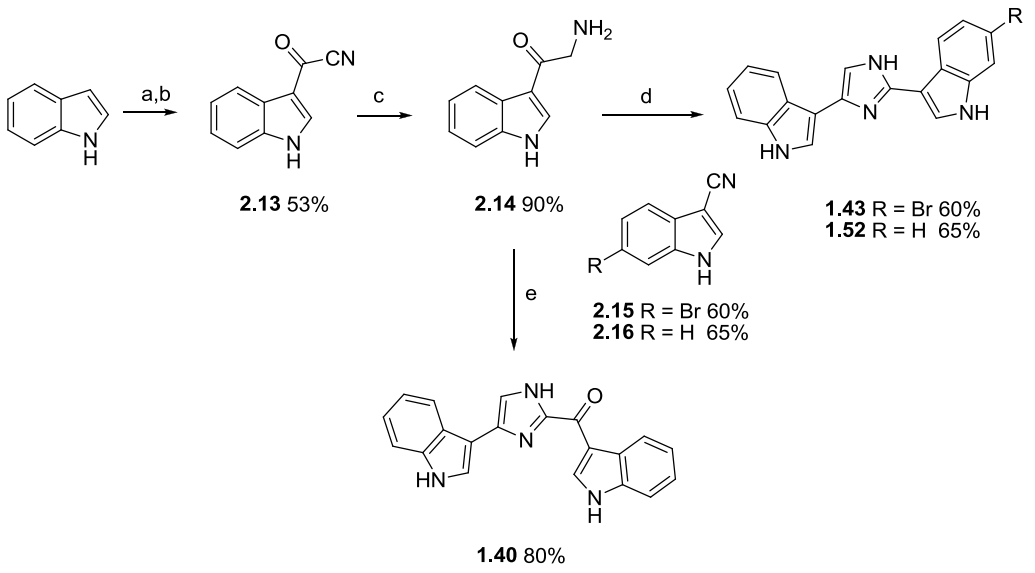

Scheme 2.7 Miyake *et al.*'s synthesis of **1.40**, **1.43** and **1.52**[87]

a) $(COCl)_2$, Et_2O, 0 °C; b) Toluene, ACN, CuCN, 110 °C; c) H_2, 10% Pd/C, AcOH; d) 190 - 210 °C; e) NH_4OH

Unfortunately, Miyake *et al.*'s proposed regioselective topsentin synthesis was not initially successful. Reaction of **2.14** and indole-3-glyoxal chloride (**2.17**) in TEA, followed by dehydrative cyclization of ketoamide **2.18** with phosphorus oxychloride yielded the first oxazole topsentin analogue (**2.19**) (**Scheme 2.8**). Miyake *et al.* subsequently unsuccessfully attempted to convert the

oxazole into imidazole by treatment with either formamide or NH_4OH. They accordingly resolved to cyclically condense two oxotryptamine subunits in the presence of NH_4OH in a non regioselective manner to yield **1.40** (**Scheme 2.7**).[87]

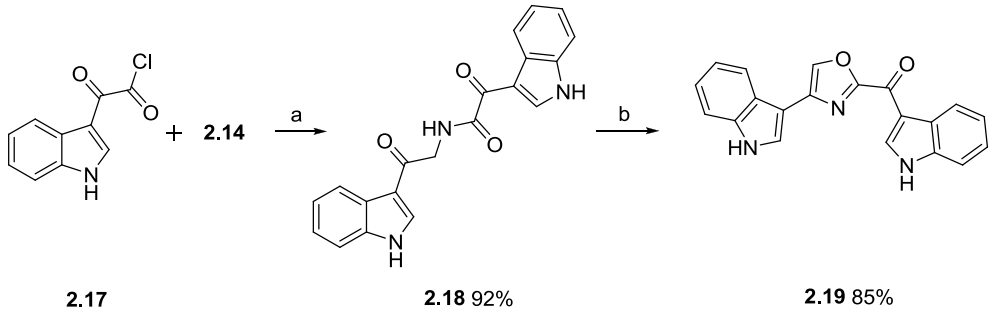

2.17 **2.18** 92% **2.19** 85%

Scheme 2.8 Miyake *et al*.'s synthesis of **2.19**[87]

a) TEA; b) $POCl_3$

The next attempt at regioselective nortopsentin synthesis was by Moody and Roffey who focused on imidazole formation by reacting an amidine with an α-halocarbonyl in a method analogous to the Hantzsch thiazole synthesis (**Scheme 2.9**).[89] *N*-Boc protected, indolyl-3-amides (**2.20** and **2.21**) were thiated to afford thioamides (**2.22** and **2.23**) via Lawesson's reagent. Methyl iodide mediated methylation yielded thioimidates, which were subsequently converted into indole-3-carboxamidines via ammonolysis. Coupling of **2.2** with the indole-3-carboxamidines was achieved in the presence of potassium carbonate to yield the *N*-Boc protected nortopsentin analogues (**2.24** and **2.25**). Unfortunately, Moody and Roffey were not able to successfully remove the Boc protecting group, and hence complete the synthesis of **1.43** and **1.52**.[89] However the authors only reported the use of two methods of *N*-Boc removal (TFA and NaOMe mediated), and speculated that nortopsentin may be unstable in acidic and basic conditions. An alternative thermolytic *N*-Boc removal as employed by ourselves and described later in this chapter may have proved more fruitful to resolve their deprotection challenge.

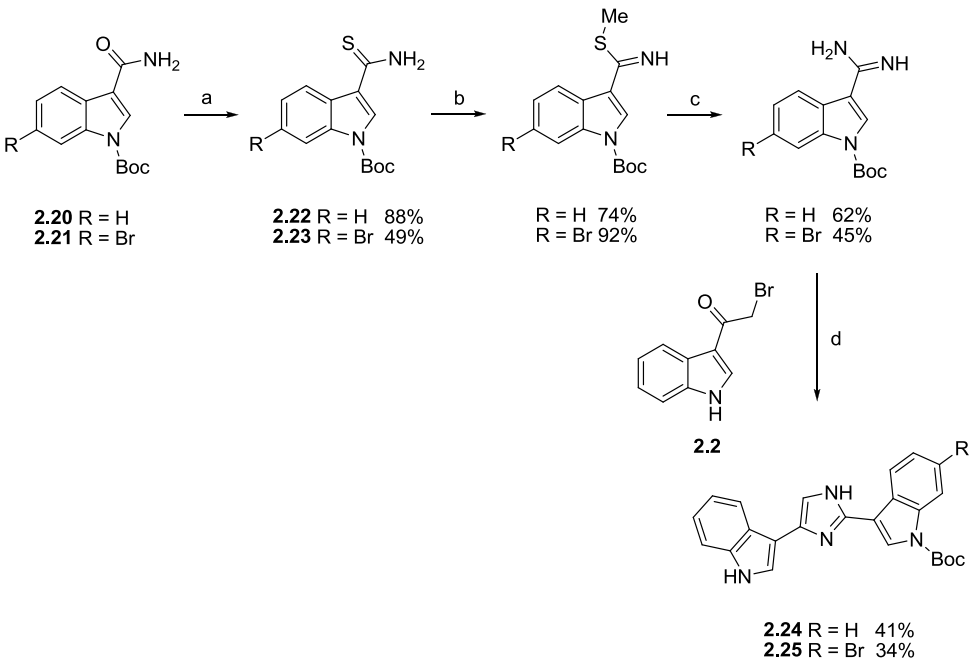

Scheme 2.9 Moody and Roffey's attempted synthesis of **1.43** and **1.52**[89]

a) Lawesson's reagent, benzene, reflux 1h; b) MeI, CH_2Cl_2, r.t. 48h Ar gas; c) NH_4Cl, MeOH, reflux, 3h; d) K_2CO_3, MeCN, reflux, 7h.

The non-naturally occurring **1.52** was most recently synthesized (**Scheme 2.10**) via cyclization of ketoamide (**2.26**) with ammonium acetate under microwave irradiation. This synthesis has regioselective potential since self cyclization of the two indole precursors **2.27** and **2.28** is not possible. Precursors **2.27** and **2.28** were condensed in the presence of tertiary phosphine to yield **2.26**.[90]

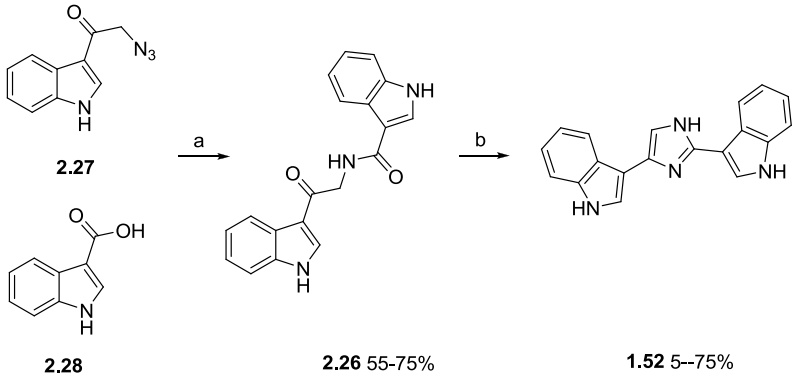

Scheme 2.10 Fresneda *et al*.'s synthesis of **1.52**[90]

a) PMe_3; b) NH_4OAc, DMF, MWI.

Guinchard *et al.*[91] described the first regiospecific topsentin syntheses not requiring the complex three ring, metal coupling method as described by Achab. Guinchard *et al.*'s synthesis of **1.40, 1.47, 1.48** and **1.51** presented in **Scheme 2.11** is also the first reported synthesis of naturally occurring isobromodeoxytopsentin (**1.47**), spongotine B (**1.48**) and topsentin D (**1.51**).[91] The synthesis of all four compounds was initiated from the common β-amino indolic *N*-hydroxylamine (**2.29**), which was transformed into the key 1-(indol-3'-yl)-1,2-diaminoethane intermediate (**2.30**) over three steps. Crucially one of the steps involved hydrogenation with the palladium based Pearlman's catalyst, which limits this method to synthesis of compounds where there is no halogen on the indole bonded directly to the imidazole because of possible halogen removal during the reduction step.[67]

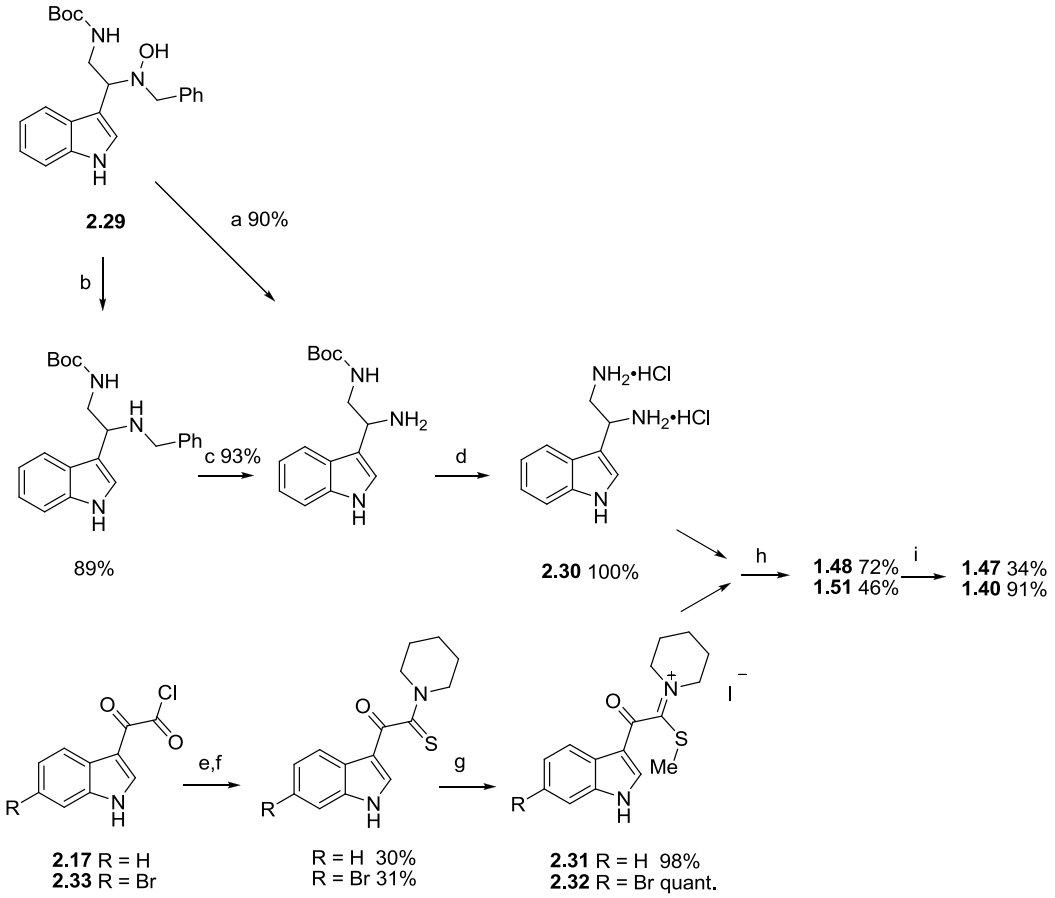

Scheme 2.11 Guinchard *et al.*'s synthesis of **1.40, 1.47, 1.48** and **1.51**[91]

a) H_2, $Pd(OH)_2$, MeOH–AcOH (96:4), r.t. 50h; b) $TiCl_3$, HCl aq. MeOH–H_2O, r.t. 15 min; c) H_2, $Pd(OH)_2$, MeOH–AcOH (96:4), r.t. 16h; d) HCl, MeOH, r.t. 1h; e) *n*-Bu_3SnH, EtOAc, 0 °C, 30 min, r.t. 16h; f) S_8, piperidine, pyridine, 80 °C, 5h; g) MeI, 80 °C, 5h; h) Amberlyst A 21, MeOH, r.t. 48h; i) IBX, DMSO, r.t. 15h.

In Guinchard *et al.*'s synthesis, 3-indolyl-α-ketothioimidate salts (**2.31** and **2.32**) were chosen as the condensation partners for **2.30**. These were prepared from indole precursors which had initially been reacted with oxalyl chloride to afford indolyl-3-glyoxalchlorides (**2.17** and **2.33**). Treatment of **2.17** and **2.33** with tributyltin hydride yielded the respective glyoxals, which were subsequently reacted with solid sulfur and piperidine in pyridine to yield the respective 3-indolyl-α-oxothioamide intermediates in low yield. These were converted to **2.31** and **2.32** by refluxing with methyliodide. The salts were finally condensed with **2.30** at room temperature in methanol in the presence of catalyst to yield racemic mixtures of **1.45** and **1.48** respectively. Oxidation of **1.48** and **1.51** converted the dihydroimidazole rings into imidazole rings and afforded **1.47** and **1.40** respectively.[91]

The limitation of one sided bromination on the topsentin scaffold was addressed in a later publication by Guinchard *et al.* (**Scheme 2.12**)[92] where the brominated analogue of **2.30** (**2.33**) was prepared over four steps. Crucially in this synthesis palladium catalysis was avoided and instead Guinchard *et al.* relied on manganese dioxide oxidation, hydroxyaminolysis of the indolic nitrones, and titanium trichloride reduction, followed by deprotection in order to access their target. The remainder of the synthesis followed their previous synthetic pathway, to yield spongotine A (**1.3**) and spongotine C (**1.49**) as a racemic mixture, in addition to bromodeoxytopsentin (**1.6**) and dibromodeoxytopsentin (**1.46**). Additionally, this was first reported synthesis of **1.3**, **1.49** and **1.46**.[92]

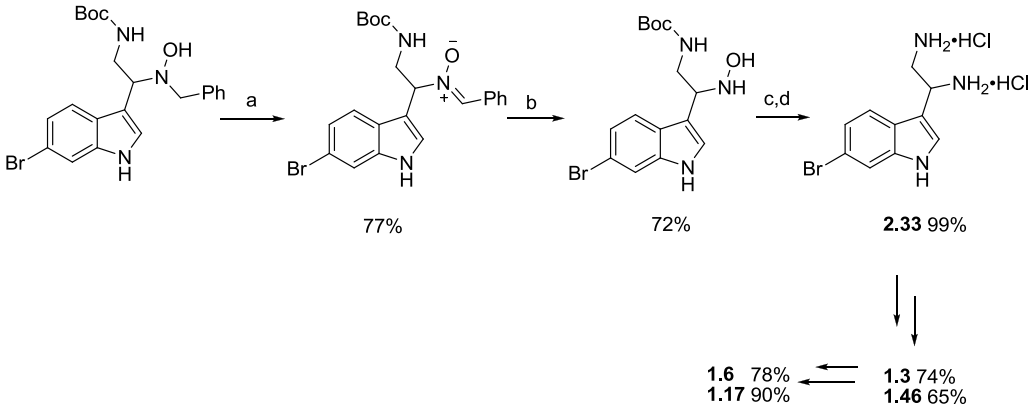

Scheme 2.12 Guinchard *et al.*'s synthesis of **1.3**, **1.6**, **1.17** and **1.46**[92]

a) MnO_2, toluene 100 °C, 10 min; b) hydroxylamine hydrochloride, MeOH, r.t. 15 min; c) $TiCl_3$, HCl, MeOH, r.t. 10 min; d) HCl, MeOH, 0 °C, 2h.

2.2 Approaches to the synthesis of other biaryl 2-acyl imidazoles

Khalili *et al.*[93] described a novel one pot procedure to synthesize 2-acyl imidazoles from aryl glyoxals in the presence of excess NH_4OAc in water, without the use of a catalyst at room temperature. They proposed the reaction scheme occurred via a reactive imine intermediate (**2.34**) which condensed to form the 1,3-diazole ring (**2.35**) (**Scheme 2.13**). They further postulated that the methane ring proton undergoes a [1,5]-hydrogen shift to yield a mixture of interconverting isomers (**Scheme 2.14**).

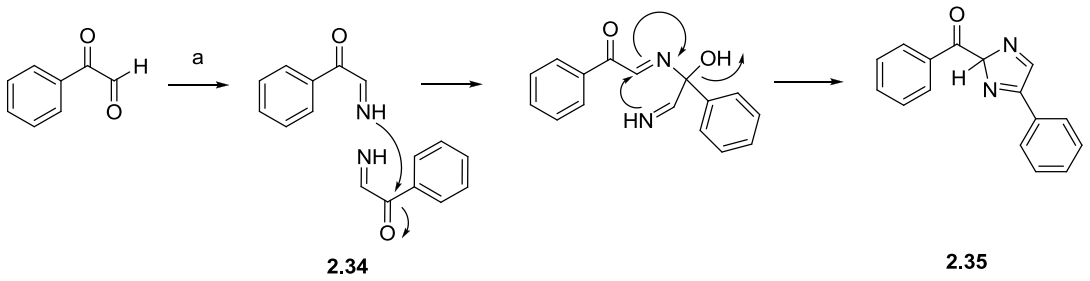

Scheme 2.13 Khalili *et al*.'s glyoxal condensation pathway[93]

a) NH_4OAc, H_2O, r.t. 69%

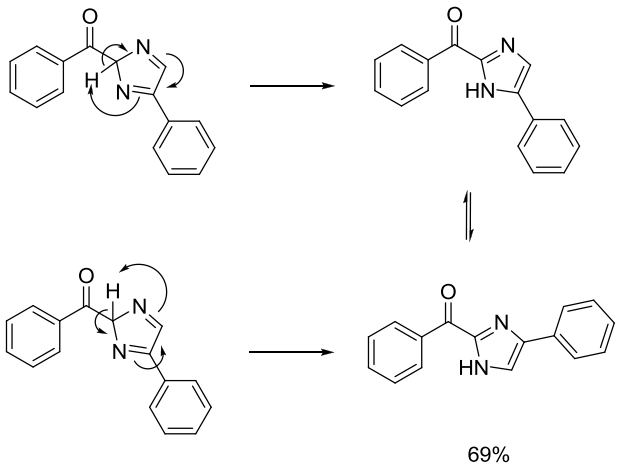

Scheme 2.14 Khalili *et al*.'s proposed [1-5] hydrogen shift resulting in interconverting tautomers[93]

While Khalili *et al.*[93] preferred to use aqueous conditions for the synthesis, they reported a marginal (2%) increase in yield to 71% when the solvent was changed to ethanol.[93]

This method was successfully used by Young in our laboratory with ethanol as the solvent of choice to condense a series of aryl glyoxals, derived from commercially available acetophenones, into their imidazole containing dimers.[94] As highlighted during our discussion of the synthetic strategies of Braekman *et al.*,[82] Tsujii *et al.*[67] and Miyake *et al.*[87] this is a non regiospecific method to synthesize 2,5 bi-functionalized imidazoles.

2.3 Rationale for the synthesis of analogues of bromodeoxytopsentin (1.6)

Based on the structure activity relationships revealed by Strangman *et al.*'s synthesis of the *cis*-3,4-dihydrohamacanthin B analogues (**1.7—1.12**),[22] And the known MRSA PK inhibition activity of the naturally occurring bromodeoxytopsentin,[16] we proposed that the synthesis of bromodeoxytopsentin analogues **1.40, 1.46** and **1.58—1.61** would provide greater insights into MRSA PK inhibition activity of **1.6**.

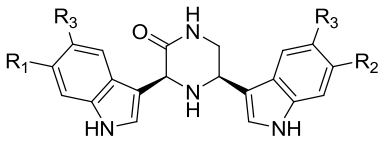

1.5 $R_1 = R_2 = Br$, $R_3 = H$ *cis*-3,4-dihydrohamacanthin B
1.7 $R_1 = R_2 = Cl$, $R_3 = H$
1.8 $R_1 = R_2 = F$, $R_3 = H$
1.9 $R_1 = R_2 = R_3 = H$
1.10 $R_1 = R_2 = H$, $R_3 = Br$
1.11 $R_1 = R_2 = Me$, $R_3 = H$
1.12 $R_1 = R_3 = H$, $R_2 = Br$

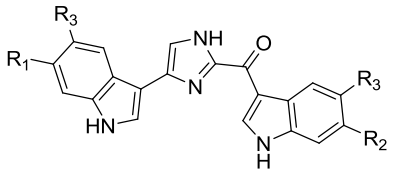

1.6 $R_1 = Br$, $R_2 = R_3 = H$ bromodeoxytopsentin
1.40 $R_1 = R_2 = R_3 = H$ deoxytopsentin
1.46 $R_1 = R_2 = Br$, $R_3 = H$ dibromodeoxytopsentin
1.58 $R_1 = R_2 = F$, $R_3 = H$
1.59 $R_1 = R_2 = Cl$, $R_3 = H$
1.60 $R_1 = R_2 = H$, $R_3 = Br$
1.61 $R_1 = R_2 = I$, $R_3 = H$

As discussed previously, the binding site of **1.5** is symmetrical due to the anti-parallel interaction of two identical α-helices,[16] which theoretically should enhance the binding of ligands that display a degree of symmetry and even pseudo symmetry as is the case with compounds **1.5, 1.7—1.12** and

evident in our proposed synthetic target imidazoles **1.40, 1.46** and **1.58—1.61.** Accordingly, our proposed synthetic targets **1.46** and **1.58—1.61** featured the same halogen substituent on each indole ring and therefore did not require a synthetic strategy that incorporated the relatively complex regioselective method used by Guinchard *et al.*.[91,92] We therefore resolved to synthesize **1.40, 1.46** and **1.58—1.61** via the cyclocondensation of suitable indolyl glyoxal analogues as per the method of Tsujii *et al.*[67] to access our desired imidazole target compounds.

The synthetic approach to topsentin type compounds of Miyake *et al.* was deemed unsuitable for our purposes since it required a Pd/C catalyzed reduction of the precursor **2.13** to afford **2.14** (**Scheme 2.7**).[87] This would have been detrimental for the formation of halogenated topsentin analogues, since Tsujii *et al.* reported the removal of bromine from indole systems by Pd/C and hydrogen (**Scheme 2.15**).[67]

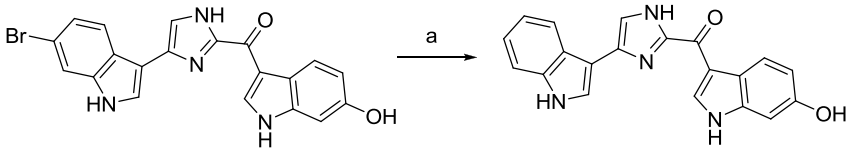

1.4 **1.41**

Scheme 2.15 Tsujii *et al.*'s bromine removal[67]

a) 10% Pd/C, H_2, EtOH, 4h, quant

Although alternative nitrile reduction[95] and amine synthetic methods[96] were considered, we felt that exploitation of the glyoxal condensation approach as utilized by Tsujii *et al.*[67], Young[94] and Khalili *et al.*[93] was more accessible.

However, syntheses involving indolyl-3-glyoxals are not common in the chemistry literature where they are occasionally reported as intermediates in reaction schemes.[67,97] Initially, we considered three possible methods for glyoxal synthesis. The first and seemingly most popular method to access

indolyl-3-glyoxals, involves reduction of indolyl-3-oxalyl chloride, **2.17**, with the very toxic and often difficult to obtain, tributyltin hydride in modest yield (**Scheme 2.16**).[21,97,99]

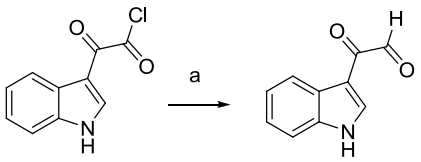

2.17

Scheme 2.16 Tributyltin hydride reduction of indolyl-3-oxalyl chloride[21,97,98].

a) *n*-Bu_3SnH, EtOAc, 0 °C – r.t.

Alternatively, Marchand *et al.*[100] and Young *et al.*[101] have shown that aryl glyoxals can be synthesized from acetophenone precursors via selenium dioxide (SeO_2) mediated oxidation in the presence of stochiometric amounts of water (**Scheme 2.17**).

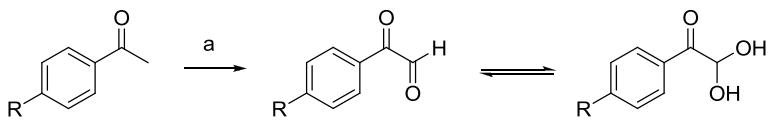

R = H 84%
R = OMe 84%
R = NO_2 62%
R = Cl 81%
R = Br 89%
R = F 87%

Scheme 2.17 Young *et al.*'s SeO_2 mediated glyoxal formation[101]

a) SeO_2, H_2O, 1,4-dioxane, MW,100 °C, 15 min

The third synthetic method which we considered was the Kornblum oxidation[102,103] which allows for the oxidation of α-bromoketones into glyoxals in the presence of DMSO at room temperature[102]

(**Scheme 2.18**). This method was later improved with the addition of base, at 100 °C allowing for the oxidation of an extended range of alkyl halides.[66] Although Kornblum oxidation appeared to require the least noxious reagents *c.f.* SeO_2 and tributyltin hydride, all attempted syntheses of indolyl-3-glyoxal via the Kornblum oxidation of **2.2** were unsuccessful in our hands. Given Young *et al.*'s [101] success in our laboratory with SeO_2 oxidations of aryl methyl ketones, under carefully controlled conditions, we proposed to adapt this method to synthesize the required indolyl-3-glyoxals from appropriate 3-acetylindole precursors.

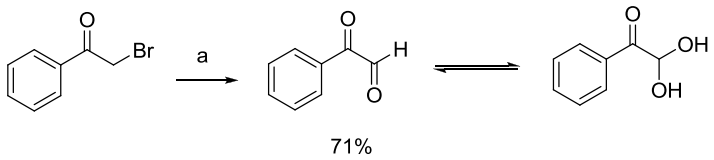

Scheme 2.18 Kornblum *et al.*'s DMSO mediated oxidation[102]

a) DMSO, r.t. 9h

2.4 Synthesis of 3-acetylindoles

2.4.1 Commercially available starting materials

Our SeO_2 mediated glyoxal synthesis was dependant on the availability of the respective 3-acetylindoles (**2.1, 2.36—2.40**) and we were disappointed, to discover that only **2.1** was commercially available. We therefore explored strategies to synthesize halogenated 3-acetylindoles from commercially available halogenated indoles. At the beginning of the project indole (**2.41**), 6-fluoro indole (**2.42**), 6-chloro indole (**2.43**) and 5-bromo indole (**2.44**) were commercially available, while the 6-bromo (**2.45**) and 6-iodo (**2.46**) analogues were not. Frustratingly, while 6-bromo indole-3-carbaldehyde (**2.47**) was commercially available, later on in the project **2.45** became available from Sigma-Aldrich after alternative methods towards the synthesis of **2.39** had been attempted.

With no ready source of **2.46** at hand it was clear that a synthesis of this compound was required (see Section **2.4.5**).

2.4.2 Possible strategies for the synthesis of 3-acetylindoles

Synthetic methodology to produce 3-acylindoles is of significant interest due to their importance in the synthesis of biologically active and versatility in alkaloids.[40,96,104–111] Two possible methods to synthesize 3-acetylindoles from indoles includes either Friedel-Crafts acylation or a Vilsmeier-Haack formylation followed by Grignard addition and alcohol oxidation.[104,110]

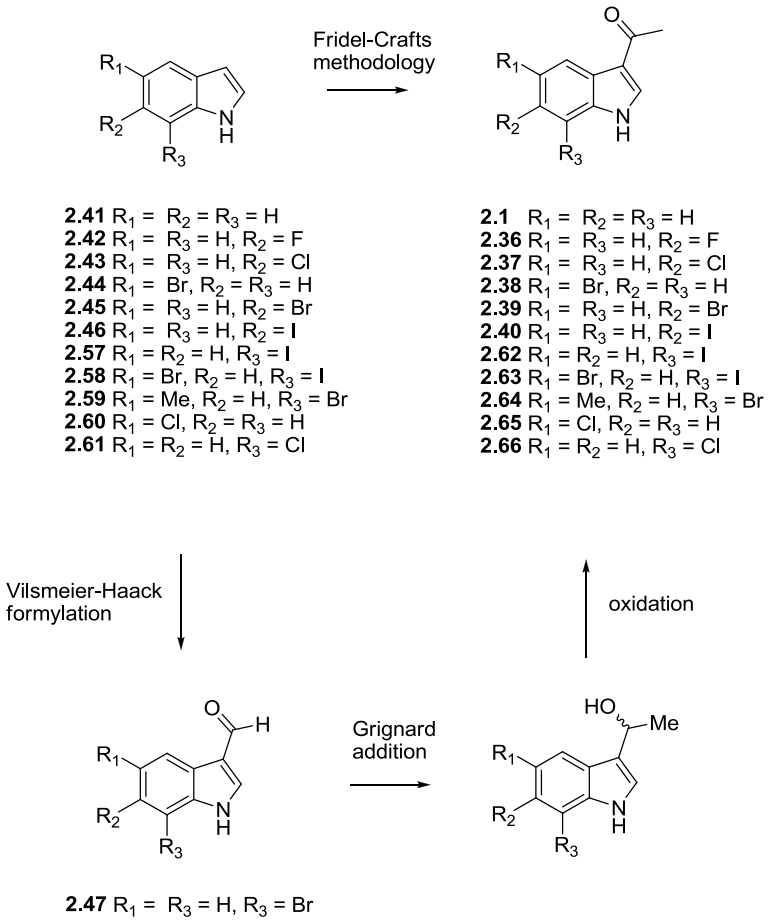

2.41 R_1 = R_2 = R_3 = H
2.42 R_1 = R_3 = H, R_2 = F
2.43 R_1 = R_3 = H, R_2 = Cl
2.44 R_1 = Br, R_2 = R_3 = H
2.45 R_1 = R_3 = H, R_2 = Br
2.46 R_1 = R_3 = H, R_2 = I
2.57 R_1 = R_2 = H, R_3 = I
2.58 R_1 = Br, R_2 = H, R_3 = I
2.59 R_1 = Me, R_2 = H, R_3 = Br
2.60 R_1 = Cl, R_2 = R_3 = H
2.61 R_1 = R_2 = H, R_3 = Cl

2.1 R_1 = R_2 = R_3 = H
2.36 R_1 = R_3 = H, R_2 = F
2.37 R_1 = R_3 = H, R_2 = Cl
2.38 R_1 = Br, R_2 = R_3 = H
2.39 R_1 = R_3 = H, R_2 = Br
2.40 R_1 = R_3 = H, R_2 = I
2.62 R_1 = R_2 = H, R_3 = I
2.63 R_1 = Br, R_2 = H, R_3 = I
2.64 R_1 = Me, R_2 = H, R_3 = Br
2.65 R_1 = Cl, R_2 = R_3 = H
2.66 R_1 = R_2 = H, R_3 = Cl

2.47 R_1 = R_3 = H, R_3 = Br

Scheme 2.19 Proposed synthetic procedures toward 3-acetylindoles

Based on the availability of starting materials we postulated that either of these two methods would deliver the desired 3-acetylindoles in acceptable yield. Theoretically 3-acylindoles e.g. 1-(6-bromo-1*H*-indol-3-yl)ethanone (**2.39**) can be accessed by Grignard methylation of indole-3-carbaldehydes such as **2.47** to afford a secondary alcohol intermediate, which on oxidation with a suitable mild oxidation agent e.g. either manganese dioxide, or *N*-morpholine oxide (NMO) would yield the desired methyl ketone.

To extrapolate this methodology to other non commercially available indole 3-carbaldehydes would require an initial standard Vilsmeier-Haack formylation of a suitably halogenated indole precursor, which we anticipated would occur regioselectively at C-3 on the indole ring.[112] Alternatively a Friedel-Crafts acylation would yield the desired products in a single step (**Scheme 2.19**). Both of these methods require strict exclusion of moisture under relatively harsh reaction conditions, while because of side reactions induced by the indole ring the Friedel-Crafts reaction often requires a prior *N*-protection strategy.[105,107,109–111]

Jiang *et al.* have recently developed a non Friedel-Crafts general method for the synthesis of non-protected 3-acylindoles via an efficient coupling of indoles and nitriles (**Scheme 2.20**).[110] This method was deemed unsuitable for our purposes since it relied upon palladium coupling, thereby potentially making the halogen substituents e.g. bromines susceptible to removal.

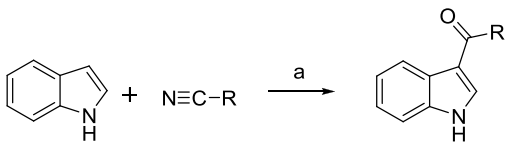

Scheme 2.20 Jiang *et al.*'s palladium catalysed indole acetylation[110]

a) $Pd(OAc)_2$, 2,2-Bipyridine, D-CSA, NMA, H_2O, 120 °C

2.4.3 Grignard methylation of indole-3-carbaldehydes

We initially explored the Grignard methodology as a route to the desired 1-(6-bromo-1*H*-indol-3-yl)ethanone (**2.39**) from the commercially available **2.47**. Both the Vilsmeier-Haack reaction and the Grignard reaction had previously been utilized in our lab to successfully synthesize a cohort of 2-deoxylapachol analogues which displayed selective activity against squamous cell esophageal cancer (**Scheme 2.21**)[113] and we were confident that we could repeat these reactions on suitably halogenated indole precursors.

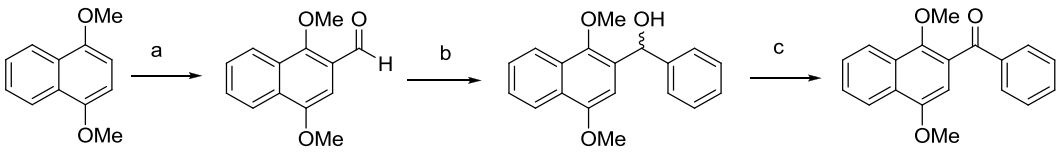

Scheme 2.21 Adpated from Sunassee *et al*.'s naphthoquinone synthesis[113]

a) $POCl_3$, DMF, $CHCl_3$, 96h, 91%; b) PhMgBr, THF, −10 °C,16h, 93%; c) NMO, TPAP, CH_2Cl_2, 2h quant

An initial trial reaction involving 4-bromobenzaldehyde (**2.50**) and Grignard reagent (MeMgBr) was successful (**Scheme 2.22**), yielding the secondary alcohol (**2.51**) (92%) with spectral data in accordance with those reported in the literature.[114]

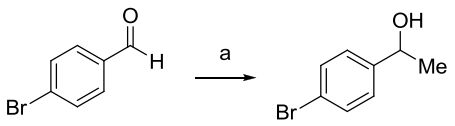

2.50 **2.51**

Scheme 2.22 Grignard methylation of 4-bromobenzaldehyde **2.50**

a) MeMgBr (3M), THF, 0 °C, 16h 92%

We then went on to apply the same Grignard methodology to 6-bromo-1*H*-indole -3-carbaldehyde **2.47**. Unfortunately, we were unable to repeat the success of the trial reaction. In every attempt at this reaction a large amount of starting material was recovered, while a ^{1}H NMR spectrum of the crude reaction mixture revealed characteristic quartet and doublet resonances corresponding to coupled methylene and methyl protons respectively, suggesting a small yield of desired product. The ^{1}H NMR spectrum also revealed a complex mixture of compounds including several aldehyde signals, possibly indicating reactivity at centres on the indole ring other than the electrophilic aldehyde. Szmuszkovicz[115] and Wang *et al.*[116] have previously noted that 3-acylindoles undergo a Michael type nucleophillic addition at C-2 on the indole ring with Grignard reagents to form disubstituted, partially dearomaticised indolines. Interestingly, the reaction procedure exhibits a degree of stereo control at C-2 depending on the quenching procedure.[116] Significantly, in all the examples presented by Wang *et al.*[116] the indole ring was *N*-alkylated and the C-3 acyl groups were ketones rather than aldehydes. However, what was encouraging and of relevance to what we had observed in the ^{1}H NMR analysis of the product mixture, was the presence of both the C-2 substituted indoline **2.52** and indolyl tertiary alcohol **2.53** synthesized from one of the least sterically hindered indolyl compounds subjected to Grignard addition (**Scheme 2.23**).[116]

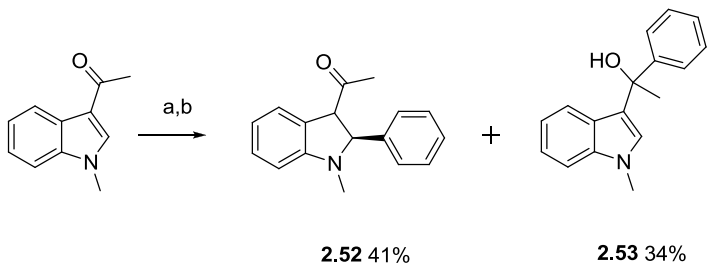

Scheme 2.23 Wang *et al.*'s Grignard reagent mediated Michael addition type synthesis of 2,3-disubstituted indolines[116]

a) PhMgBr, THF, 0 °C – r.t.; b) MeOH then Et_3N, 50 °C.

Therefore based on the results obtained by Wang *et al.* it seemed likely that indolines were amongst the side products formed in our Grignard addition reactions. We reasoned, however, that since the aldehyde is less sterically hindered than the methyl ketone, it theoretically should be a more viable centre for nucleophillic attack. We also postulated that if the reactivity of the aldehyde could be enhanced, we may be able to significantly reduce the possibility of indoline formation and increase the yield of our desired product. To this end we chose anhydrous cerium (III)chloride as an additive to improve the regioselectivity of Grignard methylation. Anhydrous cerium (III)chloride has been shown to significantly enhance Grignard addition to carbonyls whilst suppressing side reactions, even when substrates are susceptible to enolization or conjugate addition.[117–120]

Since there is some debate as to whether cerium activates the carbonyl group or creates a complex with the Grignard reagent, two methods are commonly used in which the cerium chloride is either stirred with the carbonyl compound for an hour before addition of the Grignard reagent or stirred with the Grignard reagent before addition of the carbonyl compound.[118,120] Unfortunately we were unable to achieve acceptable yields of **2.39** after several attempts at both methods, including additional efforts to exclude water co-ordinated to the cerium salt as detailed by Dimitrov *et al..*[118] Accordingly we were forced to abandon this procedure as a viable option for further synthesis of 3-acylindoles.

2.4.4 Friedel-Crafts approach to 3-acetylindoles

While the C-3 position is generally the most reactive site on the indole ring for electrophilic attack,[104] under Friedel-Crafts conditions, indole also becomes susceptible to 1-acylation, 1,3-diacylation, oligomerization and the formation of bis- and trisindole alkanes.[104,109] To reduce these side events, NH protected , or deactivated indole systems have been employed, limiting the structural variation available to synthesize a desired alkaloid.[104,109] Ottoni *et al.*[104] and more recently Guchhait *et al.*[109]

have developed high yielding Friedel-Crafts methods from a variety of acylating agents without the use of *N*-protection. Guichhait *et al.* made use of an interesting Lewis acid $ZrCl_4$ in anhydrous dichloroethane (DCE), while Ottoni *et al.* chose $SnCl_4$ in a DCM/$MeNO_2$ co-solvent system. Both methods claimed a high degree of chemo and regio-selectivity (**Scheme 2.24**).[104,109]

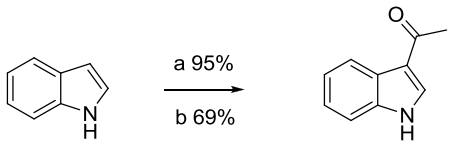

2.1

Scheme 2.24 Ottoni *et al*. (a) and Guchhait *et al*.'s (b) respective Friedel-Crafts acylation methods of NH free indoles[104,109]

a) Acetyl chloride, $SnCl_4$, DCM, $MeNO_2$, 2h,
b) Acetyl chloride, $ZrCl_4$, DCE, 3.5h

Although both Ottoni *et al.* and Guichhait *et al.* reported the synthesis of one of our target 3-acylindoles namely 1-(1*H*-indol-3-yl)ethanone **2.1**, neither group reported using their methodology to prepare the corresponding C-6 halogenated analogues. We chose to use the method of Ottoni *et al.* to prepare halogenated 3-acetylindoles because of easier access to reagents.

Ottoni *et al.* stressed the critical importance of adhering to a specific order for reagent addition. They also drew attention to the brightly coloured complexes formed upon addition of the Lewis acid to a solution of indole in DCM. The appearance of a brightly coloured complex was the signal for the further addition of the acylating agent in nitromethane. The latter solvent was critical for complex solubility, and reportedly greatly improved the reaction time and product yields.[104] Ottoni *et al.* refer to a paper published by Schmitz-Dumont and Motzkus in 1929[121] which suggests the formation of addition complexes between indole and $SnCl_4$ with a stochiometry of $SnCl_4.2C_8H_7N$. While Ottoni *et al.* were unable to isolate this addition complex, citing solubility and stability issues, they noted that

their coloured complexes share the same "physical properties" as those reported in 1929 (details of which physical properties, apart from colour, were not provided).[104] Ottoni *et al.* also provide a putative acylation mechanism in which they propose that the Lewis acid complexes at the reactive C-3 position in the indole ring, forming a polar intermediate (**2.54**) which is insoluble in non polar solvents.

The insolubility of the complex apparently justifies the addition of $MeNO_2$ which Ottoni *et al.* suggests may help dissolve **2.54** to enable further reaction with the acylating agent (**Scheme 2.25**). In support of their mechanism they further postulate that formation of this addition complex would inhibit indole oligomerization prior to addition of the acylating agent.[104]

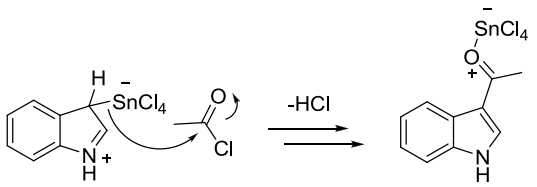

2.54

Scheme 2.25 Ottoni *et al.*'s proposed Friedel-Crafts Mechanism[104]

We repeated the method of Ottoni *et al.* initially on indoles **2.41—2.44** and similarly to Ottoni *et al.* we also obtained brightly coloured suspensions before the addition of acylating agent (**Figure 2.1**). TLC and ^{1}H NMR spectra of the crude product mixtures suggested that the reactions were successful. However, purification of these compounds proved to be challenging, with low product solubility hampering column chromatography. Traditional re-crystallization from a number of hot solvents only afforded the target compounds in low yield and purity.

Figure 2.1 Brightly coloured indole—$SnCl_4$ complexes formed before addition of acylating agent. Indoles from left **2.42, 2.43, 2.44** and **2.41.**

After our effort to locate a Friedel-Crafts methodology not requiring *N*-protection, it was with a degree of irony that SeO_2 studies conducted on the commercially available **2.1** required an *N*-Boc protection strategy to deactivate the system and prevent over oxidation to glyoxylic acid (this will be discussed later). To this end we successfully attempted *N*-Boc protection of the crude product mixture of **2.36**, which was re-crystallized from MeOH to deliver carbamate (**2.55**) in a 40% yield over two steps (**Scheme 2.26**). The downfield region of the ^{1}H NMR spectrum of re-crystallized **2.55** is presented in **Figure 2.2**

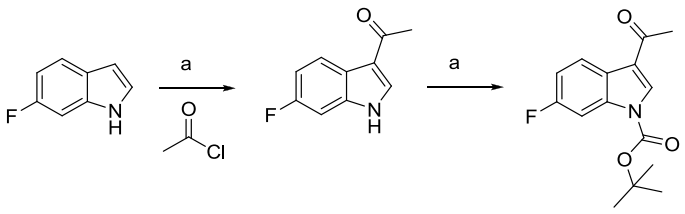

2.42 **2.36** (crude) **2.55** 42%

Scheme 2.26 Synthesis of *N*-boc protectd 6-fluoro-3-acetylindole **2.55**

a) $SnCl_4$, DCM, $MeNO_3$, 0 °C – r.t. 2h, Ar gas b) Boc_2O, DMAP, MeCN, 0 °C – r.t. 2h, Ar gas.

Based on this result, and precedent with regard to *N*-protection before Friedel-Crafts acylations, we attempted an acetylation on *N*-Boc protected indole (**2.56**) which had been prepared in a yield of 94%. (**Scheme 2.27**) Unfortunately this method was unsuccessful, we suspect due to the electron withdrawing nature of the *N*-Boc protecting group, deactivating the ring towards C-3 electrophilic attack.

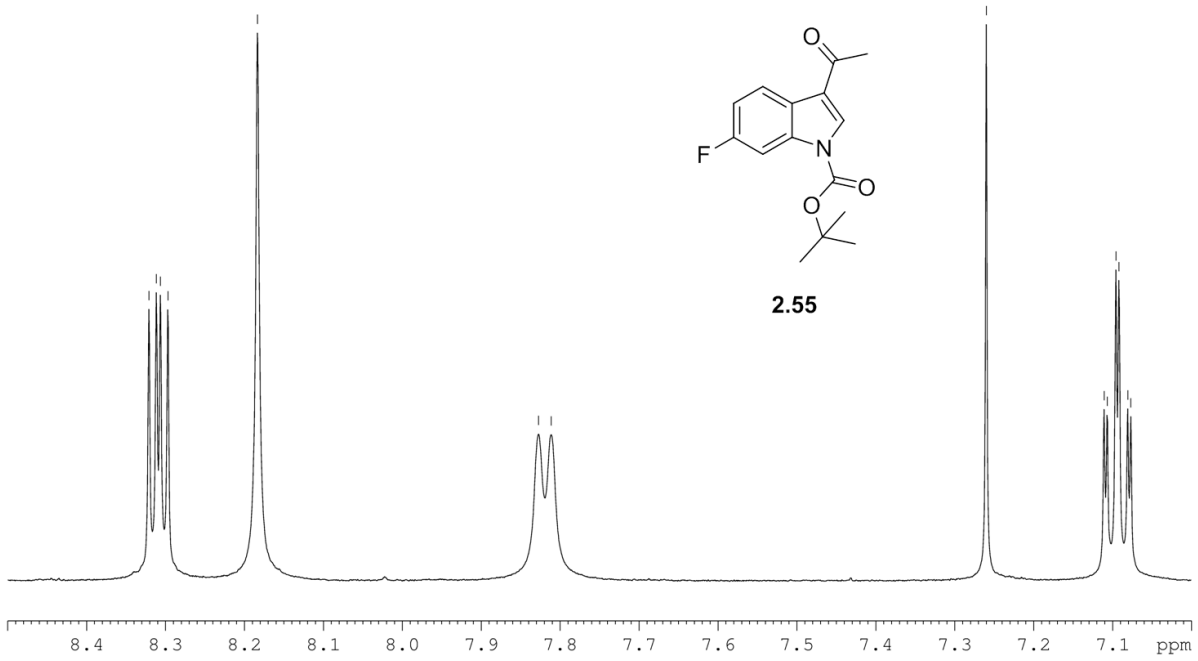

Figure 2.2 Downfield region (δ_H7— δ_H8.5) of the ^{1}H NMR spectrum (600MHz, $CDCl_3$) of **2.55.** The complex splitting pattern is a result of proton-fluorine coupling.

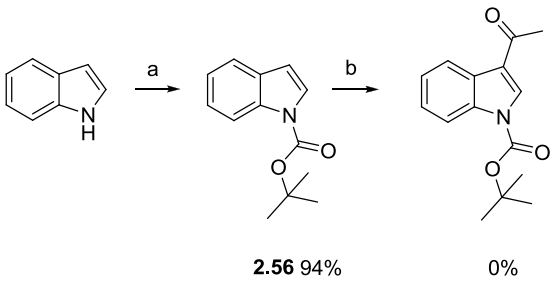

2.56 94% 0%

Scheme 2.27 Attempted acylation after *N*-Boc protection

a) Boc_2O, DMAP, MeCN, 0 °C – r.t. 2h, Ar gas b) Acetyl chloride, $SnCl_4$, DCM, $MeNO_2$, 0 °C – r.t. 2h, Ar gas

Serendipitously, the solid reaction product mixtures were all soluble in cold acetone and we were finally able to obtain pure (by ^{1}H NMR spectroscopy) halogenated 3-acetylindoles, via crystallization resulting from slow evaporation of the acetone solutions followed by the removal of impurities by washing the crystalline products with cold chloroform. This acetylation and purification method was subsequently applied to a cohort of commercially available indoles (**2.42—2.44, 2.57—2.61**), in addition to synthetically derived 6-iodoindole (**2.46**) as well as 6-bromo indole (**2.45**), (which had become commercially available in the interim in small 50 mg quantities). Yields however were not as high as those reported by Ottoni *et al.*[104] but more in line with that seen by Guichhait *et al.*.[109] Inspection of the respective yields does not point to any obvious trend (**Table 2.1**). It seems likely that yields are a function of the purification method, where some halogenated 3-acetylindoles compounds may be more soluble in the cold chloroform which was used to wash the crystals. We deemed the yields of our halogenated 3-acetylindoles to be adequate for us to proceed with the synthesis of our desired bisindole imidazole target compounds. It must be noted because of time constraints that it was not possible to take all ten of the 3-acetylindoles (**2.36—2.40, 2.62—2.66**) we prepared by Ottoni at al.'s method through to the respective bisindole imidazoles. We proceeded only with compounds **2.1, 2.36—2.40** and **2.66.**

Compound Number	Isolated Yield
2.36	56%
2.37	72%
2.38	72%
2.39	63%
2.40	64%
2.62	54%
2.63	86%
2.64	75%
2.65	65%
2.66	63%

Table 2.1 Yields of 3-acetylindoles from slow evaporation of acetone solutions of the reaction product mixtures.

2.4.5 Synthetic approaches to 6-iodoindole (2.46)

Since **2.46** was not commercially available, we were forced to explore synthetic strategies to deliver this iodinated indole. The first approach which we considered was a direct iodination. However, because molecular iodine does not share the electrophilic polarizability of bromine, It is therefore necessary to incorporate strong oxidizing agents or Lewis acids in conjunction with the iodine source, to assist direct iodination in aromatic systems.[122–124] The most commonly studied direct iodination methods involve simple six membered rings where the position on the ring targeted for iodine insertion are heavily dependent on the distribution of ring activators or deactivators.[122–124] This was a concern in our case with respect to regioselectivity, and the nucleophillic nature of the indole C-3 position and to a lesser extent C-2 position. Lista *et al.*[122] were able to achieve iodination of 5-nitroindole at the indole C-3 position, while Mongin and co-workers[125] were able to directly iodinate *N*-Boc protected indole at the C-2 position (**Scheme 2.28**). Our requirement for iodination was at the C-6 position and direct iodination was accordingly considered unsuitable.

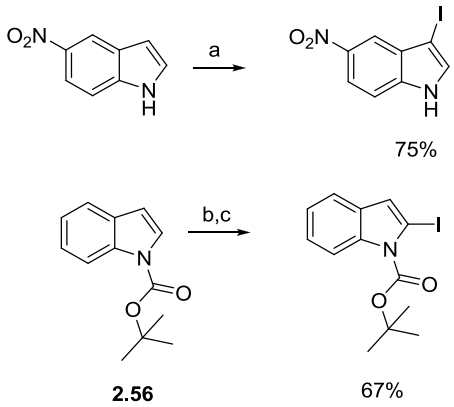

Scheme 2.28 Direct iodination of indole by Lista *et al.*[122] (top) and Mongin and co-workers[125] (bottom)

a) $NaClO_2$, NaI, H_2O, HCl r.t. 30min;
b) $ZnCl_2$•TMEDA, LTMP, THF, r.t. 2h; c) I_2

In an effort to produce potent cannabinoid agonists of the CB1 receptor as radioiodine brain imaging agents Deng *et al.*[126] developed a method of synthesizing *N*-(methylpiperidine-2-ylmethyl)-6-iodo-3-acylindole **2.67** from 6-nitroindole (**2.68**), introducing iodine through a classical nitro group reduction followed by diazotization and N_2 substitution with iodide (**Scheme 2.29**).

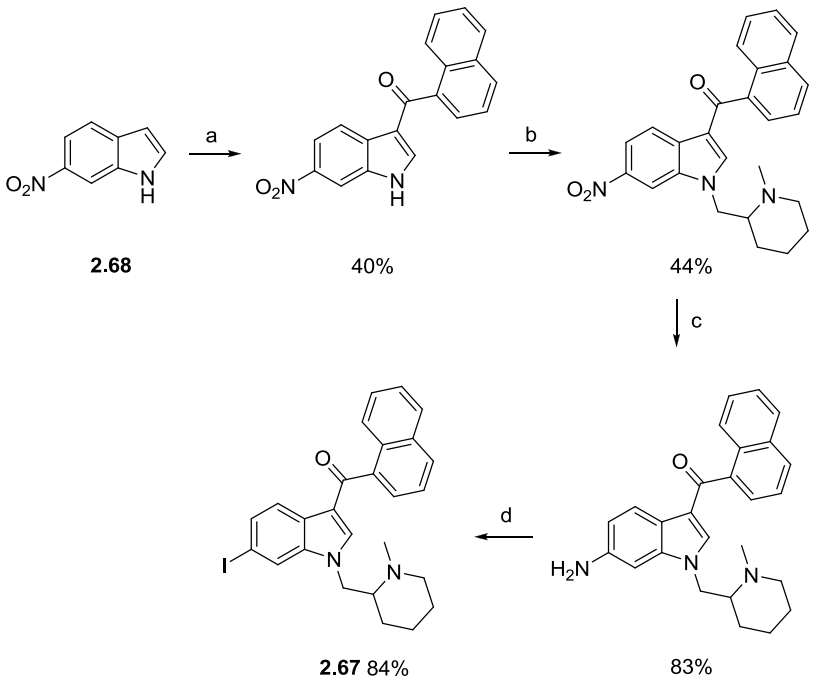

Scheme 2.29 Deng *et al.*'s synthesis of **2.67**[126]

a) MeMgBr, Et_2O, 0 °C, 15 min, Zinc Chloride, 30 min, 1-naphthoyl chloride, 2h; b) NaH, DMF, 2-chloromethyl-1-methyl-piperidine, 60–70 °C, overnight; c) hydrazine, EtOH, Raney Ni, 2h; d) HCl, 1h, $NaNO_2$, 0 °C, 1h, KI.

Similarly Irie *et al.*[127] had used a diazotization approach on non protected amino indole **2.69** in synthesizing 6-iodo indolactam precursor **2.70** (**Scheme 2.30**). We initially attempted the method of Irie *et al.* on commercially available 6-aminoindole without success.

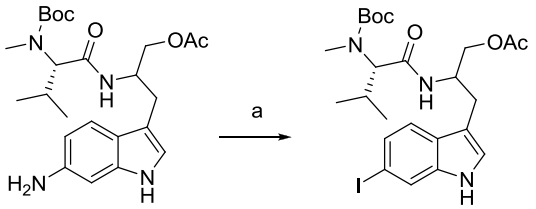

Scheme 2.30 Irie *et al.*'s diazotization of 6-aminoindole[127]

a) $NaNO_2$, H_2O, 80% AcOH, KI, Na_2SO_3.

In light of our failure to repeat Irie *et al.*'s method and the non availability of **2.68**, several indole synthesis methods were considered to obtain 6-nitro or iodoindole from available starting materials. Moskalev and Makosza[128] had described a method of obtaining nitro-indoles from condensation of 3-nitroaniline (**2.71**) and various ketones (**Scheme 2.31**). However they noted that the 4-nitro derivative **2.72** was the major product, while the 6-nitro derivative **2.73** was often isolated in yields lower than 1%.[128]

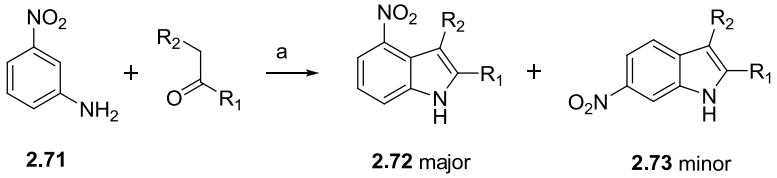

Scheme 2.31 Moskalev and Makosza's synthesis of nitroindole[128]

a) *t*-BuOK, DMSO, 3-5h.

The Bartoli reaction (**Scheme 2.32**) was suggested as a method of obtaining 6-iodoindole directly, and interestingly had previously been used in the synthesis of marine bisindoles[99,129] We ultimately

considered this method unsuitable, as it generally favours formation of C-7-substituted indoles over the required C-6 substituted indoles.[130]

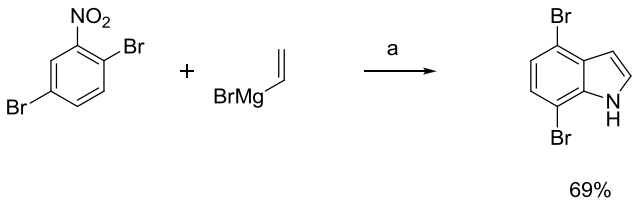

Scheme 2.32 Dobbs *et al*.'s application of the Bartoli reaction[130]

a) THF, -40 °C

Hodgkinson *et al.*[131] developed an interesting tandem copper catalyzed bond formation between aryl and alkenyl halides to yield *N*-Boc protected indoles[131] (**Scheme 2.33**). Since our needs required acetylation prior to *N*-Boc protection this method was considered unsuitable.

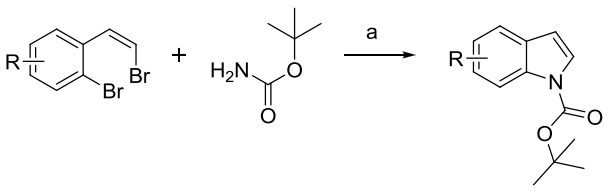

Scheme 2.33 Hodgkinson *et al*.'s synthesis of *N*-protected indole[131]

a) $CuOAc$, K_2CO_3, *N,N'*-dimethylethyldiamine, toluene, 110 °C, 24h.

McAusland *et al.*[132] developed an interesting variation of the Fischer-indole synthesis, whereby they formed benzyne *in situ* which was subsequently cyclized with *N*-tosylhydrazones to yield tosylated indole (**Scheme 2.34**).[132] Tosylation seemingly does not negatively affect Friedel-Crafts acylation,[133] but unfortunately this synthesis delivers an unwanted substituent at indole position 2.[132]

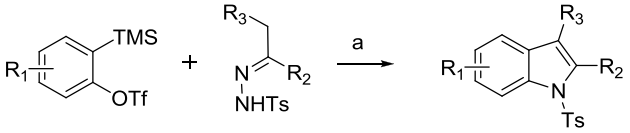

Scheme 2.34 McAusland *et al*.'s synthesis of *N*-tosylated indoles[132]

a) CsF, MeCN, r.t. 12h; b) BF_3OEt_2, reflux, 5h

Ottoni *et al.*[134] reported a regioselective nitration of **2.1**, with NO_2BF_4, in which careful control of reaction temperature will result in nitration at either indole position 5 or 6 (**Scheme 2.35**).[134] Unfortunately we accidentally overlooked this potentially high yielding one step transformation which regrettably only came to light once we had prepared **2.46** by another circuitous route adapted from Yamada *et al.*[135] starting from the commercially available 6-nitroindoline (**2.74**) (**Scheme 2.36**).

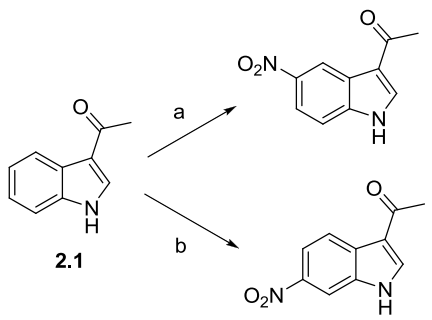

Scheme 2.35 Ottoni *et al*.'s nitration of 3-acetylindole[134]

a) NO_2BF_4, $SnCl_4$, $(CH_2Cl)_2$, $MeNO_2$ -15 – -10 °C 85%;
b) NO_2BF_4, $SnCl_4$, $CHCl_3$, $MeNO_2$ 60 °C, 85%.

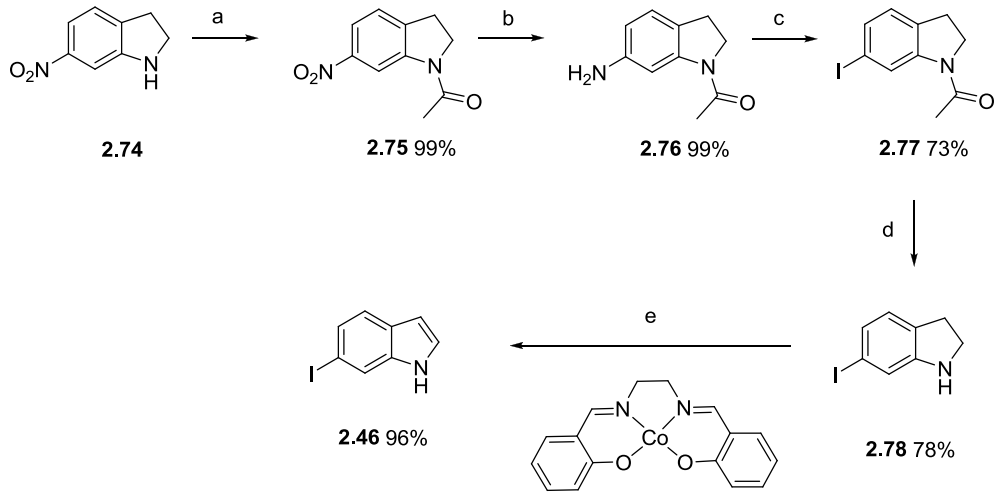

Scheme 2.36 Synthetic method to obtain 6-iodoindole adapted from Yamada *et al.*[135] and Deng *et al*.[126]

a) Ac_2O, pyridine; b) H_2/Pd, MeOH quant; c) 80% AcOH, $NaNO_2$, H_2O, sulfamic acid, KI, 4h. d) 20% NaOH aq., MeOH; e) salcomine, O_2, MeOH, 3h.

2.4.6 Synthesis of 6-Iodoindole from 6-nitroindoline

Acetylation of the basic indoline NH in acetic anhydride and pyridine yielded *N*-acetylated 6-nitroindoline (**2.75**) followed by a relatively straight forward Pd/C catalyzed reduction to yield the 6-amino derivative (**2.76**). Interestingly small baseline signals were continuously observed in the ^{1}H NMR spectrum of **2.76** with a ratio (0.13:1) from proton integrations when compared to the comparable NMR signals for **2.76**. Initially we thought that we had encountered an inseparable contaminant. However, analysis of the EXSY NMR spectrum[136] acquired for **2.76** (**Figure 2.3**) revealed the presence of two species of the same compound, which we deduced were most likely rotamers. EXSY NMR reveals correlations between protons in the same position in the same chemical structure, but in different chemical environments, as would be expected with rotamers. Correlated signals from rotamers will appear in the same phase, in contrast to correlated signals in a NOESY NMR spectrum, where NOESY correlations occur in an opposite phase relative to one another.[137]

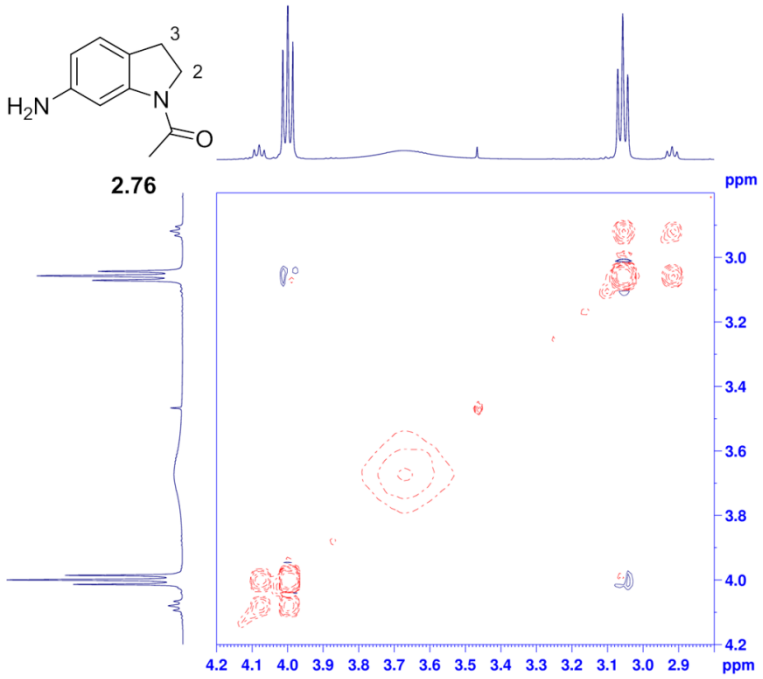

Figure 2.3 Upfield region (F1, F2 = δ_H 2.8 — 4.2) of the EXSY spectrum of **2.76** (600MHz $CDCl_3$; relaxation time [d1 = 2.00 s; EXSY mixing time [d8] = 0.449 s) showing signals corresponding to H-2 and H-3 of compound **2.75**. Correlations in the same phase highlighted in red correspond to the same proton in two separate chemical environments, as is the case with rotamers.

The critical diazotization step to yield **2.77** was initially carried out as per the method of Yamada *et al.*.[135] While Yamada *et al.* recorded a yield of 62%, our attempts at this reaction yielded a disappointing 29% yield. The diazotization process of Deng *et al.*[126] required the addition of sulfamic acid before KI until the reaction solution no longer turns starch-KI paper blue.[126] KI-starch paper is a commonly used method for the detection of strong oxidizing agents such as nitrite. KI oxidation leads to the formation of I_2 which turns the starch blue and further renders KI unavailable for reaction. Sulfamic acid is a commonly used industrial chemical with wide applications including the removal of excess nitrite used in diazotization reactions in the textile industry.[138,139] Due to the formation of diatomic iodine in the starch-KI paper test, excess nitrite is presumably detrimental to the nucleophillic iodide species required for N_2 substitution. The presence of nitrite species is limited with the addition of sulfamic acid. To ensure sufficient iodide was present for N_2 substitution, the equivalence of KI was increased from 1.1 eq. to 3 in addition to the use of sulfamic acid. Gratifyingly we were able to dramatically increase the yield of **2.77** to an acceptable 73% (**Figure 2.4**).

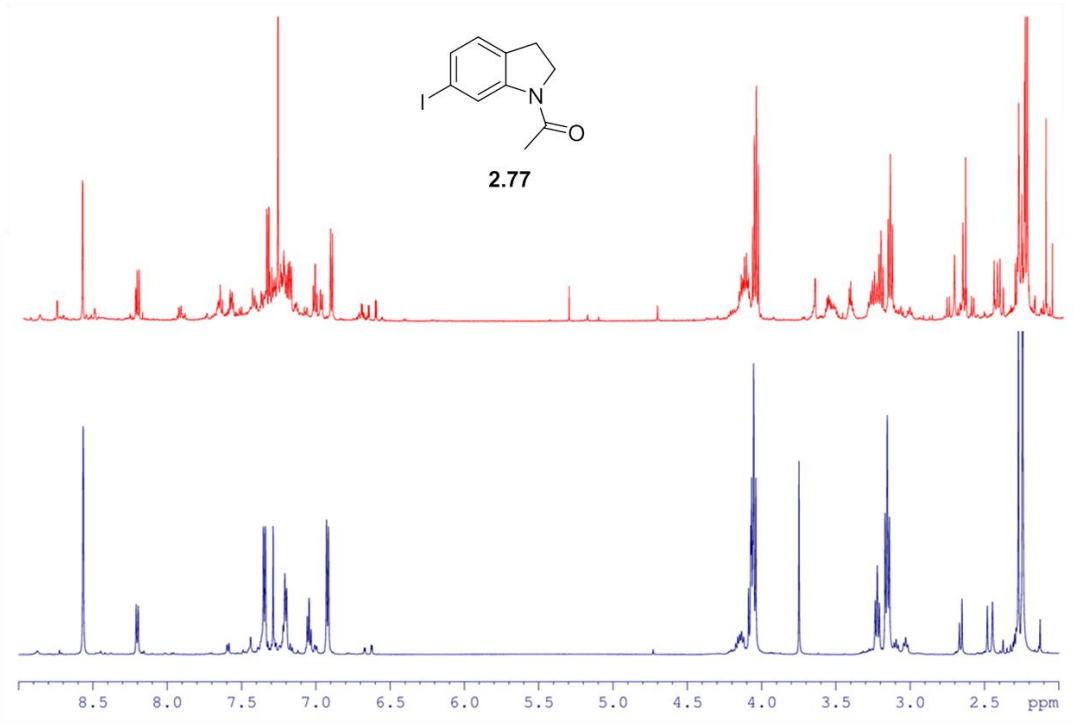

Figure 2.4 Comparative ^{1}H NMR spectra (600 MHz $CDCl_3$) of crude reaction mixtures for compound **2.77** without the use of sulfamic acid (top) and with sulfamic acid (bottom) resulting in a 'cleaner spectrum', presumably due to fewer side reaction occurring.

De-acetylation to form 6-iodoindoline **2.78** occurred in NaOH (78% yield) which was followed by oxidation, catalyzed by the cobalt—Schiff base complex salcomine[140] delivering the desired 6-iodo indole **2.46** in 96% yield and enabled us to have sufficient **2.46** (**Figure 2.5**) to feed into the synthetic pipeline with the other halogenated indoles.

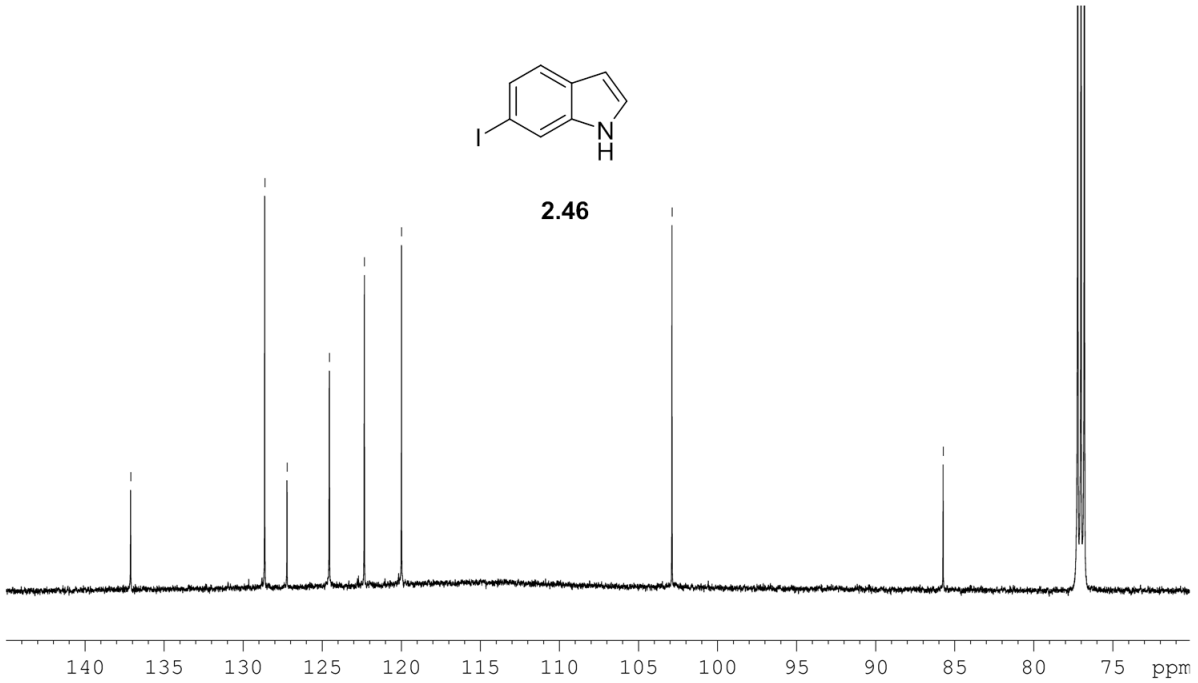

Figure 2.5 ^{13}C NMR (150 MHz $CDCl_3$) of compound **2.46** featuring the characteristic C—I signal at 85.7 ppm.

2.4.7 Summary

A key requirement of our proposed synthetic strategy was the availability of variably halogenated 3-acetylindoles. After several unsuccessful attempts at Grignard methylation of indole 3-carbaldehyde with and without the use of cerium chloride, as well as difficulties purifying Friedel-Crafts products, we were finally able to produce the desired products in acceptable yields. Additionally we were able to produce the rare 6-iodoindole over five steps in an overall acceptable yield, while encouragingly being able to improve yields in the diazotization step helped in part by adding sulfamic acid. With all

of our desired compounds in hand we were able to proceed confidently with the next step in our proposed synthetic strategy.

2.5 Selenium dioxide oxidation of 3-acetylindoles

2.5.1 Selenium dioxide oxidation of acetophenone derivatives

Marchand *et al.*[100] developed a method of synthesizing phenyl glyoxal from acetophenone via SeO_2 oxidation in 1,4-dioxane and water. This method was later modified by Young *et al.*[101] in our laboratory who utilized microwave methodology to dramatically increase yields and reduce reaction time. Young *et al.* successfully applied their method to variably substituted acetophenones (**Scheme 2.17**) where they showed that the ring activating and deactivating nature of the aromatic substituents had a significant effect on the rate of glyoxal formation.[94,101] Aryl glyoxals have been noted on numerous occasions to exist in the monohydrate form, either completely, or in equilibrium with the glyoxal species.[100,101,141] Selenium dioxide oxidations rely on the presence of stochiometric amounts of water to be present for the reaction to occur. This water acts as a nucleophile and attacks the highly reactive aldehyde, to yield the monohydrate. Young *et al.*[101] showed that this is a completely reversible reaction, in which monohydrate will revert back to an equilibrium mixture with the glyoxal upon standing in non-aqueous media.[101]

2.5.2 Attempted SeO_2 oxidation of 3-acetylindoles: requirement of *N*-Boc protection

When Young applied his microwave assisted selenium dioxide oxidation method[101] to the oxidation of 3-acetylindole **2.1**[94] he noted the methyl ketone functionality over oxidized to indolyl-3-glyoxylic acid (**2.79**)(**Scheme 2.37**), the structure of which was confirmed by NMR spectroscopy and HRMS.[94]

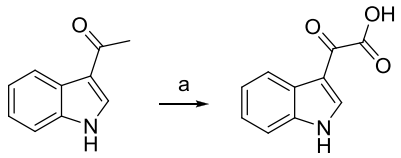

2.1 **2.79**

Scheme 2.37 Young's microwave assisted formation of **2.79**[94]

a) SeO_2, H_2O, 1,4-dioxane, MWI, 15 min 100 °C

Since they had shown a direct relationship between the activity of the aromatic ring and the rate of glyoxal formation[94,101] Young deduced that the influence of the indole nitrogen on the activity of the ring could be reduced through formation of an *N*-Boc carbamate ester (**2.80**).[94] This insight proved to be correct with the subsequent formation of an equilibrium mixture of glyoxal **2.81** and monohydrate **2.82** using 2.7 eq. of SeO_2 with 20 µl of water in 1 ml of dioxane (**Scheme 2.38**).

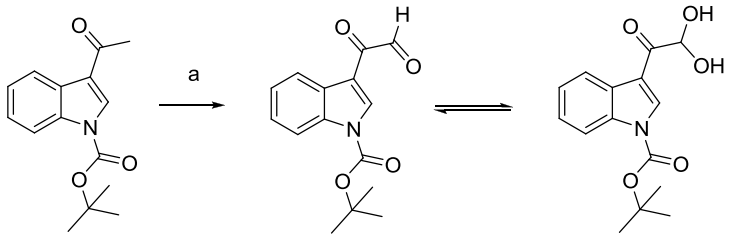

2.80 **2.81** **2.82**

Scheme 2.38 Young's microwave assisted formation of **2.81**[94]

a) SeO_2, H_2O, 1,4-dioxane, MWI, 40 min 100 °C

2.5.3 *N*-Boc protection of 3-acetylindoles

Boc protection occurred under anhydrous conditions, in HPLC grade acetonitrile, catalyzed by DMAP and under an atmosphere of argon at 0 °C. We have previously shown (**2.4.4**) that *N*-Boc protection

of indole was readily achieved on both non acetylated indole (**Scheme 2.27**), as well as crude 6-fluoro-3-acetylindole (**Scheme 2.26**). Accordingly, Boc protection of pure 3-acetylindoles (**2.1, 2.36—2.40, 2.66**) proceeded smoothly in high yield, delivering compounds **2.55, 2.80, 2.83—2.86** (**Scheme 2.39**). The one exception was the 7-chloro derivative (**2.87,** 20% yield), where presumably the close proximity of the C-7 chloro substituent inhibited Boc protection at the neighbouring N-1 position.

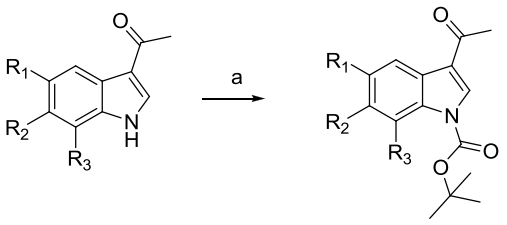

2.1 $R_1 = R_2 = R_3 = H$
2.36 $R_1 = R_3 = H$, $R_2 = F$
2.37 $R_1 = R_3 = H$, $R_2 = Cl$
2.38 $R_1 = Br$, $R_2 = R_3 = H$
2.39 $R_1 = R_3 = H$, $R_2 = Br$
2.40 $R_1 = R_3 = H$, $R_2 = I$
2.66 $R_1 = R_2 = H$, $R_3 = Cl$

2.80 $R_1 = R_2 = R_3 = H$ 96%
2.55 $R_1 = R_3 = H$, $R_2 = F$ 84%
2.83 $R_1 = R_3 = H$, $R_2 = Cl$ 94%
2.84 $R_1 = Br$, $R_2 = R_3 = H$ 65%
2.85 $R_1 = R_3 = H$, $R_2 = Br$ 67%
2.86 $R_1 = R_3 = H$, $R_2 = I$ 82%
2.87 $R_1 = R_2 = H$, $R_3 = Cl$ 20%

Scheme 2.39 *N*-Boc protection of purified 3-acylindoles

a) Boc_2O, DMAP, MeCN, 0 °C, 2h

2.5.4 Optimization of SeO_2 oxidation of *N*-Boc protected 3-acetylindoles and imidazole formation

Initial efforts to repeat Young's microwave assisted SeO_2 oxidation method (**Scheme 2.38**) proved difficult with yields of products obtained via the microwave displaying a high degree of variability. ^1H NMR spectroscopy of the crude reaction mixture revealed the expected glyoxal monohydrate equilibrium in addition to a mix of products, including the starting material, and a second aldehyde signal, which we suspected was a glyoxal species, where the Boc group had been removed. This observation provided us with a difficult problem to overcome, since the Boc group was critical to prevention of over-oxidation. Boc protecting groups are used widely in organic synthesis due to

their perceived resistance to catalytic hydrolysis and basic hydrolysis.[142,143] While generally Boc deprotection is achieved under acidic conditions, Boc deprotection has also been shown to occur under mildly basic conditions[56,143,58] as well as thermolytically[145] and in water.[146] Since our synthetic procedure required the presence of water, with the likely formation of selenous acid, at high temperature, in the microwave, in addition to possible Lewis acid like selenium dioxide by-products, we decided to explore methods to prevent this spurious deprotection during microwave mediated SeO_2 oxidation. We conducted two trial experiments in the microwave reactor at 100 °C and 150 °C (1 min ramp time, 40 min hold time, 250 W) respectively without introducing the oxidizing agent, and found that while partial deprotection occurred at 150 °C, at the lower temperature of 100 °C the Boc group was completely intact after 40 minutes, suggesting that neither the heat nor water were responsible for Boc removal, nor any other form of degradation.

We then attempted to reduce the possible influence of reduced species of selenium. Sharpless and co-workers[147] in their seminal contribution to selenium dioxide chemistry referred to the complications introduced into organic reactions by reduced selenium species. Not only do these reduced selenium species prove difficult to remove from the organic products, but they also form organo-selenium by-products, e.g. instances have been noted where addition across an olefinic double bond by an electrophilic Se (II) species have occurred.[147] In an effort to remove spurious selenium contaminants, SeO_2 was used immediately, after purification by sublimation (**Figure 2.6**).

In an attempt to further negate the influence of reduced selenium we attempted to employ the use of an additional oxidizing agent *tert*-butyl hydroperoxide (TBHP) as per the method of Umbreit and Sharpless.[147] They hypothesized that an additional oxidant would selectively and rapidly oxidize reduced selenium back into reactive SeO_2, thus minimizing the amount of reduced selenium available for side reactions.[147] Umbreit and Sharpless.[147] were able to show that olefins were oxidized to allylic alcohols using stochiometric, or in some instances catalytic amounts of SeO_2 with the addition of 90% TBHP in non-coordinating solvents such as DCM. The yields achieved were

Figure 2.6 Freshly sublimed SeO_2 after heating to over 315 °C in a sand bath, under a positive pressure of argon gas and crystallized on a cold finger.

significantly better than those achieved with stochiometric amounts of SeO_2 alone.[147] TBHP has also been used in conjunction with other catalytic oxidizing agents such as MnO_2[148] and the glutathiamine peroxidase mimic ebselen [2-phenyl-1, 2-benzisoselenazol-3(2H)-one][149] with positive results.

To add to our frustration with the inconsistent results obtained from SeO_2 oxidation experiments carried out in our microwave, we were also concerned about the use of peroxides e.g. TBHP in the microwave reactor and we decided to carry out further SeO_2 oxidation experiments under normal laboratory conditions.

We had found throughout the course of our selenium dioxide experiments that purification of the glyoxal products was difficult. Even when using semi-preparative HPLC, we found that the equilibrium mixture of the glyoxal and monohydrate streaked on the HPLC column, appearing as a large broad poorly resolved peak, with a sharp peak corresponding to unreacted methyl ketone appearing in the centre and on top of this broad peak region. For this reason, we decided to forego purification of the glyoxals and cyclize the glyoxals as crude reaction mixtures, after which they would be purified, and yields determined over two steps. As a superficial measure of glyoxal

formation, the ratio of proton integrations of relevant NMR signals were assessed to tentatively determine relative conversion, and proportions of each species present (**Figure 2.7**).

In total four TBHP experiments were conducted in which 3 equivalents of TBHP (70%), 7 equivalents of water, and stochiometric amounts of SeO_2 were reacted with **2.80** for varying lengths of time initially in DCM and later in 1,4-dioxane. Minimal conversion was observed in DCM and we concluded that either stirring at room temperature or the low temperature reflux of DCM was not hot enough to induce oxidation. Changing to the literature standard 1,4-dioxane, at reflux and slightly cooler heating conditions (75 °C) resulted in no change to the starting material. It was unclear whether the TBHP or low SeO_2 concentration was hindering the reaction, at which point we decided not to continue with the use of TBHP.

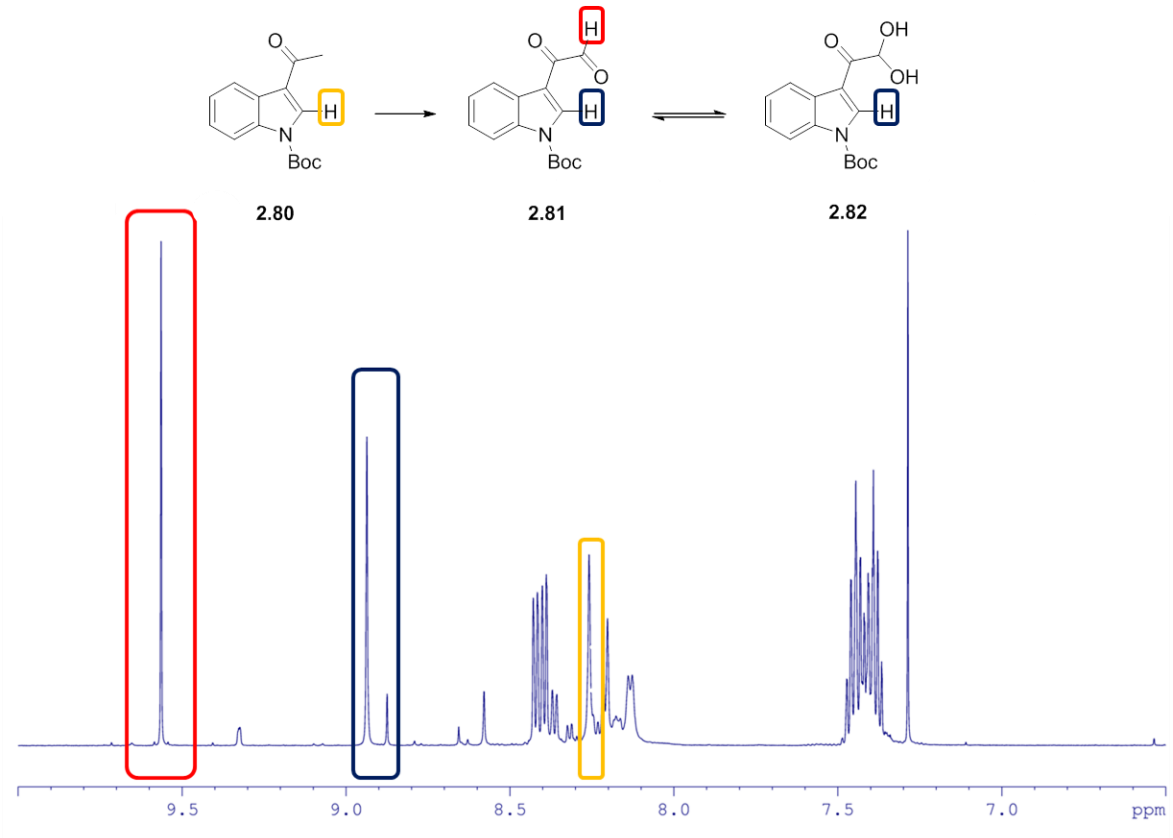

Figure 2.7 Downfield region (δ_H6.5—δ_H10) of an example ^{1}H NMR spectrum (600MHz, $CDCl_3$) of an optimized crude reaction mixture after SeO_2 oxidation of **2.80**. Highlighted are the signals used to determine relative conversion from ketone to glyoxal.

We then attempted several experiments to determine the importance of the relative equivalence of SeO_2 and water as well as the role of temperature and reaction times in the SeO_2 oxidation of **2.80** in 1,4-dioxane. At an SeO_2 equivalence of 2.7 eq. with 7 eq. of water in the microwave at 100 °C (1 min ramp time, 40 min hold time, 250 W), or with traditional mode of heating at reflux (ca. 100 °C) or controlled heating at 75 °C there seemed to be little difference between the relative conversion of methyl ketone into glyoxal/monohydrate. Interestingly we noticed that in reactions carried out in the microwave and at the higher reflux temperature of 100 °C, a precipitate of black selenium was observed, while when heating to 75 °C a blood red precipitate of selenium formed preferentially. While ^{1}H NMR analysis of the crude reaction mixtures of the three experiments revealed that under standard reflux conditions, several unidentifiable side products were forming, while at the lower temperature, these were significantly reduced (**Figure 2.8**)

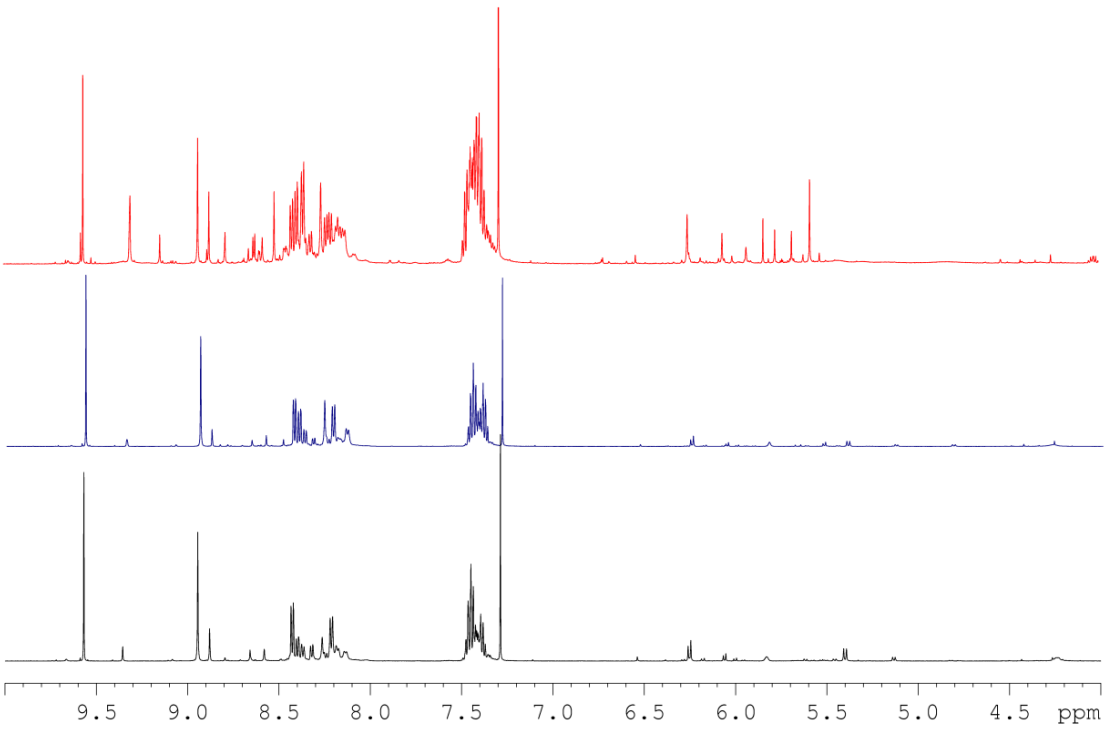

Figure 2.8 Comparison of the selected region (δ_H4—δ_H10) ^{1}H NMR spectra (600 MHz, $CDCl_3$), of the crude reaction mixtures from the SeO_2 oxidation of **2.80** carried out under reflux (top), heating at 75 °C (middle), and in the microwave reactor (1 min Ramp time, 40 min hold time, 250 W)(bottom).

While little difference was observed between the three experiments, with regard to relative conversion from tenuous NMR spectral analysis, ultimately, reaction success was assessed by measuring the yields from imidazole formation and recoverability of **2.80.** Accordingly the crude glyoxal product mixtures were dehydratively cyclized with 5eq. ammonium acetate in ethanol at room temperature as per the methods of Khalili *et al.*[93] and Young[94] to yield a bright yellow mixture which was easily purified by bench top silica chromatography (5:1 hexane: EtOAc) to yield the Boc protected deoxytopsentin (**2.88**) and the starting methyl ketone (**2.80**). We assumed that the condensation reaction would be consistent, and not vary significantly in yield over two steps.

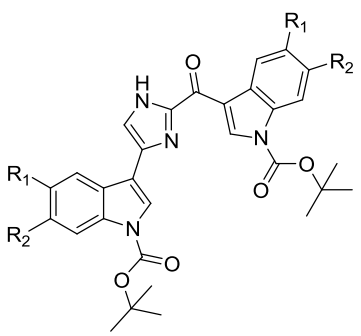

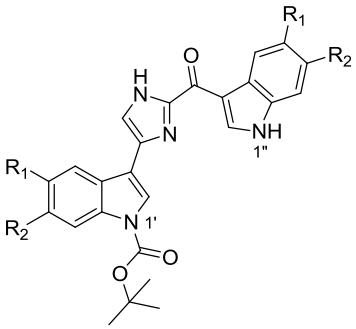

2.88 $R_1 = R_2 = H$
2.90 $R_1 = H$, $R_2 = F$
2.91 $R_1 = H$, $R_2 = Cl$
2.92 $R_1 = Br$, $R_2 = H$
2.102 $R_1 = H$, $R_2 = I$
2.103 $R_1 = H$, $R_2 = Br$

2.89 $R_1 = R_2 = H$
2.93 $R_1 = H$, $R_2 = F$
2.94 $R_1 = H$, $R_2 = Cl$
2.95 $R_1 = Br$, $R_2 = H$

The harsher conditions inflicted during reflux resulted in a similar yield to the less harsh reaction at 75 °C, but resulted in a low recovery of **2.80** while the microwave at 100 °C produced a higher yield and also unsurprisingly a lower recovery of starting material. This raised an interesting question about reaction time vs. temperature, but ultimately we felt that due to the less harsh conditions offered by reflux at 75 °C in addition to a high degree of variability observed with previous attempts of this reaction in the microwave reactor, that we would conduct experiments at a constant

temperature of 75 °C to compare the effects of other variables on yields from the experiments (**Table 2.2**).

Solvent	SeO_2	TBHP	H_2O	Temp	Time	% conversion by NMR	% Yield 2.88 over 2 steps	Recovered 2.80	% Yield 2.89
DCM	0.5eq	3eq	7eq	RT	4 days	1%	NA	NA	NA
DCM	0.5eq	3eq	7eq	reflux	10h	1%	NA	NA	NA
1,4-Dioxane	0.5eq	3eq	7eq	reflux	7h	0%	NA	NA	NA
1,4-Dioxane	1eq	3eq	7eq	75°C	6h	0%	NA	NA	NA
1,4-Dioxane	2.7eq	0eq	7eq	reflux	4h	44%	32%	13%	8%
1,4-Dioxane	2.7eq	0eq	7eq	75°C	6h	48%	30%	41%	NA
1,4-Dioxane	2.7eq	0eq	7eq	µwave	40min	45%	44%	32%	NA
1,4-Dioxane	2.7eq	0eq	11eq	75°C	6h	60%	53%	32%	NA
1,4-Dioxane	4.4eq	0eq	11eq	75°C	6h	74%	56%	9%	NA
1,4-Dioxane	6.3eq	0eq	15eq	75°C	6h	85%	58%	6%	4%
1,4-Dioxane	4.4eq	0eq	11eq	75°C	16h	98%	51%	1%	10%

Table 2.2 SeO_2 oxidations are shown to be sensitive to reaction time, temperature as well as relative concentration of SeO_2 and water. In addition to being a superficial measure of glyoxal formation, relative conversion is indicative of spurious side reactions of **2.80.**

From Table **2.2** the relative conversion of **2.80** to **2.88** was seen to increase steadily upon increasing first the stochiometric amount of water followed by SeO_2. Finally, longer reaction times seemingly resulted in total depletion of **2.80**. However, inspection of yields of **2.88** over two steps as well as the recovery of **2.80** revealed that increased eq. of water rather than simply increasing SeO_2 eq. resulted in higher yield of **2.88** as well high recovery of **2.80**, even when compared to the microwave

reaction. This is probably due to the water being involved in an increase in the rate of selenous acid formation, a likely intermediate in SeO_2 mediated oxidation.[150] Interestingly, this overall yield could not be significantly improved upon with increased eq. of SeO_2 or reaction time, and it seems that the ratio of SeO_2 to water is vital in reducing side reactions from occurring. It is clear that the increased conversion was a result of destruction of **2.80** via side reactions rather than conversion to glyoxal.

In addition, a mono deprotected product was identified in three of the experiments. Interestingly 2D NMR analysis identified the product to be N-1" deprotected product (**2.89**) rather than the alternative option deprotected at N-1' (**Figure 2.9**).

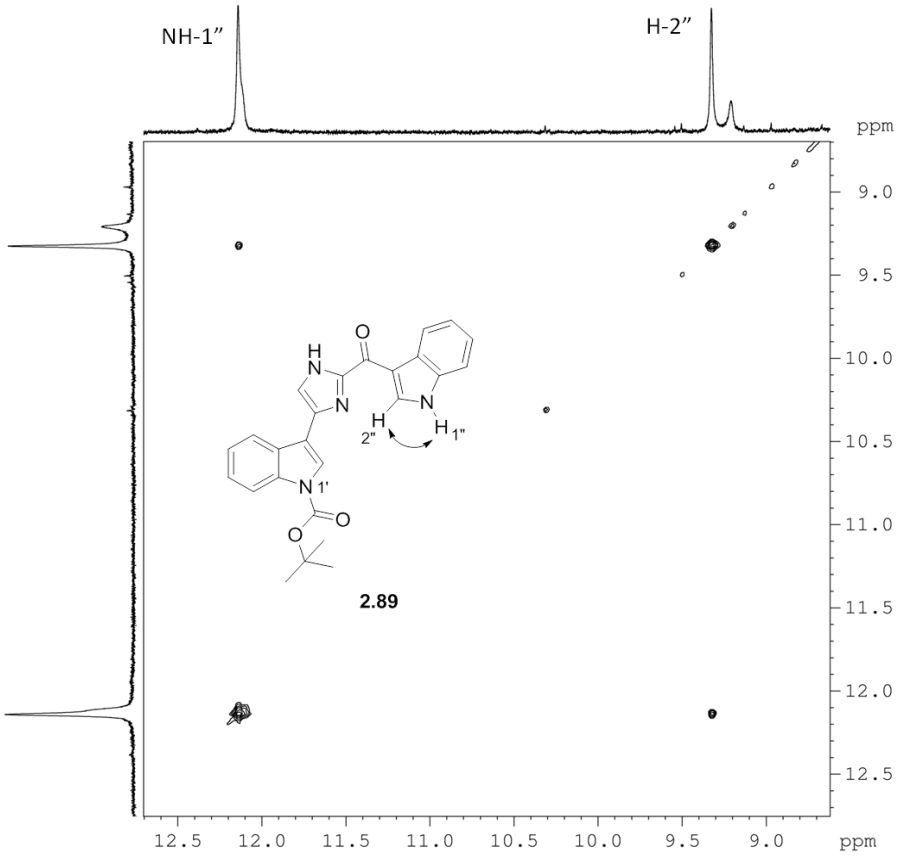

Figure 2.9 Upfield region of the COSY NMR spectrum obtained for compound **2.89** (600MHz, DMSO-d_6, relaxation time [d1] = 1.48 sec; F1 and F2 = δ_H 8.5—12.7), displaying correlation between the protons of NH-1" and H-2".

This also illustrates that Boc deprotection is occurring at some point during the two steps. Due to the mild conditions used for the cyclization it is unlikely that deprotection is occurring either during this step or during purification. If that were the case we would expect to see a more even distribution of **2.89** throughout all experiments, which is plainly not the case. At this point it was unclear whether deprotection was occurring either before or after glyoxal formation and whether deprotection was leading to glyoxylic acid formation. To this end it was concluded that the best general method to prepare our target compounds was that which resulted in a modest yield with a maximal recovery of starting material, which could then be recycled.

Compound **2.88** as predicted by Khalili *et al.*[93] was found to exist as mixture of isomers. EXSY NMR was used to show that the two sets of signals are a product of one system in two different orientations, which can be detected on an NMR time scale. However, it is not clear whether these are slowly interconverting tautomers, or restricted rotamers (**Figure 2.10**).

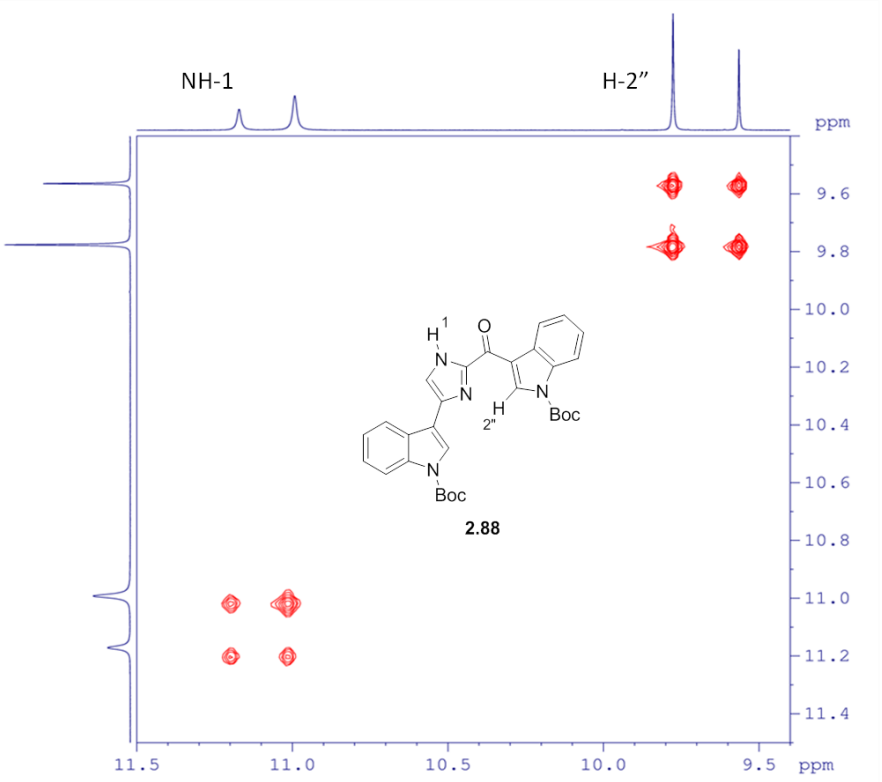

Figure 2.10 Upfield region (F1 and F2 = δ_H 9.4—11.5), of the EXSY NMR spectrum obtained for **2.88** (600 MHz, $CDCl_3$, relaxation time [d1 = 2.00 s; EXSY mixing time [d8] = 0.449 s) showing correlation between two species of NH-1 and H-2”

2.5.5 Glyoxal formation and cyclization of halogenated indole derivatives 2.55, 2.83,2.84

The low amounts of 6-bromo and 6-iodo indole which we had available required us to proceed cautiously and first optimize our methodology for glyoxal formation and cyclization using halogenated methyl ketones **2.55, 2.83** and **2.84** to yield products **2.90—2.92**. Three experiments were carried out with each indole compound to enable us to compare results with those obtained for oxidation of **2.80.** (**Table 2.3**).

Indole Substitution	SeO_2	H_2O	% Yield of product over 2 steps	Remaining Methyl Ketone	Combined yield of imidazole product and starting material	% Yield of Side Product
6-F	2.7eq	11eq	33%	45%	78%	
6-F	4.4eq	11eq	54%	21%	75%	7%
6-F	6.3eq	15eq	51%	23%	74%	7%
6-Cl	2.7eq	11eq	35%	33%	68%	
6-Cl	4.4eq	11eq	28%	39%	67%	
6-Cl	6.3eq	15eq	47%	18%	65%	6%
5-Br	2.7eq	11eq	40%	35%	75%	
5-Br	4.4eq	11eq	39%	51%	90%	
5-Br	6.3eq	15eq	53%	41%	94%	

Table 2.3 SeO_2 mediated oxidation of **2.55, 2.83** and **2.84** each under three different reaction conditions. The side product is the monoprotected bisindole imidazole.

Interestingly, the results obtained for **2.55, 2.83** and **2.84** did not mirror the results obtained for the oxidation and cyclization of **2.80.** The experimental evidence suggested that in contrast to the

pattern observed for the SeO_2 oxidation of **2.80**, increased equivalence of SeO_2 increases yields, with little increase in the occurrence of spurious side reactions on the starting material. Evidenced for this is provided by the consistent, combined yields of product and starting material, suggesting that decreased recovery of starting material was due to increased glyoxal formation. However, in the cases of the fluoro and chloro analogues, small amounts of mono Boc deprotected side products were detected. NMR spectral analysis confirmed the chlorinated analogue to be the NH-1" mono-deprotected side product **2.94**. In the case of the fluorinated analogue sufficient NMR data could not be collected to unambiguously resolve the structure as **2.93** whose mass had been confirmed by HRESMS. Compound **2.95** was not detected.

Interestingly, HRESMS (negative ion mode) on reaction mixtures prior to cyclization, detected ions corresponding to both *N*-Boc protected glyoxylic acids **2.96—2.98**, as well as Boc deprotected glyoxal **2.99—2.101** (**Figure 2.11**).

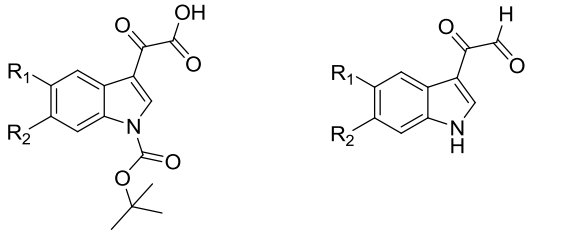

2.96 R_1 = H, R_2 = F
2.97 R_1 = H, R_2 = Cl
2.98 R_1 = Br, R_2 = H

2.99 R_1 = H, R_2 = F
2.100 R_1 = H, R_2 = Cl
2.101 R_1 = Br, R_2 = H

These results therefore provide strong evidence that firstly, glyoxylic acid formation occurs even in the presence of the Boc group, and that it is likely that Boc deprotection occurs during reaction with selenium dioxide, either from the methyl ketone, or glyoxal. While there is also a possibility that Boc deprotection occurs during MS ionization, mass peaks corresponding to this loss of the Boc group were not observed in any other Boc protected compound analyzed, which strongly implies that electrospray ionization does not induce deprotection. These samples had not been exposed to the cyclization step, providing further evidence that deprotection does not occur in that reaction.

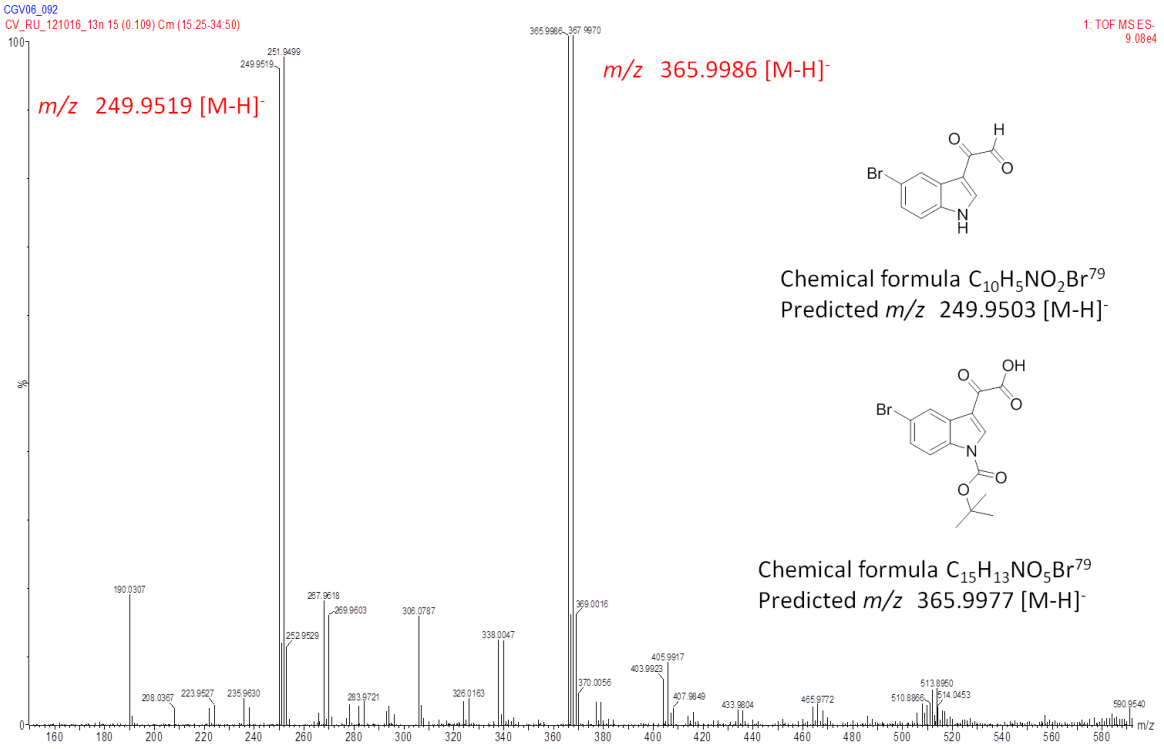

Figure 2.11 Evidence for glyoxylic acid formation and *N*-Boc deprotection was provided by MS analysis, exemplified by the above spectrum from the reaction mixture after oxidation of **2.84**. The isotope pattern confirms the presence of bromine in the molecule. Accurate masses for **2.99—2.101** calculated using ChemCalc.[151]

Since the *N*-1' deprotected variant was not detected, it further suggests that the ketone adjacent to the Boc protected indole is more susceptible to nucleophillic attack from the imine intermediate, than the alternative (**Scheme 2.40**).

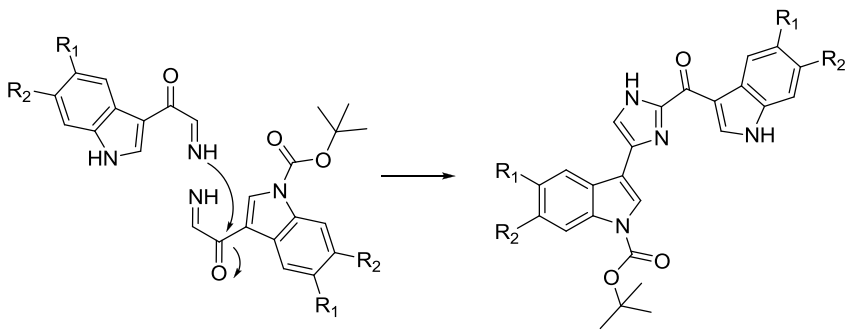

Scheme 2.40 Preferential nucleophillic attack of imine intermediate

2.5.6 Glyoxal formation and cyclization of halogenated indole derivatives 2.85 and 2.86

Based on the higher yields achieved at 6.3 equivalents of SeO_2, we decided to use this ratio of SeO_2 for the oxidation of both **2.86** and **2.87**. Disappointingly low yields for **2.102** (20 %) and **2.103** (26 %) respectively were achieved, possibly because of the small amounts of **2.85** (32 mg) and **2.86** (28 mg) used. Pleasingly, 53 % and 49 % of the respective starting materials were recovered.

2.6 *N*-Boc deprotection

Moody and Roffey[89] reported difficulties in removing Boc from indoles using both TFA and sodium methoxide. We therefore decided to rather employ a thermolytic method for the removal of the Boc protecting group[145] which proceeded smoothly yielding the fluorescent target bis-indole imidazole compounds (**1.40, 1.46, 1.58—1.61, Figure 2.12**) with a high degree of purity in quantitative yield (**Scheme 2.41**).

Figure 2.12 Compound **1.40** (1mg) fluorescing under UV irradiation (365 nm)

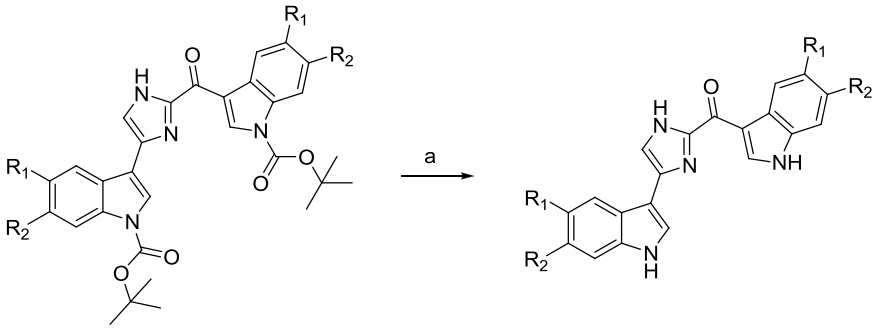

2.88 $R_1 = R_2 = H$
2.90 $R_1 = H, R_2 = F$
2.91 $R_1 = H, R_2 = Cl$
2.92 $R_1 = Br, R_2 = H$
2.102 $R_1 = H, R_2 = I$
2.103 $R_1 = H, R_2 = Br$

1.40 $R_1 = R_2 = H$
1.58 $R_1 = H, R_2 = F$
1.59 $R_1 = H, R_2 = Cl$
1.46 $R_1 = H, R_2 = Br$
1.60 $R_1 = Br, R_2 = H$
1.61 $R_1 = H, R_2 = I$

Scheme 2.41 Thermolytic Boc removal

a) 180 °C, Ar, 5 mins

In preparation for the bioassays, compounds **1.40, 1.46, 1.58—1.61** were further purified on reverse phase HPLC (3:1, MeOH: H_2O). Initial ^1H NMR analysis of the halogenated analogues **1.46, 1.58—1.61**, worryingly provided spectra where indole signals appeared as a series of non resolvable broad signals (**Figure 2.13** top) leading us to assume that our compounds had degraded during thermolytic deprotection.

Interestingly, an aromatic doublet (δ_H 7.39) in the ^1H NMR spectrum of **1.61** counter intuitively had no correlations in the COSY NMR spectrum, suggesting an unanticipated NMR phenomenon rather than thermolytic degradation was at play. HRESMS also encouragingly confirmed the expected mass of the desired compounds. Surprisingly, the broad NMR signals were not observed in the ^1H NMR spectrum of compound **1.40.** The ^1H NMR spectrum of **1.40** however revealed that this compound existed as two clearly resolvable interconverting species, which we again confirmed with EXSY. Initially we reasoned that the isomers of **1.46, 1.58—1.61** were interconverting at a time scale, not conducive to NMR resolution and the broad signals observed were as a result of signal merging.

To overcome this we added 1 eq. of TFA to the NMR solution, thereby protonating the imidazole reducing the isomeric mixture to a single species, resolvable by NMR (**Figure 2.13** bottom).

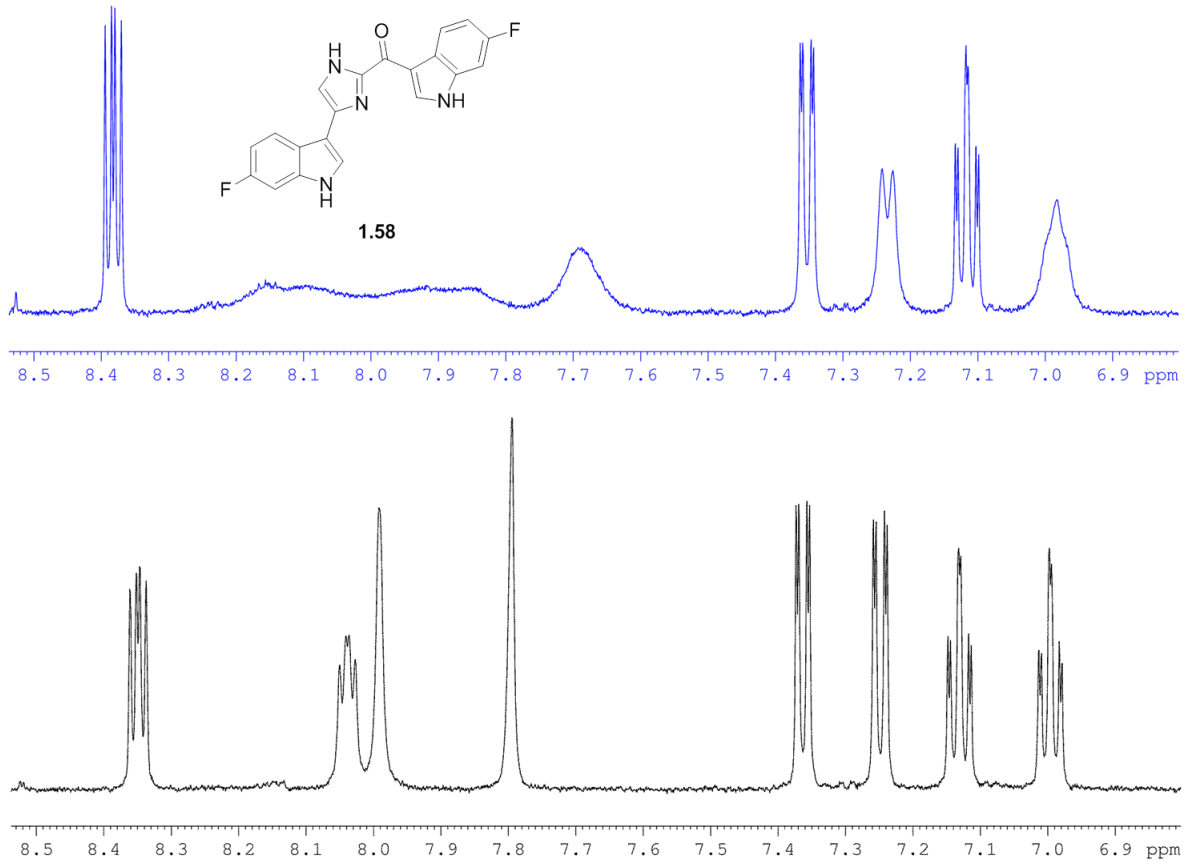

Figure 2.13 Comparative ^{1}H NMR spectra (600 MHz, DMSO-d_6 [top], DMSO-d_6, 1 eq. TFA [bottom]) showing the upfield region (δ_H 6.8—8.6) of compound **1.58.** After RP HPLC (top) we observed a mixture of sharp signals and broad unresolvable signals.

2.7 Synthesis of 7',7"-dichlorodeoxytopsenin

After analysis of the bioactivity data (**2.8**) of compounds **1.40, 1.46, 1.58—1.61**, it seemed that interchanging the position of the halogen substituent between C-5 and C-6 on the indole ring did not have a significant effect on activity, as exemplified by compounds **1.46** and **1.60**. To see if this trend was applicable to compounds halogenated at other positions on the indole ring, we decided to

synthesize one further analogue of the most potent dichloro compound **1.59** where the chlorine substituent was positioned at the indole C-7 position (**2.104**). In addition, we slightly altered our synthetic procedure, (**Scheme 2.42**) in which, after imidazole formation, we avoided bench top column purification, but rather thermolytically deprotected the crude mixture, which was then purified on reverse phase HPLC, to yield the product over 3 steps in 37% overall yield.

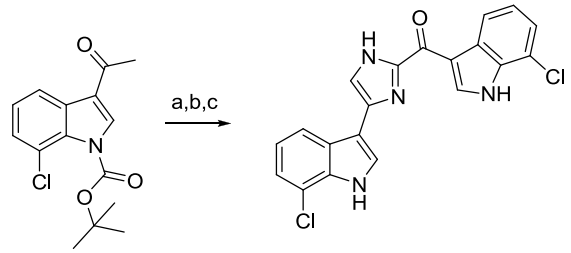

2.104 37% over 3 steps

Scheme 2.42 Synthesis of topsentin derivative **2.104**

a) SeO_2, H_2O, 1,4-dioxane, 75 °C, 6h; b) NH_4OAc, EtOH, r.t. 6h; c) 180 °C, Ar, 5 mins

The advantage of this approach apart from removing a purification step, is that if monoprotected topsentin is formed, it too will be completely deprotected, and form part of the final product yield. However, the major disadvantage is the introduced complexity of HPLC purification, in which residual deprotected 3-acetylindole, and indole glyoxylic acid need to be removed. This is particularly difficult with the 3-acetylindole precursor, since it has a similar retention time to the topsentins.

2.8 MRSA inhibition studies

After successfully synthesizing the target topsentin analogues we sent our compounds to our collaborators at the University of British Columbia who conducted both MRSA PK inhibition assays and selectivity assessments. Compounds **1.40, 1.46, 1.58—1.61** were found to be active MRSA PK

inhibitors, the most potent being the **1.59** and **1.46** analogues, which inhibited MRSA PK at an average IC_{50} of 1.4 and 2.1 nM respectively while the C-7 chlorinated **2.104** displayed a significantly lower activity that the analogues halogenated at C-5 and C-6 (**Figure 2.14**).

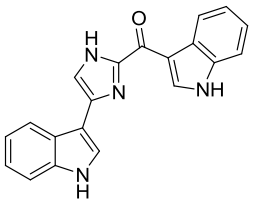

1.40 IC_{50} 238 nM
(SD = 48.93)

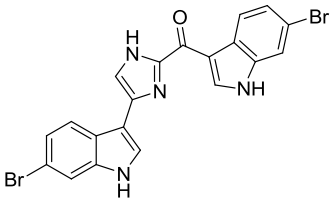

1.46 IC_{50} 2.1 nM
(SD = 1.71)

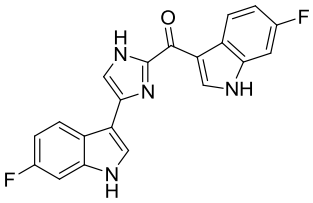

1.58 IC_{50} 23 nM
(SD = 2.62)

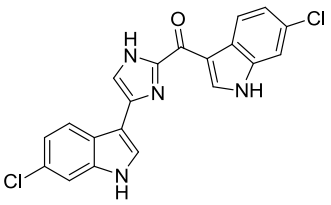

1.59 IC_{50} 1.4 nM
(SD = 0.49)

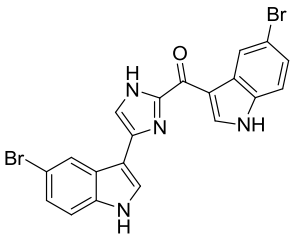

1.60 IC_{50} 6.3 nM
(SD = 1.63)

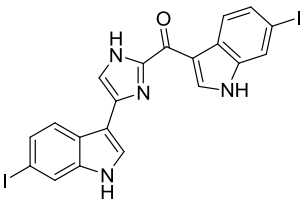

1.61 IC_{50} 3.2 nM
(SD = 0.14)

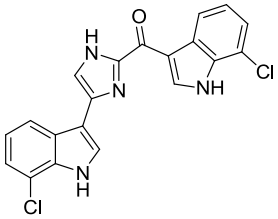

2.104 IC_{50} 25.6 μM

Figure 2.14 IC_{50} values of compounds **1.40, 1.46, 1.58—1.61, 2.104**

Additionally, both compounds **1.59** and **1.46** displayed 100% inhibition of MRSA PK at a concentration of 5 µM. Similar inhibition was observed for **1.60** and **1.61**, both of which displayed 97 and 85% inhibition of MRSA PK at 5 µM respectively, in addition to low nanomolar IC_{50} values. Compounds **1.40** and in particular **1.58** also showed encouraging inhibitory activity with nanomolar range IC_{50} data and 72—75% inhibition of MRSA PK at a concentration of 10 µM, while at the same concentration **2.104** only exhibited 19.5% inhibition (**Figure 2.15**).

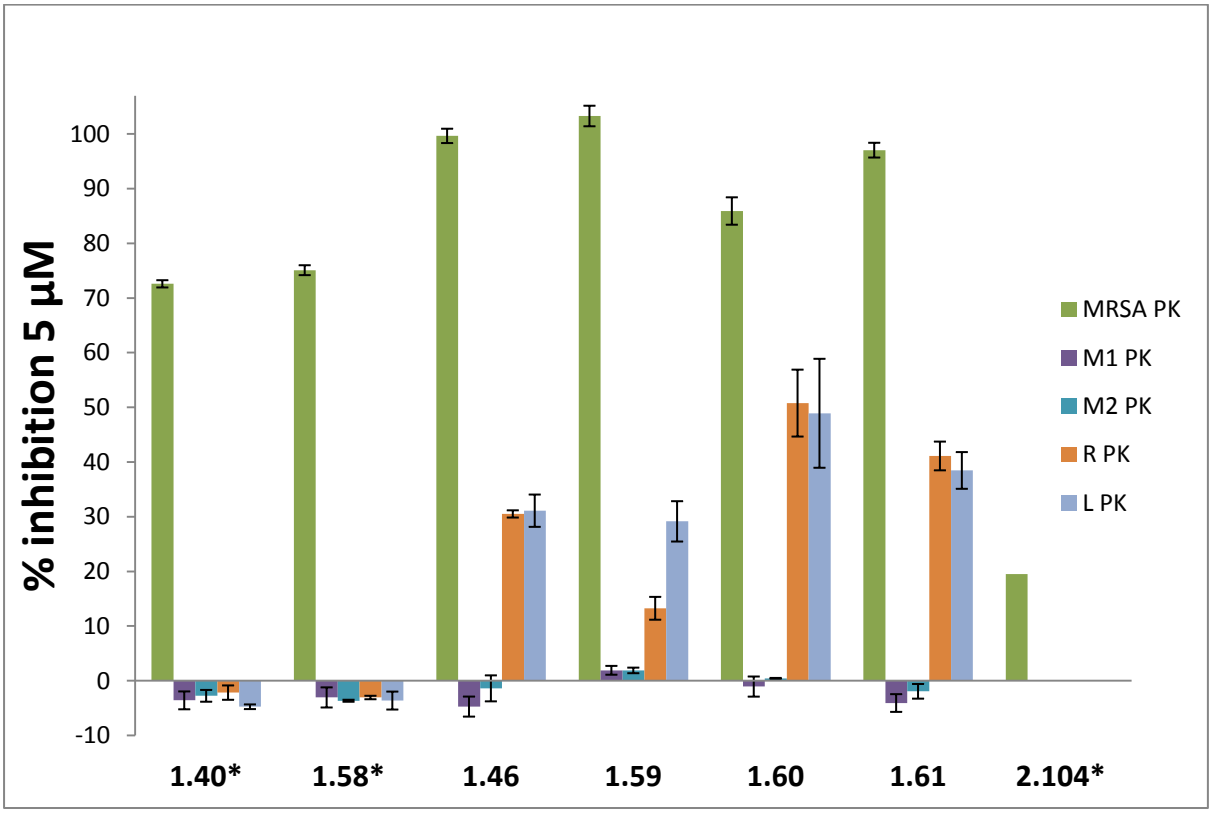

Figure 2.15 % inhibition data of compounds **1.40, 1.46, 1.58—1.61** and **2.104** against MRSA PK and 4 mammalian orthologs, where we can see the high degree of selectivity (1000—10000 fold). *% inhibition data at 10 µM.

The topsentin analogues **1.40, 1.46, 1.58—1.61** were further found to display 1000—10000 fold selectivity for MRSA PK over four human orthologs. These results were most satisfying when compared to **1.5** and **1.6** where we were able to improve activity against the target by up to a factor of 10, while improving selectivity from between 166 to 600 fold. Interestingly the SAR of these

compounds does not mirror that observed for compounds **1.5—1.12** by Strangman *et al.*[22] in which the correlation between halogen size/electronegativity and activity is not observed and the 5-bromo, fluoro and non-halogenated analogues display potent to good MRSA PK inhibitory activity. Chlorination at the C-7 position on the indole ring leads to a dramatic loss of activity. From an SAR point of view this suggests that the dihalogenated pseudo symmetry displayed by both the topsentin displayed by compounds **1.40, 1.46, 1.58—1.61** greatly improves activity, while additionally suggesting that the topsentin scaffold is more suited for MRSA inhibition than that the *cis*-3,4-dihydrohamacanthin. The major difference between the two classes is the aromatic 2-acylimidazole, which potentially may be interacting with the prominent histidine residues located in the binding site. Another possibility is that these compounds bind at a different site on the enzyme, which would account for the difference in SAR trends, which will be discussed in Chapter 4.

2.9 Conclusions

In conclusion, we successfully developed a new method to synthesize a cohort of new topsentin analogues, which showed potent, selective MRSA PK inhibitory activity. Adaptation of Ottoni *et al.*'s Friedel-Crafts method allowed us to explore the versatility of this method and synthesize a series of differentially halogenated 3-acetylindoles, while new insight into SeO_2 oxidation 3-acetylindoles as well as the role of water in this reaction was established. Comparison of SAR studies, revealed that topsentins have a privileged scaffold with regard to MRSA PK inhibition, which we will explore in more detail in the following chapter. It will be interesting to unambiguously determine the binding site of these potent compounds (discussed in Chapter 4) to assess whether this is the reason for the improved activity and selectivity.

Chapter Three

Synthesis and Biological Activity of Thiazole containing Bisindole Alkaloids

3.1 Introduction

After obtaining biological data from our cohort of halogenated topsentin analogues (**1.40, 1.46, 1.58—1.61, 2.104**), we felt it would be appropriate to test the possible effect on biological activity arising from replacing the central aromatic imidazole moiety with another five membered aromatic heterocyclic ring. We therefore resolved to attempt the synthesis of both oxazole and thiazole analogues of **1.40, 1.46, 1.58—1.61**, **2.104** since both aromatic five membered rings feature either a hydrogen bond accepting oxygen or sulfur atom respectively instead of a hydrogen bond donor as is the case with the imidazole NH functionality. IC_{50} values obtained for compounds **1.40, 1.46, 1.58—1.61** showed that repositioning of the halogen from C-6 to C-5 on the indole ring resulted in a small reduction in activity, while substitution as C-7 resulted in a dramatic loss of activity, suggesting that the C-6 position may be the optimal position for halogenation to ensure maximum MRSA PK inhibitory activity. With this in mind, and cognizant of the difficulties we had experienced in preparing 6-iodo indole, we decided that the synthesis of thiazoles **1.62—1.65** and oxazoles **2.19, 3.1—3.3** would provide an adequate addition to our SAR study.

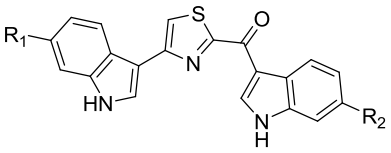

1.62 $R_1 = R_2 = H$
1.63 $R_1 = R_2 = F$
1.64 $R_1 = R_2 = Cl$
1.65 $R_1 = R_2 = Br$

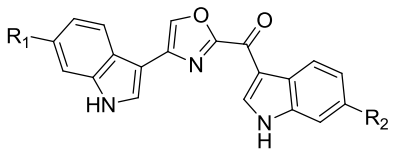

2.19 $R_1 = R_2 = H$
3.1 $R_1 = R_2 = F$
3.2 $R_1 = R_2 = Cl$
3.3 $R_1 = R_2 = Br$

While Jiang and co-workers have previously synthesized a series of thiazole containing nortopsentins with moderate anticancer activity (**Scheme 3.1**),[133,152] to date no thiazole topsentin analogue has been either synthesized or reported from a marine or terrestrial source. As reported in Chapter 2,

an oxazole containing deoxytopsentin derivative was synthesized as part of the work of Horne and co-workers (**Scheme 2.19**), but no biological data was provided for this compound.[87]

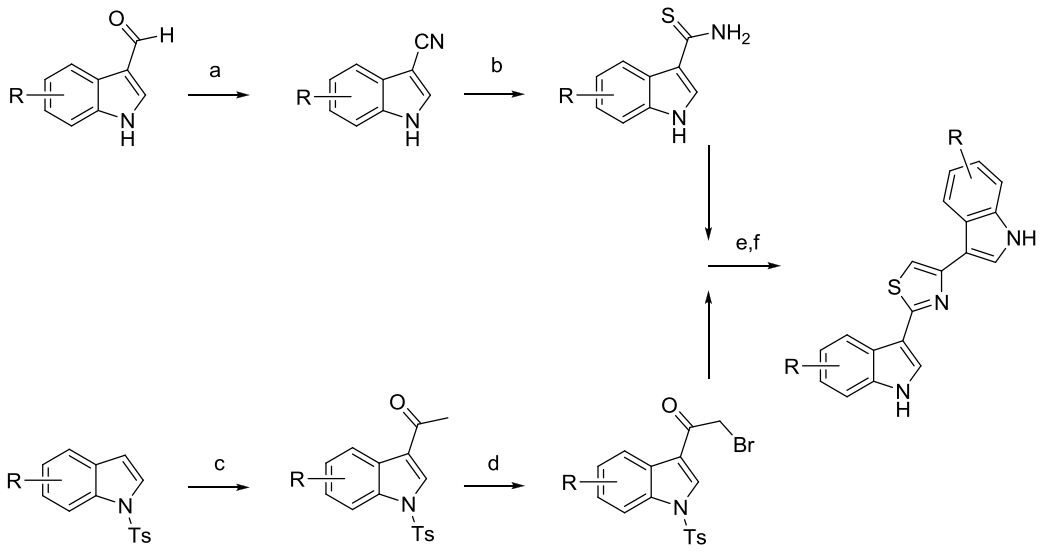

R = H, 5-Br, 6-Br, 6-OMe

Scheme 3.1 Jiang *et al.*'s synthesis of thiazole nortopsentin derivatives[133,152]

a), $(NH_4)_2HPO_4$, $CH_3CH_2CH_2NO_2$, AcOH, reflux; b), H_2S, Et_3N; c), Ac_2O, $AlCl_3$, CH_2Cl_2, 0 °C – r.t. d) $CuBr_2$, $CHCl_3$/EtOAc (1:1), reflux; e) EtOH, reflux, f) NaOH, MeOH, reflux.

3.2 Naturally occurring thiazoles and oxazoles

An ever increasing number of biologically active polyheterocyclic natural products, particularly those from the marine environment (e.g. barlingolin **3.4**),[153] are found to contain thiazole and oxazole functionalities in addition to their non-aromatic ring analogues, thiazoline and oxazoline respectively.[154,155] These heterocyclic compounds have been shown to possess anti-tumor, antimalarial, antibacterial antiviral and antihelmintic activity[155]

The most common manifestation of oxazole and thiazole containing natural products are as part of more complex heterocyclic peptides commonly found together with indole and pyridine derivatives.[156]

A specific class of these compounds with a high sulfur content, the thiopeptide antibiotics, have shown potent *in vitro* activity, with novel mechanisms of action, against a number of bacterial strains including MRSA, and as such have engendered interest from both biochemists and synthetic chemists alike.[153,155,156,157]

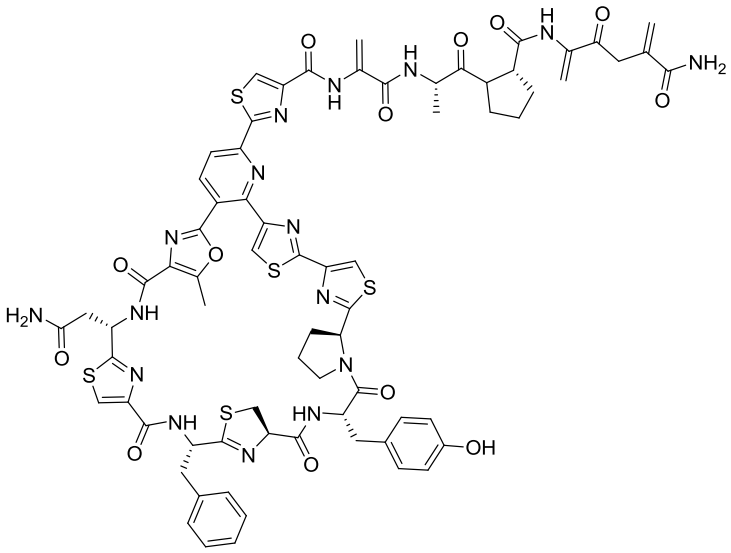

3.4 baringolin

While these macrolides are the most common source of thiazoles and imidazoles, several naturally occurring thiazole and oxazole containing small molecules which also include one or more indole rings, have been identified including the cytotoxic bacillamides (**3.5—3.7**) and diazonamide A (**3.8**),[158,159] isolated from marine *Bacillus* sp.[155] and the *Diazona chinensis* ascidian respectively,[160] the potent topoisomerase II inhibitor BE 10988 (**3.9**)[161] and the antibacterial almazoles C (**3.10**) and D (**3.11**) isolated from *Haraldiophyllum* sp. seaweed.[162,163,164]

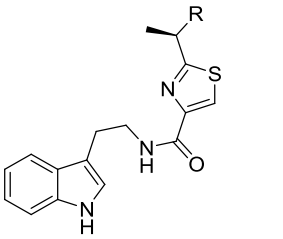

3.5 R = O bacillamide A
3.6 R = OH bacillamide B
3.7 R = NHAc bacillamide C

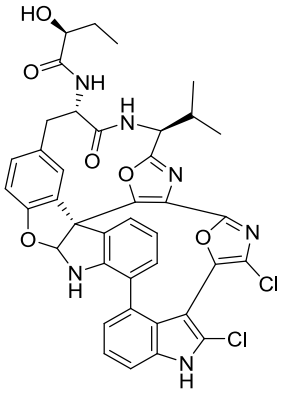

3.8 diazonamide A

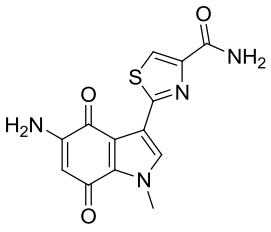

3.9 BE 10988

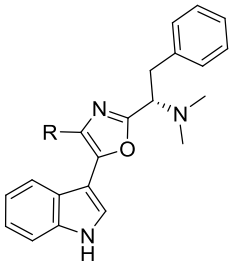

3.10 R = H almazole C
3.11 R = CO_2^- almazole D

3.3 Thiazole and oxazole biosynthesis

Biosynthetically, oxazole and thiazole containing macrolides are most likely formed from dehydrative cyclization of either cysteine or serine containing peptides to form oxazolines and thiazolines, followed by oxidation to yield oxazoles and thiazoles respectively (**Scheme 3.2**).[157,165]

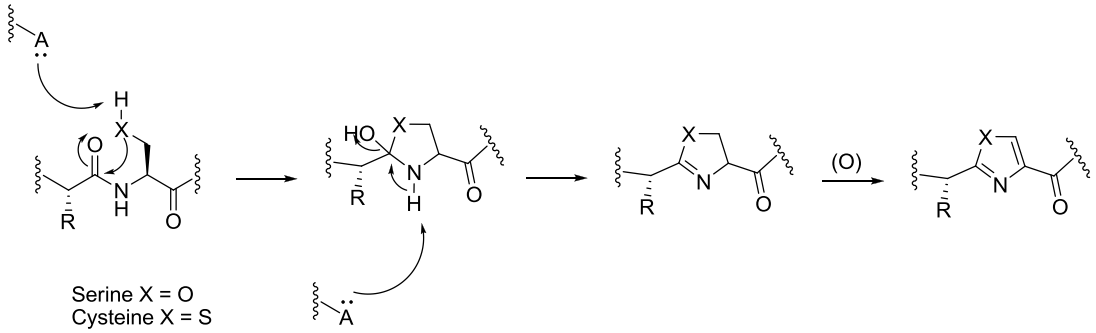

Scheme 3.2 Biosynthetic dehydrative cyclization to form oxazoles and thiazoles[157,165]

This speculative biosynthesis, outlined in **Scheme 3.2**, was confirmed from biosynthetic studies of the *Streptomyces* derived thiopeptide antibiotic berninamycin A (**3.12**) by Lau and Rinehart[166] who used 2D NMR and FABMS/MS techniques to monitor the incorporation of a series of ^{13}C enriched amino acids into berninamycin.[166]

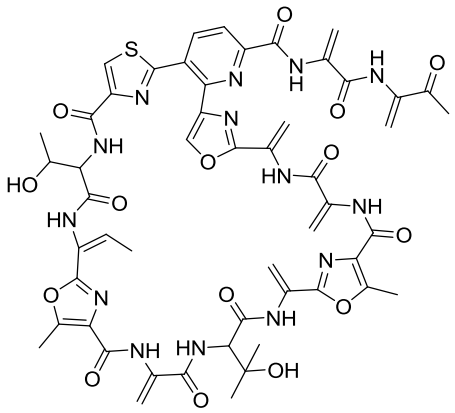

3.12 berninamycin

Conversely, the non peptide derived plant natural product camalexin (**3.13**) and the microbial derived BE10988 **3.9**,[167] are both biosynthesized from tryptophan (**3.14**) and cysteine (**3.15**). In each example the tryptophan side chain is shortened by one carbon unit before cyclization occurs (**Scheme 3.3**).[167] During the BE-10988 biosynthesis, the tryptophan is converted to pyruvic acid derivative (**3.16**), while camalexin biosynthesis occurs an via indole-3-acetaldoxime intermediate (**3.17**) which in turn is converted to the acetonitrile derivative **3.18**.[167] The mechanism of cysteine mediated cyclization is not understood at this point.

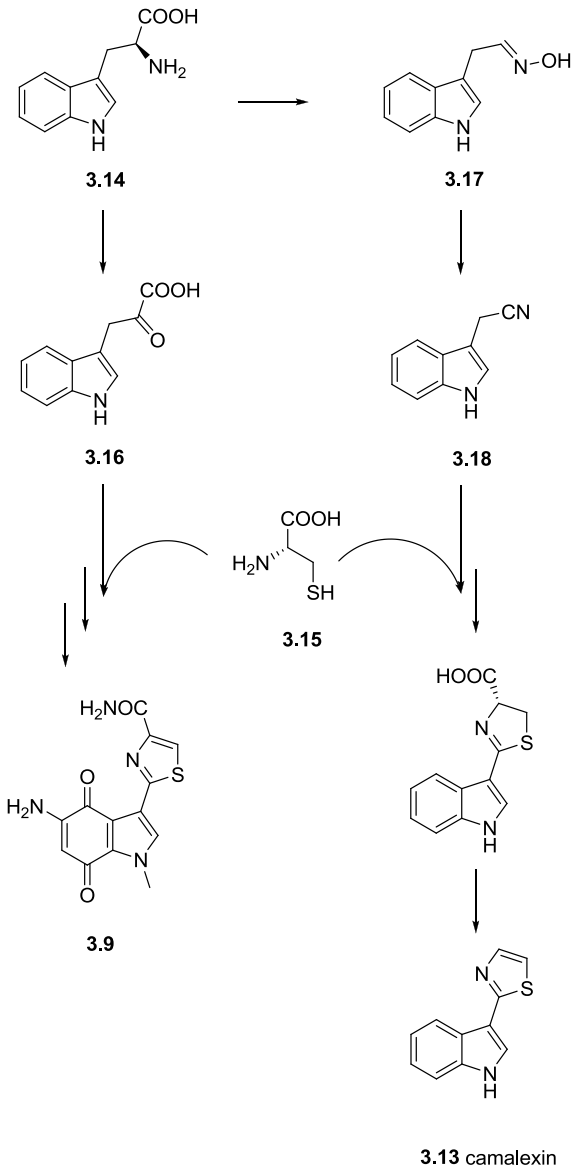

Scheme 3.3 Biosynthesis of natural thiazole containing calmexin and BA 10988[167]

Interestingly, of the three new staurosporine analogues fradcarbazoles A—C (**3.19—3.21**) isolated by Fu *et al.*[168] from a mutant strain of a marine derived *Streptomyces* spp., one metabolite fradacarbazole A, featured an indolyl-3-thiazole moiety bonded directly via C-2 of the thiazole ring to the staurosporine scaffold. Paradoxically, the indole is a C-5 substituent of the thiazole ring of **3.19** which is different to both camalexin and BE-10988 where the indole is bonded to C-2 of the thiazole suggestive of a different biogenesis for **3.19** *c.f.* **3.9** and **3.13**. The occurrence of a thioamide and a nitrile substituent on the staurosporine nucleus of **3.20** and **3.21** respectively, prompted Fu *et al.* to

speculate that the sulfur source for **3.19** and **3.20** was thiourea and not cysteine.[168] Of additional interest is the possible role of a nitrile functionality in thiazole biosynthesis, since Jiang *et al.* in their synthesis of thiazole containing nortopsentin analogues (**Scheme 3.1**),[133,152] showed that it was possible to synthetically derive thioamides from nitriles, followed by cyclization with 2-bromo-1-(1*H*-indol-3-yl)-ethanone to yield thiazoles.

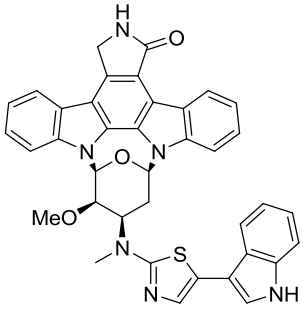

3.19 fradacarbazole A

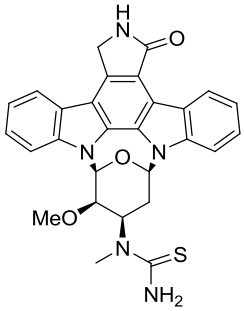

3.20 fradacarbazole B

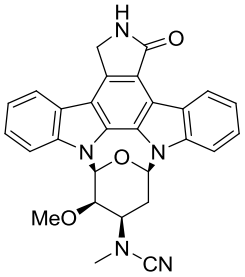

3.21 fradacarbazole C

3.4 Synthetic approaches to thiazole and oxazole topsentin analogues

While designing a synthesis for oxazole and thiazole topsentin analogues, various aspects of our successful topsentin synthesis were considered. However, as the central heterocycle contains two different heteroatoms in oxazoles and thiazoles, we could not mimic the cyclic condensation approach used for the imidazole synthesis and an alternative strategy was sought that would regiospecifically deliver the required disubstituted heterocyclic ring. An additional goal was to potentially adapt the synthesis to enable us to place differently functionalized indole rings regiospecifically onto either side of an imidazole moiety.

An organometallic approach which involves coupling modified heteroaromatics, in a method similar to that utilized by Zhang *et al.* (**Scheme 3.4**)[169] was deemed inappropriate because of the presence of potentially labile halogens, especially bromine, substituted on the indole rings of our target compounds.

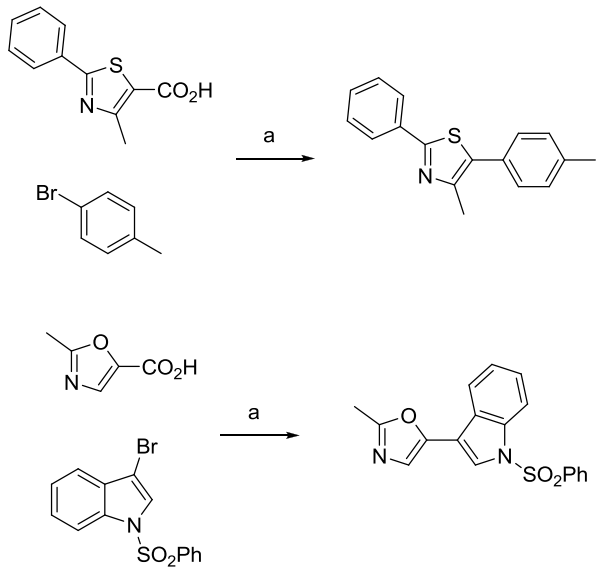

Scheme 3.4 Zhang *et al.*'s synthesis of functionalised thiazole (top) and oxazole (bottom)[169]

a) $PdCl_2$, PPh_3, Ag_2CO_3, DMA/Toluene, 135 °C, 16h.

We therefore resolved to condense functionalized indoles to form the central heterocycle moiety. Two different synthetic pathways were considered. Firstly, a cyclodehydration of ketoamides and ketothioamides adapted from the Robinson-Gabriel reaction which had previously been exploited by Miyake *et al.*[87] to synthesize an oxazole topsentin derivative (**Scheme 2.19**)[87] and was later more extensively investigated by Nicolau *et al.*[159] to synthesize a number of oxazole and thiazole heterocyclic compounds in the presence $POCl_3$ and pyridine (**Scheme 3.5**).[159]

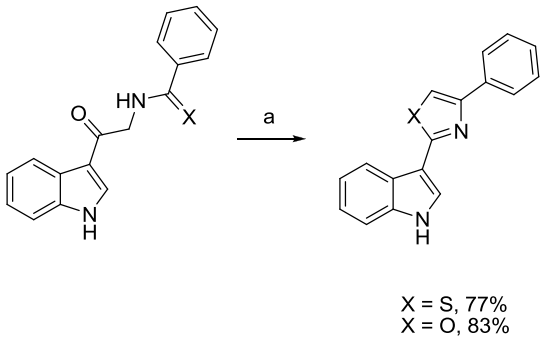

Scheme 3.5 Nicolau *et al.*'s exploration of the Robinson-Gabriel cyclodehydration reaction[159]

a) $POCl_3$, Pyridine, 0 – 25 °C, 5h.

Secondly, an adaptation of the Hantzsch thiazole synthesis as used by Moody *et al.* yielded a series of differently substituted oxazole and thiazole containing analogues of BE10988 (**Scheme 3.6**).[170]

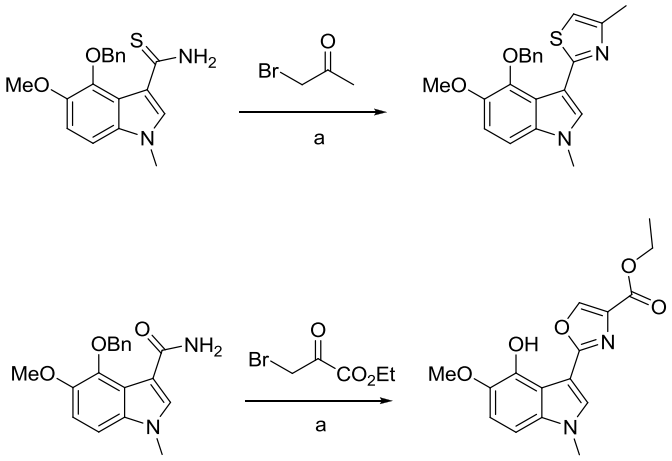

Scheme 3.6 Moody *et a*l.'s Hantzsch thiazole (top) and oxazole (bottom) synthesis[170]

a) EtOH, Heat

3.4.1 Robinson-Gabriel retrosynthesis

The Robinson-Gabriel approach, refined from the retrosynthesis presented in **Scheme 3.7** required the synthesis of either an *N*-[2-(1*H*-indol-3-yl)-2-oxoethyl]-α-oxo-1*H*-Indole-3-acetamide analogue (**3.22**) or *N*-[2-(1*H*-indol-3-yl)-2-oxoethyl]-α-oxo-1*H*-Indole-3-thioacetamide analogue (**3.23**) for oxazole(akin to that utilized by Miyake *et al.*[87]) and thiazole synthesis respectively.

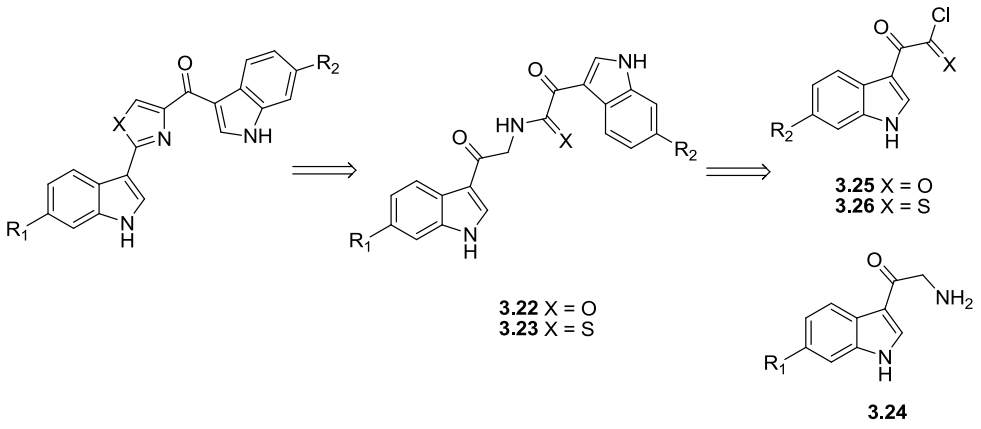

Scheme 3.7 Robinson-Gabriel retrosynthesis

We anticipated that compound **3.22** would require a condensation between an α-oxotryptamine derivative (**3.24**) and a potentially easily accessible oxalyl chloride derivative (**3.25**), while the thioacyl derivative **3.26** could be obtained from thionyl chloride oxidation of 3-acetylindoles, in a method adapted from Oka *et al.* (**Scheme 3.8**).[171] Compound **3.26** was similarly amenable to coupling with oxotryptamine to yield the key intermediate **3.23**.

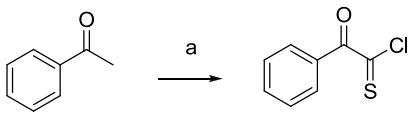

Scheme 3.8 Oka *et al.*'s synthesis of thioacyl chlorides[171]

a) $SOCl_2$, pyridine, heat, 95%

3.4.2 Hantzsch heterocycle retrosynthesis

The alternative Hantzsch style synthesis required condensation of a 2-halo-1-(1*H*-indol-3-yl)-ethanone (**3.27**) with a thioamide (**3.28**) to yield thiazole (**3.29**), or with amide (**3.30**) to yield oxazole (**3.31**) as suggested by the retrosynthesis presented in **Scheme 3.9**.

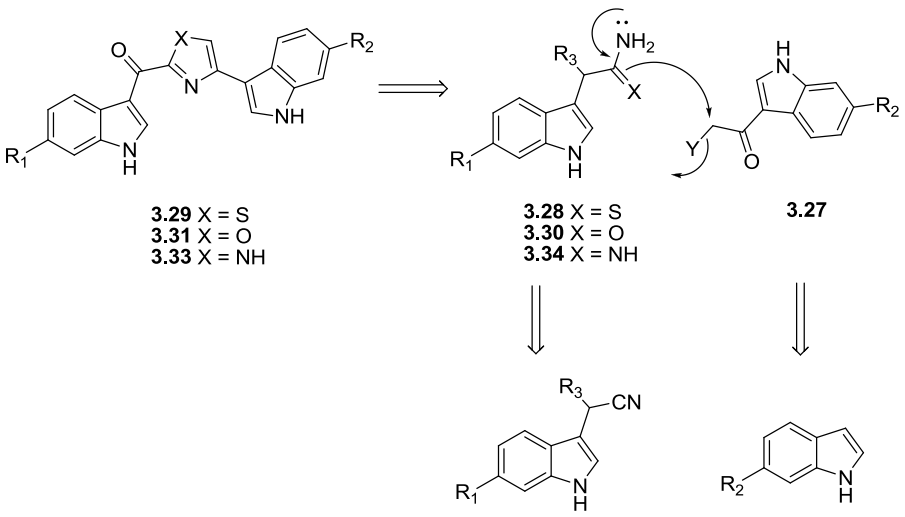

Scheme 3.9 Hantzsch heterocycle retrosynthesis

However, since the target compounds required a ketone moiety adjacent to the central heterocycle, we needed to introduce either a ketone, or a protected ketone adjacent to the amide and thioamide functionality in either **3.28** or **3.30** respectively. Therefore of interest to us was the synthesis of α-oxo-1*H*-indole-3-acetamide **3.32** has by Garg *et al.* (**Scheme 3.10**)[99] obtained by bubbling ammonia through a solution of **2.17** in DCM.[99]

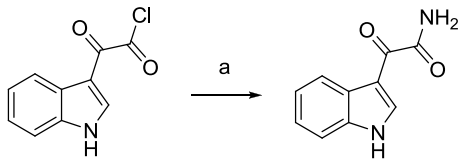

Scheme 3.10 Garg *et a*l.'s synthesis of **3.32**[98]

a) NH_3, CH_2Cl_2 r.t.

Furthermore, Moody and co-workers have shown that the thiation agent, Lawesson's reagent is useful for converting amides to thioamides (**Scheme 3.11**),[89,161] which we anticipated could also be adapted to our needs.

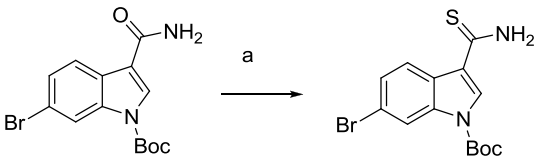

Scheme 3.11 Moody *et al*.'s thioamide synthesis[89,161]

a) Lawesson's reagent, benzene, reflux

Eftekhari-Sis *et al.* (**Scheme 3.12**)[141] and Guinchard *et al.* (**Scheme 2.11**)[91] have both shown that *N*-substituted α-oxoacetamides and α-oxothioacetamides could be synthesized from glyoxals and their

monohydrates via a Willgerodt-Kindler reaction, which we strongly considered given our previous expertise in glyoxal synthesis.

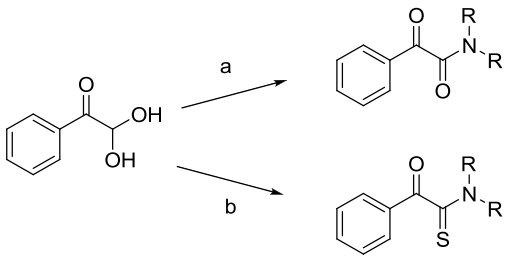

Scheme 3.12 Eftekhari-Sis *et al.*'s synthesis of α-oxoacetamides and α-oxothioacetamides[141]

a) R_2NH, Cu, air; b) R_2NH, S_8, 80 °C

Nitriles have proved to be useful intermediates in amide and thioamide synthesis. Various sulfur sources have been utilized to oxidize the nitrile functionality to afford the desired product. For example, LaMattina *et al.*[172] utilized diphenylphosphinodithioc acid[172,173] while Coleman *et al.*[174] and Jiang *et al.*[152] both bubbled H_2S through a solution of their respective nitriles in the presence of Et_3N (**Scheme 3.1**). An interesting alternative for the syntheses of thioamides, originally developed by Taylor and co-workers[175] and further applied by Gu *et al.*[133] and Chihiro *et al.* (**Scheme 3.13**),[176] utilized thioacetamide, which degrades into H_2S when exposed to warm HCl/DMF or other acidic solutions.[177]

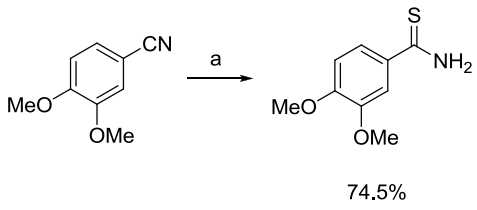

Scheme 3.13 Chihiro *et al.*'s thioamide synthesis[176]

a) Thioacetamide, 10% HCl/DMF, 100 °C, 2h.

Ferro *et al.*[178] have further shown that it is possible to oxidize nitriles to amides in the presence of NaOH and H_2O_2 (**Scheme 3.14**).

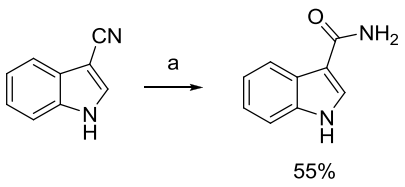

Scheme 3.14 Ferro *et al*.'s amide synthesis[178]

a) H_2O_2, NaOH, MeOH, r.t. 2h

3.4.3 Rationale for choosing the Hantzsch method to synthesize topsentin analogues

Of the two proposed methods to yield oxazole and thiazole, we concluded that, because of the accessibility of the reagents, the Hantzsch method was more appropriate than the cyclodehydration method. The additional potential application of this methodology to effect a regiospecific synthesis of topsentin type compounds e.g. **3.33** was also attractive in terms of extending the array of unsymmetrical topsentin analogues for screening. We surmised that a nitrile could be converted to an amidine **3.34**[179,180,181] and subsequently condensed with 2-halo-1-(1*H*-indol-3-yl)-ethanone to regiospecifically synthesize imidazoles (**Scheme 3.9**). This approach to the synthesis of biaryl, disubstituted imidazole compounds has been reported previously as exemplified here by Cheng *et al.* (**Scheme 3.15**).[180]

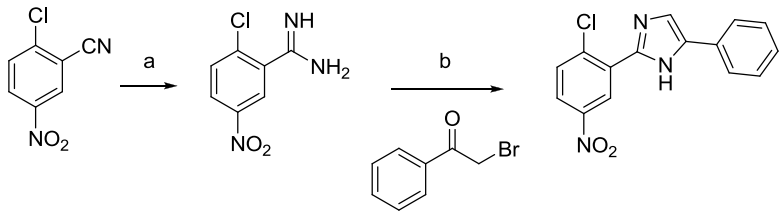

Scheme 3.15 Cheng *et al*.'s amidine and imidazole synthesis[180]

a) NH_4Cl, NaOMe, MeOH, reflux; b) $KHCO_3$, THF/H_2O, microwave, 120 °C.

In conclusion, we decided to synthesize bisindoles thiazoles and oxazole analogues via the respective condensations of α-oxo-1*H*-indole-3-thioacetamides or α-oxo-1*H*-indole-3-acetamide with 2-halo-1-

(1*H*-indol-3-yl)-ethanone analogues. The approaches to deliver the functionalized indole precursors necessary for these condensation reactions will be discussed below.

3.5 Synthesis of 2-halo-1-(1*H*-indol-3-yl)-ethanone analogues

3.5.1 Attempted synthesis of 2-halo-1-(1*H*-indol-3-yl)-ethanone analogues via direct acylation methods

In their work on Friedel-Crafts acylations of non protected NH indoles, Ottoni *et al.* also described the synthesis of both 2-chloro-1-(1*H*-indol-3-yl)-ethanone and 2-bromo-1-(1*H*-indol-3-yl)-ethanone utilizing three different acylating agents (**Scheme 3.16**).[104] Based on our previous success in utilizing their Friedel-Crafts method for the synthesis of 3-acetylindoles (Section **2.4.4**) we attempted this method using three acylating agents to deliver the desired products.

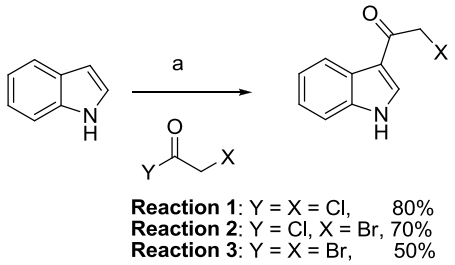

Scheme 3.16 Ottoni *et al.*'s Friedel-Crafts 2-halo-1-(1H-indol-3-yl)-ethanone synthesis[104]

a) $SnCl_4$, $MeNO_2$, 0 °C, 8 hours.

Following the Ottoni method with each of the three acylating agents, distinct colour changes were observed with the addition of $SnCl_4$ and again with the addition of acylating agent. TLC analysis after 8 hours showed that no starting indole remained, unfortunately however, the crude reaction products after work up resembled the red/brown tars described by Ottoni as representing a mixture of indole trimers.[104] Our crystallization method of purification as described in Section **2.4.4** did not

yield any product. We also attempted a method developed by Bergman *et al.*[182] in which chloracetyl chloride was added slowly to a solution of indole and pyridine in toluene at 55 °C (**Scheme 3.17**).

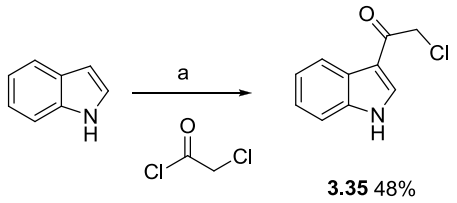

3.35 48%

Scheme 3.17 Bergman *et al.*'s indole acylation[182]

a) Toluene, pyridine, 55 °C, 1h.

The product from this reaction was a thick black oil which appeared to comprise several compounds of similar polarity from TLC analysis. Column chromatography yielded the desired product (**3.35**) in a meager 11% yield. In their paper, Bergman *et al.*[182] report a range of indole dimer side products in addition to various *N*-acetylated products in their product mixture, and we assumed we had a similar mixture in our hands. A yield of only 11% was unacceptable at the start of our synthesis and an alternative method to synthesize 2-halo-1-(1*H*-indol-3-yl)-ethanone was required.

3.5.2 α-Bromination of 3-acetylindole

While disappointingly we could not achieve the desired α-halo ketones in high yield in a single step, we attempted a selective of bromination of 3-acetylindoles, by utilizing a method for bromination of aryl methyl ketones developed by King *et al.* (**Scheme 3.18**).[183]

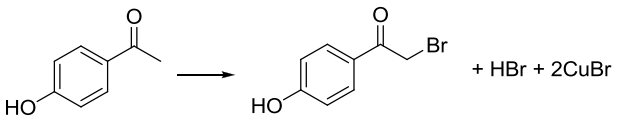

100%

Scheme 3.18 King *et al.*'s selective bromination of methyl ketones[183]

a) $2CuBr_2$, $CHCl_3$/EtOAc, reflux, 20 min

Braekman *et al.* had previously adopted this method to synthesize non protected 2-bromo-1-(1*H*-indol-3-yl)-ethanone in a low yield of 37% starting from 3-acetylindole (**Scheme 2.1**).[82] Moody *et al.* marginally increased the yield to 45% yield by first *N*-Boc protecting the 6-bromo-3-acetylindole starting material (**Scheme 3.19**).[89] As discussed previously Jiang *et al.* also exploited this bromination method to prepare a series of functionalized *N*-tosylated-2-bromo-1-(1*H*-indol-3-yl)-ethanones (**Scheme 3.1**).[133,152]

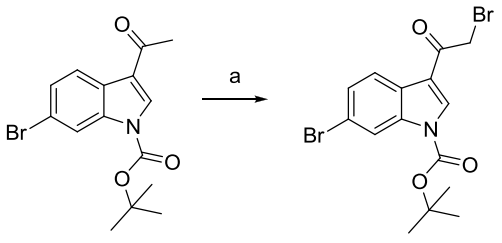

2.85 45%

Scheme 3.19 Moody *et al.*'s selective bromination of **2.85**[89]

a) $CuBr_2$, $CHCl_3$/EtOAc, 75 °C, 3h.

All of these reactions were carried out in a 1:1 $CHCl_3$: EtOAc solvent mixture which was established as a critical requirement by King *et al.* to ensure reasonable yields.[183] Interestingly Fort[184] showed that $CuBr_2$ behaves like molecular bromine when used in methanolic solution. King *et al.* used 1.6 eq. of $CuBr_2$ in their α-bromination reactions, which they explain stochiometrically translates into 0.8 eq. of available bromine and eliminates the formation of the dibrominated side product the formation of which was not reported by the authors.[183] However, Braekman *et al.*[82] who used the method of King *et al.*'s method reported the formation of the dibrominated side product in a yield of 5%.[82] Johnson and Bergman[185] also reported the formation of the dibrominated derivative when 1.2 eq. of pyridinium hydrobromide perbromide in $CHCl_3$ was used to effect α-bromination of 3-(1-benzenesulfonyl-1*H*-indolyl)-ethanone (**Scheme 3.20**).

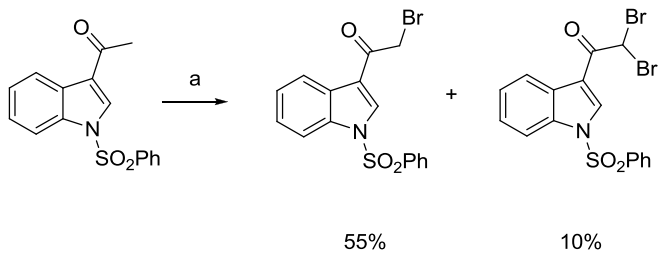

Scheme 3.20 Johnson and Bergman's bromination of 3-(1-benzenesulfonyl-1H-indolyl)-ethanone[185]

a) $PyHBr_3$, $CHCl_3$, reflux, 30 min.

Since we had previously been able to deliver the chloroform soluble *N*-Boc protected 3-acetylindole (**2.80**) in good yield, we attempted Moody's α-bromination method[89] on **2.80** as follows. A solution of 1 eq. of **2.80** in $CHCl_3$ was added to a green, vigorously stirring, refluxing suspension of 1.6 eq. of size reduced $CuBr_2$ in an equal amount of EtOAc. The reaction mixture was allowed to react for four hours, during which time the suspension had changed colour from green to amber. TLC and ^{1}H NMR analysis of the crude reaction mixture, suggested the presence of four products tentatively corresponding to two species each of 3-acetylindole, and the expected α-bromo ketone product. We suspected therefore that the mixture contained *N*-Boc protected (**2.80, 3.36**) and deprotected analogues (**2.1, 2.2**) of both 3-acetylindole and the brominated derivative respectively (**Figure 3.1**). This mixture was not purified, and the method was deemed unsuitable for our synthesis of the target compound because of the complexity of the product mixture. In an attempt to reduce the complexity of the product mixture, we performed the same reaction using non *N*-Boc protected **2.1** as the starting material (**Scheme 3.21**).

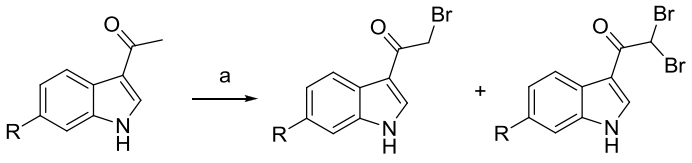

2.1 R = H
2.36 R = F
2.37 R = Cl
2.39 R = Br

2.2 R = H
3.38 R = F
3.40 R = Cl
3.41 R = Br

3.37 R = H
3.39 R = F
3.42 R = Cl
3.43 R = Br

Scheme 3.21 $CuBr_2$ mediated bromination of 3-acetylindoles **2.1, 2.36-2.39**

a) See table **3.1** for reation conditions.

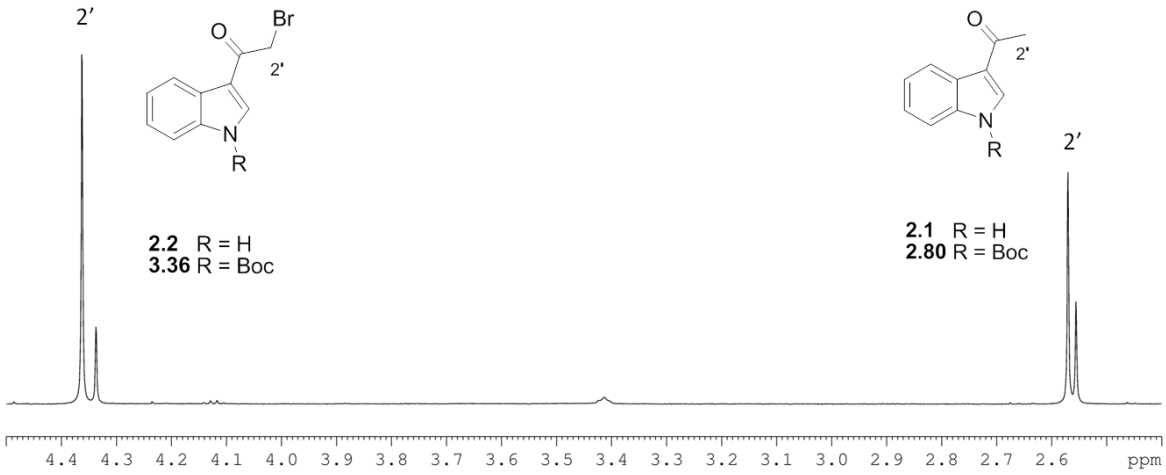

Figure 3.1 Upfield region (δ_H 2.4—4.5) of the ^{1}H NMR spectrum (600 MHz, $CDCl_3$) acquired from the crude reaction mixture after bromination of **2.1.** This region highlights the presence of four molecular species, with signals indicating two methyl ketone species, and two bromomethylene species, which we suspected were compounds **2.1, 2.80, 2.2** and **3.36** respectively.

The main, and ultimately critical, difference was the lower solubility of **2.1** in $CHCl_3$, which was added as a suspension in hot $CHCl_3$. After completion of the reaction as described above, the thick beige precipitate was filtered, and washed with EtOAc.

Following chromatography of the filtrate on silica (100% DCM), the yield of the desired product (**2.2, Figure 3.2**) was found to be a paltry 13%, with only 48% recoverable starting material and no other organic species were detected (**Table 3.1, Reaction 1**).

Increasing the amount of $CuBr_2$ (1.8 eq.) resulted in a marginally improved 22% yield of **2.2**, while when we altered our work up and eliminated the filtration step resulting in an improved 72% recovery of starting material (**Table 3.1, Reaction 2**). We then repeated the reaction with constant monitoring by TLC (**Table 3.1, Reaction 3**).

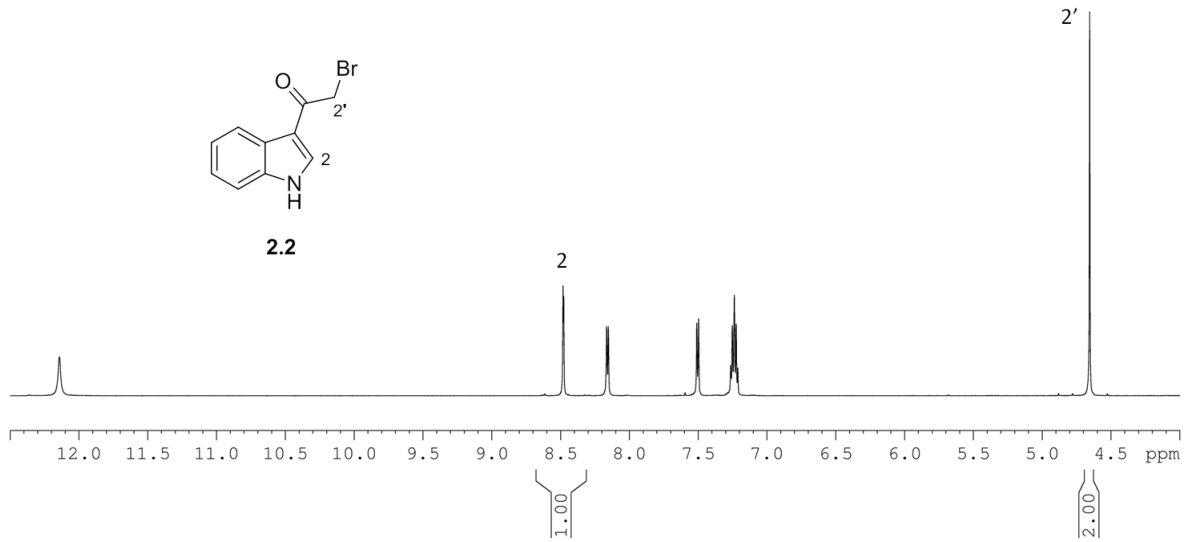

Figure 3.2 Region (δ_H 4.0—12.5) of the ^{1}H NMR spectrum (600 MHz, DMSO-d_6) of compound **2.2** showing the critical methylene signal at 4.65 ppm integrating for two protons.

After 6 hours we noticed a small third spot developing on the TLC plate with a faster retention time than **2.2**, at which time the reaction was stopped, worked up and purified, yielding 37% of **2.2** as well as a dibromo derivative (**3.37, Figure 3.3**) in a yield of 8%, corresponding to the unknown TLC spot.

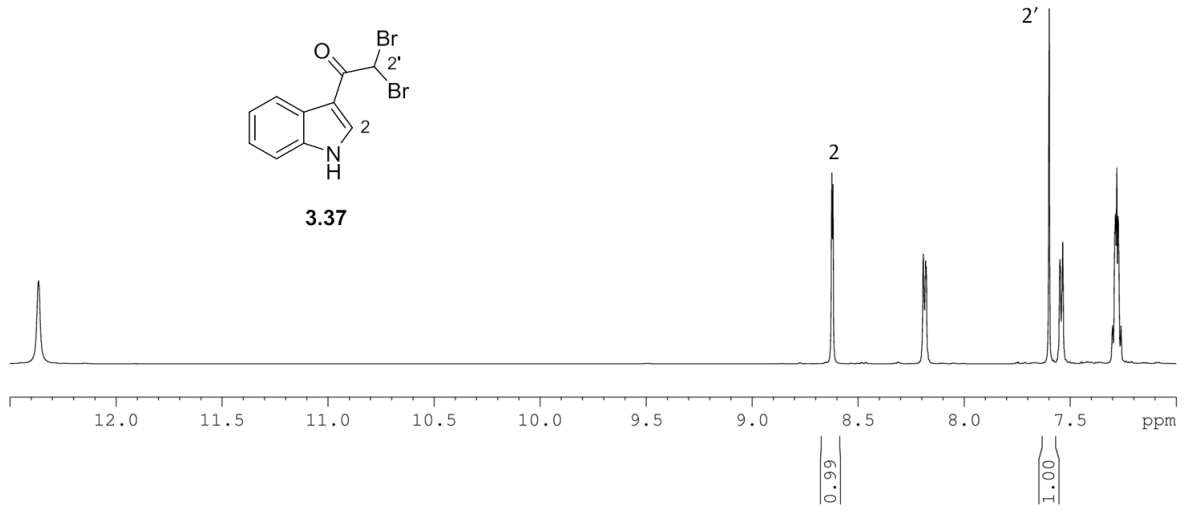

Figure 3.3 Region (δ_H 7.0—12.5) of the ^{1}H NMR spectrum (600 MHz, DMSO-d_6) of compound **3.37**. The singlet at 7.59 ppm corresponds to the proton at position 2'. The downfield shift of this signal is due to the de-shielding effect of a second electron withdrawing halogen.

We suspected that the low solubility of 3-acetylindole resulted in the unavailability of a significant proportion of this compound for reaction, and as a result the actual equivalence of bromine available was greater than that required, leading to the formation of the unwanted dibromo product **3.37**. We therefore repeated the reaction in which $CuBr_2$ (1.8 eq.) was suspended in refluxing EtOAc, to which a hot solution of **2.1** in EtOAc was added (**Table 3.1, Reaction 4**).

Reaction No.	Starting Material	$CuBr_2$ eq.	Ratio EtOAc:$CHCl_3$	Relative solvent volume	Time (hours)	Yield of mono-brominated product	Yield of dibrominated product	Recovered starting material
1	**2.1**	1.6	1:1	x	4	13%	0%	48%
2	**2.1**	1.8	1:1	x	4	22%	0%	72%
3	**2.1**	1.8	1:1	x	6	37%	8%	10%
4	**2.1**	1.8	1:0	x	3	6%	33%	61%
5	**2.1**	1.6	1:0	x	2.5	3%	20%	75%
6	**2.1**	1.8	1:1.3	5x	6	57%	3%	40%
7	**2.1**	1.1	1:1.3	5x	6	34%	0%	63
8	**2.36**	1.8	1:1.3	5x	2	47%	1%	50
9	**2.37**	1.8	1:1.3	5x	3	10%	2%	82
10	**2.37**	1.8	1:1	5x	2.5	28%	24%	31
11	**2.39**	1.8	1:1.3	5x	3	16%	4%	72%

Table 3.1 The reaction conditions used and the distribution of products from attempts to α-brominate 3-acetylindoles **2.1, 2.36, 2.37** and **2.39**.

Using TLC we noted the rapid formation of the **3.37** and after only three hours the reaction was halted and worked up in the usual manner to yield **2.1** (61%), **2.2** (6%) and **3.39** (33%).Presumably the yield of **3.39** would have been significantly larger had the reaction been allowed to proceed for a longer time. This same trend was observed when the equivalence of $CuBr_2$ was slightly reduced to 1.6 eq. (**Table 3.1, Reaction 5**) suggesting that carrying out the reaction EtOAc as the only solvent,

while a solution to the low stating material solubility problem, clearly enhanced unwanted dibromination. The possibility that the presence of $CHCl_3$ suppressed dibromination intrigued us and guided further modification of our reaction protocol.

The next modification in our attempt to boost the yield of our required monobrominated product was to increase the volume of the mixture of solvents added by a factor of 5 to aid the solubility of the reagents. In addition we changed the solvent ratio to allow a moderate excess of $CHCl_3$ to further suppress unwanted dibromination. This reaction was monitored by TLC and stopped after 6 hours after the formation of **3.37** was first observed (**Table 3.1, Reaction 6**). We were gratified to achieve a significant increase in the isolated yield of **2.2** (57%), the acceptable recovery of starting material (40%) and a minimal yield of **3.37** (3%). Our final attempt at improving the yield of **2.2** and minimizing the yield of **3.37** from this reaction was to repeat the reaction with only 1.1 eq. of $CuBr_2$ which after 6 hours had formed no **3.37**, whilst yielding **2.2** and **2.1** in 34% and 64% yields respectively (**Table 3.1, Reaction 7**). The limited quantities of 6-halogented 3-acetylindoles which we had in hand required us to gain a better fundamental understanding of the relationship between mono- and dibromination before applying the general reaction protocol (**Table 3.1, Reaction 6**) to synthesize the monobrominated derivatives of these compounds. Accordingly, the reaction was repeated and small (0.1 ml) aliquots were removed from the reaction mixture every 15 minutes over a period of 3.5 hours. The aliquots were immediately diluted with 0.4 ml of $CDCl_3$ for NMR analysis. ^1H NMR spectra were collected for each of the 15 samples and the relative concentrations of each of the three compounds of interest (**2.1, 2.2, 3.37**) were determined by normalization of a relevant compound H-2 proton signal (δ_H 7.86, 7.99, 8.23 respectively) against the EtOAc methyl signal (δ_H 2.05) which we assumed remained a relative constant in all 15 aliquots. The relative concentrations of **2.1**, **2.2** and **3.37** were plotted against time (**Figure 3.4**) and revealed that formation of **3.37** only occurs once the concentrations of **2.1** and **2.2** are roughly equal. This observation suggested to us that the reaction needed to be stopped shortly after **3.37** was detected, and yields of **2.2** greatly in

excess of 50% are effectively not possible using this method. However, the opportunity to recycle the majority of the unreacted starting material made this method acceptable for our needs and we proceeded with the selective mono α-bromination of 6-fluoro (**2.36**), chloro (**2.37**), and bromo (**2.39**) 3-acetylindoles (**Table 3.1, Reaction 8-11 and Scheme 3.21**).

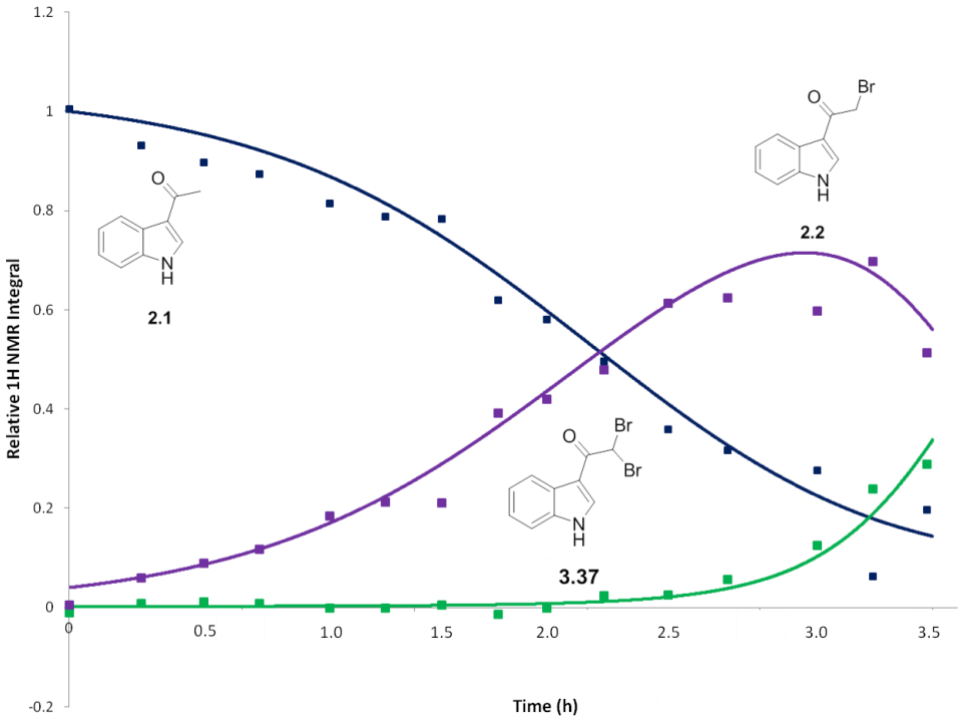

Figure 3.4 Plot of the ^{1}H NMR spectral relative intensities of species, **2.1, 2.2** and **3.37** vs. time for reaction 6 (**Table 3.1**).

Since we had limited supply of these starting materials, all reactions were monitored closely by TLC, and halted at the first sign of dibromination. The reaction of **2.36** progressed smoothly (**Table 3.1, Reaction 8**) and after 2 hours yielded 47% of the desired product (**3.38**) with negligible formation of the undesired dibrominated side product (**3.39**). Frustratingly, the monobromination of **2.37** and **2.39** (**Table 3.1, Reaction 9 and 11**) did not proceed as smoothly under the originally perceived optimal and broadly applicable reaction conditions established for the synthesis of **3.2** and **3.38** with low yields of 2-bromo-1-(6-chloro-1*H*-indol-3-yl)-ethanone (**3.40,** 10%), and 2-bromo-1-(6-bromo-1*H*-indol-3-yl)-ethanone (**3.41,** 16%). Critically, however, was the negligible formation of the

respective dibrominated analogues (**3.42** and **3.43**), which allowed for large recovery of starting materials, which were successfully recycled to increase the quantities of **3.40** and **3.41** available for further synthetic reactions. Interestingly, when we reacted **2.37** in a 1:1 EtOAc/$CHCl_3$ mixture, (**Table 3.1, Reaction 10**) which was stopped after only 2.5 hours, the yields of both **3.40** (28%) and **3.42** (24%) increased significantly with a small change in the amount of chloroform added to the reaction. Our tenuous interpretation of this single experimental result was that chlorinated (and possibly brominated) indole systems are more sensitive to a second α-bromination than the non-halogenated or 6-fluoro-3-acetylindole analogues. Regrettably the paucity of **2.37** and **2.39** prevented rigorous evaluation of this tentative assumption.

3.6 Synthesis of indolyl-3-carbonylnitriles 2.13, 3.45—3.47

As discussed in Section **3.4.2** our proposed synthetic pathway toward α-oxo-1*H*-indole-3-thioacetamide intermediates (Section **3.7**) required the initial synthesis of a carbonylnitrile precursor. Jonosik *et al.*[112] had developed a method to synthesize variably functionalized indolyl-3-carbonylnitriles over three steps from indole, via an initial Vilsmeier-Haack formylation, followed by reaction with trimethylsilyl cyanide (TMSCN) and finally a 2,3-dichloro-5,6-dicyano-1,4-benzoquinone (DDQ) mediated oxidation (**Scheme 3.22**).

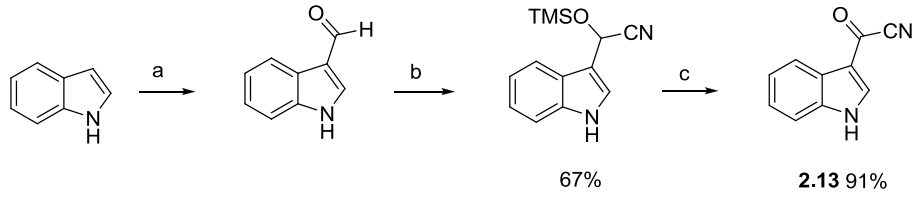

Scheme 3.22 Janosik *et al.*'s indolyl-3-carbonylnitrile synthesis[112]

a) DMF, $POCl_3$; b) TMSCN, MeCN, reflux, 2h; c) DDQ, dioxane, 2h.

However, we chose to use the method developed by Hogan and Sainsbury,[88] and utilized by Horne and co-workers on several occasions, to yield indolyl-3-carbonylnitrile (**2.13**) from indole in one pot.[87,162,186–190] In this reaction the relatively benign copper (I) cyanide , as opposed to the potentially lethal TMSCN is used as a nitrile source (**Scheme 2.7**). Although Janosik *et al.*[112] cautioned that Hogan and Sainsbury's method was low yielding when applied to halogenated indoles we considered that the potential advantages of a single low yielding reaction in one pot outweighed a three step reaction sequence. Especially a reaction sequence that required the use of TMSCN which readily generates noxious HCN on exposure to water.

3.6.1 Optimization of indolyl-3-carbonylnitrile (2.13) synthesis

We initially attempted the reaction as described by Hogan and Sainsbury, whereby oxalyl chloride was added dropwise to a solution of indole in ether under anhydrous conditions at 0 °C. After an hour, a suspension of 2 eq. of CuCN in toluene and a small portion of acetonitrile (MeCN) was added. The diethyl ether was initially distilled off from the reaction mixture which was then refluxed at 110 °C for 6 hours forming a dark brown suspension with significant insoluble material. The suspension was subsequently filtered to remove insoluble aggregates, and the dark coloured filtrate decolourized, by heating with activated charcoal. The pale yellow decolourized filtrate was concentrated under reduced pressure and the resultant residue chromatographed on silica (100% DCM) to yield **2.13** (12%) in a significantly lower yield than the yield of 53% reported by Hogan and Sainsbury.[88] Additionally we isolated a significant portion (30%) of 1*H*-3-indolecarboxylic acid (**2.28**).

The low yield of **2.13** prompted us to dissect this one pot reaction to better understand the contribution of each step in either enhancing or diminishing the yield of **2.13**. Our approach was therefore to separate out the steps from this one pot reaction to try and identify where the synthetic sequence may be susceptible to generating low yields of **2.13** (**Scheme 3.23**). The oxalyl

chloride reaction proceeded smoothly to yield a precipitate which was filtered then dried under vacuum. The precipitate was found to contain indolyl-3-glyoxal chloride (**2.17**), in excellent yield (91%) and acceptable purity by ^{1}H NMR.

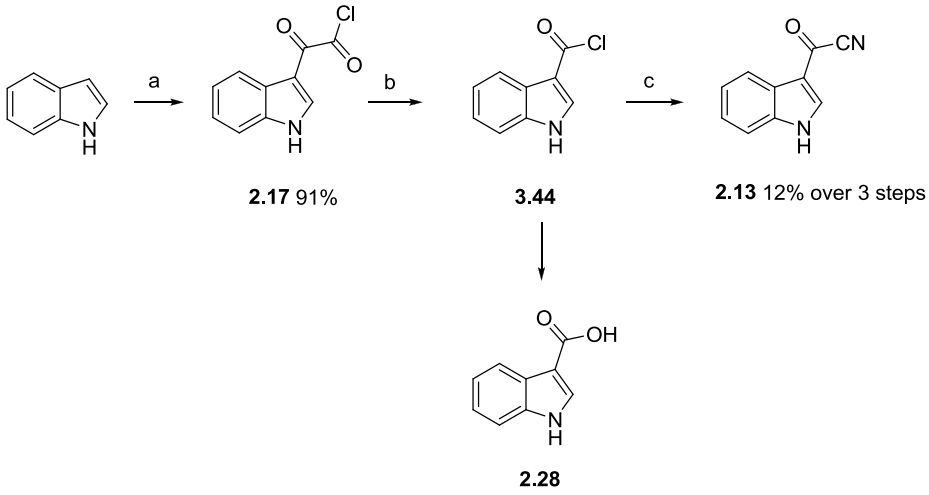

Scheme 3.23 Adaptation of Hogan and Sainsbury synthesis of **2.13**[88]

a) $(COCl)_2$, Et_2O, 0 °C, 1h. b) Toluene, reflux, 1h, c) CuCN, MeCN, reflux 16h.

The next step of the reaction was decarbonylation of **2.17** to afford 1*H*-Indole-3-carbonyl chloride (**3.44**). Glyoxal chlorides have been shown to thermolytically decarbonylate to an acid chloride when refluxed at high temperature (**Scheme 3.24).**[191,192] Accordingly compound **2.17** was refluxed in HPLC grade toluene that had been further dried over activated molecular sieves as a cautionary measure to eliminate any possible hydrolysis of **2.17** or **3.44** by trace amounts of water. The toluene was removed *in vacuo* to yield a yellow residue which was dried under vacuum. We had to assume that the yellow residue contained **3.44** as ^{1}H NMR analysis revealed the presence of the carboxylic acid **2.28** which may be due, in part, to the unavoidable presence of water in the DMSO-d_6 used for NMR data acquisition.

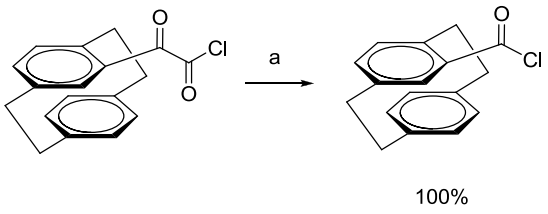

Scheme 3.24 Zitt *et al.*'s thermal decarbonylation[192]

a) PhCl, reflux, 40 h.

The yellow solid was finally added to a suspension of CuCN in HPLC grade acetonitrile and the reaction mixture refluxed for 16 hours. Moisture was excluded during refluxing by the addition of a calcium chloride drying tube. Synthesis of acyl cyanides have on several occasions been reported where cuprous cyanide is added to a refluxing solution of a corresponding acid chloride in acetonitrile (**Scheme 3.25**).[193,194] Apparently the presence of acetonitrile stabilizes the formation of cyanide ions from CuCN.[195]

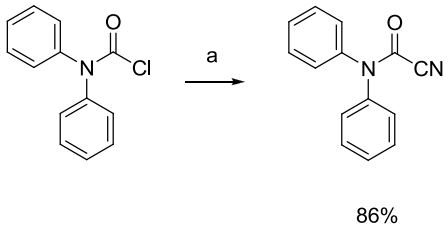

Scheme 3.25 Yu *et al.*'s carbonylnitrile synthesis[194]

a) CuCN, MeCN, reflux.

Clearly, there was no benefit in separating out the steps of the one pot reaction with a return of only 12% of **2.13** over three steps. We identified that overcoming the overwhelmingly facile hydrolysis of **3.44** to **2.28** in the presence of trace amounts of water as the key factor required to improve the yield of **2.13** from this reaction.

In addition a visual observation made during both the one pot reaction and our attempts at separating the one reaction into three separate reactions, was the formation of a significant black coloured aggregate during the reaction, which when broken up we discovered contained off white

crystalline solid which was likely unreacted CuCN. Accordingly we returned to the one pot protocol, with the intention of rigorously excluding moisture from the reaction and increasing the amount of CuCN used to introduce the nitrile functionality. All glassware was flame dried, solvents were dried according to standard protocols and redistilled directly before use, or if of HPLC grade further dried over activated molecular sieves. The reflux was conducted with the addition of a calcium chloride drying tube. Finally an increased quantity of CuCN (3 eq.) was gently introduced into the reaction flask over two minutes to avoid aggregation. We observed that the reaction mixture turned a characteristic dark brown colour after only 20 minutes. The reaction was monitored on TLC and stopped after two hours, delivering the desired product in reproducible yields of 71–73%, with the minimal formation of **2.28** (**Scheme 3.26**).

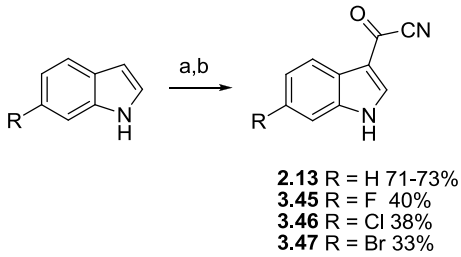

2.13 R = H 71-73%
3.45 R = F 40%
3.46 R = Cl 38%
3.47 R = Br 33%

Scheme 3.26 Successful adaptation of Hogan and Sainsbury's indolyl-3-carbonylnitrile synthesis

a) $(COCl)_2$, Et_2O, 0 °C, 1h; b) Toluene, MeCN, 3eq. CuCN (sprinkled), 110 °C, 2h (drying tube attached)

3.6.2 Synthesis of 6-halogenated indolyl-3-carbonylnitrile analogues 3.45—3.47

Although we were satisfied that the synthesis of **2.13** in reasonable yields was reproducible, application of the same one pot reaction protocol yielded halogenated carbonylnitriles 6-fluoro-3-indolyl-3-carbonylnitrile (**3.45**), 6-chloro-3-indolyl-3-carbonylnitrile (**3.46**) and 6-bromo-3-indolyl-3-carbonylnitrile (**3.47**) in lower yields (33-40%, **Scheme 3.26**) as predicted by Janosik *et al.*[112] Recently Yeung *et al.*[196] reported the substitution of bromine atom at C-7 on an indole ring by cyanide following the addition of CuCN in DMF (**Scheme 3.27**). We found no evidence of a similar nitrile

substitution occurring in any of the one pot reactions we performed in producing **3.47.** We were satisfied that we had been able to optimize this one pot reaction successfully, and that the low yields were possibly a function of the altered electronic environment arising from halogenation of the indole ring.

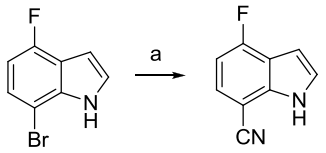

61%

Scheme 3.27 Yeung *et al*.'s nitrile bromine substitution[196]

a) CuCN, DMF, 145 °C, 17h.

3.7 Synthesis of α-oxo-1*H*-indole-3-thioacetamides 3.48—3.51

With our required carbonylnitriles in hand, we set about synthesizing the desired α-oxothioacetamides; α-oxo-1*H*-indole-3-thioacetamide (**3.48**), α-oxo-6-fluoro-1*H*-indole-3-thioacetamide (**3.49**), α-oxo-6-chloro-1*H*-indole-3-thioacetamide (**3.50**) and α-oxo-6-bromo-1*H*-indole-3-thioacetamide (**3.51**) (**Scheme 3.28**).

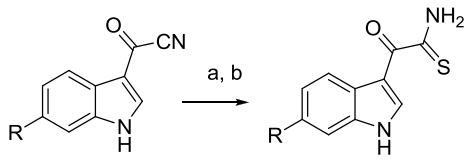

2.13 R = H
3.45 R = F
3.46 R = Cl
3.47 R = Br

3.48 R = H 58%
3.49 R = F 53%
3.50 R = Cl 58%
3.51 R = Br 51%

Scheme 3.28 Successful adaptation of the Taylor and Zoltewicz thioacetamide synthesis[175]

a) DMF, 80 °C; b) 4 eq. thioacetamide, 10% HCl/DMF, 1 eq. NaCl,

3.7.1 Synthesis of α-oxo-1*H*-indole-3-thioacetamide 3.48

The widely used method[133,176,197,198] for conversion of nitriles into thioamides originally introduced by Taylor and Zoltewicz[175] which utilizes thioacetamide in acidic conditions as an H_2S source, was deemed suitable for our purposes. Thioacetamide is easier to handle than either diphenylphosphinodithioic acid or H_2S and reportedly affords thioamides in higher yields.[197] None of these methods reported before had involved reaction with carbonylnitriles such as **2.13, 3.45—3.47**. Chihiro *et al.*'s adaption of the Taylor protocol required the addition of 2 eq. thioacetamide in HCl-DMF to a solution of nitrile followed by stirring the reaction at 100 °C for two hours.[176] The literature refers to an "HCl-saturated DMF solution"[198] and we therefore added a mixture of 35% HCl and DMF in a ratio of 1:0.78 to **2.13** and thioacetamide.

We noted a significant portion of both reactants did not initially dissolve. After stirring at 80 °C for 20 minutes the reaction mixture went pink and after two hours the colour changed to orange/brown. After the addition of ice and water the insoluble material was filtered off and the water fraction neutralized with sat. $NaHCO_3$ solution, and extracted with EtOAc. The EtOAc extract was evaporated under reduced pressure and the residue chromatograhed on silica (DCM: EtOAc 9:1) to afford **3.48** in low yield (19%).

^{1}H NMR analysis of the purified product revealed an interesting situation where the two amide proton signals appear as two independent singlets and not a broad singlet (**Figure 3.5**) in the NMR spectrum, indicating some form of coordination or restricted rotation possibly caused by the introduction of the sulfur moiety, hence differentiating between the chemical environments of the thioamide protons. Heating of the NMR sample from 298 K to 338 K did not to condense these signals.

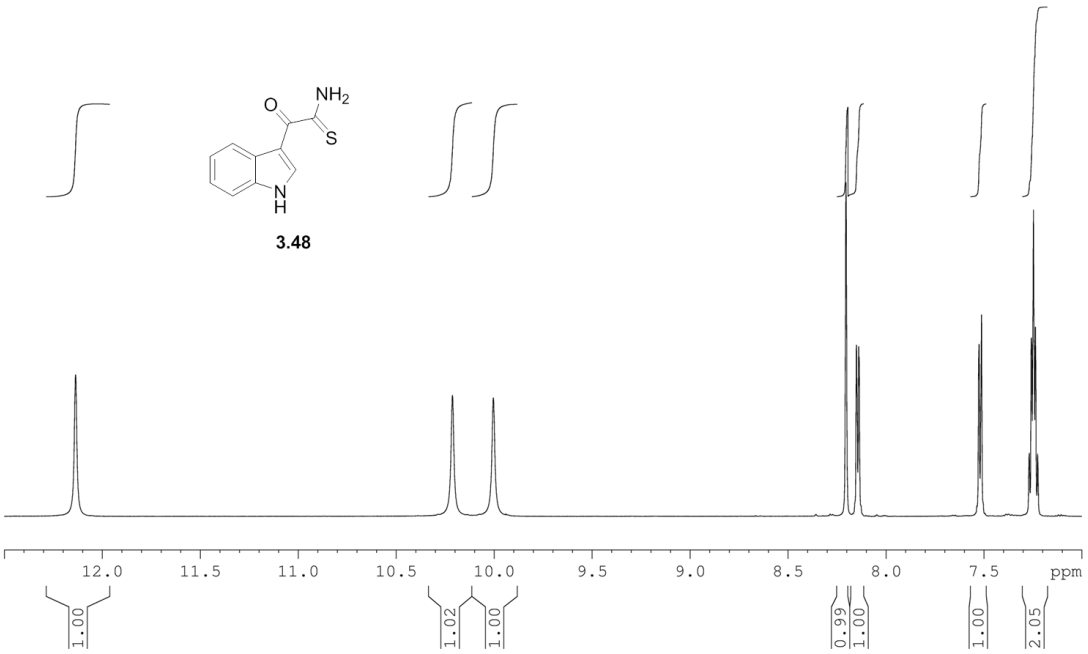

Figure 3.5 Downfield region (δ_H 7.0—12.5) of the ^{1}H NMR spectrum (600 MHz, DMSO-d_6) of compound **3.48.** The two signals at 10.21 and 10.00 ppm correspond to the NH_2 protons, which exist in different chemical environments.

3.7.2 Modification of α-oxothioacetamide synthesis and formation of *N*,*N*-dimethyl-1*H*-indole-3-carboxamide (3.52)

Based on our observations we suspected that the low yield was due in part to poor solubility of starting materials. We slightly altered our method, by dissolving **2.13** in DMF, and thioacetamide in an equal volume of HCl/DMF solution where the ratio had been changed to 2:0.78 to account for the DMF solution of **2.13**. The reaction mixture was allowed to stir at 80 °C for 1 hour, until a dark yellow colour endured. The same works up conditions were applied, and TLC indicated the presence of both starting materials with a prominent polar third spot. Purification resulted in the recovery of small quantities of starting materials, without the significant presence of desired product. What was of particular interest was a white crystalline product, corresponding to the prominent polar third TLC spot, isolated from the EtOAc column wash. ^{1}H NMR spectral analysis of this compound revealed a large singlet in the methyl region of the ^{1}H spectrum whose relative intensity indicated six protons were present (**Figure 3.6**).

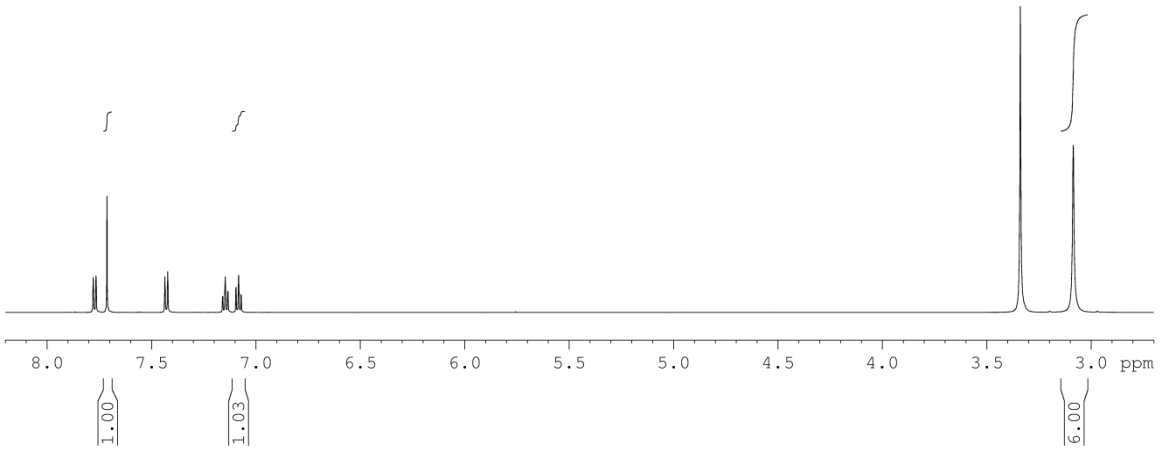

Figure 3.6 ^{1}H NMR spectrum (600 MHz, DMSO-d_6) of the unknown polar compound featuring six methyl protons, formed during attempted α-oxo-1*H*-indole-3-thioacetamide synthesis.

Strangely, no obvious ^{13}C methyl signal(s) were observed, nor was a HSQC correlation observed for the six proton signal. However, an HMBC correlation between the six proton signal and a carbonyl signal was observed. Heating of the sample in the NMR spectrometer from 298 K to 328 K resulted in the emergence of a small yet significant ^{13}C signal in the appropriate methyl region, which critically showed an HSQC correlation to the six proton signal, therefore providing evidence of C—H connectivity, and suggesting the unknown structure consisted of two methyl moieties near a carbonyl functionality (**Figure 3.7**). Since this reaction occurred in the presence of DMF, we suspected the product was *N*,*N*-dimethyl-1*H*-Indole-3-carboxamide (**3.52**).

A similar 6-flouro dimethylated analogue (**3.53**) was observed when compound **3.45** was subjected to a further modified method, in which all starting materials were dissolved in DMF, and a small portion of conc. HCl was added slowly into the solution. Interestingly, this resulted in the formation of a yellow precipitate, which dissolved upon heating. After two hours, the yellow solution was subjected to the same work up and purification as described for **3.48**. While none of the desired **3.49** was isolated, **3.53** was observed in the EtOAc wash, again providing anomalous NMR data.

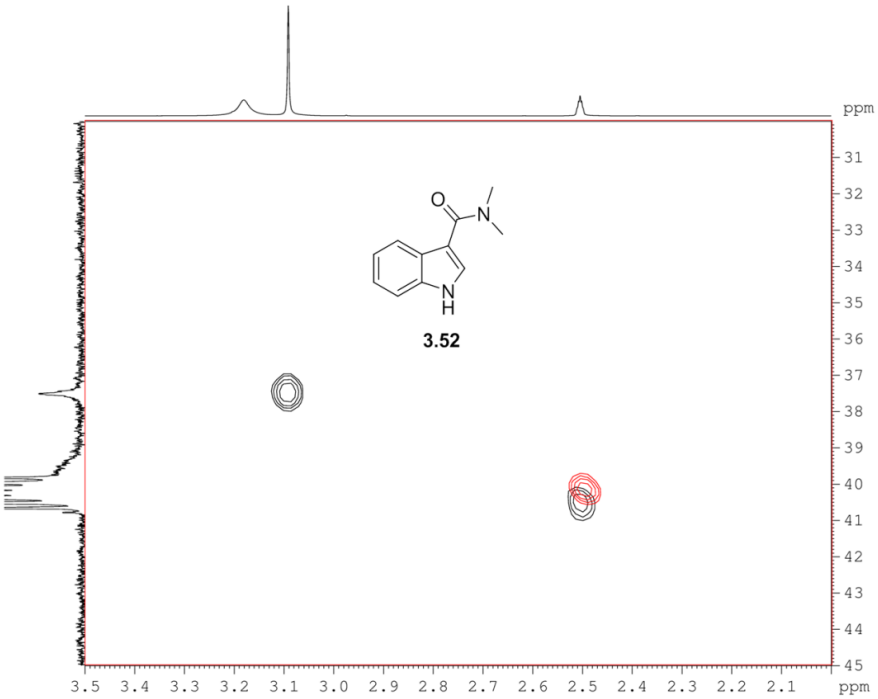

Figure 3.7 Upfield region (F1 = δ_c 30—45; F2 = δ_H 2.0—3.5) of the HSQC NMR spectrum of compound **3.52** (600 MHz, DMSO-d_6 relaxation time [d1] = 1.50 s) performed at 298 K (red) overlaid with the corresponding HSQC at 328 K (black). Note the formation of the HSQC correlation between the unresolved six proton signal in the ^{1}H NMR spectrum and a previously unseen ^{13}C methyl signal.

HRMS data of both **3.52** and **3.53** as well as X-ray crystallographic analysis of **3.52** (**Figure 3.8**) confirmed the chemical structures of these compounds as was *N*,*N*-dimethyl-1*H*-Indole-3-carboxamide (**3.52**) and was *N*,*N*-dimethyl-6-fluoro-1*H*-Indole-3-carboxamide (**3.53**) respectively.

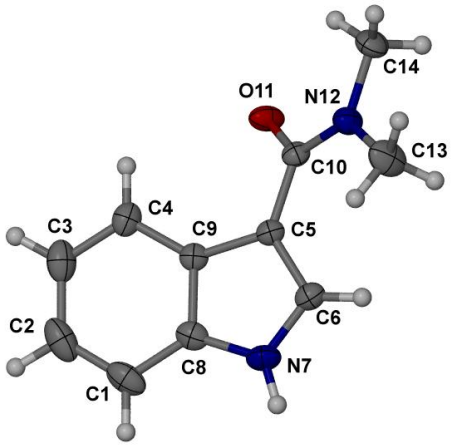

Figure 3.8 ORTEP representation of X-Ray crystal structure of compound **3.52** CCDC No. 646899.[199]

Kumar *et al.*[200] have recently reported the synthesis of *N*,*N*-dimethyl benzamide analogues via copper catalyzed oxidative coupling of aryl carboxylic acids and DMF, in which they propose an unusual decarboxylation reaction mechanism (**Scheme 3.29**).

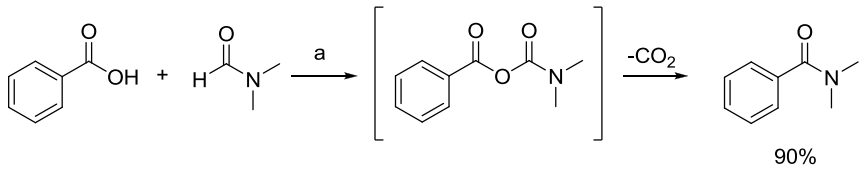

Scheme 3.29 Kumar *et al*.'s synthesis of *N*,*N*-dimethyl benzamide[200]

a) $Cu(ClO_4)_2 \bullet 6H_2O$ (10 mol%), TBHP, 100 °C,15h.

Although we considered this mechanism possibly occurring after acid hydrolysis of the carbonylnitrile into an organic acid, we remained unconvinced. We rather suspected than an amine contaminant was attacking the electrophilic carbonyl with the elimination of a cyanide ion.

^{1}H NMR analysis of our DMF solvent suggested that no amine was present as a contaminant. However, when DMF was heated in the presence of conc. HCl for 1 hour, and analyzed by NMR spectroscopy we observed a significant formation of a second methyl species consistent with dimethylamine hydrochloride, formed from acid hydrolysis of DMF. We then conducted a series of experiments, to confirm if DMF isn't formally involved in this reaction and to determine the nature of the electrophile (carboxylic acid or carbonylnitrile).

Reaction of **2.13** in DMF at both 80 °C and room temperature (**Scheme 3.30 a and b**), resulted in no change to **2.13** in either case. We then repeated the reaction of **2.13** in HCl/DMF solution at room temperature for 1 hour, which was then neutralized, and extracted with EtOAc (**Scheme 3.30 c**).

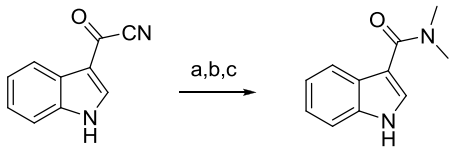

2.13 **3.52**

Scheme 3.30 Attempted formation of **3.52**

a) DMF, 80 °C 24h.
b) DMF, r.t. 24h.
c) HCl, DMF r.t. 1h.

^{1}H NMR analysis of the crude reaction mixture revealed the formation of **3.52**, along with a complex mixture of products, while no starting material remained. Importantly, no evidence of the carboxylic acid (**2.28**) was observed. To confirm that the carboxylic acid isn't involved in amide formation, 6-fluoro indolyl-3-carboxylic acid (**3.54**) was reacted with DMF and HCl/DMF at room temperature, both of which resulted in no reaction occurring (**Scheme 3.31**).

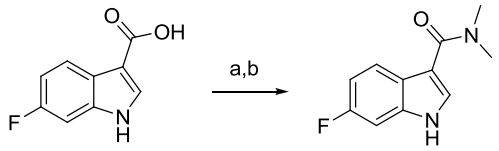

3.54 **3.53** 0%

Scheme 3.31 Attempted formation of **3.53**

a) DMF, r.t. 24h.
b) HCl, DMF r.t. 1h.

3.7.3 Attempts to avoid formation of *N*,*N*-dimethyl-1*H*-Indole-3-carboxamide

An attempt to avoid the formation of dimethylamine hydrochloride by conducting the reaction without DMF was unsuccessful. In this reaction a thioacetamide solution in 20% HCl/H_2O was added to a stirring solution of indolyl-3-carbonylnitrile in acetone. It appeared therefore that the DMF was

critical for the reaction to occur, which forced us to consider methods to ensure that H_2S evolved at a faster rate thus being available for reaction earlier, and therefore being able to compete with the side reaction that afforded *N*,*N*-dimethyl-1*H*-Indole-3-carboxamide. Rosenthal and Taylor[177] had shown that thioacetamide hydrolysis is catalyzed by both acid and base, and thioacetamide accordingly degrades into acetic acid, NH_3 and H_2S. They further showed that the rate of acid induced hydrolysis could be increased with the addition of NaCl to a warm thioacetamide HCl solution.[177] Based on Rosenthal and Taylor's findings[177] we adapted our method as follows. The indolyl-3-carbonylnitrile **2.13** was dissolved in DMF and heated to 80 °C. To this was added a warm solution of thioacetamide (4 eq.) and NaCl (0.1 eq.) in double the volume of HCl/DMF (1:0.78), resulting in an instant colour change of the solution to dark yellow. After four hours the reaction was worked up and purified in the usual manner, resulting in a much improved yield of **3.48** (58%), without the presence of any **3.52**. We then applied this method to the halogenated carbonylnitriles (**2.13, 3.45—3.47**) to yield compounds **3.49—3.51** at yields of 53, 58 and 51% respectively (**Scheme 3.28**). These compounds were found to be unstable when exposed to light and air, and as such were reacted as soon after purification as was possible.

3.8 Hantzsch thiazole synthesis of 1*H*-indol-3-yl[4-(1*H*-indol-3-yl)-thiazole-2-yl]-methanone analogues 1.62—1.68

With both the α-oxo-1*H*-indole-3-thioacetamide analogues (**3.48—3.51**) and 2-bromo-1-(1*H*-indol-3-yl)-ethanone (**2.2, 3.38, 3.40, 3.41**) required for thiazole synthesis in hand we set about utilizing a method developed by LaMattina and Mularski[172] in which an equal equivalence of thioamide (**3.55**) and α-bromoketone (**3.56**) were cyclized by allowing the reagents to simply stir in acetone at room temperature over a period of two days. Interestingly, the authors noted at the outset their intention to synthesize an acylthiazole, but opted to rather form the thiazole ring with a TMS protecting group

present, which they later removed, and oxidized over two steps to yield the 2-acylthiazole **3.57** (**Scheme 3.32**). Their rationale for this approach was that electron withdrawing groups e.g. carbonyls adjacent to the thioamide reduces reactivity towards cyclisation.[172]

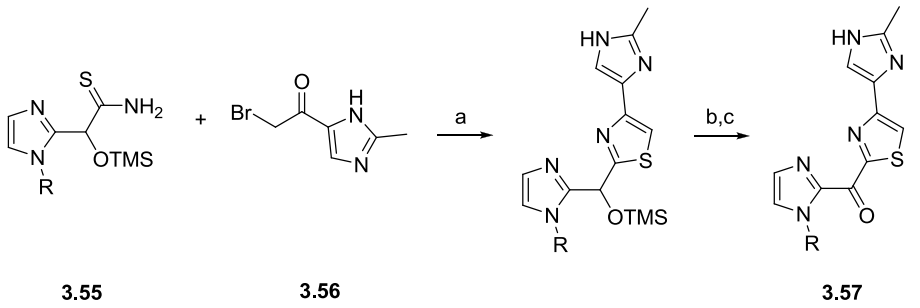

3.55 **3.56** **3.57**

Scheme 3.32 LaMattina and Mularski's synthesis of thiazole **3.57**[172]

a) Acetone, r.t. 48h; b) -10 °C, N_2, TBAF, 1h; c) MnO_2, THF 0 °C 2h.

We didn't encounter any problems with leaving our ketone functionality unprotected and we successfully adapted this method, (preferring to perform the reaction in the dark because of the light sensitivity of the thio intermediates), to afford 1*H*-indol-3-yl[4-(1*H*-indol-3-yl)-thiazole-2-yl]-methanone (**1.62**) at a reasonable yield (74%) after only 24 hours.

This method was then successfully applied to yield 6-fluoro-1*H*-indol-3-yl[4-(6-fluoro-1*H*-indol-3-yl)-thiazole-2-yl]-methanone (**1.63**), 6-chloro-1*H*-indol-3-yl[4-(6-chloro-1*H*-indol-3-yl)-thiazole-2-yl]-methanone (**1.64**) and 6-bromo-1*H*-indol-3-yl[4-(6-bromo-1*H*-indol-3-yl)-thiazole-2-yl]-methanone (**1.65**) at yields of 83, 58 and 51% respectively (**Figure 3.9**). Interestingly all these compounds were found to be highly fluorescent (**Figure 3.10**).

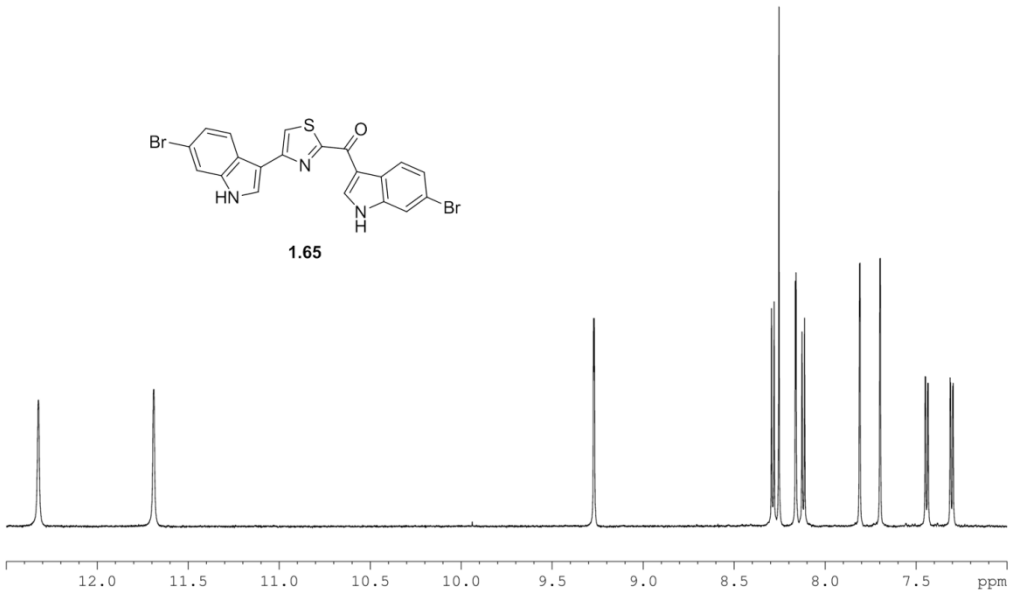

Figure 3.9 Downfield region of the ^{1}H NMR spectrum of compound **1.65** (δ_H 7.0—12.5; 600 MHz, DMSO-d_6).

Figure 3.10 Fluorescence of compound **1.64** (roughly 0.1 mg) when irradiated with ultraviolet light (365 nm) This fluorescence was observed for all thiazoles synthesized.

We further applied the regiospecificity of this method to synthesize 6-fluoro-1*H*-indol-3-yl[4-(6-bromo-1*H*-indol-3-yl)-thiazole-2-yl]-methanone (**1.66**), 6-bromo-1*H*-indol-3-yl[4-(6-fluoro-1*H*-indol-

3-yl)-thiazole-2-yl]-methanone (**1.67**) and 6-chloro-1*H*-indol-3-yl[4-(6-fluoro-1*H*-indol-3-yl)-thiazole-2-yl]-methanone (**1.68**), which were chosen based on docking data (Chapter 4) in yields of 31%, 54%, and 53% respectively (**Scheme 3.33**). Significantly we were able to retain the α-ketone moiety without additional synthetic protection and deprotection steps required.

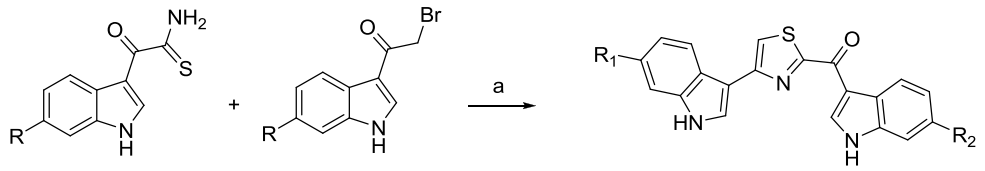

3.48 R = H
3.49 R = F
3.50 R = Cl
3.51 R = Br

2.2 R = H
3.38 R = F
3.40 R = Cl
3.41 R = Br

1.62 $R_1 = R_2 = H$ 74%
1.63 $R_1 = R_2 = F$ 83%
1.64 $R_1 = R_2 = Cl$ 58%
1.65 $R_1 = R_2 = Br$ 51%
1.66 $R_1 = Br$, $R_2 = F$ 31%
1.67 $R_1 = F$, $R_2 = Br$ 54%
1.68 $R_1 = F$, $R_2 = Cl$ 53%

Scheme 3.33 Thiazole formation to yield desired thiazole products

a) Acetone, r.t. 24h

We then attempted to determine the influence of a second bromination e.g. **3.37** would have on cyclization, and if our efforts to minimize dibromination in the preparation of **2.2, 3.38, 3.40** and **3.41** were of any consequence. We applied our method to cyclize **3.48** with **3.37** using the established synthetic protocol. After 6 days the reaction was stopped yielding only 11% of (**Scheme 3.34**) thus justifying our efforts to limit dibromination.

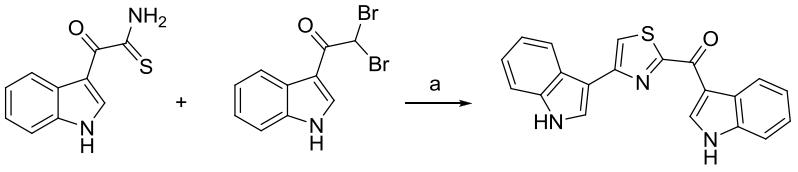

3.48 **3.37** **1.62** 11%

Scheme 3.34 Thiazole formation from **3.37**

a) Acetone, r.t. 6 days

3.9 MRSA PK inhibition activity of 1.62—1.68

As discussed in the introduction to this chapter (Section **3.1**) we were interested to determine the effect on the potent MRSA PK inhibition of the topsentin analogues by replacing the imidazole ring with an aromatic thiazole ring. The critical observations we were attempting to make were firstly the importance of a H-bond donating NH moiety on the imidazole compared to the sterically larger H-bond accepting sulfur and secondly the role of the prominent histidine residues in ligand binding which are possibly involved in π-stacking interaction with the central aromatic moiety (Chapter 4). Finally we were attempting to determine whether activity would be influenced by different halogens on each of the indole rings and whether a particular halogen on an indole ring was more suitable for biological activity as predicted my molecular docking studies (Chapter 4).

Significantly, none of the assayed compounds displayed 100% MRSA PK inhibition at concentrations as high as 100 μM (**Figure 3.11**), while both disappointingly and interestingly, IC_{50} values for MRSA PK inhibition increased by several orders of magnitude upon replacement of the imidazole with the thiazole moiety (**Figure 3.12**). However, these compounds can still be considered moderate inhibitors of MRSA PK with IC_{50} values as low as 5.1 μM.

The SAR trend observed for compounds **1.62—1.65** with regard to halogen substitution does not mirror that observed for either the topsentin analogues in Chapter 3, but rather followed that observed for the hamacanthin analogues[22] in which activity improved as the C-6 indole substituents got larger. Moderate differences in IC_{50} values are observed, it is interesting to note that while the non halogenated analogue **1.62** was still the least active, it was closer in activity to the other analogues than the previously mentioned studies. The difluorinated analogue **1.63** was moderately more active than **1.62,** while contrast to the topsentin study, the dibrominated analogue **1.65** was more active than the dichlorinated analogue **1.64**. While the differences in activity of compounds **1.62—1.65** provide further SAR information, the small changes in IC_{50} data is insignificant in comparison to the changes observed in activity when the imidazole is replaced with a thiazole. The

data at hand obtained from *in vitro* studies, strongly suggests that the potential for π-stacking interactions with the histidine residues located in our prospective binding site is not as significant a factor as the potential for hydrogen bond interaction of the imidazole NH. This is however purely speculative, since this interaction has not been predicted by *in silico* studies and the steric hindrance induced by the larger sulfur atom may be having a serious negative effect on binding. Alternatively, these compounds may be binding in an alternative site on MRSA PK.

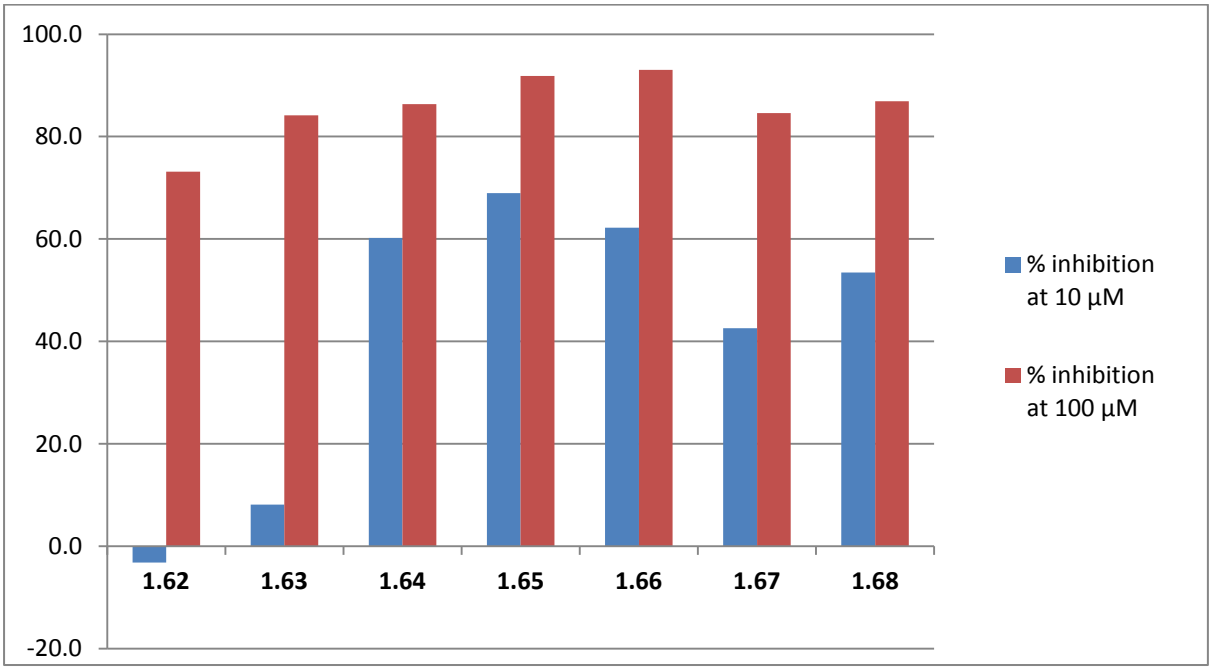

Figure 3.11 % Inhibition data for thiazole containing bisindoles **1.62—1.68** obtained at two concentrations.

The activities of differently halogenated compounds **1.66—1.68** implied that the larger bromine improved activity, while overall suggesting that for this series, optimizing molecule size by way of different sized substituents is of little significance, while the inhibitory activity of compounds **1.66** and **1.67** were similar, suggesting that the respective indole ring on which a halogen appears is of little consequence.

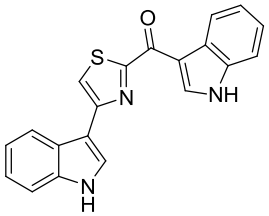

1.62 IC_{50} 20.0 μM

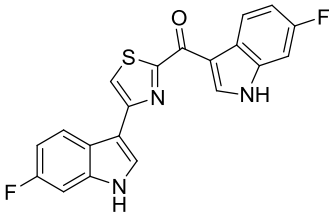

1.63 IC_{50} 12.6 μM

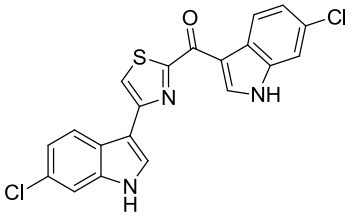

1.64 IC_{50} 11.7 μM

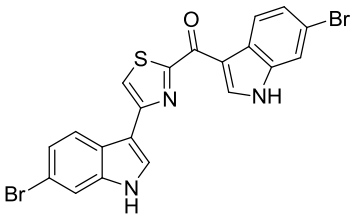

1.65 IC_{50} 5.2 μM

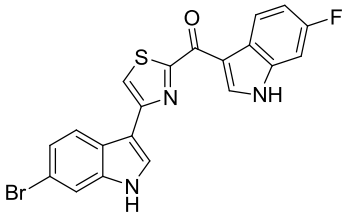

1.66 IC_{50} 5.1 μM

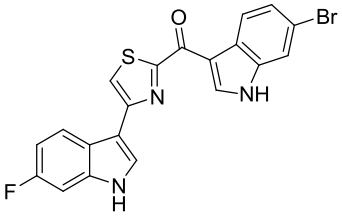

1.67 IC_{50} 6.6 μM

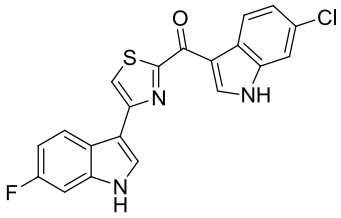

1.68 IC_{50} 7.9 μM

Figure 3.12 IC_{50} data for compounds **1.62—1.68** against MRSA PK

3.10 Attempted application of our Hantzsch methodology for oxazole and imidazole synthesis

Having been successful with our thiazole bis-indole synthesis, we turned our attention toward the regiospecific synthesis of oxazole and imidazole topsentin analogues via our established Hantzsch methodology. Since many of the required intermediates were at hand, we proposed first to synthesize oxazoles via a cyclization of 2-bromo-1-(1*H*-indol-3-yl)-ethanone analogues e.g. **2.2** with indolyl-3-α-oxoacetamide analogues e.g. **3.32**, which could be prepared from amination of indolyl-3-glyoxal chlorides (**Scheme 3.10)** Similarly we envisioned the synthesis of indolyl-3-α-oxocarboxamidine analogues e.g. **3.58** from indolyl-3-carbonylnitriles (**Scheme 3.15**) followed by cyclization with 2-bromo-1-(1*H*-indol-3-yl)-ethanone analogues e.g. **2.2** to regiospecifically deliver topsentin analogues (**Scheme 3.35**).

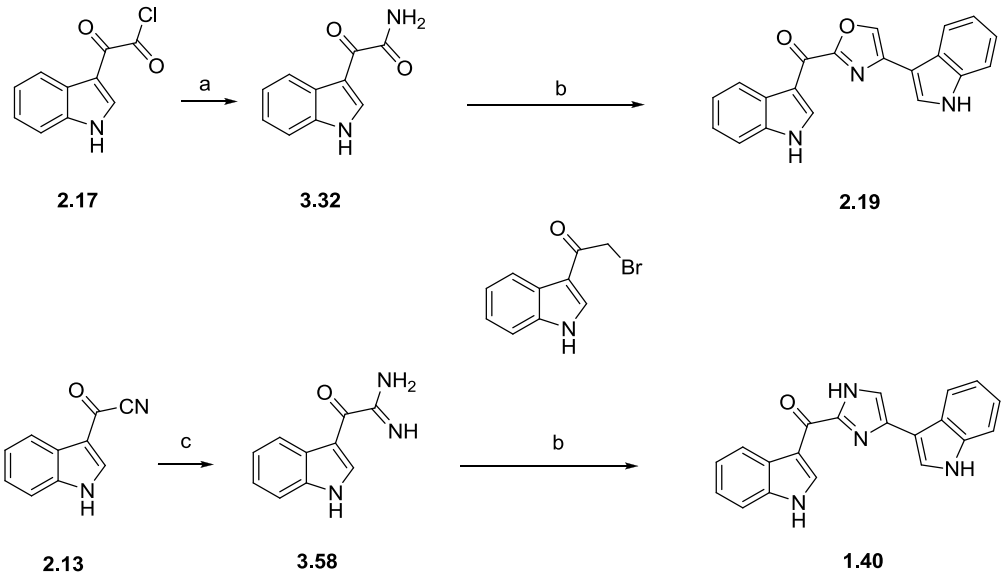

Scheme 3.35 Proposed regiospecific oxazole and imidazole synthesis

a) NH_4Cl, NaOH; b) Acetone 24 h;
c) NH_4Cl, NaOMe, MeOH, reflux

3.10.1 Synthesis of indolyl-3-α-oxoacetamide 3.32

Indolyl-3-α-oxoacetamide **3.32** was simple to access in one pot quantitatively from indole. Indolyl-3-glyoxal chloride **2.17** was synthesized via the method detailed in Section **3.4.2**. To a stirring suspension of **2.17** in ether was added an aqueous mixture of NH_4Cl and NaOH, resulting in a violent reaction to yield **3.32** (**Scheme 3.36**).

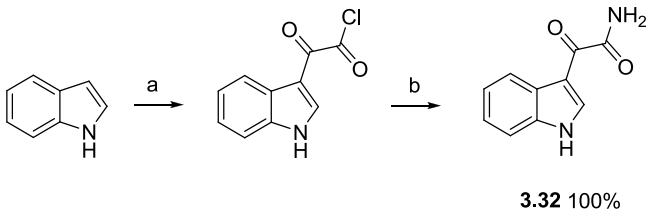

Scheme 3.36 Synthesis of **3.32**

a) $(COCl)_2$, Et_2O, 0 °C, 1h. b) NH_4Cl, NaOH, 1 min

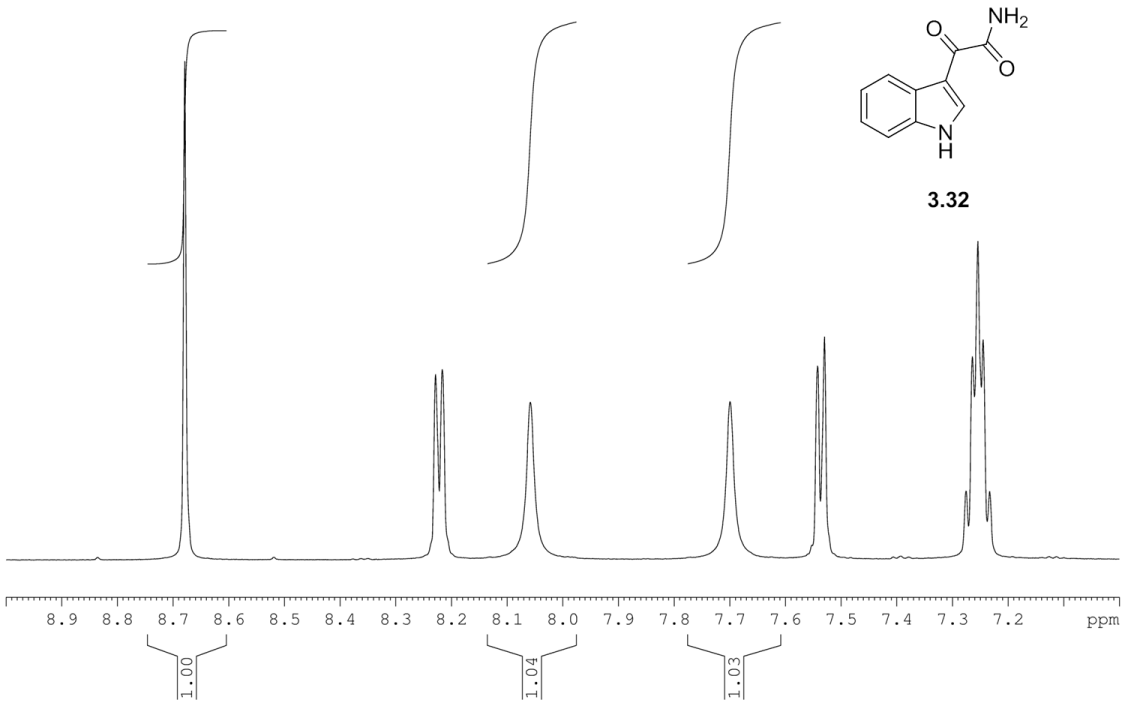

Figure 3.13 Downfield region of the ^{1}H NMR spectrum of compound **3.32** (δ_H 7.0—9.0; 600 MHz, DMSO-d_6). The NH_2 proton signals at 7.69 and 8.05 ppm appear as separate singlets indicating that each proton exists in different chemical environments.

The suspension of **3.32** was acidified with dil. HCl and washed with EtOAc, then neutralized with $NaHCO_3$ and extracted with EtOAc to quantitatively yield **3.32.** ^1H NMR spectral analysis revealed that the NH_2 proton resonances existed as individual singlets and not a single broad signal (**Figure 3.13**), which is the same pattern observed for indolyl-3-α-oxothioacetamide compounds **3.48—3.51**.

3.10.2 Attempted oxazole synthesis

Oxazole condensation between **3.32** and **2.2** to form **2.19** (**Scheme 3.37**) was initially conducted in acetone at both room temperature and reflux for 24 hours with no success, and only starting materials were recovered. We then attempted the cyclization reaction using the literature standard of ethanol as described by Moody *et al.*[170](**Scheme 3.6**) again with no success. We then turned our attention to the work of Ritson *et al.*[201] who were able to synthesize oxazole from amides and α-bromo ketones under microwave conditions with the addition of stochiometric amounts of silver salts (**Scheme 3.38**).[201] They reasoned that the halophilicity of silver salts, would drive the formation of AgBr and activate the α-bromoketone toward attack from the nucleophile.[201]

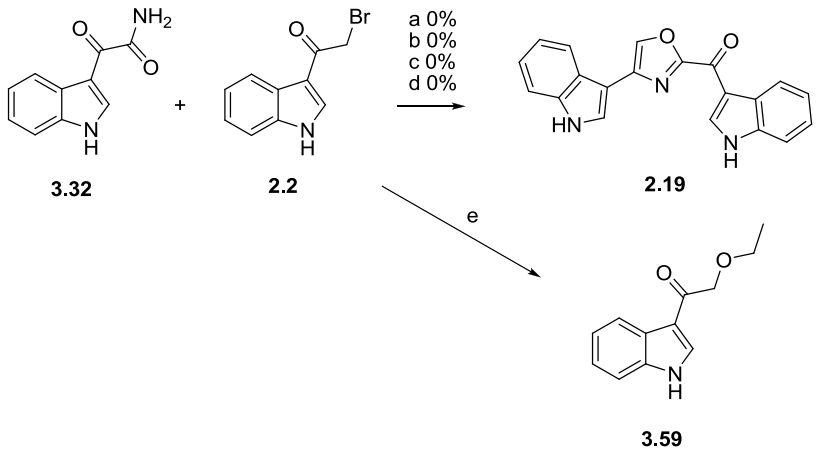

Scheme 3.37 Attempted oxazole synthesis

a) Acetone, r.t. 24h; b) acetone, reflux 24h; c) ethanol, r.t. 24h; d) $AgClO_4$, acetone, reflux, 24 hours; e) $AgClO_4$, ethanol, reflux, 24 hours.

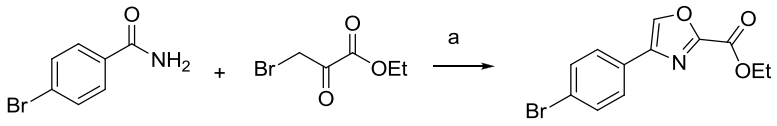

Scheme 3.38 Ritson *et al*.'s silver salt mediated oxazole synthesis[201]

a) AgX, DCE, microwave 90 °C, 30 min.

We repeated the cyclization reaction in both acetone and ethanol under reflux with the addition of silver perchlorate. After work up, the reaction in acetone yielded starting materials only, without any product, while the reaction in ethanol led to the formation and isolation of 2-ethoxy-1-(1*H*-Indol-3-yl)-ethanone (**3.59**) along with the recovery of **3.32** (**Scheme 3.37 e**). We concluded that the silver salt was successful in preparing **2.2** for nucleophillic attack, however in this instance ethanol proved to be a better nucleophile than **3.32** possibly due to the presence of the electron withdrawing ketone adjacent to the amide group reducing reactivity, as predicted by LaMattina.[172]

3.10.3 Attempted synthesis of indolyl-3-α-oxocarboxamidine 3.58

The α-ketone group adjacent to the nitrile in compound **2.13** again proved to be problematic in our attempted regioselective imidazole synthesis. We attempted to convert **2.13** into indolyl-3-α-oxocarboxamidine **3.58** via a method adapted from Cheng *et al*. (**Scheme 3.15**).[180] This method required the reaction of indolyl-3-carbonylnitrile in refluxing methanol in the presence of NH_4Cl and NaOMe. However, the sensitive carbonylnitrile was attacked by the methoxy nucleophile resulting in the formation of the 1*H* Indole-3-carboxylic acid methyl ester **3.60** (**Scheme 3.39**).

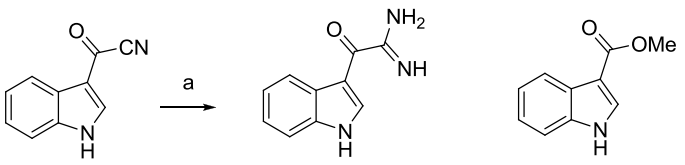

2.13 **3.58** 0% **3.60**

Scheme 3.39 Attempted synthesis of indolyl-3-α-oxocarboxamidine **3.60**

a) NH_4Cl, NaOMe, MeOH, reflux.

Due to time constraints we had to abandon the synthesis of both the imidazole and oxazole compounds. However, we felt that both our oxazole and imidazole reaction schemes may be more successful if a protected ketone, such as the TMS protected ketone used by Janosik *et al.*[112] for cyclization and amidine formation. We reason the TMS protection would negate the electron withdrawing nature of the ketone moiety, thus making **3.32** a more efficient nucleophile, as well as protecting the labile carbonylnitrile from nucleophilic attack (**Scheme 3.40**).

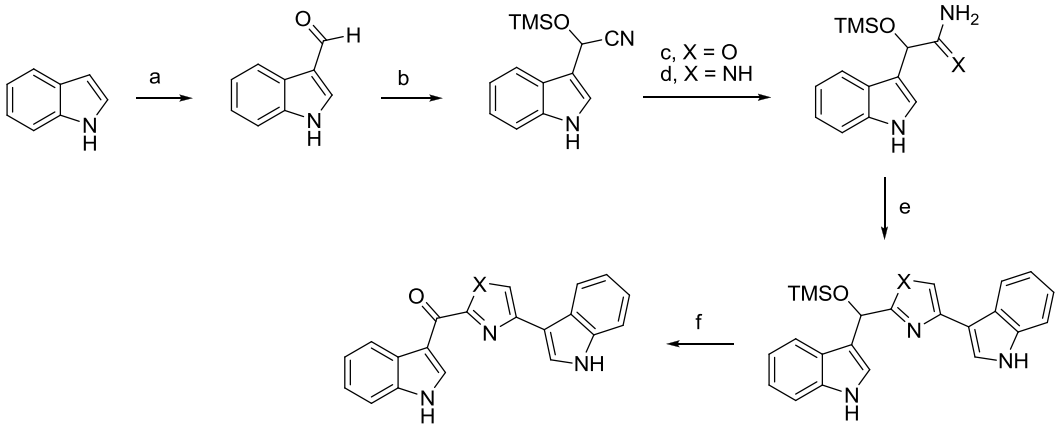

Scheme 3.40 Proposed oxazole and imidazole synthesis

a) DMF, $POCl_3$; b) TMSCN, MeCN, reflux; c) H_2O_2, NaOH, MeOH, r.t. d) NH_4Cl, NaOMe, MeOH, reflux; e) **2.2**, EtOH; e) DDQ, dioxane, 2h.

3.11 Conclusions

In conclusion, we were successful in developing a new method to regiospecifically synthesize a cohort of unknown thiazole containing bisindole topsentin analogues. The indolyl-3-carbonylnitrile synthesis of Hogan and Sainsbury was applied to previously untested indoles, while new insight was gained on α-bromination of methyl ketones, and thioacetamide mediated synthesis of thioamides, here being the first attempt to use a thioacetamide based methodology to synthesize α-oxothioacetamides. With regard to oxazole synthesis, it was interesting to note the lowered reactivity of α-oxoacetamides toward cyclization when compared to their sulfur analogues. This problem, together with the challenging indolyl-3-α-oxocarboxamidine synthesis could potentially be solved by a ketone protecting scheme.

While it was unfortunate that MRSA PK inhibitory activity was significantly lower that of the imidazole containing topsentin analogues discussed in Chapter three, these new compounds provide greater insight and depth to our growing SAR study. The lower MRSA PK inhibition activity may be due to ligand binding at a different site to the hamacanthin analogues which will be discussed in the following chapter (Chapter 4).

Chapter Four

In Silico Docking Studies

4.1 Introduction

In a drug discovery context, protein-ligand docking provides a platform to accurately predict non-covalent binding interactions of ligands within the constrained environment of a known receptor binding site of a biomacromolecule.[202,203] From random conformations within the receptor binding site, the ligand is allowed to explore multiple conformations and orientations until a duplicate energetically favourable state is determined, from which the probable orientation and binding affinity with the receptor are ranked by a scoring function. The scoring function provides a measure of how a chosen small molecule interacts with a biomacromolecule.[203,204,205,206,207]

In a practical sense computer assisted drug design allows for large scale screening of small molecules to obtain leads against a specific target,[203] or alternatively, as part of a rational drug design approach, can assist in optimizing a known lead compound by exploring the chemical space located in the binding site.[207,208]

Protein–ligand docking has proven to be a powerful tool in medicinal chemistry, with over 4000 publications involving docking studies appearing in the chemistry literature in 2011 alone.[202] The technique does, however, offer several limitations, the most critical being receptor flexibility.[205] Commonly 3D structures of a holo-receptor are sourced from NMR spectroscopy or X-ray crystallography, or if this information has not been determined, homology modeling can be used to obtain an adequate 3D representation of this receptor.[205,206] These are however static representations of a protein that changes conformation dynamically in solution and the dynamic process of ligand binding, whereby both the ligand and the receptor may well be subject to changes in conformation before optimal binding is achieved.[205] In fact enzyme inhibition is often achieved by ligand binding resulting in changes in protein conformation.[16] A comprehensive account of receptor flexibility greatly expands the possible search space for a ligand interaction and is therefore much more computationally expensive, and in most cases is impractical.[205] The implications of this for docking means that any given ligand can only be assessed against the receptor conformation, pre-

determined by another ligand, which was present during structural determination of the receptor. Therefore the potency of a small molecule against a target may be over or underestimated, depending on how it may bind to an apo-receptor *in vitro*.

A compromise has recently been achieved in this regard with selected regions of the receptor being allowed limited degrees of flexibility, which in the cases of AutoDock 4[209] and AutoDock Vina[203] allows amino acid side chains selected by the user to be separated from the protein and modeled explicitly allowing for conformational changes due to bond rotation, in a similar manner to how the ligand conformation is explored in the receptor site.[203,205,209]

4.2 Lamarckian genetic algorithm and scoring functions

The docking software used in this study, AutoDock Vina[203] utilizes a Lamarckian genetic algorithm to perform adaptive global—local searches of optimal ligand binding.[203,204] The arrangement of a ligand with respect to a receptor is defined by the values describing translation, orientation and conformation representing a 'genotype'.[204] Genetic algorithms randomly assign these values to generate a random population of 'genetically' diverse individuals. These individuals evolve over several generations, by a process of crossover between two parents, in addition to random mutations of the genotype, producing offspring that that are phenotypically either more or less fit for the environment. Fitness is assessed by total interaction energy, whereby the individuals with the most optimal binding properties are selected to produce further generations, and those less fit not taken into consideration.[204] The Lamarckian element of the genetic algorithm allows for local searches around a specific state to find a local energy minimum. This phenotypic information is inversely mapped back onto the genotype and incorporated into the genetic algorithm, therefore allowing the local minima search to influence future generations (**Figure 4.1**).[204,207]

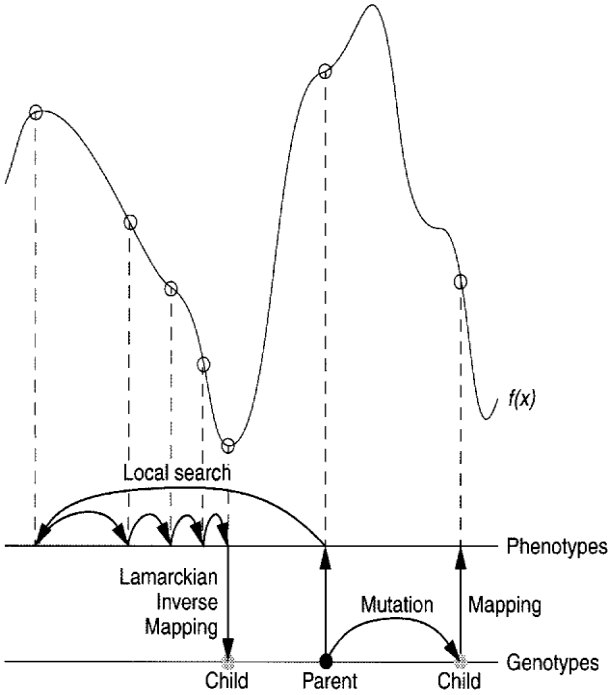

Figure4.1 Illustrating contrasting Darwinian and Lamarckian searches. The lower horizontal line represents the genotype, while the phenotype is represented by the upper horizontal line. Genotypic mutation (right) is mapped on to the phenotype, whose fitness is assessed by a fitness function *f(x).* A local phenotypic search (left) employs information about the local fitness landscape allowing for the discovery of a local minimum. Lamarckian genetics allows for the phenotypic information obtained from the local search to be inversely mapped back onto the Genotype, thereby replacing the genotype of the parent and affecting future generations. Image reproduced with permission of Arthur Olson.[204]

The AutoDock Vina scoring function considers three terms describing Van der Waal's interactions, in addition to one each for hydrophobic interactions, hydrogen bonding and ligand flexibility.[203] The scoring function has however not formally been extended to include halogen bonding interactions.

4.3 Halogen bonding

Halogens, especially the smaller, more electronegative fluorine and chlorine appear widely as substituents in medicinal chemistry, and until relatively recently were thought of purely as hydrophobic moieties.[23] Superficially, halogen bonding is a non-covalent interaction analogous to

hydrogen bonding, between a halogen atom and a Lewis base such as oxygen and nitrogen atoms which are distributed widely in biomacromolecules and critically feature a lone pair of electrons.[210] From the perspective of biological chemistry, halogens are present in synthetic ligands, as well as natural product ligands (particularly marine)[28] and native biological ligands e.g. thyroid hormones.[23,211] Additionally halogen bonding has been observed in both protein—ligand and RNA—ligand interactions.[211] This interaction is due to an electron deficient region on the surface of the halogen, referred to as the σ-hole,[212,213] the size and charge of which is variable, and depends on both the nature of the moieties to which the halogen is bound, as well as the electronegativity of the halogen.[211] A survey of the Protein Data Base (PDB) found that the majority of halogen bonding ligands involved halogens bonded to aromatic compounds.[211] The heavier halogens e.g. Br, due to the trend in periodic electronegativity tend towards σ-holes with a greater partial positive charge, and therefore have a greater likelihood of interaction with a Lewis base, and hence halogen bonding.[211] In fact fluorine rarely forms a σ-hole, and is not considered as a halogen bonding moieyy.[211] Halogen bonds are highly directional in nature, with the bond angle between the atoms C—X---D roughly linear (X representing the halogen and D the halogen bond donor), with a maximum angle range of 140°—180° and a bond length, smaller than the Van der Waal's radii of the participating atoms, generally in the region of 3.0—3.5 Å depending on the halogen.[214,215]

The possibility that a halogen bond is unaccounted for, such as is possible with AutoDock Vina, and rather being assigned as a hydrophobic interaction, will further deviate the docked model from a realistic binding scenario, and is an important consideration when assessing data obtained from docking studies.

In the context of the SAR study conducted by Strangman *et al.*(Chapter 1)[22] a trend was observed between compounds **1.5** and **1.7—1.9** where activity reduced with an increase in electronegativity of the C-6 halogen substituent, finally resulting in the nonhalogenated compound **1.9** being inactive.

This trend superficially pointed toward the possibility of halogen bonding being a factor in defining MRSA PK inhibitory activity.

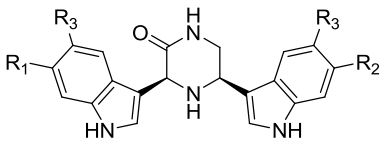

1.5 $R_1 = R_2 = Br$, $R_3 = H$ *cis*-3,4-dihydrohamacanthin B
1.7 $R_1 = R_2 = Cl$, $R_3 = H$
1.8 $R_1 = R_2 = F$, $R_3 = H$
1.9 $R_1 = R_2 = R_3 = H$
1.10 $R_1 = R_2 = H$, $R_3 = Br$
1.11 $R_1 = R_2 = Me$, $R_3 = H$
1.12 $R_1 = R_3 = H$, $R_2 = Br$

This hypothesis was further enhanced by the lower activity of compound **1.11** whose bulky methyl substituents would interact with a hydrophobic site, without resulting in halogen bonding. The activity closely resembled that of compound **1.8**, whose fluorine substituents are unlikely to induce halogen bonding. Inspection of the X-ray co-crystal of compound **1.5** and MRSA PK,[16] revealed that halogen bonding was not occurring, since bond length and bond angle of all available Lewis acids were not conducive to halogen bonding (**Figure 4.2**).

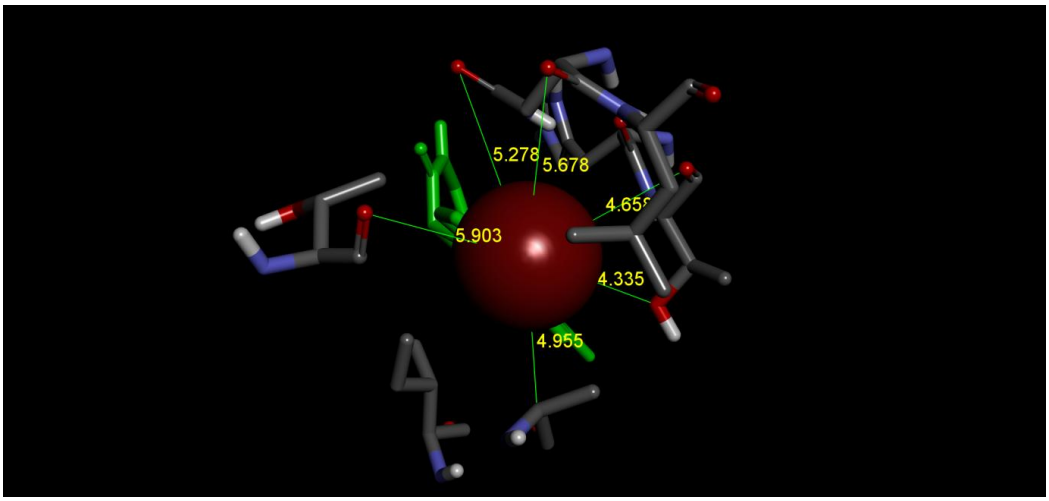

Figure 4.2 View of ligand **1.5** from the hydrophobic binding pocket visualising along the Br-C bond. Note the bond distances between bromine and the pocket Lewis acids are not concordant with known values for halogen bonding, while none of the residues are aligned appropriately for such an interaction.

Therefore the trend observed between compounds **1.5** and **1.7—1.9** was more likely related to the increasing size of the halogen better occupying a hydrophobic binding pocket, rather than decreasing electronegativity. Further, this assumption allowed us to continue with our docking experiments without consideration of halogen bonding.

4.4 Docking preparation and validation

Docking studies were performed using AutoDock Vina to provide evidence that topsentin analogues **1.6, 1.40, 1.46** and **1.58—1.61** bind in the same pocket as compound **1.5**. as well as to inform the synthesis of thiazole analogues **1.62—1.68**.

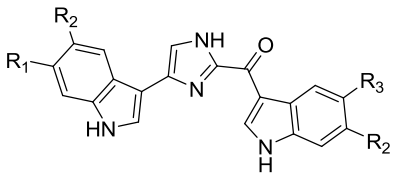

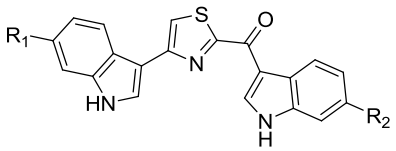

1.6 R_1 = Br, R_2 = R_3 = H bromodeoxytopsentin
1.40 R_1 = R_2 = R_3 = H deoxytopsentin (topsentin A)
1.46 R_1 = R_2 = Br, R_3 = H dibromodeoxytopsentin
1.58 R_1 = R_2 = F, R_3 = H
1.59 R_1 = R_2 = Cl, R_3 = H
1.60 R_1 = R_2 = H, R_3 = Br
1.61 R_1 = R_2 = I, R_3 = H

1.62 R_1 = R_2 = H
1.63 R_1 = R_2 = F
1.64 R_1 = R_2 = Cl
1.65 R_1 = R_2 = Br
1.66 R_1 = Br, R_2 = F
1.67 R_1 = F, R_2 = Br
1.68 R_1 = F, R_2 = Cl

Having determined that halogen bonding interactions are not a factor, docking studies in which halogen bonding was not considered were deemed sufficient in this study. Ligand and receptor visualizations were performed on Discovery Studio 3.5 Visualizer.[21] All receptors were prepared by initially removing the ligand present in the active site then equipped for docking in AutoDock tools whereby all non-polar hydrogens were merged, and polar-hydrogens were added. Electrostatic charges were calculated as Gasteiger charges and atoms were assigned by the AutoDock 4 typing rules.

Observation of the ligand present in the MRSA co-crystal structure showed the structure of the ligand to be different to that of compound **1.5** as reported in the publication.[16] Instead the co-

crystallized ligand featured a pyrazinone ring with a Δ^3 olefin presenting a compound not previously reported in the literature referred to here as compound **4.1**. A reinspection of the original NMR data of the natural product submitted for screening confirmed the presence a proton at position C-3, and thus supported the structure of the ligand as **1.5** and not **4.1** (**Figure 4.3**).

While oxidation during co-crystallization is highly unlikely, the most reasonable explanation is that errors in data resolution and assignments were made during the crystal structure refinement, where the double bond may have been assumed based on a shortened bond length. It is important to note as well that the bond angles of carbons 3 and 5 are neither perfectly tetrahedral, nor trigonal planar, and the orientation of the indole moieties results in overlap of the Van der Waal's radii of the hydrogens at indole position 2 (**Figure 4.4**). While this is considered an energetically unfavourable orientation, the constraints inflicted by the protein under crystallization conditions could account for this.

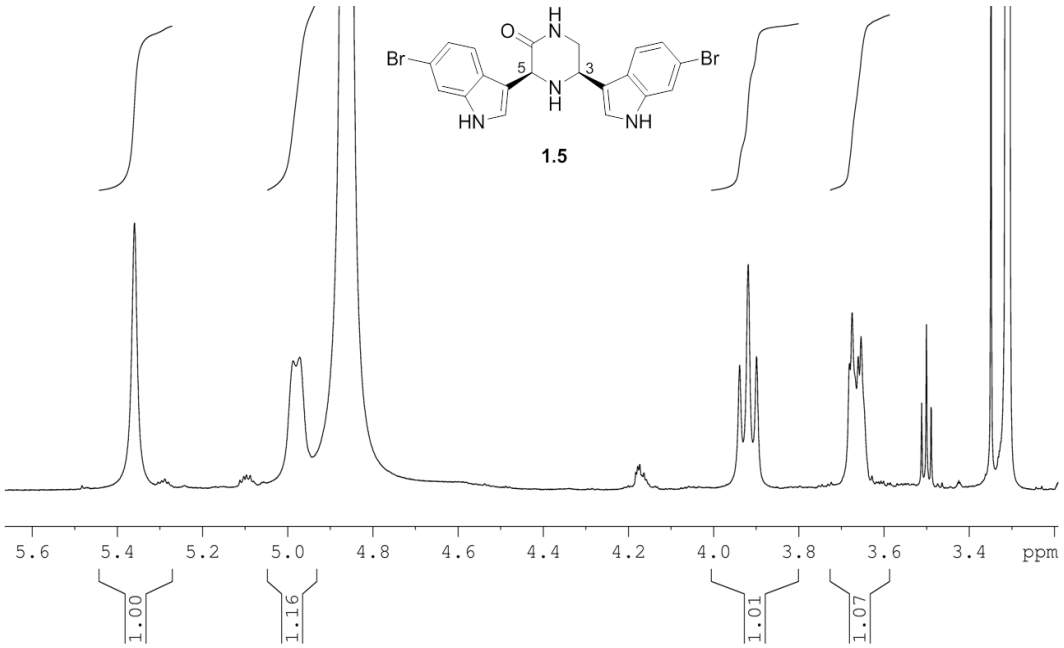

Figure 4.3 Selected region (δ_H 3.3—5.6) of the ^{1}H NMR spectrum of **1.5** (MeOD, 600MHz). The two signals at 5.3 and 4.9 ppm correspond to the protons at positions 3 and 5 on the piperazine ring respectively.

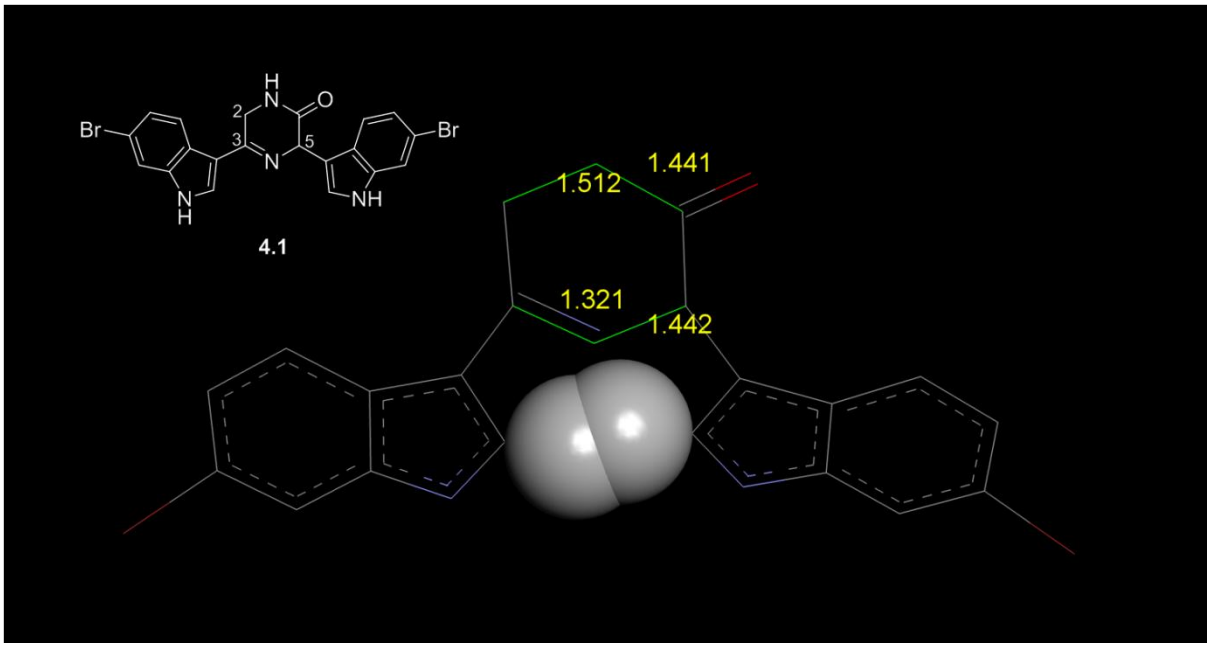

Figure 4.4 Stick representation of the ligand present in X-ray co-crystal 3T07 (compound **4.1**). Highlighted are the respective bond lengths, and the overlapping Van der Waal's radii of the protons at indole position 2.

Initially, we attempted to validate our binding docking procedure, by re-docking **4.1** in its bound conformation to the crystal structure of MRSA PK. The X-ray co-crystal structure reveals that two molecules of **4.1** were bound in two respective identical binding sites located directly opposite each other. For the purposes of our docking study we chose one, without any preference, since they are both identical. The docking site was defined by X, Y and Z coordinates located on the originally crystallized ligand. The search space was a cube of 30 Å in each of the three dimensions, centred on the docking site.

Initially a global search exhaustiveness of 32 searches in the area were performed to adequately search the desired binding site, which was then repeated at an exhaustiveness of 8. AutoDock Vina output consists of a series of active conformations, which are ranked according to binding energy. The highest ranking conformations at both exhaustiveness settings were identical, implying that the experiment conducted at an exhaustiveness of 8 was sufficient for the rest of the experiment. The best fit conformation from both experiments overlaid on the position of the co-crystal ligand with a

root mean square distance (RMSD) of 0.2868 Å and a binding energy of —11.5 kcal/mol. The second best fit was positioned as a mirror image, which is to be expected with the symmetrical nature of both the binding site and ligand, which gratifyingly demonstrated that our model consistently achieves a minimum binding energy (**Figure 4.5** left). We further went on to add the missing hydrogens **4.1**, to reproduce the structure of **1.5**, whilst still maintaining its bound conformation. Once more this overlaid with the co-crystal ligand with a slightly better binding affinity of —11.7 kcal/mol, implying that the missing hydrogens have little effect on ligand binding, and are simply an oversight by the crystallographer. To determine the importance of the unusual conformation of compound **4.1** from the co-crystal structure, compound **1.5** was re-drawn displaying the more conventional tetrahedral bond angles associated with sp^3 hybridized carbons, with the indoles in a less sterically hindered position and re-docked. Interestingly the resultant binding energy was found to be lower (—8.1 kcal/mol), displaying little homogeneity with the active binding orientation (**Figure 4.5** right).

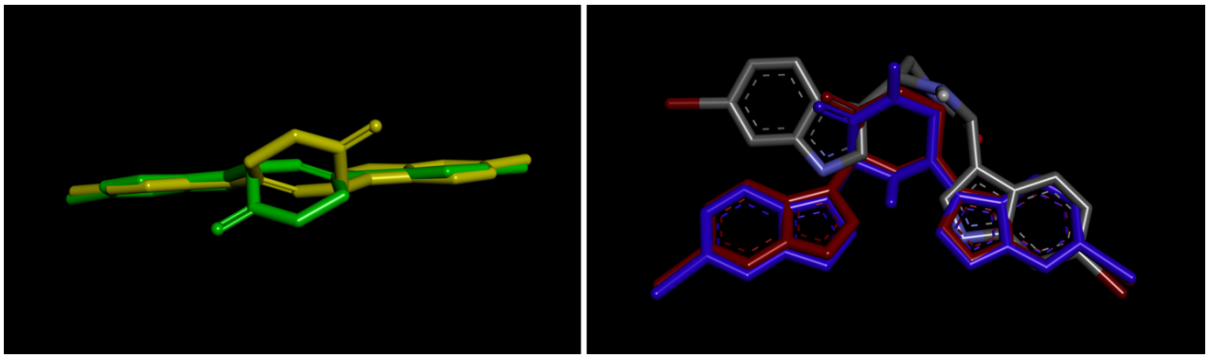

Figure 4.5 (Left) The top two ranking binding orientations for docked 4.1 showing C2 symmetry. (Right) Overlaid image of the crystallised ligand **4.1** (red) as well as **1.5** in both the stained conformation (blue) and low energy conformation (CPK colouring) after docking. Thus highlighting the importance of the strained conformation of **4.1** for ligand docking.

Additionally, we introduced flexibility to the two histidine residues in the binding site, hoping that for docking of compound **4.1** they would remain in their original position, while potentially revealing π-stacking interactions with topsentin. Unfortunately, however, histidine flexibility resulted in a

binding event which was significantly different to that seen in the crystal structure and was attributed to the extensive conformational space that is inadequately explored upon introduction of this flexibility, in reasonable time. We therefore concluded that the flexible residue model was inappropriate for this study (**Figure 4.6**).

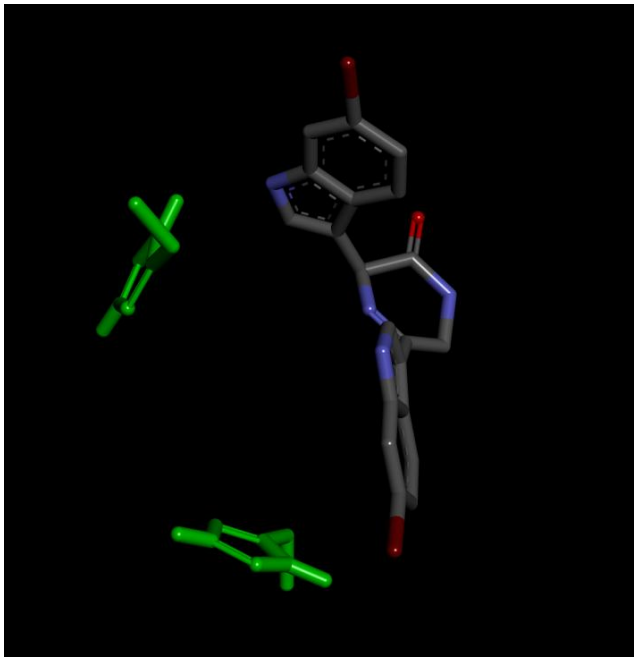

Figure 4.6 Binding orientation utilizing flexible histidine residues (green) shows complete displacement of ligand **4.1** (Remainder of protein removed for clarity).

4.5 Topsentin docking study

We then turned our attention to docking of topsentin analogues **1.6, 1.40, 1.46, 1.58—1.61** against the same target under conditions deemed sufficient from the validation study. All topsentin ligands were constructed as .pdb files in Discovery Studio Visualizer,[21] with hydrogens added and geometry 'cleaned'. This was followed by calculation of charges, defining of torsions and saving to .pdbqt files using AutoDock tools, prior to docking.

Both possible tautomeric forms of each topsentin derivative were docked against the target. Docking was assessed by two main criteria, firstly a visual inspection of the position and orientation of ligand in the binding site, compared with **4.1** with a particular emphasis on the position of the halogens in the binding site. Secondly, by comparing binding affinity with that of the re-docked **4.1**. In most instances the first and second ranked docking orientation with the same binding affinity were found to be mirror images, due to the nature of the binding site, in which case they were considered equally.

Visual inspection of C-6 halogenated and non-halogenated **1.6, 1.40, 1.46, 1.58, 1.59** and **1.61** docked topsentin data revealed that neither tautomer was significantly more suited for binding than the other, with overlays showing identical orientation with the exception of the exchangeable proton (**Figure 4.7a**). Any noticeable difference would presumably be inconsequential since tautomerisation would likely occur in the biological medium to form the most stable binding complex if necessary. As mentioned above a mirror image orientation with perfect C2 symmetry and equal binding energy was observed as the second ranking orientation, consistent with the results obtained for hamacanthin, implying a high degree of consistency in the method (**Figure 4.7b**). The single exception to this trend was that of tautomer 1 of compound **1.58**, whose highest ranking orientation did not fit the same binding trend, but rather mirrored the binding trend of the lower ranking non-halogenated topsentins. However the second and third ranking orientations of this analogue had equal binding energy as the first ranking orientation, and maintained the observed trend (**Figure 4.7c and d)**. The C-5 brominated compound **1.60** was also found to dock in the target site, but unsurprisingly with a different binding orientation.

In contrast to the experimental data obtained for the topsentin analogues (Chapter 2), **1.58** displayed the greatest affinity (—11.0 kcal/mol) for the binding pocket *in silico* when compared to any of the other docked analogues.

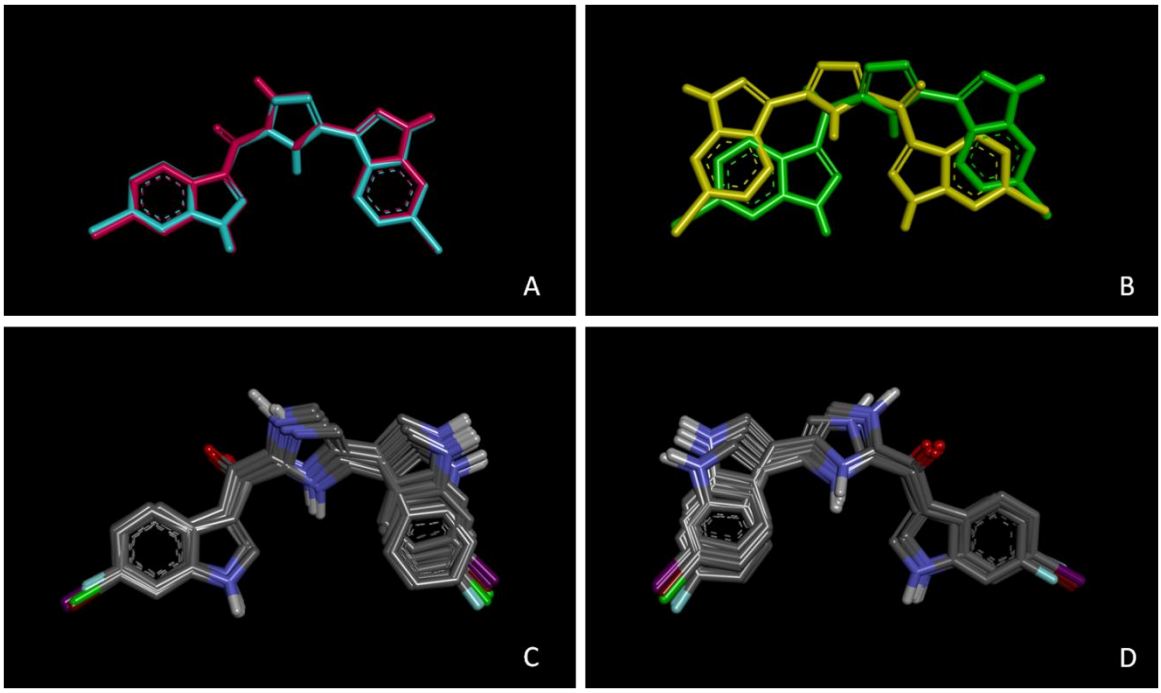

Figure 4.7 (A) The overlaid binding orientation of tautomer 1 (pink) and tautomer 2 (blue) of compound **1.59**. (B) C2 symmetrical binding orientation of compound **1.46** tautomer 2. (C and D) Overlaid image of docked ligands from both orientations showing consistency of binding within the preferred orientation.

Comparison of the docking binding energies showed **4.1** to have the greatest affinity for the binding site, which is not altogether surprising since the conformation of the receptor has been altered by the bound ligand for optimal binding and vice versa. The overwhelmingly consistent feature of topsentin docking was the positioning of the halogen moieties, all of which were positioned inside the same hydrophobic pocket where the bromines of **4.1** were situated. However this was not the sole reason for the consistency in docking orientation, since the non halogenated compound **1.40** also displayed the same binding mode. The indole NH on each of the indole moieties of compound **4.1** formed a single hydrogen bond with the two respective Ser 362 residues present at the site.[16] Interestingly with the topsentin ligands, only the indole adjacent to the carbonyl lies in a similar orientation to the hamacanthin indole, where a hydrogen bond is formed between the N-1" hydrogen and Ser362. The second indole is flipped around with the NH pointing out of the binding pocket, not forming a second hydrogen bond, while still allowing the halogen to occupy the hydrophobic binding pocket (**Figure 4.8**). This is not the case observed with the anomalous docking

compound **1.58**, where both indole NH's point out the pocket, and the carbonyl points in, forming no hydrogen bonds (**Figure 4.9**). It is curious what maintains this orientation for the non halogenated analogue.

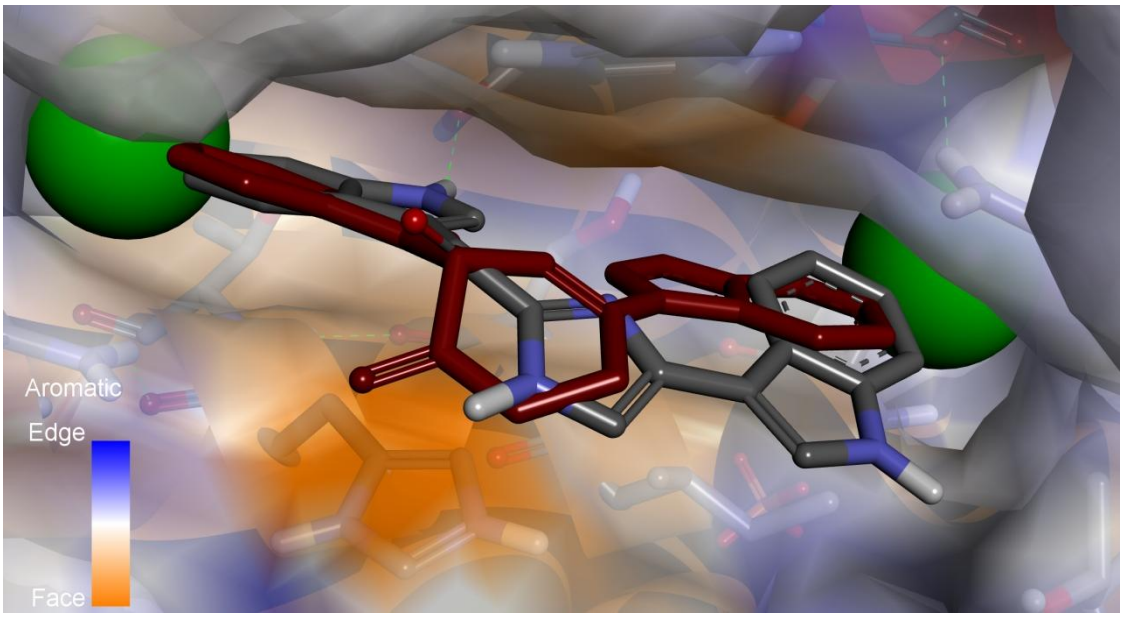

Figure 4.8 Docked binding orientation of compound **1.59** overlaid with **4.1** whereby the large chlorine atoms are orientated toward the hydrophobic binding pockets, with the single hydrogen bond detected between NH 1" and Ser 362. The other indole NH points out the pocket, not forming the second hydrogen bond as seen with **4.1** (hydrogen bond removed here for clarity). Note the aromatic face from the histidine residues, potentially interacting with the imidazole face *in vitro*.

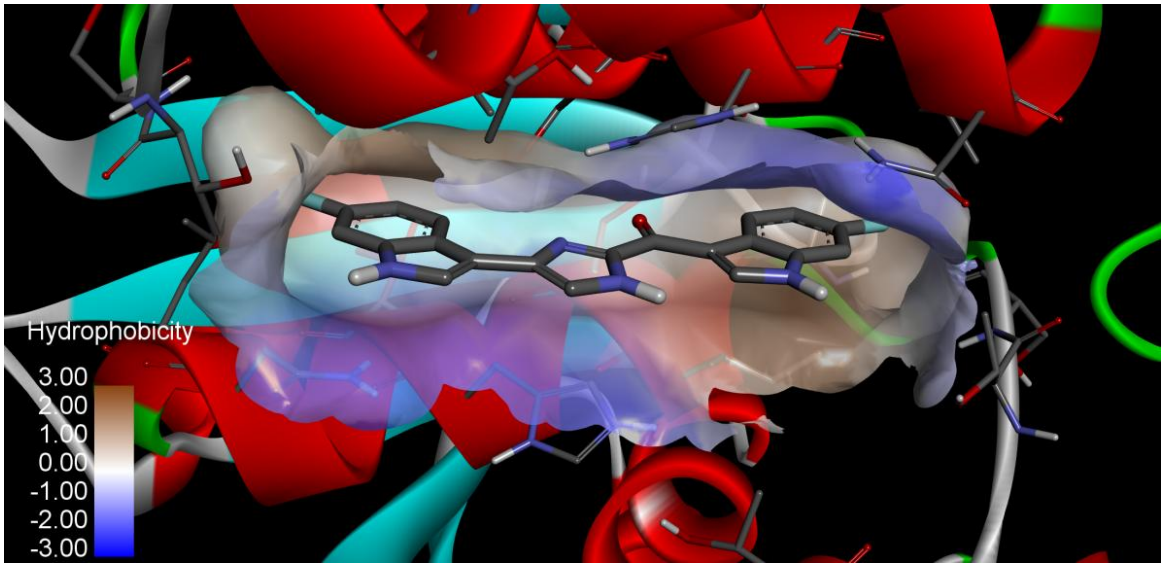

Figure 4.9 Compound **1.58** docked in the binding pocket. Note the halogen and indole NH orientation, sacrificing the hydrogen bond, consequently forcing the carbonyl into the binding pocket.

Overall visual inspection seems to favour two particular orientations, while not heavily favouring any particular analogue, which importantly place the ligands in the same evolutionary conserved binding pocket as **1.5**, strengthening the possibility that this is the viable binding site for these ligands, and making them suitable candidates for potential MRSA PK inhibition. Based on binding energy, while not being as active as the original hamacanthin inhibitor, the closely ranked **1.46, 1.58** and **1.59,** were predicted to be the best inhibitors, while the **1.6, 1.40, 1.60** and **1.61** were predicted to be less likely inhibitors. While the docking study did suggest that all of the compounds would bind, it could not predict the *in vitro* activity trend, and seemingly rather correlated with the relative differences in C-6 substituent (**Figure 4.10**).

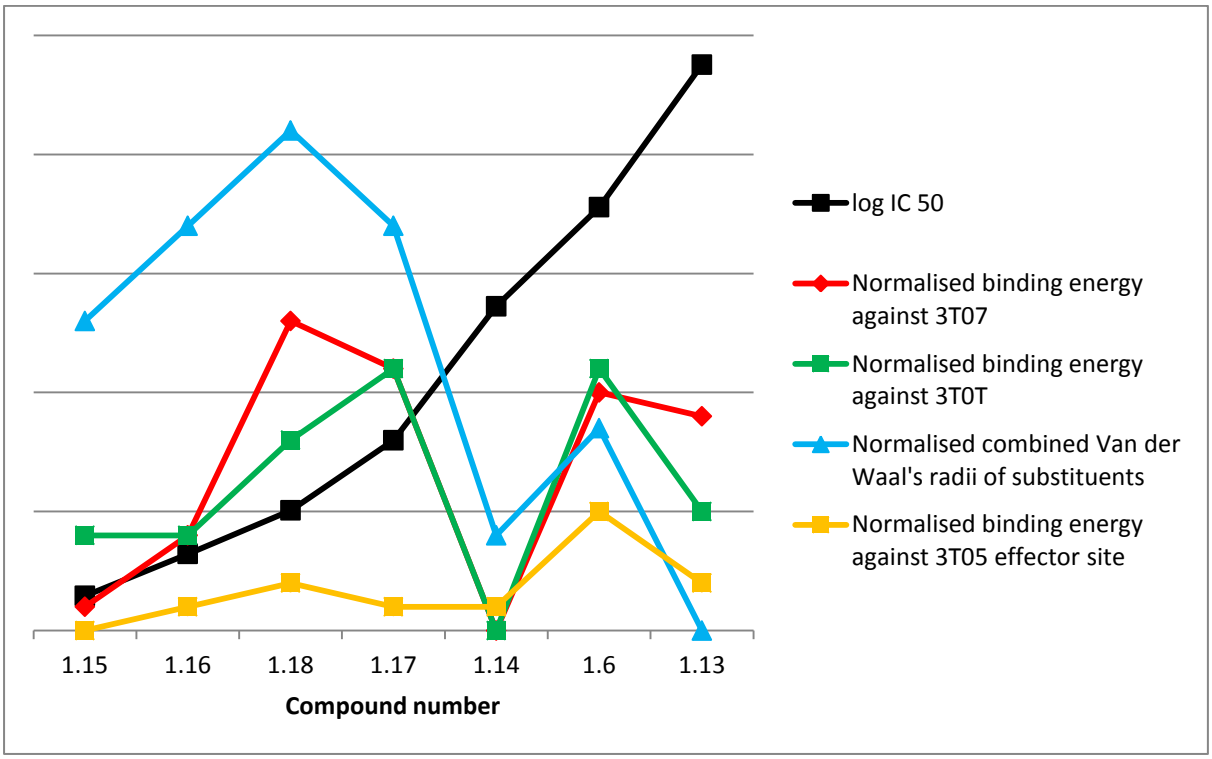

Figure 4.10 Scatter plots of normalised docking binding energy of ligands in the 3T07, 3T0T hydrophobic pocket and 3T05 effector site along with log values of *in vitro* inhibition data, and normalised combined Van der Waal's radii of indole substituents. The data suggests the docking method provided little insight into the SAR of indole substitution. The relative size of the ligand seemingly plays a major role in binding affinity. This may be a negative factor in docking against a static receptor. Normalised here refers to the lowest value in any series is subtracted from all the values in the series, so that the lowest value equals zero and the data can be compared on similar axes.

None of the docked compounds had predicted binding energies greater than compound **4.1**, yet four of the seven were more active. This is however is not surprising since, as it was discussed previously, the receptor conformation was defined by the presence of the ligand with which it was crystallized, and therefore any ligand would have to occupy a similar molecular space to achieve the same binding.

Perhaps this is the reason derivative **1.58** derivative displayed the best docking, while also having the most similar *in vitro* activity to hamacanthin. The smaller halogen size would have allowed a tighter fit into the pocket, whilst sacrificing the hydrogen bond *in silico*. In the case of the even smaller non halogenated derivative, the hydrogen bond would likely not be sacrificed, since there is no moiety to access the hydrophobic pocket, hence the orientation homology with the rest of the series. The predicted binding energy difference between the **1.58** and **1.61** was 1.2 kcal/mol, while the difference between **1.40** and **1.61** was 0.4 kcal/mol, where **1.40** was predicted as having the better fit underlining the disparity between results obtained *in vitro* and *in silico* (**Table 4.1**).

Compound number	IC_{50} nM	3T07 binding energy (kcal/mol)	3T0T binding energy (kcal/mol)
1.59	1.4	-10.9	-10
1.46	2.1	-10.6	-10
1.61	3.2	-9.7	-9.6
1.60	6.3	-9.9	-9.3
4.1/1.5	16	-11.5	-10.2
1.58	23	-11	-10.4
1.6	60	-10	-9.3
4.2	91	-9.7	-9.6
1.40	238	-10.1	-9.9

Table 4.1 Table displaying binding energy against two targets *in silico* in conjunction with *in vitro* inhibition data.

To further probe this binding site from a docking perspective, additional docking studies were conducted against apo MRSA PK enzyme (PDB code 3T05)[16] and an X-ray co-crystal structure (PDB code 3T0T) obtained from an SAR study which revealed a series of potent nanomolar range hydrazone MRSA PK inhibitors that bind to the same hydrophobic pocket as *cis*-3,4-dihydrohamacanthin B.[13] Both proteins were prepared in the same manner as described for 3T07. Since the apo enzyme 3T05 has no bound ligand, no docking validation was possible and a starting co-ordinate was selected from His365 located in the desired binding site (**Figure 4.11** left), with a search space of 30 Å and an exhaustiveness of 32. Docking of both tautomers of compound **1.46** and **1.59** was performed, with both being unable to penetrate the hydrophobic binding pocket. Rather, docking resulted in both ligands binding in a cleft at the large interface, for which they showed a low binding affinity and displayed a single hydrogen bond between the indole proton and NH-1' and the backbone carbonyl of Lys260. (**Figure 4.11** right) This result was assessed visually as an unsuccessful dock, so no other analogues were assessed in this experiment.

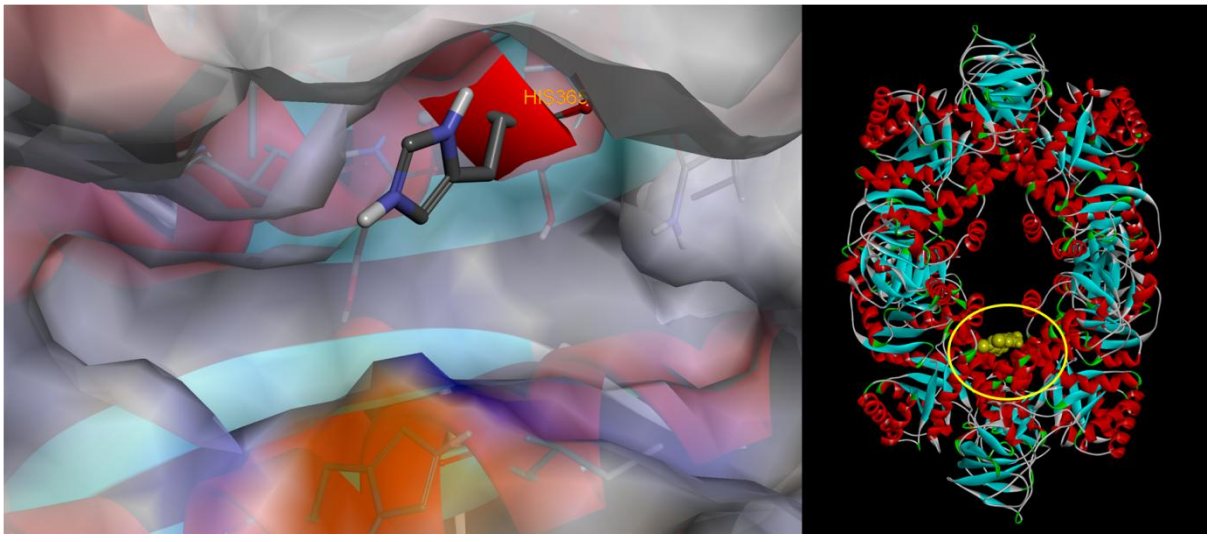

Figure 4.11 Right: hydrophobic binding pocket of apo MRSA PK enzyme (PDB ID 3T05). Docking coordinate was defined by HIS 365. Even in the apo form this enzyme retains this binding pocket unlike mammalian orthologs (see **Fig. 1.4**) Left: Docking of compound **1.46** (CPK view in yellow) against 3T05. The ligand could not access the binding site, and found a lower energy conformation at the large interface.

Crystal structure 3T0T was the next target for assessment. A binding coordinate was taken from the bound ligand (**4.2**), and re-docked for validation firstly, unsatisfactorily at an exhaustiveness of 8 and successfully at an exhaustiveness of 32, reproducing a similar orientation to the co-crystallized ligand displaying the same hydrogen bond between Ser 362 and the ligand NH with an RMSD of 0.5949 Å, and a binding energy of —9.6 kcal/mol. Importantly, in their publication Kumar *et al.* note four hydrogen bonding events,[13] while here we note just one according to results gleaned from the software we had available. We therefore conducted the remainder of this part of the docking study at an exhaustiveness of 32.

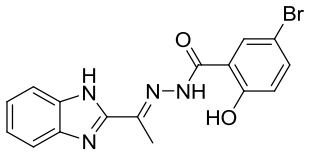

4.2

The same trends were observed for topsentin docking here as were observed against 3T07, whereby the ligands adopted the same binding orientation, with the two highest ranking orientations displaying C2 symmetry. Again there seemed to be little difference between tautomers and a single hydrogen bond formed between Ser362 and the indole NH-1" as observed in the 3T07 experiments. Again **1.58** proved to be the anomaly with regard to binding orientation, however on this occasion this binding orientation was observed for both tautomers, first and second ranked orientation, the explanation of which remains the same.

The binding affinity, whilst showing results consistent with the previous study, again did not mirror the results obtained *in vitro* (**Figure 4.10**) with the **1.60** predicted to have the lowest activity, followed by **1.61**, while the binding affinity of the **1.40** was only 0.1 kcal/mol less than **1.46** and **1.59**, which were identical. Again **1.58** had the highest binding affinity. Interestingly the all of the docked analogues with the exception of the **1.60** displayed higher binding affinities for the pocket than the co-crystal ligand **4.2**. *In vitro* assay of this compound revealed an IC_{50} 91 nM, which is significantly

lower than that determined for the halogenated topsentin analogues **1.6, 1.46, 1.58—1.61** (**Table 4.1**).

4.6 Interpretation of results and alternative binding sites

The trend observed with the hamacanthin SAR study,[22] suggested that activity of the topsentin analogues **1.40** and **1.60** should be low, while activity should follow a trend of increased activity with increased halogen size, while experimentally we can see **1.40** is marginally active, with **1.60** being potently active, and the halogen trend is nonexistent.

For the purpose of interpretation, if we assume that the hamacanthin binding site is indeed the topsentin binding site, we can infer some interesting points. The 'halogen binding' pocket does not induce halogen bonding, but is rather a hydrophobic site. However the more hydrophobic methyl (**1.11**) and fluorine (**1.8**) substituted hamacanthins were significantly less active than the larger bromine substituted compound **1.5**, which in turn was moderately more active than the slightly smaller chlorine substituted compound **1.7** (Chapter 1). The dichlorinated topsentin analogue **1.59** was significantly more active than compound **1.5**, while was only slightly more active than the larger bromine (**1.46**) and iodine (**1.61**) substituted topsentin analogues and moderately more active than the smaller fluorine substituted **1.58** (**Table 4.1**). This suggests potentially, that the initial halogen observation was correct from a non halogen bonding point of view. It is possible that the binding pocket has an optimal size for an inhibitor, which was not adequately filled by the more hydrophobic **1.8** and **1.11**, hence explaining their reduced activity. If the topsentin indoles were allowed to adopt the same orientation as that seen for hamacanthin, a second hydrogen bond could form, and since topsentins are generally slightly bigger molecules than hamacanthins, compounds **1.40** and **1.58** may well have occupied the binding site better than their hamacanthin counterparts, **1.8** and **1.11** therefore explaining their greater activity *in vitro*. Additionally **1.59** may be slightly more suitable for

the active site than the larger **1.46** followed by **1.61**, hence explaining the trend as a mild form of an activity cliff,[216] whereby this activity trend is governed by an optimal size of ligand. It might therefore be possible to better inhibit the enzyme by optimizing the ligand size with different halogens on the respective indoles, something we were not able to achieve.

Alternatively the dispute in activity trends between the topsentins and hamacanthins may be because topsentin binds at a different site on the enzyme. To monitor this we performed global searches on all three protein crystals used during this study, whereby the same original docking coordinate was used, but the search area expanded from 30 Å in each of the three spacial dimensions to 80 Å at an exhaustiveness of 64, so to allow a more comprehensive search of the binding regions. Beginning with the apo 3T05 a single tautomer of each of **1.58** and **1.59** were docked, and were found to occupy a 13 amino acid binding cleft located near the effector site, at the interface of two C domains featuring residues Leu355, Gly460, Thr463, Asn465 from one subunit and Leu449, Lys468, Ile469, His470, Leu471, Asp571, Gln574, Lys576 and Asn583 from the other (**Figure 4.12**).

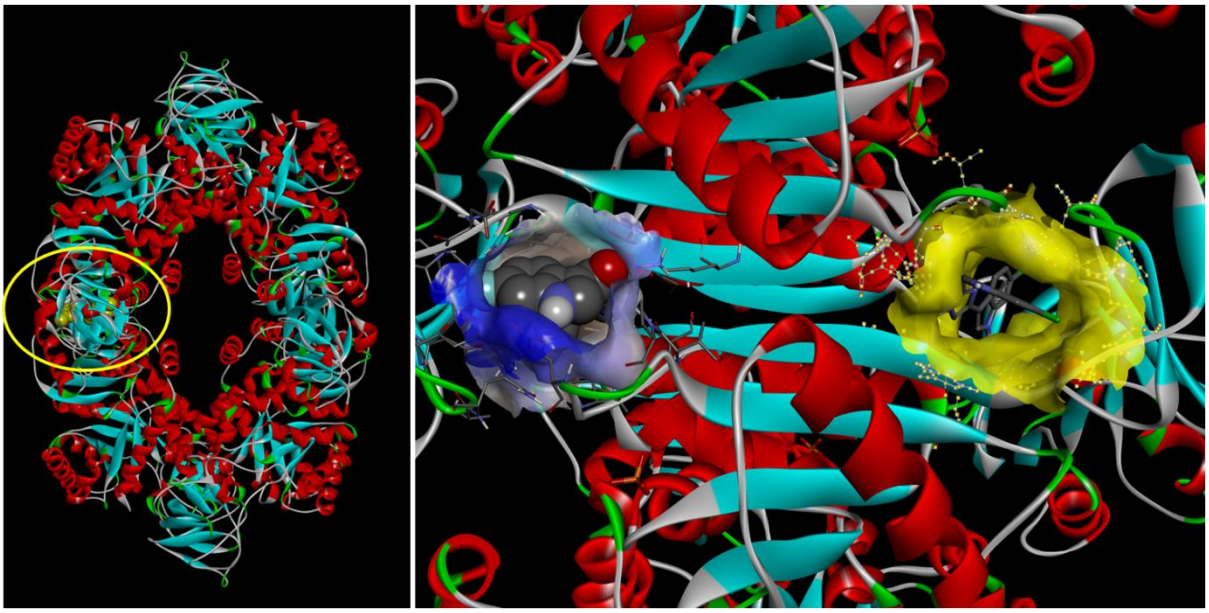

Figure 4.12 Left: global search of 3T0T revealed a possible binding cleft near the effector site. Right: side view of the binding pockets located as the C domain interface. The binding site exists as a tunnel wherein the ligands **1.58** (left) and **1.59** (right) can dock.

Two hydrogen bonds were detected between the imidazole N and Leu471 backbone NH, as well as the imidazole NH and the backbone carbonyl of Ile469. Due to the nature of the enzyme four such binding sites exist, all of which were occupied.

This preliminary result was followed by a full docking study to assess whether predicted binding affinity may more closely mirror experimentally determined inhibitory activity. The chosen coordinate was taken from the docked ligand, and the search area reduced to 30 Å at an exhaustiveness of 32. Both tautomers of **1.59** were initially assessed by this method, with no difference between the two, as was consistent with all previous studies. Satisfyingly they also adopted the same conformation with the same binding energy as that obtained in the global search. Since this binding pocket does not present as a symmetrical binding pocket, we did not expect to see C2 symmetry between the binding orientations, however visual inspection of the docked ligand by rank revealed a low degree of binding homology perhaps bringing into question the consistency of this study, and further suggesting this is unlikely to be the actual ligand binding site. Again accurate correlation was not observed between *in vitro* and *in silico* results. However, binding affinities between the ligands were similar, whilst still showing a less prominent correlation between binding affinity and ligand size (**Figure 4.10**).

As a final inspection of the possible binding sites, a global search was conducted on both 3T07 and 3T0T, to ascertain whether **1.59** would preferentially bind in the site described above, or in the hydrophobic site discovered from X-ray co-crystallography. Both global searches occurred at an exhaustiveness of 64, and were each replicated from coordinates taken from the respective crystallized ligands and Thr463. On all four occasions, docking was found to occur at the hydrophobic binding site, originally occupied by compound **1.5** suggesting a preference for this site over the effector site.

Interpretation of these results leaves many questions unresolved. This docking study was unable to replicate the results determined *in vitro*, if we assume a direct correlation between binding affinity

and inhibitory activity. This may however be an over simplification of the processes behind enzyme inhibition, with unknown secondary variables effecting the results *in vitro*.

4.7 Discussion of topsentin docking results

Based on results obtained from docking, a purely *in silico* based drug design approach would have likely deferred us away from the most active inhibitor of MRSA PK. However, if we keep in mind the limitations of docking which were discussed above, it can help to establish whether a compound will likely fit into a receptor and binding pocket, which should be interpreted in the face of other data made available. Additionally, it would be erroneous to assume high inhibitory activity if factors like solubility, pKa or cell wall permeability - in the case of cell based screens- would not be major contributors to activity, and are not reflected in a pure docking study. The attempted docking in the hydrophobic site of 3T05, suggested that the size and shape of the pocket is highly reliant on the presence of a ligand, while the alternative binding site found from global docking on 3T05, may simply be an open crevice naturally occurring in apo MRSA PK. It is interesting to note that global docking of 3T0T and 3T07 preferably bound to the hydrophobic binding site, suggesting without certainty that it is the *in vitro* topsentin binding site.

4.8 Docking study of thiazole bisindole topsentin analogues

A series of thiazole based topsentin analogues (**1.62—1.65**) were synthesized as part of our SAR study, and were subsequently docked against 3T07. We expected the models to follow a similar trend to the topsentin docking, with the halogens and indole nitrogen providing the main receptor interaction, with the more bulky sulfur potentially having a slight effect. Since only analogues featuring a C-6 fluorine (**1.63**), chlorine (**1.64**) and bromine (**1.65**) substitution were synthesized, in

addition to a non halogenated derivative (**1.62**), only those compounds were docked. Not surprisingly the same C2 symmetry was seen between the top two ranking docks, with the ligands occupying an almost identical orientation to that observed for topsentin docking.

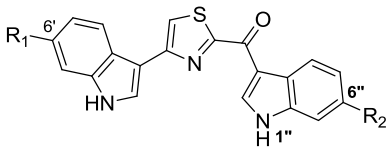

1.62 $R_1 = R_2 = H$
1.63 $R_1 = R_2 = F$
1.64 $R_1 = R_2 = Cl$
1.65 $R_1 = R_2 = Br$
1.66 $R_1 = Br$, $R_2 = F$
1.67 $R_1 = F$, $R_2 = Br$
1.68 $R_1 = F$, $R_2 = Cl$
4.3 $R_1 = Br$, $R_2 = Cl$
4.4 $R_1 = Cl$, $R_2 = Br$
4.5 $R_1 = Cl$, $R_2 = F$

The fluorinated derivative on this occasion however, did not occupy a non-uniform orientation as was seen in the topsentin docking study. Only the highest ranking non halogenated derivative broke the trend, with the second ranking derivative which had an equal binding affinity resuming the trend. Interestingly the preferred orientation had the sulfur pointing out the binding pocket. None of the binding affinities were found to be better than the originally re-docked **4.1** with the best being compounds **1.64** and **1.65** both at —10.5 kcal/mol followed by **1.63** and **1.62** at —10.4 and —10.3 kcal/mol respectively (**Table 4.2**).

Since the method for synthesizing the thiazole analogues (Chapter 3) allowed for regiospecific synthesis, we decided to synthesize differentially halogenated thiazole analogues, to test our optimal ligand size hypothesis. Docking of the six possible combinations of halogenated analogues (**1.66—1.68, 4.3—4.5**) was conducted in an effort to further study the consistency of docking as well as help guide synthesis since starting materials were limited.

Compound number	IC_{50} µM	3T07 binding energy (kcal/mol)
1.66	5.1	-10.2
1.65	5.2	-10.5
1.67	6.6	-10.8
1.68	7.9	-10.7
1.64	11.7	-10.5
1.63	12.6	-10.4
1.62	20	-10.3
4.3	N/A	-10.3
4.4	N/A	-10.7
4.5	N/A	-10.2

Table 4.2 Binding energies obtained for thiazole containing topsentin analogues against the hydrophobic pocket of 3T07 *in silico* and IC_{50} data obtained *in vitro*

Unsurprisingly, binding orientations were consistent with previously seen data, and C2 symmetry was again noted for the top two ranking orientations, with the same halogen orientation and single hydrogen bond between Ser362 and NH-1". On this occasion however, no analogues broke the binding trend with an alternative orientation. Interestingly in the context of the symmetrical binding pocket, binding affinity was heavily dependent on which side of the molecule a given halogen was located, i.e. **1.67** displayed the greatest binding affinity (—10.8 kcal/mol), while the lowest binding affinity (—10.2 kcal/mol) was observed in its regioisomer **1.66** (**Table 4.2**). This trend held true for the entire series, in which greater binding affinity was observed when the larger halogen was located at C-6" on the indole adjacent to the carbonyl rather than the alternative 6'and vice versa. The hydrogen bond seen in the docking studies features the indole NH adjacent to the carbonyl (i.e. NH-1"), maintaining the indole orientation as seen in the hamacanthin co-crystal structure. It therefore stands to reason that if the larger halogen is positioned to interact with the hydrophobic binding site, it is likely to have a greater *in silico* binding affinity than its regioisomer. In an effort to

test the optimal size hypothesis, as well as the trend observed above, both compounds **1.66** and **1.67** were synthesized and well as the second most active compound *in silico* **1.68**.

Comparison of *in silico* and *in vitro* obtained for compounds **1.62—1.68** revealed again that no trend in activity was accurately predicted by docking. All the thiazole compounds assayed against MRSA PK were found to be moderate inhibitors of the enzyme, while docking studies predicted that compound **1.68** (—10.7 kcal/mol) would have a slightly greater binding energy than **1.46** (—10.6 kcal/mol), activity was found to be 1000 times lower.

Additionally the trend difference in binding energy predicted between compounds **1.66** and **1.67** (—10.2 and —10.8 kcal/mol respectively) did not mirror the experimentally obtained biological data, with **1.66** displaying slightly better MRSA PK inhibition. The reasons for the differences in binding energy were discussed above, and reflect the sometimes superficial nature of results obtained from docking studies.

4.9 Conclusion

While *in silico* docking studies strongly suggested that both the topsentin analogues and thiazole analogues bound to the same active site as *cis*-3,4-dihydrohamacanthin B, they were unable to accurately predict any trend observed with *in vitro* biological data. While in many cases differences in IC_{50} value were small to a point of being insignificant, in some cases large differences in binding energy were predicted, which were not reflected *in vitro*.

In the beginning of this chapter we discussed the main areas where docking has shortfalls, with particular reference to the static representation of proteins offered by X-ray crystallography. It seems at least in the case of the compounds used in this study that this limitation significantly

limited the predictive power of docking studies, while the question of an alternative binding site is still a possibility.

Chapter Five

Experimental Data

5.1 General Experimental Procedures

5.1.1 Analytical

Melting points were determined using either a Reichert hot stage microscope or a Stuart SMP30 (Bibby scientific ltd.) and are uncorrected. NMR spectra were acquired using standard pulse sequences on a Bruker 600 MHz Avance II spectrometer. Chemical shifts are reported in ppm, referenced to residual solvent resonances ($CDCl_3$ δ_H 7.26, δ_C 77.0; DMSO-d_6 δ_H 2.50, δ_C 39.50; MeOD δ_H 3.31, δ_C 49.00 ppm),[217] and coupling constants are reported in Hz taken directly from the NMR spectra. Infrared spectra were recorded on a Perkin Elmer Spectrum 2000 FT-IR. High resolution mass spectrometry was performed on a Waters Synapt G2 TOF instrument with an ESI source. Spectra were acquired in both the positive and negative ion mode by the University of Stellenbosch Central Analytical Facility. Predicted accurate masses for compounds **2.99—2.101** were performed using ChemCalc.[151]

5.1.2 Chromatography

Reactions were monitored by thin layer chromatography in the normal phase (NP) on DC-Plastikfolien Kieselgel 60 F254 plates and visualized under UV light (254 nm). Reversed phase (RP) thin layer chromatography was performed on DC-Ferigplatten RP18 F245 plates and visualized under UV light (254 nm). Flash chromatography was performed using Kieselgel 60 (230-400 mesh) silica gel. Semi-preparative NP-HPLC was performed using a Whatman's Magnum 9 Partisil 10 column with a Physics Spectra-Series P100 isocratic pump and a Waters 410 Differential Refractometer. Semi preparative RP-HPLC was performed using an Onyx Monolithic C18 column on an Agilent 1100 Series quad pump and an Agilent 1100 diode array detector.

5.1.3 Synthesis

All reactions requiring anhydrous conditions were performed in oven dried apparatus under an inert atmosphere of argon gas or using an anhydrous calcium chloride drying tube. Anhydrous solvents were prepared by standard procedures outlined by Perrin and Amerego[218] as well as Casey, Leonard, Lygo and Procter.[219] Immediately prior to their use THF and Et_2O were distilled from Na/ benzophenone ketyl, while CH_2Cl_2 was distilled from calcium hydride. All solvents were stored over 4 Å molecular sieves under anhydrous argon. General laboratory solvents were distilled before use and all reactions were magnetically stirred with organic extracts dried over anhydrous $MgSO_4$. Microwave reactions were carried out in a CEM Discover single-mode microwave apparatus, producing controlled irradiation at 2450 MHz, using standard 10 ml silicon-septum sealed glass pressure vials. Temperature was monitored using an IR sensor directed at the outside wall of the reaction vial. Once the reaction was complete the reaction vessel was cooled to 50 °C by means of propelled airflow.

5.1.4 X-ray crystallography

Full intensity data for crystals was collected on a Nonius Kappa CCD diffractometer with the crystals cooled in a steady nitrogen stream at -100 °C. The crystal structures were solved by Professor Caira at the University of Cape Town. Only one crystal structure (**Figure 3.8**) is presented in this thesis. The original structure of **3.52** was originally acquired by Jakše *et al.*[199] CCDC No. 646899. The X-ray crystal lattice dimensions determined by Professor Caira for **3.52** were consistent with those deposited by Jakše *et al.* in the CCDC and are reproduced here on page 206.

5.1.5 Docking studies

All models were constructed and visualized using Discovery Studio 3.5 Visualizer.[21] Docking studies were performed using AutoDock Vina.[203] Particular details of algorithms used are stated in the text.

5.1.6 MRSA PK inhibition studies

Biological assay was performed by Roya Zoraghi from the University of British Columbia.[16] PK activity was determined by measuring the change in absorbance at 340 nm of NADH in a continuous assay coupled to rabbit muscle lactate dehydrogenase (L-LDH). UV absorbance was measured using a Benchmark Plus microplate spectrophotometer (Bio-Rad). The reaction contained 60 mM Na+-HEPES, pH 7.5, 5% glycerol, 67 mM KCl, 6.7 mM $MgCl_2$, 0.24 mM NADH, 5.5 units L-LDH, 2 mM ADP and 10 mM PEP. Assayed compounds were dissolved in DMSO with the final concentration of the solvent never exceeding 1% of the assay volume. IC_{50} values were calculated by curve fitting on a four-parameter dose-response model with variable slope using Graphpad Prism 5.0.[220] All values determined represent three measurements, each in triplicate

5.2 Chapter Two Experimental

5.2.1 Grignard methylation

5.2.1.1 Grignard methylation of 4-bromo benzaldehyde 2.50[113]

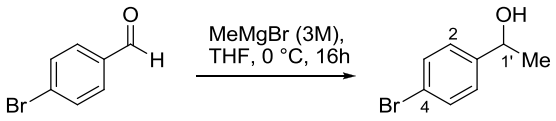

2.50 **2.51**

MeMgBr (3 M, 1.08 mol, 3 eq.) was added dropwise to a stirring solution of 4-bromobenzaldehyde (200 mg, 1.08 mmol) in dry THF (2.5 ml) under an inert atmosphere at 0 °C. The reaction mixture was allowed to stir under argon for 16 hours, resulting in an orange solution. The reaction was quenched with NH_4Cl (sat) and extracted with 3 x 10 ml Et_2O. The combined organic fractions were washed with saturated brine (10 ml), and dried over $MgSO_4$. Solvent was removed under reduced pressure to yield 4-bromophenyl ethanol **2.51** (198 mg, 0.99 mmol, 92%).

4-bromophenyl ethanol (**2.51**): yellow oil (92%), ^{1}H NMR ($CDCl_3$, 600 MHz) δ 7.46 (2H, m, H-2, H-6), 7.24 (2H, m, H-3, H-5), 4.86 (1H, q, *J* = 6.6 Hz, H-1'),1.46 (3H, d, *J* = 6.6 Hz, H-2').

5.2.1.2 Attempted Grignard methylation of 6-bromoindole-3-carbaldehyde 2.47

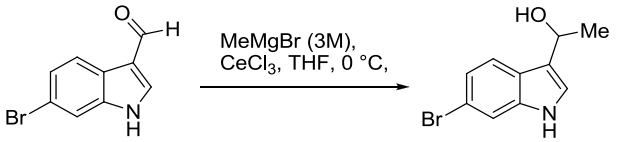

2.47

Dry $CeCl_3$ (827 mg, 3.35 mol, 1.5 eq.) was suspended in dry THF (6 ml) under argon at room temperature and allowed to stir for two hours until a fine white suspension formed. After cooling to -10 °C, MeMgBr (3 M, 6.69 mol 3 eq.) was added dropwise to the suspension and allowed to react for 1.5 hours forming a yellow suspension. 6-Bromoindole-3-carbaldehyde (500 mg, 1 eq.) was added to the reaction mixture as a solution in 2 ml THF via syringe. The reaction mixture was allowed to stir under argon for 16 hours proceeding from -10 °C to room temperature. The reaction was quenched with NH_4Cl (sat) and extracted with 3 x 10 ml Et_2O. The combined organic fractions were washed with water (3 x 10 ml) and sat. brine (3 x 10 ml), and dried over $MgSO_4$. Solvent was removed under reduced pressure yielding an orange solid which was revealed to be a complex mixture of products.

5.2.1.3 A second attempted Grignard methylation of 6-bromoindole-3-carbaldehyde 2.47

To a solution of 6-bromoindole-3-carbaldehyde (500 mg, 2.23 mol, 1 eq.) in dry THF (8 ml) under argon at room temperature was added $CeCl_3$ (827 mg, 1.5 eq.). The suspension was allowed to stir for two hours after which time the suspension was cooled to -10 °C and MeMgBr (3 M, 6.69 mol, 3 eq.) was added via syringe and allowed to stir under argon for 16 hours proceeding from -10 °C to room temperature. The reaction was quenched with NH_4Cl (sat) and extracted with 3 x 10 ml Et_2O. The combined organic fractions were washed with 3 x 10 ml water and 3 x 10 ml sat. brine, and dried

over $MgSO_4$. Solvent was removed under reduced pressure again yielding an orange solid and no significant desired product.

5.2.2 Friedel Crafts acetylation of indoles 2.42—2.46 and 2.57—2.61[104]

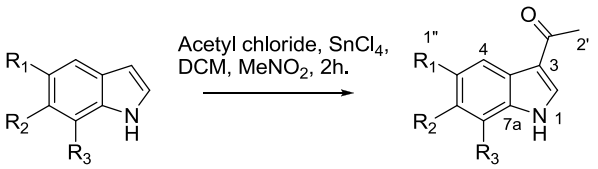

2.42 R_1 = R_3 = H, R_2 = F
2.43 R_1 = R_3 = H, R_2 = Cl
2.44 R_1 = Br, R_2 = R_3 = H
2.45 R_1 = R_3 = H, R_2 = Br
2.46 R_1 = R_3 = H, R_2 = I
2.57 R_1 = R_2 = H, R_3 = I
2.58 R_1 = Br, R_2 = H, R_3 = I
2.59 R_1 = Me, R_2 = H, R_3 = Br
2.60 R_1 = Cl, R_2 = R_3 = H
2.61 R_1 = R_2 = H, R_3 = Cl

2.36 R_1 = R_3 = H, R_2 = F
2.37 R_1 = R_3 = H, R_2 = Cl
2.38 R_1 = Br, R_2 = R_3 = H
2.39 R_1 = R_3 = H, R_2 = Br
2.40 R_1 = R_3 = H, R_2 = I
2.62 R_1 = R_2 = H, R_3 = I
2.63 R_1 = Br, R_2 = H, R_3 = I
2.64 R_1 = Me, R_2 = H, R_3 = Br
2.65 R_1 = Cl, R_2 = R_3 = H
2.66 R_1 = R_2 = H, R_3 = Cl

This method is representative. To a stirred solution of indole **2.42** (500 mg, 3.70 mmol, 1 eq.) in dry CH_2Cl_2 (7.5 ml) under argon at 0 °C was added $SnCl_4$ (519.5 µl, 1.2 eq.). The ice bath was removed and the reaction suspension was allowed to stir for a further 30 minutes. Acetyl chloride (3.70 mmol 1 eq.) was added dropwise to the reaction mixture, followed by nitromethane (4.5 ml). After four hours the reaction was quenched with ice and water. Organic material was extracted with EtOAc (100ml), washed with water (2 x 20ml) and sat. brine (2x 30ml) and dried over anhydrous $MgSO_4$. Solvent was removed *in vacuo* to afford a brown tarry solid which was dissolved in cold acetone. The acetone was allowed to slowly evaporate over several days, affording brown prisms which were washed with cold chloroform to yield **2.36** (367 mg, 2.07 mmol, 56%).

The same procedure was applied to varying quantities of indoles **2.43—2.46** and **2.57—2.61** depending on availability using the same equivalents and solvent ratios above.

1-(6-Fluoro-1*H*-indol-3-yl)ethanone[110] (**2.36**): brown prisms from acetone (56% yield), mp 210 °C, lit 236 °C[221]; IR (film) ν_{max} cm^{-1} 3016 2970 2025 1700 1529 1438 1217 950 ; ^{1}H NMR (MeOD, 600 MHz) δ 8.31 (1H, s, H-2), 8.14 (1H, dd, *J* = 8.7, 5.6 Hz, H-4), 7.25 (1H, dd, *J* = 9.7, 2.4 Hz, H-7), 7.03 (1H, m, H-5), 2.33 (3H, s, H-2'); ^{13}C NMR (MeOD, 150 MHz) δ 192.6 (q_c, C-1'), 159.2 (q_c, d, $J_{F,C}$ = 236.6 Hz, C-6), 136.7 (q_c, d, $J_{F,C}$ = 13.0 Hz, C-7a), 134.9 (CH, C-2), 122.4 (CH, d, $J_{F,C}$ = 9.9 Hz, C-4), 121.9 (q_c, C-3a), 116.7 (q_c, C-3), 109.9 (CH, d, $J_{F,C}$ = 23.5 Hz, C-5), 98.3 (CH, d, $J_{F,C}$ = 25.6 Hz, C-7), 27.1 (CH_3, C-2') ppm; ESMS *m/z* (rel. int.) 136 $[M+H]^+$ (63), 109 (100), 107 (46), 83 (12); HRESMS *m/z* 178.0664 (calcd for $C_{10}H_9NOF$ $[M+H]^+$ 178.0668).

1-(6-Chloro-1*H*-indol-3-yl)ethanone[222] (**2.37**): pale yellow prisms from acetone (72% yield), mp 220 °C (charred), lit 209 °C (decomp)[222]; IR (film) ν_{max} cm^{-1} 3117 3029 1737 1517 1442 1219 938; ^{1}H NMR (MeOD, 600 MHz) δ 8.17 (1H, d, *J* = 8.5 Hz, H-4), 8.15 (1H, s, H-2), 7.44 (1H, d, *J* = 1.8 Hz, H-7), 7.17 (1H, dd, *J* = 8.5, 1.8 Hz, H-5), 2.51 (3H, s, H-2'); ^{13}C NMR (MeOD, 150 MHz) δ 196.3 (q_c, C-1'), 138.9 (q_c, C-7a), 136.1 (CH, C-2), 130.1 (q_c, C-6), 125.5 (q_c, C-3a), 123.9 (CH, C-4), 123.6 (CH, C-5), 118.5 (q_c, C-3), 112.7 (CH, C-7), 27.1 (CH_3, C-2') ppm; ESMS *m/z* (rel. int.) 152 $[M+H]^+$ (5), 144 (10), 117 (100), 89 (45), 77 (4); HRESMS *m/z* 194.0366 (calcd for $C_{10}H_9NOCl^{35}$ $[M+H]^+$ 194.0373)

1-(5-Bromo-1*H*-indol-3-yl)ethanone[223] (**2.38**): pink needles from acetone (72% yield), mp 241—243 °C, lit 250—252 °C[223] IR (film) ν_{max} cm^{-1} 3115 2935 1707 1523 1438 1226 938; ^{1}H NMR (MeOD, 600 MHz) δ 8.39 (1H, d, *J* = 1.5 Hz, H-4), 8.12 (1H, s, H-2), 7.34 (2H,m, H-6, H-7), 2.50 (3H, s, H-2'); ^{13}C NMR (MeOD, 150 MHz) δ 194.7 (q_c, C-1'), 135.7 (q_c, C-7a), 134.6 (CH, C-2), 127.1, (q_c, C-3a), 125.7 (CH, C-6), 124.0 (CH, C-4), 116.7 (q_c, C-3), 115.2 (q_c, C-6), 113.0 (CH, C-7), 25.7 (CH_3, C-2') ppm; ESMS *m/z* (rel. int.) 236 $[M+H]^+$ (47), 224 (93), 222 (100), 194 (12), 143 (21); HRESMS *m/z* 237.9862 (calcd for $C_{10}H_9NOBr^{79}$ $[M+H]^+$ 237.9886).

1-(6-Bromo-1*H*-indol-3-yl)ethanone[223] (**2.39**): orange prisms from acetone (63% yield), mp 243—244 °C, lit 247—249 °C[223]; IR (film) ν_{max} cm^{-1} 3160 2970 1700 1626 1517 1420 1365 1217 938; ^{1}H NMR (MeOD, 600 MHz) δ 8.14 (1H, s, H-2), 8.12 (1H, d, *J* = 8.5 Hz, H-4), 7.61 (1H, s, H-7), 7.31 (1H, d, *J* = 8.5 Hz, H-5), 2.51 (3H, s, H-2'); ^{13}C NMR (MeOD, 150 MHz) δ 196.3 (q_c, C-1'), 139.3 (q_c, C-7a), 136.0 (CH, C-2), 126.3, (CH, C-5), 125.8 (q_c, C-3a), 124.3 (CH, C-4), 118.5 (q_c, C-3), 117.5 (q_c, C-6), 115.8 (CH, C-7), 27.2 (CH_3, C-2') ppm; ESMS *m/z* (rel. int.) 223 $[M+H]^+$ (10), 193 (8), 144 (100), 136 (14), 116 (100), 89 (57); HRESMS *m/z* 237.9862 (calcd for $C_{10}H_9NOBr^{79}$ $[M+H]^+$ 237.9886).

1-(6-Iodo-1*H*-indol-3-yl)ethanone (**2.40**): white crystals from acetone (64% yield), mp 189—192 °C; IR (film) ν_{max} cm^{-1} 3106 2980 2301 1703 1630 1572 1381 1268 923; ^{1}H NMR (MeOD, 600 MHz) δ 8.09 (1H, s, H-2), 8.00 (1H, d, *J* = 8.3 Hz, H-4), 7.81 (1H, s, H-7), 7.48 (1H, d, *J* = 8.2 Hz, H-5), 2.51 (3H, s, H-2'); ^{13}C NMR (MeOD, 150 MHz) δ 196.3 (q_c, C-1'), 139.7 (q_c, C-7a), 135.8 (CH, C-2), 131.9, (CH, C-5), 126.2 (q_c, C-3a), 124.5 (CH, C-4), 122.0 (CH, C-7), 118.5 (q_c, C-3), 87.6 (q_c, C-6), 27.2 (CH_3, C-2') ppm; ESMS *m/z* (rel. int.) 144 $[M+H]^+$ (100), 116 (15), 89 (4); HRESMS *m/z* 285.9732 (calcd for $C_{10}H_9NOI$ $[M+H]^+$ 285.9729).

1-(7-Iodo-1*H*-indol-3-yl)ethanone (**2.62**): clear prisms from acetone (64% yield), mp 199 °C; IR (film) ν_{max} cm^{-1} 3191 2160 1705 1628 1525 1295 942; ^{1}H NMR (MeOD, 600 MHz) δ 8.23 (1H, d, *J* = 7.8 Hz, H-6), 8.15 (1H, s, H-2), 7.60 (1H, d, *J* = 7.6 Hz, H-4), 6.97 (1H, t, *J* = 7.6 Hz, H-5), 2.51 (3H, s, H-2'); ^{13}C NMR (MeOD, 150 MHz) δ 196.5 (q_c, C-1'), 140.3 (q_c, C-7a), 135.6 (CH, C-2), 133.5 (CH, C-4), 127.3 (q_c, C-3a), 124.7 (CH, C-5), 122.9 (CH, C-6), 119.4 (q_c, C-3), 76.8 (q_c, C-7), 27.3 (CH_3, C-2') ppm; ESMS *m/z* (rel. int.) 144 $[M+H]^+$ (100), 116 (15), 89 (4); HRESMS *m/z* 285.9727 (calcd for $C_{10}H_9NOI$ $[M+H]^+$ 285.9729).

1-(5-Bromo-7-Iodo-1*H*-indol-3-yl)ethanone (**2.63**): yellow needles from acetone (86% yield), mp 248 °C; IR (film) ν_{max} cm^{-1} 3225 2159 1702 1630 1523 1286 1239 945; ^{1}H NMR (MeOD, 600 MHz) δ 8.39 (1H, s, H-4), 8.19 (1H, s, H-2), 7.73 (1H, s, H-6), 2.51 (3H, s, H-2'); ^{13}C NMR (MeOD, 150 MHz) δ 196.2

(q_c, C-1'), 139.5 (q_c, C-7a), 136.6 (CH, C-2), 135.2 (CH, C-6), 128.3 (q_c, C-3a), 125.5 (CH, C-4), 118.5 (q_c, C-3), 116.5 (q_c, C-5), 77.5 (q_c, C-7), 27.2 (CH_3, C-2') ppm; ESMS *m/z* (rel. int.) 269 $[M+H]^+$ (72), 221 (100), 195 (16), 166 (4), 143 (75), 115 (20); HRESMS *m/z* 363.8833 (calcd for $C_{10}H_8NOBr^{79}I$ $[M+H]^+$ 363.8834).

1-(5-Methyl-7-Bromo-1*H*-indol-3-yl)ethanone (**2.64**): brown prisms from acetone (75% yield), mp 207 °C; IR (film) ν_{max} cm^{-1} 3217 1738 1635 1522 1420 1198 951; ^1H NMR (MeOD, 600 MHz) δ 8.11 (1H, s, H-2), 8.01 (1H, s, H-4), 7.24 (1H, s, H-6), 2.50 (3H, s, H-2'), 2.42 (3H, s, H-1"); ^{13}C NMR (MeOD, 150 MHz) δ 196.4 (q_c, C-1'), 135.9 (CH, C-2), 135.3 (q_c, C-7a), 134.6 (q_c, C-5), 128.5 (q_c, C-3a), 128.1 (CH, C-6), 122.0 (CH, C-4), 118.5 (q_c, C-3), 105.4 (q_c, C-7), 37.5 (CH_3, C-2'), 21.4 (CH_3, C-1") ppm; ESMS *m/z* (rel. int.) 158 $[M+H]^+$ (100), 130 (45), 103 (10), 77 (3); HRESMS *m/z* 252.0021 (calcd for $C_{11}H_{11}NOBr^{79}$ $[M+H]^+$ 252.0024).

1-(5-Chloro-1*H*-indol-3-yl)ethanone[221] (**2.65**)**:** yellow crystals from acetone (65% yield), mp 227—229 °C, lit 246—247 °C[221]; IR (film) ν_{max} cm^{-1} 3125 2938 1697 1523 1439 1172 938; ^1H NMR (MeOD, 600 MHz) δ 8.19 (1H, d, *J* = 2.0 Hz, H-4), 8.16 (1H, s, H-2), 7.39 (1H, d, *J* = 8.6 Hz, H-7), 7.18 (1H, dd, *J* = 8.6, 2.1 Hz, H-6), 2.49 (3H, s H-2'); ^{13}C NMR (MeOD, 150 MHz) δ 196.2 (q_c, C-1'), 136.8 (q_c, C-7a), 136.5 (CH, C-2), 129.1 (q_c, C-5), 127.9 (q_c, C-3a), 124.5 (CH, C-6), 122.2 (CH, C-4), 118.1 (q_c, C-3), 114.1 (CH, C-7), 27.1 (CH_3, C-2') ppm; ESMS *m/z* (rel. int.) 150 $[M+H]^+$ (15), 144 (17), 130 (10), 123 (10), 117 (100), 103 (5), 89 (10); HRESMS *m/z* 194.0377 (calcd for $C_{10}H_9NOCl^{35}$ $[M+H]^+$ 194.0377).

1-(7-Chloro-1*H*-indol-3-yl)ethanone (**2.66**)**:** yellow prisms from acetone (63% yield), mp 188—190 °C; IR (film) ν_{max} cm^{-1} 3168 1740 1632 1521 1438 1167 951; ^1H NMR (MeOD, 600 MHz) δ 8.18 (1H, s, H-2), 8.17 (1H, d, *J* = 8.1 Hz, H-4), 7.24 (1H, d, *J* = 7.7 Hz, H-6), 7.16 (1H, t, *J* = 7.8 Hz, H-5), 2.53 (3H, s, H-2'); ^{13}C NMR (MeOD, 150 MHz) δ 196.4 (q_c, C-1'), 135.9 (CH, C-2), 135.4 (q_c, C-7a), 128.6 (q_c, C-3a), 124.0 (CH, C-5), 123.8 (CH, C-6), 121.7 (CH, C-4), 119.3 (q_c, C-3), 118.3 (q_c, C-7), 27.3 (CH_3, C-2') ppm;

ESMS *m/z* (rel. int.) 178 $[M+H]^+$ (6), 150 (8), 144 (17), 117 (100), 89 (20); HRESMS *m/z* 194.0372 (calcd for $C_{10}H_9NOCl^{35}$ $[M+H]^+$ 194.0373).

5.2.3 Synthesis of 6-iodoindole 2.46[126,135]

5.2.3.1 *N*-Acetylation of 6-nitroindoline 2.74

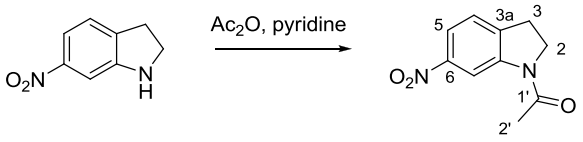

2.74 **2.75**

Pyridine (0.5ml) was added to a stirring solution of **2.74** (2020 mg, 12.3 mmol, 1eq.) in Ac_2O (10.34 ml, 9 eq.) resulting in an instant colour change to bright yellow. After stirring for 1 hour, a small portion of ice was added to quench the reaction. Toluene (1 x 30 ml) was added and removed *in vacuo* to assist in azeotropically removing acetic acid. Further drying under vacuum to remove excess pyridine yielded a yellow crystalline solid. Recrystallisation from methanol yielded **2.75** (2059 mg, 12.2 mmol, 99%).

***N*-Acetyl-6-nitroindoline**[135] (**2.75**): yellow needles from methanol (99% yield), mp 160—163 °C, lit 152—156 °C[135]; IR (film) ν_{max} cm^{-1} 3134 1664 1591 1397 894; ^1H NMR ($CDCl_3$, 600 MHz) δ 8.97 (1H, d, *J* = 1.5 Hz, H-7), 7.88 (1H,dd, *J* = 7.9, 1.9 Hz, H-5), 7.26 (1H, d, *J* = 8.0 Hz, H-4), 4.17 (2H, t, *J* = 8.6 Hz, H-2), 3.29 (2H, t, *J* = 8.5 Hz, H-3), 2.25 (3H, s, H-2'); ^{13}C NMR ($CDCl_3$, 150 MHz) δ 169.2 (q_c, C-1'), 147.9 (CH, C-6), 143.8 (q_c, C-7a), 138.4 (q_c, C-3a), 124.4 (CH, C-4), 119.1 (CH, C-5), 111.7 (CH, C-7), 49.2 (CH_2, C-2), 27.9 (CH_2, C-3), 24.1 (CH_3, C-2') ppm; ESMS *m/z* (rel. int.) 118$[M+H]^+$ (100), 91 (26), 65 (3); HRESMS *m/z* 207.0762 (calcd for $C_{10}H_{11}N_2O_3$ $[M+H]^+$ 207.0770).

5.2.3.2 Hydrogenation of *N*-acetyl-6-nitroindoline 2.75

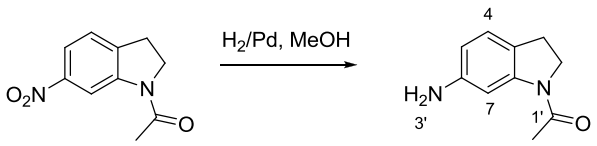

2.75 **2.76**

10% Pd/C (250 mg) was added to a vigorously stirring yellow suspension of **2.75** (2.45 g, 11.89 mmol, 1 eq.) in methanol (120 ml) under an atmosphere of H_2 gas. The reaction was allowed to stir for three hours at room temperature until the yellow colour has disappeared, after which time the Pd/C was carefully filtered. The methanolic solution was concentrated *in vacuo* to yield **2.76** as pink crystals (2072 mg, 11.77 mmol, 99%).

***N*-Acetyl-6-aminoindoline**[135] (**2.76**): pink crystals from methanol (99% yield) mp 180—185 °C, lit 187—191[135]; IR (film) ν_{max} cm^{-1} 3409 3319 2918 1650 1495 1308 1204 1029; ^{1}H NMR ($CDCl_3$, 600 MHz) δ 7.66 (1H, d, *J* = 1.8 Hz, H-7), 6.92 (1H,d, *J* = 7.9 Hz, H-4), 6.34 (1H, dd, *J* = 7.8, 2.2 Hz, H-5), 4.01 (2H, t, *J* = 8.4 Hz, H-2) 3.66 (2H, br, NH_2-3'), 3.06 (2H, t, *J* = 8.4 Hz, H-3), 2.19 (3H, s, H-2'); ^{13}C NMR ($CDCl_3$, 150 MHz) δ 168.7 (q_c, C-1'), 146.1 (CH, C-6), 143.8 (q_c, C-7a), 124.8 (CH, C-4), 120.9 (q_c, C-3a), 110.2 (CH, C-5), 104.5 (CH, C-7), 49.5 (CH_2, C-2), 27.2 (CH_2, C-3), 24.3 (CH_3, C-2') ppm; ESMS *m/z* (rel. int.) 135 $[M+H]^+$ (52), 118 (100), 107 (18), 91 (51), 80 (5), 65 (11); HRESMS *m/z* 177.1024 (calcd for $C_{10}H_{13}N_2O$ $[M+H]^+$ 177.1028).

5.2.3.3 Diazotization of *N*-acetyl-6-aminoindoline 2.76

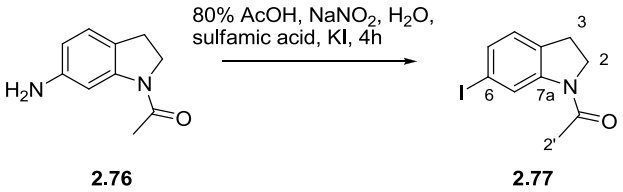

2.76 **2.77**

To a solution of **2.76** (2.12 g, 12.03 mmol, 1 eq.) in 80% AcOH (250 ml) under an atmosphere of argon gas was added $NaNO_2$ (912 mg, 1.1 eq.) in 7,5 ml cold water. The mixture was allowed to stir for 30 minutes resulting in a dark yellow solution. Sulfamic acid was then added until the reaction mixture no longer turned KI starch paper blue, followed by KI (6.005 g, 3 eq.) in 7.5 ml cold water. After four hours $NaHSO_4$ was added and the reaction halted. AcOH was concentrated as an azeotrope with toluene (200 ml) to yield a brown yellow residue. The residue was dissolved in EtOAc (100ml) and washed with water (2 x 20 ml) and sat. brine (2 x 20 ml) to yield a brown solid (2.99g). Flash chromatography in hexane: EtOAc (1:1) yielded **2.77** (2520 mg, 8.78 mmol, 73%).

***N*-Acetyl-6-iodoindoline**[224] (**2.77**)**:** fine yellow needles from hexane (73% yield), mp 132—133 °C, lit 131—132 °C[224]; IR (film) ν_{max} cm^{-1} 3115 2962 2160 1737 1652 1548 1478 1125 1030; ^{1}H NMR ($CDCl_3$, 600 MHz) δ 8.57 (1H, d, *J* = 1.4 Hz, H-7), 7.32 (1H,dd, *J* = 7.8, 1.3 Hz, H-5), 6.89 (1H, d, *J* = 7.8 Hz, H-4), 4.03 (2H, t, *J* = 8.5 Hz, H-2) 3.13 (2H, t, *J* = 8.5 Hz, H-3), 2.21 (3H, s, H-2'); ^{13}C NMR ($CDCl_3$, 150 MHz) δ 168.8 (q_c, C-1'), 144.1 (q_c, C-7a), 132.5 (CH, C-4), 130.9 (q_c, C-3a), 126.0 (CH, C-5), 126.5 (CH, C-7), 92.2 (CH, C-6), 48.9 (CH_2, C-2), 27.7 (CH_2, C-3), 24.2 (CH_3, C-2') ppm; ESMS *m/z* (rel. int.) 245 $[M+H]^+$ (5), 161 (10), 118 (100), 91 (30); HRESMS *m/z* 287.9880 (calcd for $C_{10}H_{11}NOI$ $[M+H]^+$ 287.9885).

5.2.3.4 De-acetylation of *N*-acetyl-6-iodoindoline 2.77

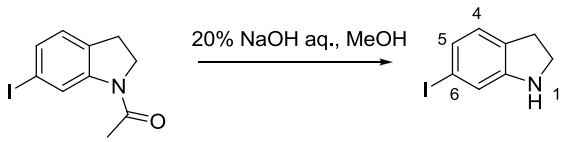

2.77 **2.78**

A 20% aq. NaOH solution (80 ml) was added to a solution of **2.77** (1.65 g, 5.75 mmol, 1 eq.) in methanol (100 ml). The reaction mixture was heated to 75 °C and allowed to react for four hours, after which time the methanol was concentrated *in vacuo* and the mixture diluted with EtOAc (100 ml) and washed with water (3 x 20 ml) and sat. brine (1 x 30 ml). Concentration of the EtOAc solution yielded an orange oil (1.31 g). Flash column chromatography (hexane: EtOAc, 10:1) yielded **2.78** (1102 mg, 4.48 mmol, 78 %).

6-Iodoindoline[224] (**2.78**): purple needles from hexane (78% yield), mp 94 °C, lit 92.5 °C[224]; IR (film) ν_{max} cm^{-1} 3383 2951 1737 1600 1485 1320 1254 1050; ^{1}H NMR ($CDCl_3$, 600 MHz) δ 6.99 (1H, d, *J* = 7.6 Hz, H-5), 6.94 (1H, s, H-7), 6.83 (1H, d, *J* = 7.6 Hz, H-4), 3.54 (2H, t, *J* = 8.4 Hz, H-2) 2.97 (2H, t, *J* = 8.38 Hz, H-3); ^{13}C NMR ($CDCl_3$, 150 MHz) δ 153.5 (q_c, C-7a), 129.1 (q_c, C-3a), 127.4 (CH, C-5), 126.2 (CH, C-4), 117.9 (CH, C-7), 91.9 (CH, C-6), 47.4 (CH_2, C-2), 29.4 (CH_2, C-3) ppm; ESMS *m/z* (rel. int.) 245 $[M+H]^+$ (35), 119 (100), 104 (15), 91 (14); HRESMS *m/z* 245.9788 (calcd for $C_{10}H_9NI$ $[M+H]^+$ 245.9780).

5.2.3.5 Oxidation of 6-iodoindoline 2.78

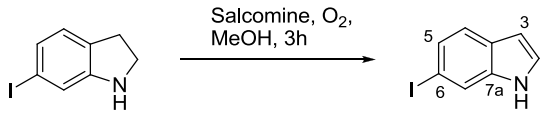

2.78 **2.46**

Salcomine (50 mg, 0.1 eq.)was added to a methanolic solution (8 ml) of **2.78** (380 mg, 1.55 mmol, 1 eq.). After stirring for three hours, the methanol was removed *in vacuo* and the crude mixture subjected to flash column chromatography (hexane: EtOAc, 8:1) yielding **2.46** (360 mg, 1.48 mmol, 96%)

6-Iodoindole[135] (**2.46**): purple needles from chloroform (96% yield), mp 105 °C, lit 70—71 °C[135]; IR (film) ν_{max} cm^{-1} 3409 3079 2161 1884 1598 1490 1332 1089; ^{1}H NMR ($CDCl_3$, 600 MHz) δ 8.14 (1H, br s, NH-1), 7.76 (1H, s, H-7), 7.39 (2H, m, H-4, H-5), 7.15 (1H, t, *J* = 2.7 Hz, H-2), 6.53 (1H, m, H-3); ^{13}C NMR ($CDCl_3$, 150 MHz) δ 137.1 (q_c, C-7a), 128.6 (CH, C-5), 127.2 (q_c, C-3a), 124.5 (CH, C-2), 122.3 (CH, C-4), 119.9 (CH, C-7), 102.9 (q_c, C-3), 85.7 (q_c, C-6) ppm; ESMS *m/z* (rel. int.) 245 $[M+H]^+$ (15), 215 (5), 190 (5), 170 (15), 161 (12), 118 (100), 101 (5), 92 (8); HRESMS *m/z* 243.9645 (calcd for C_8H_7NI $[M+H]^+$ 243.9623).

5.2.3.6 Attempted diazotization of 6-aminoindole[127]

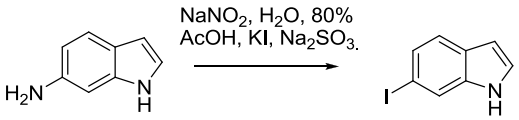

2.46

An aq. solution of $NaNO_2$ (43 mg, 1.1 eq.) in 0.5 ml water was added to a solution of 6-amino indole (75 mg, 0.57 mol, 1 eq.) in 80% acetic acid (21 ml), resulting in a colour change to dark brown. This was directly followed by the addition of an aq. solution of KI (104 mg (1.1 eq.) in 0.5 ml water. After 30 minutes $NaHSO_3$ was added and allowed to stir for five minutes. The reaction was stopped and toluene was added to allow for azeotroptic removal of acetic acid. The concentrated reaction mixture was diluted in EtOAc (10 ml) and washed with water (2 x 10 ml) and sat. brine (2 x 10 ml). The organic fraction was dried over $MgSO_4$ and solvent removed under reduced pressure. Analysis of the crude reaction mixture revealed no observable **2.46**

5.2.4 *N*-Boc protection of indole[94]

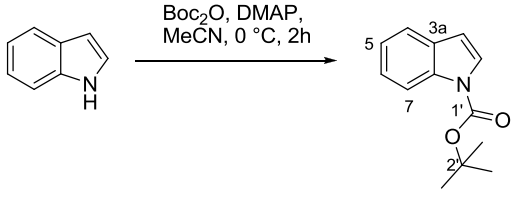

2.56

Boc_2O (545 mg, 1.5 eq.) and DMAP (19 mg, 0.1 eq.) were added to a stirring solution of indole (200 mg, 1.7 mmol, 1 eq.) in HLPC grade MeCN (3 ml) at 0 °C under an atmosphere of argon. After three

hours the MeCN was removed *in vacuo* and the volatile reagents removed under reduced pressure to yield **2.56** (344 mg, 1.6 mmol, 94%).

***N*-*tert*-Butoxycarbonyl indole**[225] **(2.56)**: yellow white oil (94%), ^{1}H NMR ($CDCl_3$, 600 MHz) δ 8.15 (1H, d, *J* = 6.2 Hz, H-7), 7.60 (1H, d, *J* = 3.3 Hz, H-3), 7.56 (1H, d, *J* = 7.7 Hz, H-4), 7.31 (1H, t, *J* = 7.6 Hz, H-6), 7.23 (1H, t, *J* = 7.3 Hz, H-5), 6.57 (1H, d, *J* = 3.4 Hz, H-2), 1.68 (9H, s, H-3'); ^{13}C NMR ($CDCl_3$, 150 MHz) δ 149.8 (q_c, C-1'), 135.1 (q_c, C-7a), 130.5 (q_c, C-3a), 125.8 (CH, C-3), 124.1 (CH, C-6), 122.5 (CH, C-5), 120.9 (CH, C-4), 115.1 (CH, C-7), 107.2 (CH, C-2), 83.6 (q_c, C-2'), 28.1 (3 x CH_3, C-3').

5.2.5 *N*-Boc protection of 1-(1*H*-indol-3-yl)ethanones 2.1, 2.36—2.40, and 2.66[94]

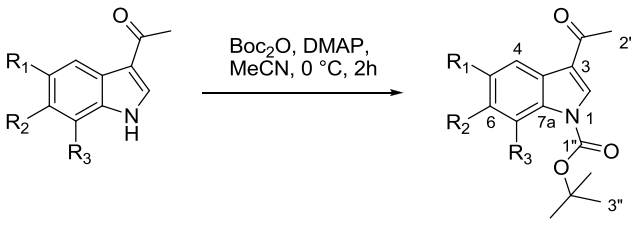

2.1 $R_1 = R_2 = R_3 = H$
2.36 $R_1 = R_3 = H, R_2 = F$
2.37 $R_1 = R_3 = H, R_2 = Cl$
2.38 $R_1 = Br, R_2 = R_3 = H$
2.39 $R_1 = R_3 = H, R_2 = Br$
2.40 $R_1 = R_3 = H, R_2 = I$
2.66 $R_1 = R_2 = H, R_3 = Cl$

2.80 $R_1 = R_2 = R_3 = H$
2.55 $R_1 = R_3 = H, R_2 = F$
2.83 $R_1 = R_3 = H, R_2 = Cl$
2.84 $R_1 = Br, R_2 = R_3 = H$
2.85 $R_1 = R_3 = H, R_2 = Br$
2.86 $R_1 = R_3 = H, R_2 = I$
2.87 $R_1 = R_2 = H, R_3 = Cl$

This method is representative. Boc_2O (2020 mg, 1.5 eq.) and DMAP (77 mg, 0.1 eq.) was added to a stirring solution of **2.1** (1000 mg, 6.3 mmol, 1 eq.) in HPLC grade MeCN (15 ml) at 0 °C under an atmosphere of argon. After three hours the MeCN was removed *in vacuo* and the solid re-crystallized from methanol to yield **2.80** (1565 mg, 6.04 mmol, 96%)

The same procedure was applied to varying quantities of 3-acetylindoles **2.36—2.40, 2.65** and **2.66** depending on availability using the same equivalents and solvent ratios above.

3-Acetyl-1-(*tert*-butoxycarbonyl)indole [226] (**2.80**) white needles from methanol (96 % yield), mp 148 °C, lit. 148 °C[226]; IR (film) ν_{max} cm^{-1} 2981 1739 1664 1545 1449 1359 1150; ^{1}H NMR ($CDCl_3$, 600 MHz) δ 8.36 (1H, m, H-4), 8.22 (1H, s, H-2), 8.10 (1H, d, *J*= 7.9 Hz, H-7), 7.35 (2H, m, H-5, H-6), 2.55 (3H, s, H-2'), 1.70 (9H, s, H-3"); ^{13}C NMR ($CDCl_3$, 150 MHz) δ 193.9 (q_c, C-1'), 149.1 (q_c, C-1"), 135.5 (q_c, C-7a), 132.4 (CH, C-2), 127.4, (q_c, C-3a), 125.5 (CH, C-6), 124.4 (CH, C-5), 122.7 (CH, C-4), 120.7 (q_c, C-3), 114.9 (CH, C-7), 85.4 (q_c, C-2"), 28.1 (3x CH_3, C-3"), 27.7 (CH_3, C-2') ppm; ESMS *m/z* (rel. int.) 204 $[M+H]^+$ (5), 160 (6), 118 (100), 91 (38), 57 (5); HRESMS *m/z* 260.1281 (calcd for $C_{15}H_{18}NO_3$ $[M+H]^+$ 260.1287).

6-Fluoro-3-acetyl-1-(*tert*-butoxycarbonyl)indole (**2.55**): white needles from methanol (84% yield over 1 step, 43% over 2 steps), mp 142—143 °C; IR (film) ν_{max} cm^{-1} 2983, 1732, 1659, 1428, 1350, 1153; ^{1}H NMR ($CDCl_3$, 600 MHz) δ 8.31 (1H,dd, *J* = 8.8, 5.7 Hz, H-4), 8.18 (1H, s, H-2), 7.82 (1H, d, *J* = 9.5 Hz, H-7), 7.09 (1H, m, H-5), 2.55 (3H, s, H-2'), 1.71 (9H, s, H-3"); ^{13}C NMR ($CDCl_3$, 150 MHz) δ 193.7 (q_c, C-1'), 161.3 (q_c, d, $J_{F,C}$ = 243.2 Hz, C-6), 148.8 (q_c, C-1"), 135.8 (q_c, d, $J_{F,C}$ = 12.6 Hz, C-7a), 132.4 (CH, C-2), 123.7 (CH, d, $J_{F,C}$ = 9.8 Hz C-4), 123.6 (q_c, C-3a), 120.4 (q_c, C-3), 112.6 (CH, d, $J_{F,C}$ = 23.5 Hz, C-5), 102.3 (CH, d, $J_{F,C}$ = 28.7 Hz, C-7), 85.8 (q_c, C-2"), 28.1 (3x CH_3, C-3"), 27.5 (CH_3, C-2') ppm; ESMS *m/z* (rel. int.) 222 $[M+H]^+$ (11), 178 (15), 118 (100), 109 (80), 83 (10), 57 (15); HRESMS *m/z* 278.1181 (calcd for $C_{15}H_{17}NO_3F$ $[M+H]^+$ 278.1192).

6-Chloro-3-acetyl-1-(*tert*-butoxycarbonyl)indole (**2.83**): white needles from methanol (94% yield), mp 180—182 °C; IR (film) ν_{max} cm^{-1} 2970 2162 1732 1665 1548 1361 1272 1150; ^{1}H NMR ($CDCl_3$, 600 MHz) δ 8.28 (1H, d, *J* = 8.4 Hz, H-4), 8.18 (1H, s, H-2), 8.15 (1H, s, H-7), 7.32 (1H, dd, *J* = 8.5, 1.7 Hz, H-5), 2.55 (3H, s, H-2'), 1.71 (9H, s, H-3"); ^{13}C NMR ($CDCl_3$, 150 MHz) δ 193.6 (q_c, C-1'), 148.7 (q_c, C-1"), 135.9 (q_c, C-7a), 132.5 (CH, C-2), 131.5, (q_c, C-6), 125.8 (q_c, C-3a), 124.9 (CH, C-5), 123.5 (CH, C-4), 120.3 (q_c, C-3), 115.3 (CH, C-7), 85.9 (q_c, C-2"), 28.0 (3x CH_3, C-3"), 27.6 (CH_3, C-2') ppm; ESMS *m/z* (rel. int.) 238 $[M+H]^+$ (5), 194 (7), 152 (17), 117 (100), 89 (10), 57 (15); HRESMS *m/z* 294.0889 (calcd for $C_{15}H_{17}NO_3Cl^{35}$ $[M+H]^+$ 294.0897).

5-Bromo-3-acetyl-1-(*tert*-butoxycarbonyl)indole (**2.84**): purple needles from methanol (65% yield), mp 170—173 °C; IR (film) ν_{max} cm^{-1} 2880 2162 1746 1662 1546 1439 1361 1272 1150; ^{1}H NMR ($CDCl_3$, 600 MHz) δ 8.54 (1H, d, *J* = 1.7 Hz, H-4), 8.19 (1H, s, H-2), 7.98 (1H, d, *J* = 8.7 Hz, H-7), 7.47 (1H, dd, *J* = 8.3, 1.9 Hz, H-6), 2.55 (3H, s, H-2'), 1.71 (9H, s, H-3"); ^{13}C NMR ($CDCl_3$, 150 MHz) δ 193.5 (q_c, C-1'), 148.8 (q_c, C-1"), 134.3 (q_c, C-7a), 132.9 (CH, C-2), 128.9 (q_c, C-3a), 128.5 (CH, C-6), 125.4 (CH, C-4), 119.8 (q_c, C-3), 118.1 (q_c, C-5), 116.3 (CH, C-7), 85.9 (q_c, C-2"), 28.1 (3x CH_3, C-3"), 27.6 (CH_3, C-2') ppm; ESMS *m/z* (rel. int.) 281 $[M+H]^+$ (5), 237 (5), 188 (5), 159 (6), 144 (100), 116 (24), 89 (8); HRESMS *m/z* 338.0377 (calcd for $C_{15}H_{17}NO_3Br^{79}$ $[M+H]^+$ 338.0392).

6-Bromo-3-acetyl-1-(*tert*-butoxycarbonyl)indole[89] (**2.85**): white needles from methanol (75% yield), mp 186°C, lit. 150—152 °C;[89] IR (film) ν_{max} cm^{-1} 2971 2161 2033 1665 1548 1461 1360 1152; ^{1}H NMR ($CDCl_3$, 600 MHz) δ 8.32 (1H, s, H-7), 8.22 (1H, d, *J* = 8.4 Hz, H-4), 8.16 (1H, s, H-2), 7.46 (1H, dd, *J* = 8.5, 1.7 Hz, H-5), 2.55 (3H, s, H-2'), 1.71 (9H, s, H-3"); ^{13}C NMR ($CDCl_3$, 150 MHz) δ 193.6 (q_c, C-1'), 148.7 (q_c, C-1"), 136.2 (q_c, C-7a), 132.4 (CH, C-2), 127.7 (CH, C-5), 126.2 (q_c, C-3a), 123.9 (CH, C-4), 120.3 (q_c, C-3), 119.3, (q_c, C-6), 118.2 (CH, C-7), 85.9 (q_c, C-2"), 28.0 (3x CH_3, C-3"), 27.6 (CH_3, C-2') ppm; ESMS *m/z* (rel. int.) 292 $[M+H]^+$ (32), 261 (37), 251 (100), 203 (11), 183 (84), 162 (10), 109 (21), 92 (34), 57 (20); HRESMS *m/z* 338.0377 (calcd for $C_{15}H_{17}NO_3Br^{79}[M+H]^+$ 338.0392).

6-Iodo-3-acetyl-1-(*tert*-butoxycarbonyl)indole (**2.86**): white needles from methanol (81% yield), mp 181—182 °C; IR (film) ν_{max} cm^{-1} 2970 2159 1700 1662 1546 1363 1275 1154; ^{1}H NMR ($CDCl_3$, 600 MHz) δ 8.54 (1H, s, H-7), 8.11 (2H, m, H-2, H-4), 7.65 (1H, d, *J* = 8.3 Hz, H-5), 2.54 (3H, s, H-2'), 1.71 (9H, s, H-3"); ^{13}C NMR ($CDCl_3$, 150 MHz) δ 193.6 (q_c, C-1'), 148.7 (q_c, C-1"), 136.4 (q_c, C-7a), 133.3 (CH, C-5), 132.2 (CH, C-2), 126.7 (q_c, C-3a), 124.2 (CH, C-4), 124.1 (CH, C-7), 120.4 (q_c, C-3), 90.2 (q_c, C-6), 85.9 (q_c, C-2"), 28.04 (3x CH_3, C-3"), 27.7 (CH_3, C-2') ppm; ESMS *m/z* (rel. int.) 329 $[M+H]^+$ (12), 285 (4), 203 (27), 188 (62), 144 (100), 116 (3); HRESMS *m/z* 386.0251 (calcd for $C_{15}H_{17}NO_3I$ $[M+H]^+$ 386.0253).

7-Chloro-3-acetyl-1-(*tert*-butoxycarbonyl)indole (**2.87**): beige amorphous solid (20% yield); ^{1}H NMR ($CDCl_3$, 600 MHz) δ 8.34 (1H, d, *J* = 7.9 Hz, H-4), 8.14 (1H, s, H-2), 7.38 (1H, d, *J* = 7.7 Hz, H-6), 7.28 (1H, t, *J* = 7.8 Hz, H-5), 2.55 (3H, s, H-2'), 1.68 (9H, s, H-3"); ^{13}C NMR ($CDCl_3$, 150 MHz) δ 193.3 (q_c, C-1'), 148.3 (q_c, C-1"), 135.5 (CH, C-2), 132.3 (q_c, C-7a), 130.6 (q_c, C-3a), 127.5 (CH, C-6), 125.3 (CH, C-5), 121.4 (CH, C-4), 120.0 (q_c, C-7), 119.9 (q_c, C-3), 86.2 (q_c, C-2"), 27.8 (3x CH_3, C-3"), 27.7 (CH_3, C-2') ppm; ESMS *m/z* (rel. int.) 263 $[M+H]^+$ (13), 228 (43), 201 (23), 174 (8), 152 (28), 117 (100),112 (22), 90 (4), 68 (12); HRESMS *m/z* 294.0889 (calcd for $C_{15}H_{17}NO_3Cl^{35}$ $[M+H]^+$ 294.0897).

5.2.6 SeO_2 oxidation of 3-acetyl-1-(*tert*-butoxycarbonyl)indole 2.80 and cyclization[93,94]

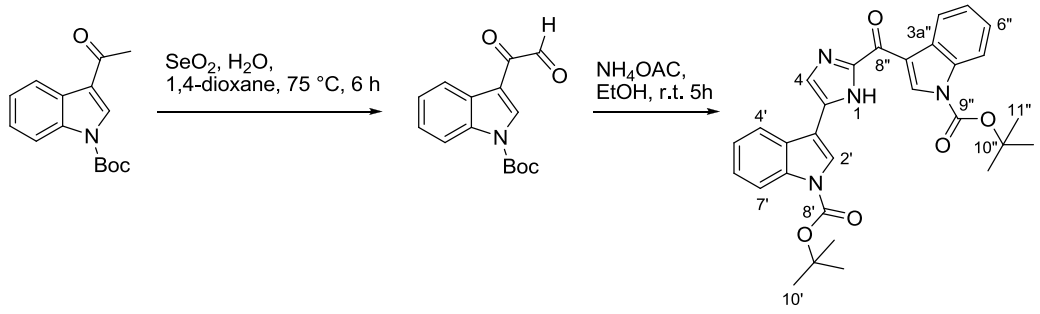

2.80 **2.88**

Freshly sublimed SeO_2 (286 mg, 2.59 mmol, 2.7 eq.) was added to a mixture of 1,4-dioxane (7 ml) and water (200 µl, 11 eq.) after which the reaction mixture was heated to 60 °C to allow all the SeO_2 to dissolve. To this was added **2.80** (250 mg, 0.96 mmol, 1eq.) and the temperature increased to 75 °C. After six hours the crude reaction mixture was filtered through celite, which was washed with CH_2Cl_2 (20 ml). The combined fractions were washed with water (2 x 10ml) and sat. brine (2 x 10 ml), dried over anhydrous $MgSO_4$ and the organic fraction concentrated *in vacuo* to yield an orange oil (287 mg). The crude reaction mixture was dissolved in EtOH (7 ml) followed by the addition of NH_4OAc (374 mg, 5 eq.) and allowed to stir for five hours. The bright orange solution was

concentrated *in vacuo*, and redissolved in CH_2Cl_2 (15 ml). The organic solution was once again washed with water (2 x 10ml) and sat. brine (2 x 10 ml) and dried over anhydrous $MgSO_4$ to yield a yellow amorphous solid (248 mg). Purification via flash chromatography (hexane : EtOAc, 5:1), yielded **2.88** (141.5 mg, 0.27 mmol, 53% over two steps).

(*N*1', *N*1"- di-*tert*-Butoxycarbonyl)-Indol-3-yl[5-(indol-3-yl)-1*H*-imidazole-2-yl]-methanone[94] (**2.88**): yellow amorphous solid (53%); IR (film) ν_{max} cm^{-1} 2980, 1741, 1667, 1370, 1150, 749; ^{1}H NMR (DMSO-d_6, 600 MHz) δ 13.62 (1H, s, NH-1), 9.69 (1H, s, H-2"), 8.45 (1H, d, *J* = 7.8 Hz, H-4"), 8.38 (1H, d, *J* = 7.7 Hz, H-4'), 8.19 (1H, d, *J* = 8.1 Hz, H-7"), 8.14 (2H, m, H-2', H-7'), 8.09 (1H, s, H-4), 7.42 (4H, m, H-5', H-5", H-6', H-6"), 1.69 (9H, s, H-11"), 1.68 (9H, s, H-10') ; ^{13}C NMR (DMSO-d_6, 150 MHz) δ 176.2 (q_c, C-8"), 149.1 (q_c, C-9"), 148.6 (q_c, C-8'), 144.8 (q_c, C-2), 136.6 (CH, C-2"), 136.4 (q_c, C-5), 135.1 (q_c, C-7a"), 134.7 (q_c, C-7a'), 127.9 (q_c, C-3a"), 127.8 (q_c, C-3a'), 125.5 (CH, C-6"), 124.7 (CH, C-6'), 124.4 (CH, C-5"), 123.1 (CH, C-5'), 122.3 (CH, C-4"), 122.0 (CH, C-2'), 121.1 (CH, C-4'), 118.6 (CH, C-4), 116.6 (q_c, C-3"), 116.5 (CH, C-3'), 114.9 (CH, C-7"), 114.8 (CH, C-7'), 85.4 (q_c, C-10"), 84.1 (q_c, C-9'), 27.7 (3 x CH_3, C-11"), 27.6 (3 x CH_3, C-10') ppm; ESMS *m/z* (rel. int.) 415 $[M+H]^+$ (9), 371 (10), 254 (50), 228 (5), 210 (10), 182 (15), 155 (100), 144 (18), 116 (5); HRESMS *m/z* 527.2308 (calcd for $C_{30}H_{31}N_4O_5$ $[M+H]^+$ 527.2294).

5.2.7 SeO_2 oxidation of 3-acetyl-1-(*tert*-butoxycarbonyl)indoles 2.55, 2.83—2.86 and cyclization[93,94]

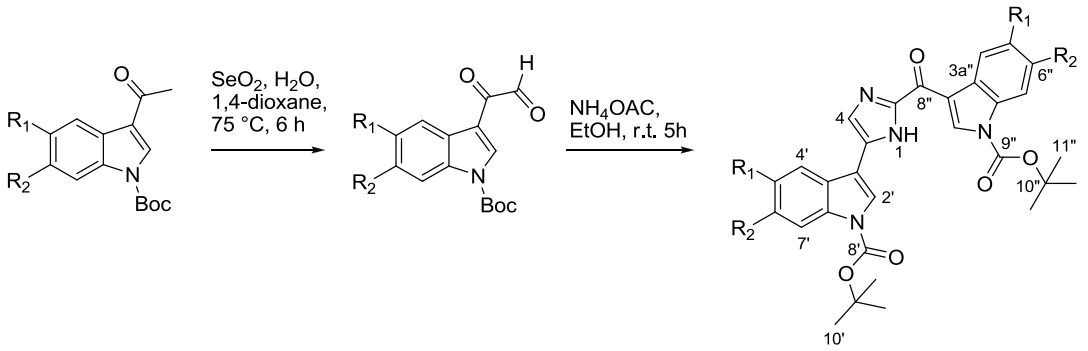

2.55 R_1 = H, R_2 = F
2.83 R_1 = H, R_2 = Cl
2.84 R_1 = Br, R_2 = H
2.85 R_1 = H, R_2 = Br
2.86 R_1 = H, R_2 = I

2.90 R_1 = H, R_2 = F
2.91 R_1 = H, R_2 = Cl
2.92 R_1 = Br, R_2 = H
2.102 R_1 = H, R_2 = I
2.103 R_1 = H, R_2 = Br

This method is representative. Freshly sublimed SeO_2 (248 mg, 2.25 mmol, 6.3 eq.) was added to a mixture of 1,4-dioxane (4 ml) and water (101 µl, 15 eq.) after which the reaction mixture was heated to 60 °C to allow all the SeO_2 to dissolve. To this was added **2.55** (100 mg, 0.36 mmol, 1eq.) and the temperature increased to 75 °C. After six hours the crude reaction mixture was filtered through celite, which was washed with CH_2Cl_2 (15 ml). The combined fractions were washed with water (2 x 10ml) and sat. brine (2 x 10 ml), dried over anhydrous $MgSO_4$ and the organic fraction concentrated *in vacuo* to yield an orange oil (118 mg). 45.6 mg of the crude reaction mixture was dissolved in EtOH (2 ml) followed by the addition of NH_4OAc (60 mg, 5 eq.) and allowed to stir for five hours. The bright orange solution was concentrated *in vacuo*, and redissolved in CH_2Cl_2 (10 ml). The organic solution was once again washed with water (2 x 10ml) and sat. brine (2 x 10 ml) and dried over anhydrous $MgSO_4$ to yield a yellow amorphous solid (40 mg). Purification via flash chromatography (hexane: EtOAc, 5:1), yielded **2.90** (19.9 mg, 0.035 mmol, 51% over two steps).

The same procedure was applied to varying quantities of *N*-Boc protected 3-acetylindoles **2.83—2.86** depending on availability using the same equivalents and solvent ratios above.

(*N*1', *N*1"- di-*tert*-Butoxycarbonyl)-6"-fluoroindol-3-yl[5-(6'-fluoroindol-3-yl)-1*H*-imidazole-2-yl]-methanone (**2.90**): yellow amorphous solid (51% over two steps); IR (film) ν_{max} cm^{-1} 2970 2161 1739 1608 1488 1217 1152; ^{1}H NMR (DMSO-d_6, 600 MHz) δ 13.66 (1H, s, NH-1), 9.66 (1H, s, H-2"), 8.42 (1H, dd, *J* = 8.7, 5.7 Hz, H-4"), 8.38 (1H, dd, *J* = 8.6, 5.7 Hz, H-4'), 8.13 (1H, s, H-2'), 8.11 (1H, s, H-4), 7.88 (2H, m, H-7', H-7"), 7.32 (1H, m, H-5"), 7.20 (1H, m, H-5'), 1.68 (9H, s, H-11"), 1.67 (9H, s, H-10') ; ^{13}C NMR (DMSO-d_6, 150 MHz) δ 175.9 (q_c, C-8"), 160.4 (q_c, d, $J_{F,C}$ = 239.5 Hz, C-6"), 160.2 (q_c, d, $J_{F,C}$ = 238.8 Hz, C-6'), 148.8 (q_c, C-9"), 148.3 (q_c, C-8'), 144.6 (q_c, C-2), 136.6 (CH, C-2"), 136.2 (q_c, C-5), 134.9 (q_c, C-7a"), 134.8 (q_c, C-7'), 124.5 (2 x q_c, C- 3a', C-3a"), 123.3 (CH, d, $J_{F,C}$ = 9.9 Hz, C-4"), 122.6 (CH, C-2'), 122.4 (CH, d, $J_{F,C}$ = 9.9 Hz, C-4'), 118.8 (CH, C-4), 116.3 (q_c, C-3"), 114.6 (q_c, C-3'), 112.5 (CH, d, $J_{F,C}$ = 23.7 Hz, C-5"), 110.0 (CH, d, $J_{F,C}$ = 23.6 Hz, C-5'), 101.9 (2 x CH, C-7', C-7"), 85.9 (q_c, C-10"), 84.6 (q_c, C-9'), 27.6 (3 x CH_3, C-11"), 27.5 (3 x CH_3, C-10') ppm; ESMS *m/z* (rel. int.) 451 $[M+H]^+$ (18), 407 (25), 290 (10), 272 (100), 246 (10), 228 (28), 200 (25), 173 (70), 162 (13); HRESMS *m/z* 563.2115 (calcd for $C_{30}H_{29}N_4O_5F_2$ $[M+H]^+$ 563.2106).

(*N*1', *N*1"- di-*tert*-Butoxycarbonyl)-6"-chloroindol-3-yl[5-(6'-chloroindol-3-yl)-1*H*-imidazole-2-yl]-methanone (**2.91**): yellow amorphous solid (47% over two steps); IR (film) ν_{max} cm^{-1} 2980 2160 1739 1601 1430 1365 1236 1098; ^{1}H NMR (DMSO-d_6, 600 MHz) δ 13.65 (1H, s, NH-1), 9.58 (1H, s, H-2"), 8.38 (1H, d, *J* = 8.4 Hz, H-4"), 8.34 (1H, d, *J* = 8.4 Hz, H-4'), 8.14 (1H, s, H-7"), 8.12 (1H, s, H-2'), 8.11 (1H, s, H-7'), 8.08 (1H, d, *J* = 2.2 Hz, H-4), 7.45 (1H, d, *J* = 8.5 Hz, H-5"), 7.34 (1H, d, *J* = 8.4 Hz, H-5'), 1.68 (9H, s, H-11"), 1.67 (9H, s, H-10') ; ^{13}C NMR (DMSO-d_6, 150 MHz) δ 175.8 (q_c, C-8"), 148.7 (q_c, C-9"), 148.2 (q_c, C-8'), 144.5 (q_c, C-2), 136.8 (CH, C-2"), 136.1 (q_c, C-5), 135.4 (q_c, C-7a"), 134.9 (q_c, C-7a'), 129.9 (q_c, C-6"), 129.2 (q_c, C-6'), 126.7 (q_c, C-3a"), 126.6 (q_c, C-3a'), 124.5 (CH, C-5"), 123.3 (CH, C-5'), 123.2 (CH, C-4"), 122.7 (CH, C-2'), 122.4 (CH, C-4'), 118.8 (CH, C-4), 116.2 (q_c, C-3"), 114.7 (CH, C-7"), 114.6 (2 x CH, C-7', C-3'), 85.9 (q_c, C-10"), 84.7 (q_c, C-9'), 27.6 (3 x CH_3, C-11"), 27.5 (3 x CH_3, C-

10') ppm; ESMS *m/z* (rel. int.) 483 $[M+H]^+$ (17), 439 (22), 306 (9), 288 (100), 262 (13), 244 (28), 219 (15), 189 (70), 181 (22); HRESMS *m/z* 595.1515 (calcd for $C_{30}H_{29}N_4O_5Cl_2^{35}[M+H]^+$ 595.1515)

(*N*1', *N*1"- di-*tert*-Butoxycarbonyl)-5"-bromoindol-3-yl[5-(5'-bromoindol-3-yl)-1*H*-imidazole-2-yl]-methanone (**2.92**): yellow amorphous solid (53% over two steps); IR (film) ν_{max} cm^{-1} 2970 2161 1739 1610 1447 1367 1217 1152; ^{1}H NMR (DMSO-d_6, 600 MHz) δ 13.69 (1H, s, NH-1), 9.62 (1H, s, H-2"), 8.55 (1H, s, H-4"), 8.49 (1H, s, H-4'), 8.16 (2H, m, H-2', H-4), 8.10 (1H, d, *J* = 8.8 Hz, H-7"), 8.06 (1H, d, *J* = 8.9 Hz, H-7'), 7.62 (1H, d, *J* = 8.7 Hz, H-6"), 7.65 (1H, d, *J* = 8.8 Hz, H-6'), 1.67 (9H, s, H-11"), 1.66 (9H, s, H-10'); ^{13}C NMR (DMSO-d_6, 150 MHz) δ 175.8 (q_c, C-8"), 148.7 (q_c, C-9"), 148.2 (q_c, C-8'), 144.5 (q_c, C-2), 137.4 (CH, C-2"), 136.0 (q_c, C-5), 133.9 (q_c, C-7a'), 133.5 (q_c, C-7a"), 129.8 (q_c, C-3a"), 129.6 (q_c, C-3a') 128.1 (CH, C-6"), 127.4 (CH, C-6'), 124.2 (CH, C-4"), 123.5 (CH, C-2'), 123.4 (CH, C-4'), 118.7 (CH, C-4), 117.1 (q_c, C-5"), 116.9 (q_c, C-5'), 116.8 (CH, C-7"), 116.7 (CH, C-7'), 115.6 (CH, C-3"), 114.1 (CH, C-3'), 85.9 (q_c, C-10"), 84.6 (q_c, C-9'), 27.6 (3 x CH_3, C-11"), 27.4 (3 x CH_3, C-10') ppm; ESMS *m/z* (rel. int.) 572 $[M+H]^+$ (32), 528 (37), 349 (16), 331 (100), 287 (11), 253 (65), 221 (16), 209 (40), 181 (29), 150 (15), 132 (5), 106 (7); HRESMS *m/z* 683.0532 (calcd for $C_{30}H_{29}N_4O_5Br_2^{79}$ $[M+H]^+$ 683.0505).

(*N*1', *N*1"-di-*tert*-Butoxycarbonyl)-6"-iodoindol-3-yl[5-(6'-iodoindol-3-yl)-1*H*-imidazole-2-yl]-methanone (**2.102**): yellow amorphous solid (20% over two steps); IR (film) ν_{max} cm^{-1} 2900 1739 1590 1425 1366 1240 1150; ^{1}H NMR (DMSO-d_6, 600 MHz) δ 13.64 (1H, s, NH-1), 9.53 (1H, s, H-2"), 8.51 (2H, m, H-7', H-7"), 8.20 (1H, d, *J* = 8.2 Hz, H-4"), 8.15 (1H, d, *J* = 8.5 Hz, H-4'), 8.07 (1H, s, H-4), 8.06 (1H, s, H-2'), 7.73 (1H, d, *J* = 8.2 Hz, H-5"), 7.62 (1H, d, *J* = 8.5 Hz, H-5'), 1.68 (9H, s, H-11"), 1.67 (9H, s, H-10'); ^{13}C NMR (DMSO-d_6, 150 MHz) δ 175.9 (q_c, C-8"), 148.7 (q_c, C-9"), 148.2 (q_c, C-8'), 144.6 (q_c, C-2), 136.4 (q_c, C-7a'), 136.2 (2 x CH, C-2", C-5), 135.7 (q_c, C-7a"), 132.8 (CH, C-5"), 131.6 (CH, C-5'), 127.4 (q_c, C-3a"), 127.2 (q_c, C-3a'), 123.9 (CH, C-4"), 123.5 (2 x CH, C-7', C-7"), 123.1 (CH, C-4'), 122.5 (CH, C-2'), 118.9 (CH, C-4), 116.3 (CH, C-3"), 114.7 (CH,C-3'), 90.4 (q_c, C-6"), 89.5 (q_c, C-6'), 85.9 (q_c, C-10"), 84.6 (q_c, C-9'), 27.6 (3 x CH_3, C-11"), 27.5 (3 x CH_3, C-10') ppm; ESMS *m/z* (rel. int.) 666 $[M+H]^+$ (67), 622 (27), 495 (8), 451 (20), 410 (12), 379 (100), 353 (15), 280 (13), 271 (17), 253 (60),

225 (11), 209 (23), 181.0 (47), 109 (11); HRESMS *m/z* 779.0242 (calcd for $C_{30}H_{29}N_4O_5I_2$ $[M+H]^+$ 779.0227).

(*N*1', *N*1"- di-*tert*-Butoxycarbonyl)-6"-bromoindol-3-yl[5-(6'-bromoindol-3-yl)-1*H*-imidazole-2-yl]-methanone (**2.103**): yellow amorphous solid (26% over two steps); IR (film) ν_{max} cm^{-1} 3248 2901 1740 1604 1536 1427 1367 1312 1241 1150 1101 854 763; ^{1}H NMR (DMSO-d_6, 600 MHz) δ 13.66 (1H, s, NH-1), 9.56 (1H, s, H-2"), 8.35 (1H, d, *J* = 8.5 Hz, H-4"), 8.29 (3H, m, H-4', H-7', H-7"), 8.12 (1H, s, H-2'), 8.09 (1H, s, H-4), 7.58 (1H, d, *J* = 8.4 Hz, H-5"), 7.47 (1H, d, *J* = 8.5 Hz, H-5'), 1.68 (9H, s, H-11"), 1.67 (9H, s, H-10'); ^{13}C NMR (DMSO-d_6, 150 MHz) δ 175.8 (q_c, C-8"), 148.7 (q_c, C-9"), 148.2 (q_c, C-8'), 144.5 (q_c, C-2), 136.7 (CH, C-2"), 136.1 (q_c, C-5), 135.8 (q_c, C-7a'), 135.3 (q_c, C-7a"), 127.2 (CH, C-5"), 127.0 (q_c, C-3a"), 126.9 (q_c, C-3a'), 125.9 (CH, C-5'), 123.6 (CH, C-4"), 122.9 (2 x CH, C-2', C-4'), 118.9 (CH, C-4), 118.1 (q_c, C-6"), 117.6 (CH, C-7"), 117.5 (CH, C-7'), 117.1 (q_c, C-6'), 116.2 (CH, C-3"), 114.7 (CH,C-3'), 85.9 (q_c, C-10"), 84.7 (q_c, C-9'), 27.6 (3 x CH_3, C-11"), 27.5 (3 x CH_3, C-10') ppm; ESMS *m/z* (rel. int.) 572 $[M+H]^+$ (20), 528 (22), 429 (10), 400 (11), 355 (20), 340 (75), 331 (100), 289 (20), 281 (26), 266 (32), 253 (40), 234 (25), 221 (34), 209 (71), 181 (28), 147 (30); HRESMS *m/z* 683.0518 (calcd for $C_{30}H_{29}N_4O_5Br_2^{79}$ $[M+H]^+$ 683.0505).

5.2.8 Mono-Boc protected topsentin species 2.89, 2.93 and 2.94

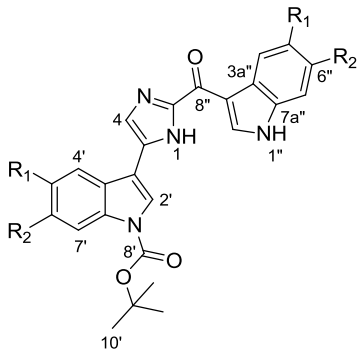

2.89 $R_1 = R_2 = H$
2.93 $R_1 = H$, $R_2 = F$
2.94 $R_1 = H$, $R_2 = Cl$

(*N*1'-*tert*-Butoxycarbonyl)-1*H*"-indol-3-yl[5-(indol-3-yl)-1*H*-imidazole-2-yl]-methanone (**2.89**): yellow amorphous solid; IR (film) ν_{max} cm^{-1} 2927 1732 1602 1370 1240 1150; ^1H NMR (DMSO-d_6, 600 MHz) δ 13.34 (1H, s, NH-1), 12.14 (1H, s, NH-1"), 9.32 (1H, s, H-2"), 8.40 (1H, d, *J* = 7.4 Hz, H-4"), 8.15 (2H, m, H-4', 7'), 7.98 (1H, s, H-4), 7.69 (1H, s, 2'), 7.56 (1H, d, *J* = 7.6 Hz, H-7"), 7.40 (2H, m, H-5', H-6'), 7.26 (2H, m, H-5", H-6"), 1.69 (9H, s, H-10') ; ^{13}C NMR (DMSO-d_6, 150 MHz) δ 175.9 (q_c, C-8"), 149.1 (q_c, C-8'), 145.6 (q_c, C-2), 136.9 (CH, C-2"), 136.2 (q_c, C-7a"), 135.1 (q_c, C-7a'), 131.5 (q_c, C-5), 128.6 (CH, C-2'), 127.9 (q_c, C-3a"), 126.6 (q_c, C-3a'), 124.6 (CH, C-6'), 122.9 (2 x CH, C-5', 6"), 121.9 (2 x CH, C-5", 4'), 121.6 (CH, C-4"), 117.3 (CH, C-4), 115.2 (CH, C-7'), 114.8 (CH, C-3"), 113.6 (CH, C-3'), 112.3 (CH, C-7"), 83.9 (q_c, C-9'), 27.7 (3 x CH_3, C-10') ppm; ESMS *m/z* (rel. int.) 371 $[M+H]^+$ (3), 272 (5), 254 (35), 228 (10), 210 (12), 184 (35), 155 (100), 144 (20), 130 (5), 116 (4); HRESMS *m/z* 427.1761 (calcd for $C_{25}H_{23}N_4O_3[M+H]^+$ 427.1770).

(*N*1'-*tert*-Butoxycarbonyl)-1*H*"-6"-fluoroindol-3-yl[5-(6'-fluoroindol-3-yl)-1*H*-imidazole-2-yl]-methanone (**2.93**): yellow amorphous solid; IR (film) ν_{max} cm^{-1} 2927 2160 1731 1615 1519 1446 1370 1143; ESMS *m/z* (rel. int.) 290 $[M+H]^+$ (4), 272 (31), 246 (5), 228 (17), 200 (17), 173 (100), 162 (28), 134 (5), 114 (2); HRESMS *m/z* 463.1577 (calcd for $C_{25}H_{21}N_4O_3F_2$ $[M+H]^+$ 463.1582).

(*N*1'-*tert*-Butoxycarbonyl)-1*H*"-6"-chloroindol-3-yl[5-(6'-chloroindol-3-yl)-1*H*-imidazole-2-yl]-methanone (**2.94**): yellow amorphous solid; IR (film) ν_{max} cm^{-1} 2927 1727 1618 1370 1285 1150; ^{1}H NMR (DMSO-d_6, 600 MHz) δ 13.43 (1H, s, NH-1), 12.18 (1H, s, NH-1"), 9.29 (1H, s, H-2"), 8.36 (1H, d, *J* = 8.2 Hz, H-4"), 8.25 (1H, d, *J* = 8.3 Hz, H-4'), 8.16 (1H, s, H-7'), 8.01 (1H, s, H-4), 7.70 (1H, s, H-2'), 7.62 (1H, s, H-7"), 7.48 (1H, d, *J* = 8.1 Hz, H-5'), 7.39 (1H, d, *J* = 8.1 Hz, H-5"), 1.67 (9H, s, H-10') ; ^{13}C NMR (DMSO-d_6, 150 MHz) δ 175.9 (q_c, C-8"), 147.9 (q_c, C-8'), 145.3 (q_c, C-2), 137.8 (CH, C-2"), 136.7 (q_c, C-5), 135.6 (q_c, C-7a"), 135.5 (q_c, C-7a'), 128.8 (CH, C-2'), 128.6 (q_c, C-6'), 127.5 (q_c, C-6"), 126.1 (q_c, C-3a"), 125.4 (q_c, C-3a'), 124.9 (CH, C-5'), 123.3 (CH, C-5"), 123.0 (CH, C-4'), 122.8 (CH, C-4"), 117.8 (CH, C-4), 114.9 (CH, C-3"), 114.5 (CH, C-7'), 113.5 (CH, C-3'), 112.1 (CH, C-7"), 86.4 (q_c, C-9'), 27.6 (3 x CH_3, C-10') ppm; ESMS *m/z* (rel. int.) 306 $[M+H]^+$ (5), 288 (42), 262 (6), 244 (20), 218 (20), 189 (100), 178 (33), 150 (9); HRESMS *m/z* 495.0981 (calcd for $C_{25}H_{21}N_4O_3Cl_2^{35}$ $[M+H]^+$ 495.0991).

5.2.9 *N*-Boc protected glyoxylic acids 2.96—2.98

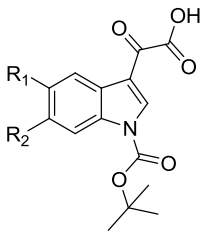

2.96 R_1 = H, R_2 = F
2.97 R_1 = H, R_2 = Cl
2.98 R_1 = Br, R_2 = H

The *N*-Boc protected glyoxylic acids **2.96—2.98** were not separated from the reaction mixture and their presence was confirmed from ESMS data.

***N*-(*tert*-Butoxycarbonyl)-6-fluoro-α-oxo-indole-3-acetic acid** (**2.96**); ESMS *m/z* (rel. int.) 160 $[M-H]^-$ (100), 140 (5), 132 (10), 112 (9); HRESMS *m/z* 306.0804 (calcd for $C_{15}H_{13}NO_5F$ $[M-H]^-$ 306.0778).

***N*-(*tert*-Butoxycarbonyl)-6-chloro-α-oxo-indole-3-acetic acid** (**2.97**); ESMS *m/z* (rel. int.) 275 $[M-H]^-$ (6), 250 (7), 220 (15), 205 (12), 175 (69), 160 (10), 150 (100), 140 (26), 121 (20), 110 (6); HRESMS *m/z* 322.0498 (calcd for $C_{15}H_{13}NO_5Cl^{35}$ $[M-H]^-$ 322.0482).

***N*-(*tert*-Butoxycarbonyl)-5-bromo-α-oxo-indole-3-acetic acid** (**2.98**); ESMS *m/z* (rel. int.) 294 $[M-H]^-$ (4), 265 (5), 221 (100), 195 (23), 173 (4), 156 (4), 140 (10), 118 (5), 80 (23); HRESMS *m/z* 365.9986 (calcd for $C_{15}H_{13}NO_5Br^{79}$ $[M-H]^-$ 365.9977).

5.2.10 1*H*-Indole-3-glyoxals 2.99—2.101

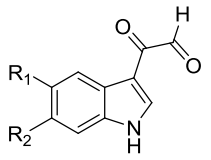

2.99 R_1 = H, R_2 = F
2.100 R_1 = H, R_2 = Cl
2.101 R_1 = Br, R_2 = H

The 1*H*-Indole-3-glyoxals **2.99—2.101** were not separated from the reaction mixture and their presence was confirmed from ESMS data.

6-Fluoro-indole-3-glyoxal (**2.99**); HRESMS *m/z* 190.0318 (calcd for $C_{10}H_5NO_2F$ $[M-H]^-$ 190.0304).

6-Chloro-indole-3-glyoxal (**2.100**); HRESMS *m/z* 206.0028 (calcd for $C_{10}H_5NO_2Cl^{35}$ $[M-H]^-$ 206.0009).

5-Bromo-indole-3-glyoxal[227] (**2.101**); HRESMS *m/z* 249.9519 (calcd for $C_{10}H_5NO_2Br^{79}$ $[M-H]^-$ 249.9503).

5.2.11 Thermal deprotection of topsentin precursors 2.88, 2.90—2.92, 2.102 and 2.103[145]

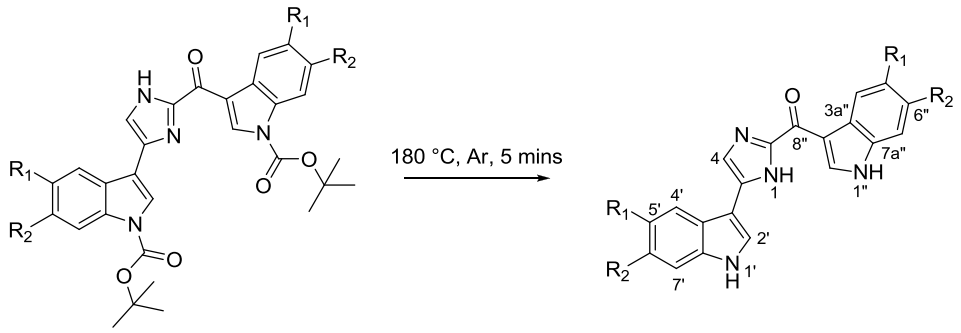

2.88 $R_1 = R_2 = H$
2.90 $R_1 = H, R_2 = F$
2.91 $R_1 = H, R_2 = Cl$
2.92 $R_1 = Br, R_2 = H$
2.102 $R_1 = H, R_2 = I$
2.103 $R_1 = H, R_2 = Br$

1.40 $R_1 = R_2 = H$
1.58 $R_1 = H, R_2 = F$
1.59 $R_1 = H, R_2 = Cl$
1.60 $R_1 = Br, R_2 = H$
1.61 $R_1 = H, R_2 = I$
1.46 $R_1 = H, R_2 = Br$

Compounds **2.88, 2.90—2.92, 2.102** and **2.103** were heated to 180 °C as dry solids under an inert atmosphere of argon. Once the desired temperature was achieved, gas bubbles appeared in the solution, which subsided after five minutes, at which time the heat source was removed and the compounds were allowed to reach room temperature yielding compounds **1.40, 1.46, 1.58—1.61** in quantitative yield. All compounds were routinely subjected to RP-HPLC (MeOH : H_2O, 3:1), to deliver compounds suitably pure for bioassay.

1*H*"-indol-3-yl[5-(1*H*'-indol-3-yl)-1*H*-imidazole-2-yl]-methanone; (deoxytopsentin)[66] (1.40) - tautomer 1: yellow amorphous solid (30 mg, 100 %, 0.091 mmol); IR (film) ν_{max} cm^{-1} 2924, 2160, 1725, 1589, 1613, 1449, 1354, 1149; ^{1}H NMR (DMSO-d_6, 600 MHz) δ 13.21 (1H, s, NH-1), 12.10 (1H, s, NH-1"), 11.45 (1H, s, NH-1'), 9.40 (1H, d, *J* = 2.6 Hz, H-2"), 8.4 (1H, m, H-4"), 8.17 (1H, d, *J* = 7.9 Hz, H-4'), 8,12 (1H, d, *J* = 2.5 Hz, H-2'), 7.70 (1H, s, H-4), 7.55 (1H, m, H-7"), 7.46 (1H, d, *J* = 7.9 Hz, H-7'), 7.25 (2H, m, H-5", H-6"), 7.15 (2H, m, H-5', H-6'); ^{13}C NMR (DMSO-d_6, 150 MHz) δ 176.1 (q_c, C-8"), 145.2 (q_c, C-2), 136.6 (CH, C-2"), 136.5 (q_c, C-7a'), 136.1 (q_c, C-7a"), 130.3 (q_c, C-5), 126.7 (q_c, C-3a") 124.5 (q_c, C-3a'), 124.1 (CH, C-2'), 121.8 (CH, C-4"), 121.7 (2 x CH, C-5", C-6"), 121.6 (CH, C-6'), 120.2

(CH, C-4'), 119.5 (CH, C-5'), 114.9 (CH, C-4), 113.8 (q_c, C-3"), 112.3 (CH, C-7"), 111.9 (CH, C-7'), 110.0 (q_c, C-3') ppm; ESMS *m/z* (rel. int.) 210 $[M+H]^+$ (7), 184 (10), 155 (100), 144 (15), 130 (5), 116 (4); HRESMS *m/z* 327.1241 (calcd for $C_{20}H_{15}N_4O$ $[M+H]^+$ 327.1246)

Deoxytopsentin - tautomer 2, ^{1}H NMR (DMSO-d_6, 600 MHz) δ 13.12 (1H, s, NH-1), 12.04 (1H, s, NH-1"), 11.23 (1H, s, NH-1'), 9.19 (1H, d, *J* = 2.7 Hz, H-2"), 8.41 (1H, m, H-4"), 7.91 (1H, d, *J* = 7.9 Hz, H-4'), 7.84 (1H, d, *J* = 2.3 Hz, H-2'), 7.63 (1H, s, H-4), 7.55 (1H, m, H-7"), 7.44 (1H, d, *J* = 7.9 Hz, H-7'), 7.25 (2H, m, H-5", H-6"), 7.12 (2H, m, H-5', H-6'); ^{13}C NMR (DMSO-d_6, 150 MHz) δ 176.0 (q_c, C-8"), 141.1 (q_c, C-2), 138.5 (q_c, C-5), 136.9 (CH, C-2"), 136.4 (q_c, C-7a'), 136.1 (q_c, C-7a"), 126.7 (q_c, C-3a") 125.8 (CH, C-4), 125.0 (q_c, C-3a'), 122.9 (CH, C-2'), 122.8 (2 x CH, C-5", C-6"), 121.8 (CH, C-4"), 121.3 (CH, C-6'), 119.5 (CH, C-4'), 119.2 (CH, C-5'), 113.7 (q_c, C-3"), 112.3 (CH, C-7"), 111.6 (CH, C-7'), 104.8 (q_c, C-3').

6"-Bromo-1*H*"-indol-3-yl[5-(6'-bromo-1*H*'-indol-3-yl)-1*H*-imidazole-2-yl]-methanone; (6',6"-dibromo-deoxytopsentin)[51] (**1.46**): yellow amorphous solid (5.1 mg, 100 %, 0.011 mmol); IR (film) ν_{max} cm^{-1} 2924 1606 1520 1444 1238 1140; ^{1}H NMR (DMSO-d_6, 1eq. TFA, 600 MHz) δ 12.23 (1H, s, NH-1"), 11.54 (1H, s, NH-1'), 9.18 (1H, s, H-2"), 8.30 (1H, d, *J* = 8.5 Hz, H-4"), 8.01 (2H, m, H-2', H-4'), 7.77 (1H, s, H-4), 7.76 (1H, d, *J* = 1.7 Hz, H-7"), 7.65 (1H, d, *J* = 1.5 Hz, H-7'), 7.41 (1H, dd, *J* = 8.4, 1.6 Hz, H-5"), 7.25 (1H, dd, *J* = 8.5, 1.6 Hz, H-5'); ^{13}C NMR (DMSO-d_6, 150 MHz) δ 175.1 (q_c, C-8"), 144.2 (q_c, C-2), 137.8 (2x CH, C-2", C-5), 137.3 (q_c, C-7a"), 137.1 (q_c, C-7a'), 125.6 (CH, C-2'), 124.9 (CH, C-5"), 124.8 (q_c, C-3a") 123.6 (q_c, C-3a'), 123.1 (CH, C-4"), 122.5 (CH, C-5'), 121.6 (CH, C-4'), 115.5 (CH, C-4), 115.1 (CH, C-7"), 114.4 (CH, C-7'), 114.3 (q_c, C-6"), 113.6 (q_c, C-6') 112.4 (2 x q_c, C-3', C-3") ppm; ESMS *m/z* (rel. int.) 367 $[M+H]^+$ (7), 289 (12), 232 (49), 221 (8), 209 (77), 181 (100), 154 (12), 127 (8); HRESMS *m/z* 482.9451 (calcd for $C_{20}H_{13}N_4OBr_2^{79}$ $[M+H]^+$ 482.9456).

6”-Fluoro-1*H*”-indol-3-yl[5-(6’-fluoro-1*H*’-indol-3-yl)-1*H*-imidazole-2-yl]-methanone; (6’,6”-difluoro-deoxytopsentin) (**1.58**): yellow amorphous solid (15.5 mg, 100 %, 0.042 mmol); IR (film) ν_{max} cm^{-1} 2900 1672 1523 1449 1232 1150 1024; ^{1}H NMR (DMSO-d_6, 1 eq. TFA, 600 MHz) δ 12.23 (1H, s, NH-1”), 11.48 (1H, s, NH-1’), 9.14 (1H, s, H-2”), 8.35 (1H, dd, *J* = 8.6, 5.6 Hz, H-4”), 8.04 (1H, dd, *J* = 8.2, 5.6 Hz, H-4’), 7.99 (1H, s, H-2’), 7.79 (1H, s, H-4), 7.36 (1H, dd, *J* = 9.5, 2.2 Hz, H-7”), 7.25 (1H, dd, *J* = 9.9, 2.2 Hz, H-7’), 7.13 (1H, m, H-5”), 6.99 (1H, m, H-5’); ^{13}C NMR (DMSO-d_6, 150 MHz) δ 175.0 (q_c, C-8”), 159.4 (q_c, d, $J_{F,C}$ = 236.2 Hz, C-6”), 159.0 (q_c, d, $J_{F,C}$ = 236.2 Hz, C-6’), 144.1 (q_c, C-2), 137.9 (2x CH, C-2”, C-5), 136.4 (q_c, d, $J_{F,C}$ = 12.4 Hz, C-7a”), 136.3 (q_c, d, $J_{F,C}$ = 12.3 Hz, C-7a’), 124.5 (2 x CH, m, C-4”, C-4’), 123.2 (CH, C-2’), 122.6 (2 x q_c, C-3a’, C-3a”), 121.5 (CH, C-4), 120.9 (q_c, C-3”), 113.6 (q_c, C-3’), 110.4 (CH, d, $J_{F,C}$ = 22.3 Hz, C-5”), 108.2 (CH, d, $J_{F,C}$ = 23.7 Hz, C-5’), 98.8 (CH, d, $J_{F,C}$ = 25.3 Hz, C-7”), 97.9 (CH, d, $J_{F,C}$ = 26.9 Hz, C-7’) ppm; ESMS *m/z* (rel. int.) 228 $[M+H]^+$ (6), 202 (8), 173 (100), 162 (10), 148 (5), 134 (4); HRESMS *m/z* 363.1054 (calcd for $C_{20}H_{13}N_4OF_2$ $[M+H]^+$ 363.1057).

6”-Chloro-1*H*”-indol-3-yl[5-(6’-chloro-1*H*’-indol-3-yl)-1*H*-imidazole-2-yl]-methanone; (6’,6”-dichloro-deoxytopsentin) (**1.59**): yellow amorphous solid (11.5 mg, 100 %, 0.029 mmol); IR (film) ν_{max} cm^{-1} 2880 1672 1519 1445 1241 1137; ^{1}H NMR (DMSO-d_6, 1eq. TFA, 600 MHz) δ 12.26 (1H, s, NH-1”), 11.54 (1H, s, NH-1’), 9.19 (1H, s, H-2”), 8.35 (1H, d, *J* = 8.5 Hz, H-4”), 8.06 (1H, d, *J* = 8.4 Hz, H-4’), 8.03 (1H, s, H-2’), 7.79 (1H, s, H-4), 7.62 (1H, d, *J* = 1.6 Hz, H-7”), 7.51 (1H, d, *J* = 1.6 Hz, H-7’), 7.29 (1H, dd, *J* = 8.5, 1.8 Hz, H-5”), 7.14 (1H, dd, *J* = 8.5, 1.7 Hz, H-5’); ^{13}C NMR (DMSO-d_6, 150 MHz) δ 175.2 (q_c, C-8”), 144.3 (q_c, C-2), 138.0 (CH, C-2”), 136.8 (q_c, C-7a”), 136.7 (q_c, C-7a’), 129.8 (q_c, C-6”), 128.3 (q_c, C-6’), 127.6 (q_c, C-3a”), 126.4 (q_c, C-3a’), 125.3 (q_c, C-5), 124.8 (CH, C-5”), 123.4 (CH, C-5’), 122.7 (CH, C-4”), 122.4 (CH, C-4’), 122.3 (CH, C-2’), 121.2 (CH, C-4), 120.0 (q_c, C-3”), 113.6 (CH, C-3’), 112.2 (CH, C-7”) 111.5 (CH, C-7’) ppm; ESMS *m/z* (rel. int.) 244 $[M+H]^+$ (5), 191 (22), 189 (100), 181 (18), 177 (12), 149 (8); HRESMS *m/z* 395.0455 (calcd for $C_{20}H_{13}N_4OCl_2{}^{35}[M+H]^+$ 395.0466).

5”-Bromo-1*H*”-indol-3-yl[5-(5’-bromo-1*H*’-indol-3-yl)-1*H*-imidazole-2-yl]-methanone; (5’,5”-dibromo-deoxytopsentin) (**1.60**): yellow amorphous solid (6.2 mg, 98 %, 0.013 mmol); IR (film) ν_{max} cm^{-1} 2880 1672 1519 1433 1231 1137 1024; ^{1}H NMR (DMSO-d_6, 1eq. TFA, 600 MHz) δ 12.42 (1H, s, NH-1”), 11.63 (1H, s, NH-1’), 9.16 (1H, s, CH-2”), 8.50 (1H, s, CH-4”), 8.21 (1H, s, H-4’), 8,02 (1H, s, H-2’), 7.84 (1H, s, H-4), 7.55 (1H, d, *J* = 8.6 Hz, H-7”), 7.44 (1H, d, *J* = 8.6 Hz, H-7’), 7.42 (1H, dd, *J* = 8.6, 1.9 Hz, H-6”), 7.29 (1H, dd, *J* = 8.6, 1.7 Hz, H-6’); ^{13}C NMR (DMSO-d_6, 150 MHz) δ 174.9 (q_c, C-8”), 144.1 (q_c, C-2), 138.1 (2x CH, C-7a”,7a’), 135.2 (CH, C-2”), 135.1 (q_c, C-5), 128.3 (CH, 2’), 126.4 (CH, C-6”), 125.8 (q_c, C-3a”) 124.3 (q_c, C-3a’), 123.7 (CH, C-6’), 123.5 (CH, C-4”), 122.1 (CH, C-4’), 121.9 (CH, C-4), 114.7 (CH, C-7”), 114.6 (CH, C-7’), 113.9 (2 x q_c, C-5’, C-5”), 113.2 (q_c, C-3”) 112.5 (q_c, C-3’) ppm; ESMS *m/z* (rel. int.) 289 $[M+H]^+$ (12), 232 (43), 223 (10), 209 (100), 181 (61), 154 (31), 127 (5); HRESMS *m/z* 482.9460 (calcd for $C_{20}H_{13}N_4OBr_2^{79}$ $[M+H]^+$ 482.9456).

6”-Iodo-1*H*”-indol-3-yl[5-(6’-iodo-1*H*”-indol-3-yl)-1*H*-imidazole-2-yl]-methanone; (6’,6”-diiodo-deoxytopsentin) (**1.61**): yellow amorphous solid (6.1 mg, 100 %, 0.01 mmol); IR (film) ν_{max} cm^{-1} 2880 1672 1516 1440 1203 1136; ^{1}H NMR (DMSO-d_6, 1eq. TFA, 600 MHz) δ 12.25 (1H, s, NH-1”), 11.53 (1H, s, NH-1’), 9.07 (1H, s, H-2”), 8.16 (1H, d, *J* = 8.4 Hz, H-4”), 7.97 (1H, s, H-2’) 7.94 (1H, s, H-7”), 7.88 (1H, d, *J* = 8.5 Hz, H-4’), 7.83 (1H, s, H-7’), 7.81 (1H, s, H-4), 7.56 (1H, d, *J* = 8.4 Hz, H-5”), 7.41 (1H, d, *J* = 8.5 Hz, H-5’); ^{13}C NMR (DMSO-d_6, 150 MHz) δ 174.6 (q_c, C-8”), 144.5 (q_c, C-2), 137.9 (CH, C-2”, q_c, C-7a’), 137.8 (2 x q_c, C-7a”, C-5), 130.6 (CH, C-5”), 128.2 (CH, C-5’), 125.9 (CH, C-2’), 123.9 (CH, C-4”), 123.5 (q_c, C-3a”) 123.4 (q_c, C-3a’), 121.9 (CH, C-4’), 121.1 (CH, C-4), 121.0 (CH, C-7”), 120.5 (CH, C-7’), 113.6 (2x q_c, C-3”, C-3’), 87.5 (q_c, C-6”), 86.0 (q_c, C-6’) ppm; ESMS *m/z* (rel. int.) 235 $[M+H]^+$ (47), 280 (59), 269 (16), 209 (100), 181 (72), 154 (38), 142 (7); HRESMS *m/z* 578.9184 (calcd for $C_{20}H_{13}N_4OI_2$ $[M+H]^+$ 578.9179).

5.2.12 Synthesis of 7',7"-dichloro-deoxytopsentin 2.104

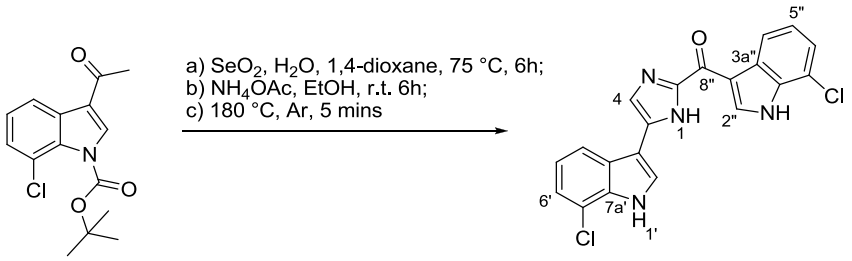

2.104

Compound **2.104** was synthesized as per the method described above for halogenated topsentin analogues **1.46, 1.58—1.61** with the exception of the bench top purification step which was omitted in favour of deprotection of the crude reaction mixture. Routine RP-HPLC (MeOH:H_2O, 3:1) delivered compound **2.104** as a yellow amorphous solid (14 mg, 0.035 mmol, 35% over three steps).

7"-Chloro-1*H*"-indol-3-yl[5-(7'-chloro-1*H*"-indol-3-yl)-1*H*-imidazole-2-yl]-methanone; (7',7"-dichloro-deoxytopsentin) (**2.104**): yellow amorphous solid (14 mg, 0.035 mmol 35% over three steps); IR (film) ν_{max} cm^{-1} 2970 2161 1737 1584 1433 1364 1200 1109 1051; ^{1}H NMR (DMSO-d_6, 1eq. TFA, 600 MHz) δ 12.80 (1H, s, NH-1"), 11.96 (1H, s, NH-1'), 8.94 (1H, d, *J* = 2.8 Hz, H-2"), 8.28 (1H, d, *J* = 7.8 Hz, H-4"), 8.14 (1H, d, *J* = 2.5 Hz, H-2'), 8.07 (CH, s, H-4), 8.03 (1H, d, *J* = 7.9 Hz, H-4'), 7.41 (1H, d, *J* = 7.6 Hz, H-6"), 7.31 (2H, m, H-5", H-6'), 7.18 (1H, t, *J* = 7.8 Hz, H-5'); ^{13}C NMR (DMSO-d_6, 150 MHz) δ 173.6 (q_c, C-8"), 142.5 (q_c, C-2), 138.7 (CH, C-2"), 133.7 (q_c, C-7a"), 133.5 (q_c, C-7a'), 132.2 (q_c, C-5), 128.2 (q_c, C-3a") 126.4 (q_c, C-3a'), 126.1 (CH, C-2'), 123.8 (CH, C-6'), 123.4 (CH, C-6"), 121.8 (CH, C-5"), 121.2 (CH, C-5'), 120.5 (CH, C-4"), 118.8 (CH, C-4'), 118.3 (CH, C-4), 117.1 (CH, C-7"), 116.6 (CH, C-7'),114.5 (q_c, C-3"), 105.9 (q_c, C-3') ppm; ESMS *m/z* (rel. int.) 244 $[M+H]^+$ (10), 218 (3), 189 (100), 181 (17), 178 (10), 153 (7); HRESMS *m/z* 395.0468 (calcd for $C_{20}H_{13}N_4OCl_2^{35}$ $[M+H]^+$ 395.0466).

5.3 Chapter Three Experimental

5.3.1 Synthesis of 2-chloro-1-(1*H*-indol-3-yl)-ethanone 3.35 via Friedel-Crafts acylation of indole[104]

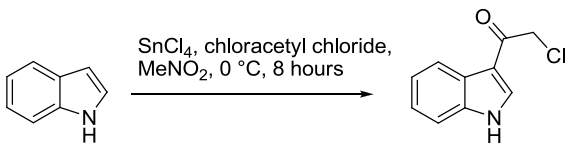

3.35

This method is representative. $SnCl_4$ (519.5 µl, 1.2 eq.) was added to a stirred solution of indole (500mg 3.70 mmol, 1 eq.) in dry CH_2Cl_2 (7.5 ml) under argon at 0 °C. The ice bath was removed and the reaction suspension was allowed to stir for a further 30 minutes. Chloracetyl chloride (3.70 mmol 1 eq.) was added dropwise to the reaction mixture, followed by nitromethane (4.5 ml). After eight hours the reaction was quenched with ice and water. Organic material was extracted with EtOAc (100ml), washed with water (2 x 20ml) and sat. brine (2x 30ml) and dried over anhydrous $MgSO_4$. Solvent was removed *in vacuo* to afford a red/brown tarry solid which did not yield the desired product **3.37**.

The procedure detailed above was repeated exactly on two further occasions with the single change being the acylating agent used on each occasion namely bromacetyl chloride and bromacetyl bromide respectively.

5.3.2 Synthesis of 3.35 via direct acylation of indole[182]

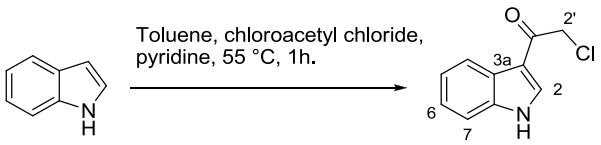

3.35

Pyridine (690 µl, 8.54 mmol, 1 eq.) was added to a solution of indole (1 g, 1 eq.) in toluene (20 ml). The reaction mixture was heated to 55 °C and chloroacetyl chloride (680 µl, 1 eq.) was added slowly over an hour. After a further hour of stirring, MeOH (5 ml) and water (25 ml) were added. The reaction mixture was washed with water (2 x 10 ml) and sat. brine (2 x 10 ml), and dried over anhydrous $MgSO_4$. Solvents were removed *in vacuo*. Normal phase flash chromatography (100% $CHCl_3$) yielded **3.35** (182 mg, 0.94 mmol, 11% yield).

2-Chloro-1-(1*H*-indol-3-yl)-ethanone[182] (**3.35**): red amorphous solid (11% yield); IR (film) ν_{max} cm^{-1} 2391 1739 1638 1514 1427 1150; ^{1}H NMR (DMSO-d_6, 600 MHz) δ 12.14 (1H, s, NH-1), 8,45 (1H, d, *J* = 3.2 Hz, H-2), 8.19 (1H, d, *J* = 7.4 Hz, H-4), 7.51 (1H, d, *J* = 7.5 Hz, H-7), 7.23 (2H, m, H-5, H-6), 4.89 (2H, s, H-2'); ^{13}C NMR (DMSO-d_6, 150 MHz) δ 186.2 (q_c, C-1'), 136.6 (q_c, C-7a), 134.7 (CH, C-2), 125.4 (q_c, C-3a), 123.2 (CH, C-5), 122.2 (CH, C-6), 121.2 (CH, C-4), 113.6 (q_c, C-3) 112.3 (CH, C-7), 46.4 (CH_2, C-2') ppm; ESMS *m/z* (rel. int.) 159 $[M+H]^+$ (7), 144 (23), 130 (100), 117 (68), 103 (11), 91 (8), 77 (2); HRESMS *m/z* 194.0373 (calcd for $C_{10}H_9NOCl^{35}$ $[M+H]^+$ 194.0373).

5.3.3 Attempted selective bromination of 3-acetyl-1-(*tert*-butoxycarbonyl)indole 2.80[89]

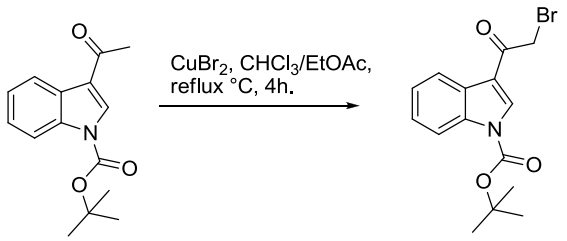

2.80 **3.36**

A solution of **2.80** (250 mg, 0.96 mmol, 1 eq.) in $CHCl_3$ (5 ml) was added to a green, vigorously stirring, refluxing suspension of $CuBr_2$ (344 mg, 1.6 eq.) in an equal volume of EtOAc. The reaction mixture was maintained at reflux for four hours, during which time the suspension changed colour from green to amber. After cooling the organic reaction mixture was filtered, and the organic supernatant was washed with water (2 x 10 ml) and sat. brine (2 x 10 ml) and dried over anhydrous $MgSO_4$ and the organic phase was concentrated *in vacuo* to yield a pink/amber solid (232.8 mg) ^1H NMR analysis of the crude reaction mixture, suggested the presence of uncontrolled side products. The crude reaction mixture was not purified.

5.3.4 Selective bromination of 1-(1*H*-indol-3-yl)ethanone 2.1, 2.36, 2.37 and 2.39[183]

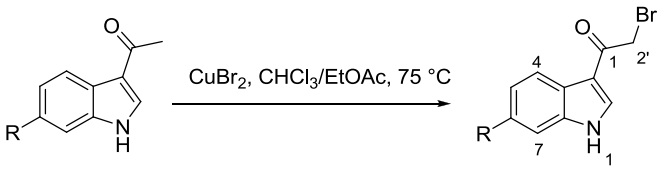

2.1 R = H
2.36 R = F
2.37 R = Cl
2.39 R = Br

2.2 R = H
3.38 R = F
3.40 R = Cl
3.41 R = Br

This method is representative. To a vigorously stirring suspension of $CuBr_2$ (252 mg, 1,13 mmol, 1.8 eq.) in EtOAc (15 ml) at reflux, was added **2.1** (100 mg, 0.63 mmol, 1 eq.) in hot $CHCl_3$ (20 ml). The reaction was maintained at 75 °C for six hours, while being constantly monitored by TLC, after which time the reaction mixture was allowed to cool. The organic phase was washed with water (2 x 20 ml) and sat. brine (2 x 20 ml) and dried over anhydrous $MgSO_4$.The organic phase was concentrated *in vacuo* and purified via normal phase flash chromatography (100% CH_2Cl_2) yielding **2.2** as a beige amorphous solid (85.5 mg, 0.36 mmol, 57%).

This is a representative method, and was applied to varying quantities of 1-(-1*H*-indol-3-yl)ethanones **2.36, 2.37** and **2.39** depending on availability using the same equivalents and solvent ratios above. Reaction time varied, and was determined by TLC analysis.

2-Bromo-1-(1*H*-indol-3-yl)-ethanone[82] (**2.2**): beige amorphous solid (57% yield); IR (film) ν_{max} cm^{-1} 2161 1738 1617 1517 1428 1133; ^{1}H NMR (DMSO-d_6, 600 MHz) δ 12.14 (1H, s, NH-1), 8.47 (1H, d, *J* = 3.1 Hz, H-2), 8.15 (1H, d, *J* = 7.5 Hz, H-4), 7.49 (1H, d, *J* = 7.8 Hz, H-7), 7.23 (2H, m, H-5, H-6), 4.65 (2H, s, H-2'); ^{13}C NMR (DMSO-d_6, 150 MHz) δ 186.4 (q_c, C-1'), 136.7 (q_c, C-7a), 135.3 (CH, C-2), 125.5 (q_c, C-3a), 123.2 (CH, C-5), 122.2 (CH, C-6), 121.2 (CH, C-4), 113.5 (q_c, C-3) 112.3 (CH, C-7), 33.5 (CH_2, C-2') ppm; ESMS *m/z* (rel. int.) 159 $[M+H]^+$ (99), 144 (100), 130 (28), 117 (65), 103 (2), 90 (4); HRESMS *m/z* 237.9866 (calcd for $C_{10}H_9NOBr^{79}$ $[M+H]^+$ 237.9868).

2-Bromo-1-(6-fluoro-1*H*-indol-3-yl)-ethanone (**3.38**): beige amorphous solid (47% yield); IR (film) ν_{max} cm^{-1} 2159 1739 1634 1520 1416 1125; ^{1}H NMR (MeOD, 600 MHz) δ 8.27 (1H, s, H-2), 8.19 (1H, dd, *J* = 8.8, 5.5 Hz, H-4), 7.17 (1H, dd, *J* = 9.4, 2.2 Hz, H-7), 7.01 (1H, m, H-5), 4.48 (2H, s, H-2'); ^{13}C NMR (MeOD, 150 MHz) δ 189.4 (q_c, C-1'), 161.9 (q_c, d, $J_{F,C}$ = 238.6 Hz), 138.7 (q_c, d, $J_{F,C}$ = 12.0 Hz, C-7a), 136.4 (CH, C-2), 124.0 (CH, d, $J_{F,C}$ = 9.9 Hz, C-4), 123.7 (q_c, C-3a), 115.4 (q_c, C-3) 111.8 (CH, d, $J_{F,C}$ = 24.1 Hz, C-5), 99.2 (CH, d, $J_{F,C}$ = 26.2 Hz, C-7), 32.3 (CH_2, C-2') ppm; ESMS *m/z* (rel. int.) 177 $[M+H]^+$ (23), 162 (100), 148 (50), 135 (85), 107 (22), 92 (2); HRESMS *m/z* 255.9769 (calcd for $C_{10}H_8NOBr^{79}F$ $[M+H]^+$ 255.9773).

2-Bromo-1-(6-chloro-1*H*-indol-3-yl)-ethanone (**3.40**): beige amorphous solid (10 % yield); IR (film) ν_{max} cm^{-1} 2922 1742 1634 1575 1132 1055; ^{1}H NMR (MeOD, 600 MHz) δ 8.29 (1H, s, H-2), 8.18 (1H, d, *J* = 8.6 Hz, H-4), 7.49 (1H, d, *J* = 1.7 Hz, H-7), 7.22 (1H, dd, *J* = 8.5, 1.8 Hz, H-5), 4.48 (2H, s, H-2'); ^{13}C NMR (MeOD, 150 MHz) δ 189.3 (q_c, C-1'), 139.2 (q_c, C-7a), 136.3 (CH, C-2), 130.6 (q_c, C-6), 128.8 (q_c, C-3a), 124.3 (CH, C-5), 123.9 (CH, C-4), 113.2 (CH, C-7), 113.0 (CH, C-3), 32.4 (CH_2, C-2') ppm; ESMS *m/z* (rel. int.) 193 $[M+H]^+$ (22), 178 (100), 164 (27), 151 (90), 141 (5), 122 (12), 116 (10), 89 (5); HRESMS *m/z* 271.9470 (calcd for $C_{10}H_8NOCl^{35}Br^{79}[M+H]^+$ 271.9478).

2-Bromo-1-(6-bromo-1*H*-indol-3-yl)-ethanone (**3.41**): beige amorphous solid (16 % yield); IR (film) ν_{max} cm^{-1} 2160 1738 1597 1403 1128; ^{1}H NMR (MeOD, 600 MHz) δ 8.27 (1H, s, H-2), 8.13 (1H, d, *J* = 8.7 Hz, H-4), 7.65 (1H, s, H-7), 7.35 (1H, d, *J* = 8.4 Hz, H-5), 4.48 (2H, s, H-2'); ^{13}C NMR (MeOD, 150 MHz) δ 189.3 (q_c, C-1'), 139.3 (q_c, C-7a), 136.5 (CH, C-2), 126.7 (CH, C-5), 126.1 (q_c, C-3a), 124.2 (CH, C-4) 117.9 (q_c, C-6), 116.1 (CH, C-7), 115.4 (CH, C-3), 32.4 (CH_2, C-2') ppm; ESMS *m/z* (rel. int.) 236 $[M+H]^+$ (30), 221 (100), 207 (27), 194 (70), 166 (8), 144 (40), 130 (40), 116 (40), 102 (5), 89 (5); HRESMS *m/z* 315.8983 (calcd for $C_{10}H_8NOBr_2{}^{79}[M+H]^+$ 315.8973).

5.3.5 2,2-Dibromo-1-(1*H*-indol-3-yl)-ethanone analogues 3.37, 3.39, 3.42 and 3.43

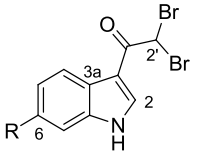

3.37 R = H
3.39 R = F
3.42 R = Cl
3.43 R = Br

2,2-Dibromo-1-(1*H*-indol-3-yl)-ethanone[82] (**3.37**) yellow amorphous solid (3% yield); IR (film) ν_{max} cm^{-1} 2229 1715 1635 1513 1423 1151; ^{1}H NMR (DMSO-d_6, 600 MHz) δ 12.36 (1H, s, NH-1), 8.61 (1H, d, *J* = 3.1 Hz, H-2), 8.18 (1H, d, *J* = 8.3 Hz, H-4), 7.59 (1H, s, H-2'), 7.53 (1H, d, *J* = 8.1 Hz, H-7), 7.27 (2H, m, H-5, H-6); ^{13}C NMR (DMSO-d_6, 150 MHz) δ 181.6 (q_c, C-1'), 137.0 (q_c, C-7a), 135.5 (CH, C-2), 125.7 (q_c, C-3a), 123.7 (CH, C-6), 122.7 (CH, C-5), 121.3 (CH, C-4), 112.7 (CH, C-7), 109.2 (q_c, C-3) 43.7 (CH_2, C-2') ppm; ESMS *m/z* (rel. int.) 236 $[M+H]^+$ (72), 221 (3), 207 (5), 158 (6), 144 (100), 130 (28), 117 (65), 103 (2), 90 (4); HRESMS *m/z* 315.8983 (calcd for $C_{10}H_8NOBr_2^{79}$ $[M+H]^+$ 315.8973).

2,2-Dibromo-1-(6-fluoro-1*H*-indol-3-yl)-ethanone (**3.39**) yellow amorphous solid (1% yield); IR (film) ν_{max} cm^{-1} 2291 1738 1642 1517 1413 1221 1125; ^{1}H NMR (MeOD, 600 MHz) δ 8.39 (1H, s, H-2), 8.21 (1H, dd, *J* = 8.7, 5.5 Hz, H-4), 7.23 (1H, s, H-2'), 7.20 (1H, dd, *J* = 9.1, 2.2 Hz, H-7), 7.05 (1H, m, H-5); ^{13}C NMR (MeOD, 150 MHz) δ 184.2 (q_c, C-1'), 162.1 (q_c, d, $J_{F,C}$ = 239.9 Hz), 138.8 (q_c, d, $J_{F,C}$ = 12.7 Hz, C-7a), 136.4 (CH, C-2), 124.1 (CH, d, $J_{F,C}$ = 9.9 Hz, C-4), 123.9 (q_c, C-3a), 112.1 (CH, d, $J_{F,C}$ = 24.0 Hz, C-5), 111.2 (q_c, C-3), 99.6 (CH, d, $J_{F,C}$ = 26.5 Hz, C-7), 42.3 (CH_2, C-2') ppm; ESMS *m/z* (rel. int.) 213 $[M+H]^+$ (100), 183 (6), 159 (6), 146 (10), 126 (2), 80 (60); HRESMS *m/z* 333.8865 (calcd for $C_{10}H_7NOBr_2^{79}F$ $[M+H]^+$ 333.8878).

2,2-Dibromo-1-(6-chloro-1*H*-indol-3-yl)-ethanone (**3.42**)yellow amorphous solid (2% yield); IR (film) ν_{max} cm^{-1} 2923 2160 1744 1570 1420 1132; ^{1}H NMR (MeOD, 600 MHz) δ 8.41 (1H, s, H-2), 8.19 (1H, d, *J* = 8.5 Hz, H-4), 7.51 (1H, s, H-7), 7.26 (1H, d, *J* = 8.5 Hz, H-5), 7.24 (1H, s, H-2'); ^{13}C NMR (MeOD, 150 MHz) δ 184.1 (q_c, C-1'), 139.1 (q_c, C-7a), 136.6 (CH, C-2), 130.9 (q_c, C-6), 126.1 (q_c, C-3a), 124.3 (CH, C-5), 124.0 (CH, C-4), 113.2 (CH, C-7), 111.1 (CH, C-3), 42.3 (CH_2, C-2') ppm; ESMS *m/z* (rel. int.) 272 $[M+H]^+$ (10), 178 (14), 164 (27), 151 (100), 124 (7), 116 (5), 89 (2); HRESMS *m/z* 349.8577 (calcd for $C_{10}H_7NOCl^{35}Br_2^{79}[M+H]^+$ 349.8583).

2,2-Dibromo-1-(6-bromo-1*H*-indol-3-yl)-ethanone (**3.43**) yellow amorphous solid (4% yield), IR (film) ν_{max} cm^{-1} 2922 2160 1737 1635 1513 1436 1157; ^{1}H NMR (MeOD, 600 MHz) δ 8.35 (1H, s, H-2), 8.10 (1H, d, *J* = 8.6 Hz, H-4), 7.63 (1H, d, *J* = 1.3 Hz, H-7), 7.35 (1H, dd, *J* = 8.4, 1.4 Hz, H-5), 7.12 (1H, s, H-2'); ^{13}C NMR (MeOD, 150 MHz) δ 184.1 (q_c, C-1'), 139.5 (q_c, C-7a), 136.5 (CH, C-2), 127.0 (CH, C-5), 126.5 (q_c, C-3a), 124.3 (CH, C-4) 118.3 (q_c, C-6), 116.3 (CH, C-7), 111.2 (CH, C-3), 42.3 (CH_2, C-2') ppm; ESMS *m/z* (rel. int.) 316 $[M+H]^+$ (24), 221 (19), 207 (35), 194 (100), 157 (10), 149 (9), 129 (33), 116 (30), 102 (3), 89 (5); HRESMS *m/z* 393.8065 (calcd for $C_{10}H_7NOBr_3^{79}[M+H]^+$ 393.8078).

5.3.6 Synthesis of indolyl-3-carbonylnitrile analogues 2.13, 3.45—3.47[88]

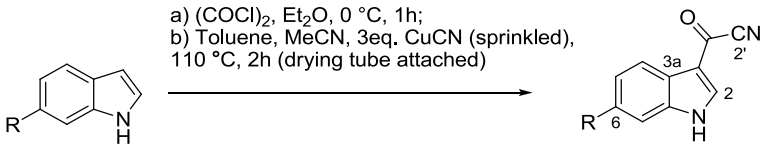

2.13 R = H
3.45 R = F
3.46 R = Cl
3.47 R = Br

Oxalyl chloride (420 µl, 4.8 mmol, 1.13 eq.) was added dropwise to a stirring solution of indole (500 mg, 4.26 mmol, 1 eq.) in dry Et_2O (10 ml) at 0 °C under an inert atmosphere of dry argon gas, resulting in an instant colour change to yellow. After one hour dry toluene (20 ml) and HPLC grade MeCN (4 ml) were added, followed by CuCN (1144.5 mg, 3 eq.) which was sprinkled in over two minutes to avoid aggregation. The reaction mixture was set up for reflux with a drying tube attached, and heated to 110 °C, allowing the Et_2O to boil off. After two hours the reaction mixture was cooled and concentrated *in vacuo* to yield a black solid which was subjected to flash chromatography (100% CH_2Cl_2) yielding **2.13** as a yellow crystalline solid (529 mg, 3.10 mmol, 73%).

This is a representative method, and was applied in the synthesis of **3.45—3.47** from varying quantities of starting material depending on availability using the same equivalents and solvent ratios above.

Indolyl-3-carbonylnitrile[88] (**2.13**): yellow needles from acetone (71-73 % yield), mp 222 °C, lit 224—226 °C[112]; IR (film) ν_{max} cm^{-1} 3222 2222 1780 1616 1514 1232; ^{1}H NMR (DMSO-d_6, 600 MHz) δ 12.89 (1H, s, NH-1), 8.62 (1H, s, H-2), 8.04 (1H, d, *J* = 7.6 Hz, H-4), 7.58 (1H, d, *J* = 8.0 Hz, H-7), 7.34 (2H, m, H-5, H-6); ^{13}C NMR (DMSO-d_6, 150 MHz) δ 158.6 (q_c, C-1'), 141.3 (CH, C-2), 137.6 (q_c, C-7a), 124.9 (CH, C-5), 124.2 (q_c, C-3a), 123.8 (CH, C-6) 120.9 (CH, C-4), 116.2 (q_c, C-3), 114.4 (q_c, C-2'), 113.3 (CH,

C-7) ppm; ESMS *m/z* (rel. int.) 144 $[M+H]^+$ (21), 117 (100), 89 (30); HRESMS *m/z* 171.0550 (calcd for $C_{10}H_7NO_2$ $[M+H]^+$ 171.0558).

6-Fluoroindolyl-3-carbonylnitrile (**3.45**): yellow needles from acetone (40 % yield), mp 218—220 °C; IR (film) ν_{max} cm^{-1} 3248 2225 1736 1614 1519 1224; ^1H NMR (DMSO-d_6, 600 MHz) δ 12.93 (1H, s, NH-1), 8.64 (1H, s, H-2), 8.01 (1H, dd, *J* = 8.2, 5.4 Hz, H-4), 7.39 (1H, dd, *J* = 9.2, 1.8 Hz, H-7), 7.20 (1H, m, H-5); ^{13}C NMR (DMSO-d_6, 150 MHz) δ 160.1 (q_c, d, $J_{F,C}$ = 238.0 Hz, C-6), 158.7 (q_c, C-1'), 142.1 (CH, C-2), 137.8 (q_c, d, $J_{F,C}$ = 12.5 Hz, C-7a), 122.3 (CH, d, $J_{F,C}$ = 10.4 Hz, C-4), 120.8 (q_c, C-3a), 116.1 (q_c, C-3), 114.2 (q_c, C-2'), 112.1 (CH, d, $J_{F,C}$ = 24.1 Hz, C-5), 99.9 (CH, d, $J_{F,C}$ = 26.1 Hz, C-7) ppm; ESMS *m/z* (rel. int.) 162 $[M+H]^+$ (20), 148 (5), 135 (100), 107 (75); HRESMS *m/z* 189.0453 (calcd for $C_{10}H_6N_2OF$ $[M+H]^+$ 189.0464).

6-Chloroindolyl-3-carbonylnitrile (**3.46**): yellow needles from acetone (38 % yield), mp 240—243 °C; IR (film) ν_{max} cm^{-1} 3218 2223 1731 1603 1518 1231; ^1H NMR (DMSO-d_6, 600 MHz) δ 12.96 (1H, s, NH-1), 8.67 (1H, s, H-2), 8.01 (1H, d, *J* = 8.4 Hz, H-4), 7.63 (1H, d, *J* = 1.8 Hz, H-7), 7.37 (1H, dd, *J* = 8.4, 1.8 Hz, H-5); ^{13}C NMR (DMSO-d_6, 150 MHz) δ 158.7 (q_c, C-1'), 142.1 (CH, C-2), 138.0 (q_c, C-7a), 129.3 (q_c, C-6), 124.0 (CH, C-5), 122.9 (q_c, C-3a), 122.2 (CH, C-4), 115.9 (q_c, C-3), 114.1 (q_c, C-2'), 113.1 (CH, C-7) ppm; ESMS *m/z* (rel. int.) 178 $[M+H]^+$ (36), 151 (100), 130 (44), 123 (65), 116 (21), 103 (5), 89 (20); HRESMS *m/z* 205.0173 (calcd for $C_{10}H_6N_2OCl^{35}$ $[M+H]^+$ 205.0169).

6-Bromoindolyl-3-carbonylnitrile[188] (**3.47**): orange needles from acetone (33 % yield), mp 249—250 °C; IR (film) ν_{max} cm^{-1} 3212 2223 1737 1602 1516 1229; ^1H NMR (DMSO-d_6, 600 MHz) δ 12.99 (1H, s, NH-1), 8.68 (1H, s, H-2), 7.96 (1H, d, *J* = 8.4 Hz, H-4), 7.77 (1H, s, H-7), 7.48 (1H, d, *J* = 8.3 Hz, H-5); ^{13}C NMR (DMSO-d_6, 150 MHz) δ 158.8 (q_c, C-1'), 142.2 (CH, C-2), 138.5 (q_c, C-7a), 126.8 (CH, C-5), 123.3 (q_c, C-3a), 122.7 (CH, C-4), 117.4 (q_c, C-6), 116.1 (CH, C-7), 116.0 (q_c, C-3), 114.2 (q_c, C-2') ppm; ESMS *m/z* (rel. int.) 194 $[M+H]^+$ (9), 169 (14), 144 (100), 130 (12), 116 (35), 89 (8); HRESMS *m/z* 248.9772 (calcd for $C_{10}H_6N_2OBr^{79}$ $[M+H]^+$ 248.9664).

5.3.7 Synthesis of indolyl-3-carbonylnitrile 2.13 over three steps[191,192,193,194,228]

5.3.7.1 Synthesis of indolyl-3-oxalyl chloride 2.17[228]

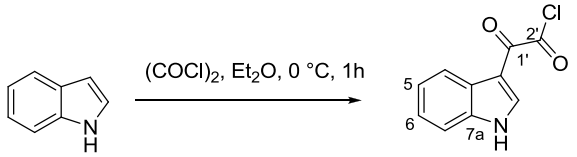

2.17

Oxalyl chloride (420 µl, 4.8 mmol, 1.13 eq.) was added dropwise to a stirring solution of indole (500 mg, 4.26 mmol, 1 eq.) in dry Et_2O (10 ml) at 0 °C under an inert atmosphere of dry argon gas, resulting in an instant colour change to yellow. After one hour the reaction mixture was filtered and washed with dry Et_2O yielding **2.17** a yellow powder (803 mg, 91%, 3.88 mmol)

Indolyl-3-α-oxoacetyl chloride[228] (**2.17**): yellow powder (91% yield); ^{1}H NMR (DMSO-d_6, 600 MHz) δ 12.45 (1H, s, NH-1), 8.41 (1H, d, *J* = 3.3 Hz, H-2), 8.17 (1H, d, *J* = 7.2 Hz, H-4), 7.55 (1H, d, *J* = 8.0 Hz, H-7), 7.26 (1H, m, H-5, H-6); ^{13}C NMR (DMSO-d_6, 150 MHz) δ 180.8 (q_c, C-2'), 165.3 (q_c, C-1'), 137.9 (CH, C-2), 136.7 (q_c, C-7a), 125.6 (q_c, C-3a), 123.7 (CH, C-6), 122.7 (CH, C-5), 121.1 (CH, C-4), 112.7 (CH, C-7), 112.3 (q_c, C-3) ppm.

5.3.7.2 Decarbonylation of indolyl-3-α-oxoacetyl chloride 2.17[191,192]

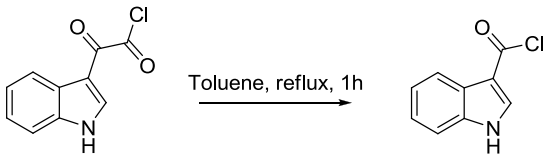

2.17 **3.44**

Compound **2.17** (800mg, 3.86 mmol) was refluxed at 110 °C in HPLC grade toluene, which had been dried over activated molecular sieves (30 ml) for 1 hour resulting in a light yellow solution. Toluene was removed under reduced pressure yielding a yellow solid (545.9 mg) which was taken forward to the next step

5.3.7.3 Indolyl-3-carbonylnitrile synthesis from crude 1*H*-Indole-3-carbonyl chloride **3.44**[193,194]

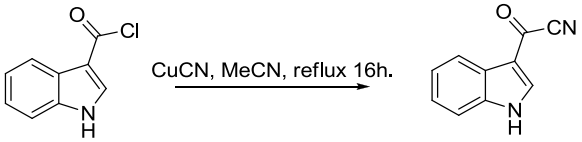

3.44 **2.13**

CuCN (765 mg, 8.54 mmol) was added to a stirring solution of the crude reaction mixture of **3.44** (545.9 mg) in HPLC grade MeCN (30 ml). The reaction mixture was heated to reflux and left to react for 16 hours. After cooling solvent was removed under reduced pressure yielding a black solid (1071.8 mg). Flash chromatography (100 % DCM) yielded **2.13** (12 % over three steps, 0.51 mmol, 87 mg).

5.3.8 Isolated 1*H*-indole-3-carboxylic acids 2.28 and 3.54

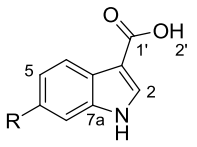

2.28 R = H
3.54 R = F

1*H* Indole-3-carboxylic acid[229] (**2.28**): red solid; IR (film) ν_{max} cm^{-1} 3389 2852 1615 1580 1441 1157; ^{1}H NMR (DMSO-d_6, 600 MHz) δ 11.91 (1H, s, OH-2'), 11.80 (1H, s, NH-1), 8.00 (2H, m, H-2, H-4), 7.47 (1H, d, *J* = 7.9 Hz, H-7), 7.17 (2H, m, H-5, H-6); ^{13}C NMR (DMSO-d_6, 150 MHz) δ 165.9 (q_c, C-1'), 136.4 (q_c, C-7a), 132.2 (CH, C-2), 125.9 (q_c, C-3a), 122.1 (CH, C-6), 120.9 (CH, C-5) 120.6 (CH, C-4), 112.2 (CH, C-7), 107.3 (q_c, C-3) ppm; ESMS *m/z* (rel. int.) 144 $[M+H]^+$ (35), 116 (100), 89 (22); HRESMS *m/z* 162.0552 (calcd for $C_9H_8NO_2$ $[M+H]^+$ 162.0555).

6-Fluoro-1*H* indole-3-carboxylic acid (**3.54**): red solid; IR (film) ν_{max} cm^{-1} 3342 2815 1625 1537 1436 1189; ^{1}H NMR (DMSO-d_6, 600 MHz) δ 12.01 (1H, s, OH-2'), 11.8 (1H, s, NH-1), 7.99 (1H, d, *J* = 2.8 Hz, H-2), 7.97 (1H, dd, *J* = 8.7, 5.6 Hz, H-4), 7.24 (1H, dd, *J* = 9.7, 2.3 Hz, H-7), 7.01 (1H, m, H-5); ^{13}C NMR (DMSO-d_6, 150 MHz) δ 165.7 (q_c, C-1'), 158.9 (q_c, d, $J_{F,C}$ = 236.5 Hz, C-6), 136.3 (q_c, d, $J_{F,C}$ = 12.7 Hz, C-7a), 132.8 (CH, C-2), 122.6 (q_c, C-3a), 121.6 (CH, d, $J_{F,C}$ = 10.1 Hz, C-4), 109.4 (CH, d, $J_{F,C}$ = 24.1 Hz, C-5), 107.5 (q_c, C-3), 98.3 (CH, d, $J_{F,C}$ = 25.5 Hz, C-7) ppm; ESMS *m/z* (rel. int.) 162 $[M+H]^+$ (12), 134 (78), 117 (5), 107 (100), 98 (5), 89 (7), 83 (10), 63 (4); HRESMS *m/z* 180.0471 (calcd for $C_9H_7N_2OF$ $[M+H]^+$ 180.0461).

5.3.9 Synthesis of indolyl-3-α-oxothioacetamides 3.48—3.51[175,177]

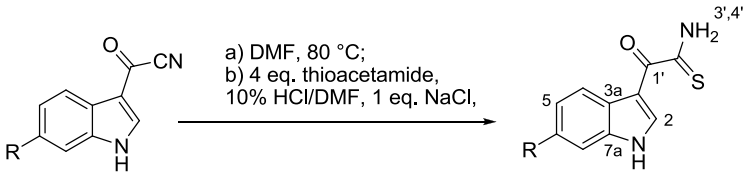

2.13 R = H
3.45 R = F
3.46 R = Cl
3.47 R = Br

3.48 R = H
3.49 R = F
3.50 R = Cl
3.51 R = Br

Thioacetamide (87.9 mg, 1.17 mmol, 4 eq.) and NaCl (1.6 mg, 0.1 eq.) was added to 2ml of a conc. HCl/DMF solution (1:0.78), and gently heated until dissolved. This solution was then added to a solution of **2.13** (50 mg, 1 eq.) in 1 ml DMF heated to 80 °C resulting in an instant colour change to dark yellow. After stirring for four hours at 80 °C the reaction was cooled with the addition of ice, and filtered. The filtrate was neutralized with sat. $NaHCO_3$ and the extracted with EtOAc (3 x 15 ml). The combined organic fractions were washed with water (1 x 10 ml) and sat. brine (1x 10 ml) and concentrated *in vacuo*. Flash column chromatography with 5% EtOAc/CH_2Cl_2 yielded **3.48** (34.6 mg, 0.17 mmol, 58%) as a bright yellow solid.

This is a representative method, and was applied in the synthesis of **3.49—3.51** from varying quantities of starting material depending on availability using the same equivalents and solvent ratios above.

Indolyl-3-α-oxothioacetamide (**3.48**): yellow amorphous solid (58 % yield); IR (film) ν_{max} cm^{-1} 2160 1785 1620 1514 1244 1114; ^{1}H NMR (DMSO-d_6, 600 MHz) δ 12.15 (1H, s, NH-1), 10.21 (1H, s, NH-3'), 10.00 (1H, s, NH-4') 8.20 (1H, d, *J* = 3.1 Hz, H-2), 8.14 (1H, d, *J* = 7.2 Hz, H-4), 7.51 (1H, d, *J* = 7.8 Hz, H-7), 7.24 (1H, m, H-5, H-6); ^{13}C NMR (DMSO-d_6, 150 MHz) δ 201.1 (q_c, C-2'), 185.4 (q_c, C-1'), 136.7 (q_c, C-7a), 136.6 (CH, C-2), 125.6 (q_c, C-3a), 123.2 (CH, C-5), 122.3 (CH, C-6), 121.1 (CH, C-4), 112.5

(CH, C-7), 111.7 (q_c, C-3) ppm; ESMS *m/z* (rel. int.) 144 $[M+H]^+$ (100), 116 (25), 89 (6); HRESMS *m/z* 205.0441 (calcd for $C_{10}H_9N_2OS$ $[M+H]^+$ 205.0436).

6-Fluoroindolyl-3-α-oxothioacetamide (**3.49**): yellow amorphous solid (53 % yield); IR (film) ν_{max} cm^{-1} 2160 1736 1627 1567 1120; ^1H NMR (DMSO-d_6, 600 MHz) δ 12.15 (1H, s, NH-1), 10.23 (1H, s, NH-3'), 10.01 (1H, s, NH-4') 8.21 (1H, d, *J* = 2.9 Hz, H-2), 8.11 (1H, dd, *J* = 8.7, 5.5 Hz, H-4), 7.31 (1H, dd, *J* = 9.5, 2.2 Hz, H-7), 7.11 (1H, m, H-5); ^{13}C NMR (DMSO-d_6, 150 MHz) δ 200.7 (q_c, C-2'), 185.2 (q_c, C-1'), 159.4 (q_c, d, $J_{F,C}$ = 237.8 Hz, C-6), 137.3 (CH, C-2), 136.8 (q_c, d, $J_{F,C}$ = 13.0 Hz, C-7a), 122.3 (q_c, C-3a), 122.2 (CH, d, $J_{F,C}$ = 10.0 Hz, C-4), 111.6 (q_c, C-3), 110.6 (CH, d, $J_{F,C}$ = 24.1 Hz, C-5), 98.9 (CH, d, $J_{F,C}$ = 26.1 Hz, C-7) ppm; ESMS *m/z* (rel. int.) 184 $[M+H]^+$ (3), 162 (65), 134 (100), 107 (62); HRESMS *m/z* 223.0337 (calcd for $C_{10}H_8N_2OSF$ $[M+H]^+$ 223.0341).

6-Chloroindolyl-3-α-oxothioacetamide (**3.50**): yellow amorphous solid (58 % yield); IR (film) ν_{max} cm^{-1} 2161 1715 1600 1511 1225 1128; ^1H NMR (DMSO-d_6, 600 MHz) δ 12.21 (1H, s, NH-1), 10.25 (1H, s, NH-3'), 10.03 (1H, s, NH-4') 8.25 (1H, d, *J* = 3.1 Hz, H-2), 8.11 (1H, d, *J* = 8.5 Hz, H-4), 7.57 (1H, d, *J* = 1.8 Hz, H-7), 7.26 (1H, dd, 8.5, 1.8 Hz H-5); ^{13}C NMR (DMSO-d_6, 150 MHz) δ 200.6 (q_c, C-2'), 185.2 (q_c, C-1'), 137.5 (q_c, C-7a), 137.1 (CH, C-2), 127.7 (q_c, C-6), 124.4 (q_c, C-3a), 122.5 (CH, C-5), 122.3 (CH, C-4), 112.3 (CH, C-7), 111.7 (q_c, C-3) ppm; ESMS *m/z* (rel. int.) 178 $[M+H]^+$ (70), 150 (100), 123 (100), 117 (23), 88 (2); HRESMS *m/z* 239.0046 (calcd for $C_{10}H_8N_2OSCl^{35}$ $[M+H]^+$ 239.0046).

6-Bromoindolyl-3-α-oxothioacetamide (**3.51**): yellow amorphous solid (51 % yield); IR (film) ν_{max} cm^{-1} 2160 1600 1509 1234 1127; ^1H NMR (DMSO-d_6, 600 MHz) δ 12.21 (1H, s, NH-1), 10.25 (1H, s, NH-3'), 10.03 (1H, s, NH-4') 8.23 (1H, d, *J* = 3.2 Hz, H-2), 8.06 (1H, d, *J* = 8.5 Hz, H-4), 7.71 (1H, d, *J* = 1.7 Hz, H-7), 7.38 (1H, dd, 8.5, 1.8 Hz H-5); ^{13}C NMR (DMSO-d_6, 150 MHz) δ 200.6 (q_c, C-2'), 185.2 (q_c, C-1'), 137.6 (q_c, C-7a), 137.4 (CH, C-2), 125.1 (CH, C-5), 124.7 (q_c, C-3a), 122.7 (CH, C-4), 115.7 (q_c, C-6), 115.2 (CH, C-7), 111.7 (q_c, C-3) ppm; ESMS *m/z* (rel. int.) 221 $[M+H]^+$ (100), 193 (58), 166 (52), 143 (73), 115 (80), 88 (8); HRESMS *m/z* 282.9552 (calcd for $C_{10}H_8N_2OSBr^{79}$ $[M+H]^+$ 282.9541).

5.3.10 Attempted synthesis of indolyl-3-α-oxothioacetamide 3.48 and subsequent formation of *N,N*-dimethyl-1*H*- indolyl-3-α-carboxamide 3.52[176,198]

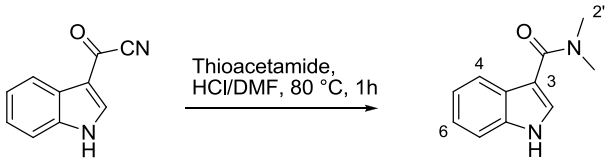

2.13 **3.52**

A solution of thioacetamide (44 mg, 0.59 mmol, 2 eq.) in 2 ml of HCl/DMF (2 : 0.78) was added to a stirring solution of **2.13** (50 mg, 0.29 mmol, 1 eq.) in DMF (2ml). The reaction mixture was heated to 80 °C for 1h resulting in a colour change to dark yellow. The reaction was cooled with the addition of ice, and filtered. The filtrate was neutralized with sat. $NaHCO_3$ and the extracted with EtOAc (3 x 5 ml). The combined organic fractions were washed with water (1 x 10 ml) and sat. brine (1x 10 ml) and concentrated *in vacuo*. After flash chromatography with 5% EtOAc/CH_2Cl_2 yielded no desired product, the column was washed with EtOAc to yield **3.55** (20.6 mg, 0.11 mmol, 37%) as a white crystalline solid.

***N,N*-dimethyl-1*H*- indolyl-3-α-carboxamide**[230] (**3.52**): white needles from EtOAc (37 % yield), mp 237 °C, lit 237—239 °C[230]; IR (film) ν_{max} cm^{-1} 2911 2161 1585 1394 1237 1133; ^{1}H NMR (DMSO-d_6, 600 MHz) δ 11.54 (1H, s, NH-1), 7.77 (1H, d, *J* = 7.9 Hz, H-4), 7.71 (1H, s, H-2), 7.42 (1H, d, *J* = 8.1 Hz, H-7), 7.14 (1H, t, *J* = 7.4 Hz, H-6), 7.08 (1H, t, *J* = 7.4 Hz, H-5), 3.08 (6H, s, H-2'); ^{13}C NMR (DMSO-d_6, 150 MHz) δ 166.2 (q_c, C-1'), 135.5 (q_c, C-7a), 127.8 (CH, C-2), 126.5 (q_c, C-3a), 121.8 (CH, C-6), 120.7 (CH, C-4), 119.9 (CH, C-5), 111.7 (CH, C-7), 109.9 (q_c, C-3), 36.7 (2 x CH_3, C-2') ppm; ESMS *m/z* (rel. int.) 144 $[M+H]^+$ (100), 116 (81), 89 (30); HRESMS *m/z* 189.1022 (calcd for $C_{11}H_{13}N_2O$ $[M+H]^+$ 189.1028). CCDC No. 646899.[199] X-ray data:

Formula	$C_{11}H_{12}N_2O$
Rel. formula weight	188.23
Crystal System	orthorhombic
Space group	P 212121
a (Å)	7.8327(6)
b (Å)	8.9283(7)
c (Å)	13.6410(12)
α (°)	90
β (°)	90
γ (°)	90
V (Å3)	953.95(13)
Z	4
ρ (Mg m-3)	1.3105 (2)
μ (mm-1)	0.082
Crystal Size (max)	0.38
Crystal Size (mid)	0.28
Crystal Size (min)	0.24
Temperature (K)	173 (2)
Wavelength (Å)	0.71073

5.3.11 Attempted synthesis of indolyl-3-α-oxothioacetamide 3.49 and subsequent formation of *N,N*-dimethyl-6-fluoro-1*H*- indolyl-3-α-carboxamide 3.53

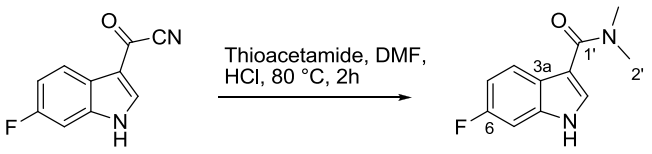

3.45 **3.53**

A solution of thioacetamide (40.3 mg, 0.53 mmol, 2 eq.) and **3.45** (50 mg, 0.26 mmol, 1 eq.) in DMF (4 ml) was heated to 60 °C. 400 µl of conc. HCl was added to the reaction mixture resulting in the formation of a yellow precipitate. The reaction temperature was increased to 80 °C resulting in the formation of a yellow solution. After 2h the reaction was cooled with the addition of ice, and filtered. The filtrate was neutralized with sat. $NaHCO_3$ and the extracted with EtOAc (3 x 5 ml). The combined organic fractions were washed with water (1 x 10 ml) and sat. brine (1x 10 ml) and concentrated *in vacuo*. After flash chromatography with 5% EtOAc/CH_2Cl_2 yielded no desired product, the column was washed with EtOAc to yield **3.53** (29.5 mg, 0.14 mmol, 55%) as a white crystalline solid.

***N,N*-dimethyl-6-fluoro-1*H*- indolyl-3-α-carboxamide**[231] (**3.53**) white needles from EtOAc (55 % yield), mp 238 °C, lit 245 °C[231]; IR (film) ν_{max} cm^{-1} 2904 2160 1550 1395 1224 1146 1094; ^{1}H NMR (DMSO-d_6, 600 MHz) δ 11.60 (1H, s, NH-1), 7.78 (1H, dd, *J* = 8.7, 5.7 Hz, H-4), 7.73 (1H, d, *J* = 2.6 Hz, H-2), 7.19 (1H, dd, *J* = 9.9, 2.1 Hz, H-7), 6.94 (1H, m, H-6), 3.08 (6H, s, H-2'); ^{13}C NMR (DMSO-d_6, 150 MHz) δ 165.8 (q_c, C-1'), 158.9 (q_c, d, $J_{F,C}$ = 236.0 Hz, C-6), 135.4 (q_c, d, $J_{F,C}$ = 12.3 Hz, C-7a), 128.4 (CH, C-2), 123.5 (q_c, C-3a), 121.9 (CH, d, $J_{F,C}$ = 10.0 Hz, C-4), 109.9 (q_c, C-3), 108.5 (CH, d, $J_{F,C}$ = 24.1 Hz, C-5), 97.6 (CH, d, $J_{F,C}$ = 25.9 Hz, C-7), 36.1 (2 x CH_3, C-2') ppm; ESMS *m/z* (rel. int.) 162 $[M+H]^+$ (54), 134 (100), 107 (61); HRESMS *m/z* 207.0926 (calcd for $C_{11}H_{12}N_2OF$ $[M+H]^+$ 207.0934).

5.3.12 Attempted synthesis of indolyl-3-α-oxothioacetamide 3.51 without using DMF

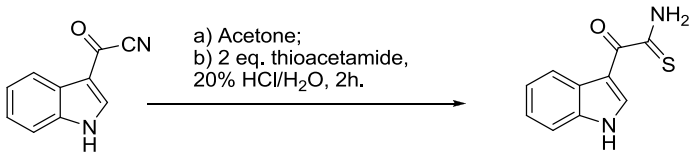

2.13 **3.51** 0%

A solution of thioacetamide (26.5 mg, 0.35 mmol, 2 eq.) in 2 ml of 20% HCl in water was added to a stirring solution of **2.13** (30 mg, 0.176 mmol, 1 eq.) in acetone (1ml). The reaction mixture was heated to reflux and reacted for 2h after which time the reaction was cooled with the addition of ice, and filtered. The filtrate was neutralized with sat. $NaHCO_3$ and the extracted with EtOAc (3 x 5 ml). The combined organic fractions were washed with water (1 x 10 ml) and sat. brine (1x 10 ml) and concentrated *in vacuo*. Flash chromatography with 5% EtOAc/CH_2Cl_2 followed by a column wash with EtOAc yielded only starting materials.

5.3.13 Synthesis of *N,N*-dimethyl-1*H*- indolyl-3-α-carboxamide 3.52 from indolyl-3-carbonylnitrile 2.13

2.13 **3.52**

Conc. HCl (100 µl) was added to a solution of indolyl-3-carbonylnitrile 2.13 in DMF (0.5 ml) and allowed to stir for 1h at room temperature. After work up in the usual manner, ^{1}H NMR analysis of the crude reaction mixture revealed the formation of compound **3.52** as part of a complex organic mixture.

5.3.14 Attempted synthesis of *N,N*-dimethyl-6-fluoro-1*H*- indolyl-3-α-carboxamide 3.53 from 6-fluoro-1*H* indole-3-carboxylic acid 3.54

3.54 **3.53** 0%

Conc. HCl (250 µl) was added to a solution of 6-fluoro-1*H* indole-3-carboxylic acid **3.54** (20mg, 0.097 mmol) in DMF (1 ml) and allowed to stir for 1h at room temperature. After work up in the usual manner, ^{1}H NMR analysis of the crude reaction mixture revealed only compound **3.54** to be present.

5.3.15 Hantzsch thiazole synthesis of compounds 1.62—1.68[172]

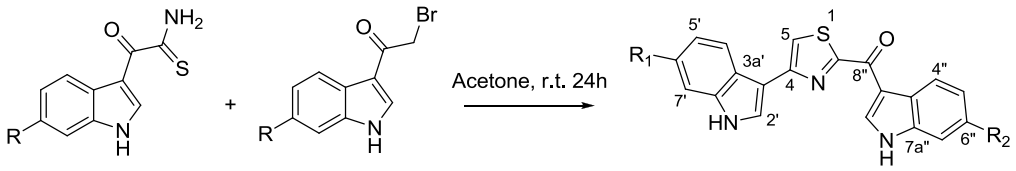

3.48 R = H
3.49 R = F
3.50 R = Cl
3.51 R = Br

2.2 R = H
3.38 R = F
3.40 R = Cl
3.41 R = Br

1.62 $R_1 = R_2 = H$
1.63 $R_1 = R_2 = F$
1.64 $R_1 = R_2 = Cl$
1.65 $R_1 = R_2 = Br$
1.66 $R_1 = Br$, $R_2 = F$
1.67 $R_1 = F$, $R_2 = Br$
1.68 $R_1 = F$, $R_2 = Cl$

This method is representative. Compounds **3.48** (39.6 mg, 0.19 mmol, 1 eq.) and **2.2** (45 mg, 1 eq.) were dissolved in acetone (4 ml) and allowed to stir for 24 hours in the dark forming a dark orange solution. Routine NP-HPLC (hexane: EtOAc, 3:2) yielded **1.62** (48.1 mg, 0.14 mmol, 74%) as a yellow solid.

This is a representative method, and was applied in the synthesis of **1.63—1.68** from varying quantities of starting material depending on availability using the same equivalents and solvent ratios above.

1*H*-Indol-3-yl[4-(1*H*-indol-3-yl)-thiazole-2-yl]-methanone (**1.62**): yellow amorphous solid (74% yield); IR (film) ν_{max} cm^{-1} 3250 2160 1575 1434 1241 1131 1101; ^{1}H NMR (DMSO-d_6, 600 MHz) δ 12.29 (1H, s, NH-1"), 11.54 (1H, s, NH-1'), 9.31 (1H, d, *J* = 2.9 Hz, H-2"), 8.37 (1H, d, *J* = 7.2 Hz, H-4"), 8.19 (1H, s, H-5), 8.16 (1H, d, *J* = 7.8 Hz, H-4'), 8.13 (1H, d, *J* = 2.5 Hz, H-2'), 7.59 (1H, d, *J* = 7.5 Hz, H-7"), 7.51 (1H, d, *J* = 7.9 Hz, H-7'), 7.29 (2H, m, H-5", H-6"), 7.22 (1H, t, *J* = 7.6 Hz, H-6'), 7.20 (1H, t, *J* = 7.4 Hz, H-5'); ^{13}C NMR (DMSO-d_6, 150 MHz) δ 177.3 (q_c, C-8"), 168.4 (q_c, C-2), 152.9 (q_c, C-4), 137.7 (CH, C-2"), 136.7 (q_c, C-7a'), 136.4 (q_c, C-7a"), 126.6 (q_c, C-3a"), 125.5 (CH, C-2'), 124.5 (q_c, C-3a'), 123.4 (CH, C-6"), 122.4 (CH, C-5"), 121.7 (CH, C-6'), 121.5 (CH, C-4"), 120.0 (CH, C-5'), 119.7 (CH, C-4'), 116.0 (CH, C-5), 112.6 (q_c, C-3"), 112.5 (CH, C-7"), 112.0 (CH, C-7'), 110.5 (q_c, C-3') ppm; ESMS *m/z* (rel. int.) 227 $[M+H]^+$ (15), 201 (100), 174 (21), 144 (80), 141 (45), 130 (15), 116 (10), 89 (2); HRESMS *m/z* 344.0856 (calcd for $C_{20}H_{14}N_3OS$ $[M+H]^+$ 344.0858).

6"-Fluoro-1*H*"-indol-3-yl[4-(6'-fluoro-1*H*'-indol-3-yl)-thiazole-2-yl]-methanone (**1.63**): yellow amorphous solid (83% yield); IR (film) ν_{max} cm^{-1} 3184 2916 1621 1576 1498 1150; ^{1}H NMR (DMSO-d_6, 600 MHz) δ 12.29 (1H, s, NH-1"), 11.61 (1H, s, NH-1'), 9.26 (1H, d, *J* = 3.1 Hz, H-2"), 8.33 (1H, dd, *J* = 8.7, 5.6 Hz, H-4"), 8.23 (1H, s, H-5), 8.14 (1H, dd, *J* = 8.7, 5.5 Hz, H- 4'), 8.12 (1H, d, *J* = 2.5 Hz, 2'), 7.39 (1H, dd, *J* = 9.5, 2.2 Hz, H-7"), 7.29 (1H, dd, *J* = 9.8, 2.3 Hz, H-7'), 7.16 (1H, m, H-5"), 7.03 (1H, m, H-5'); ^{13}C NMR (DMSO-d_6, 150 MHz) δ 177.2 (q_c, C-8"), 168.1 (q_c, C-2), 159.5 (q_c, d, $J_{F,C}$ = 237.3 Hz, C-6"), 158.9 (q_c, d, $J_{F,C}$ = 235.0 Hz, C-6'), 152.4 (q_c, C-4), 138.4 (CH, C-2"), 136.6 (q_c, d, $J_{F,C}$ = 12.6 Hz, C-7a'), 136.5 (q_c, d, $J_{F,C}$ = 12.5 Hz, C-7a"), 126.2 (CH, C-2'), 123.2 (q_c, C-3a"), 122.6 (CH, d, $J_{F,C}$ = 9.8 Hz, C-4"), 121.4 (q_c, C-3a'), 120.8 (CH, d, $J_{F,C}$ = 10.0 Hz, C-4'), 116.6 (CH, C-5), 112.6 (q_c, C-3"), 110.8 (CH, d, $J_{F,C}$ = 23.9 Hz, C-5"), 110.7 (q_c, C-3'), 108.4 (CH, d, $J_{F,C}$ = 24.1 Hz, C-5'), 98.9 (CH, d, $J_{F,C}$ = 25.6 Hz, C-7"), 98.0

(CH, d, $J_{F,C}$ = 25.6 Hz, C-7') ppm; ESMS *m/z* (rel. int.) 219 $[M+H]^+$ (42), 192 (25), 162 (63), 159 (100), 148 (33), 134 (25), 107 (6); HRESMS *m/z* 380.0674 (calcd for $C_{20}H_{12}N_3OSF_2$ $[M+H]^+$ 380.0669).

6"-Chloro-1*H*"-indol-3-yl[4-(6'-chloro-1*H*'-indol-3-yl)-thiazole-2-yl]-methanone (**1.64**): yellow amorphous solid (58% yield); IR (film) ν_{max} cm^{-1} 3260 2916 2160 1573 1449 1110; ^1H NMR (DMSO-d_6, 600 MHz) δ 12.32 (1H, s, NH-1"), 11.68 (1H, s, NH-1'), 9.28 (1H, d, *J* = 3.1 Hz, H-2"), 8.33 (1H, d, *J* = 8.5 Hz, H-4"), 8.25 (1H, s, H-5), 8.16 (2H, m, H-2', H-4') 7.66 (1H, d, *J* = 1.6 Hz, H-7"), 7.55 (1H, d, *J* = 1.7 Hz, H-7'), 7.32 (1H, dd, *J* = 8.5, 1.8 Hz, H-5"), 7.29 (1H, dd, *J* = 8.6, 1.8 Hz, H-5'); ^{13}C NMR (DMSO-d_6, 150 MHz) δ 177.2 (q_c, C-8"), 168.1 (q_c, C-2), 152.3 (q_c, C-4), 138.6 (CH, C-2"), 137.1 (q_c, C-7a'), 136.1 (q_c, C-7a"), 127.9 (q_c, C-6"), 126.6 (CH, C-2'), 126.5 (q_c, C-6'), 125.3 (q_c, C-3a"), 123.4 (q_c, C-3a'), 122.8 (CH, C-4"), 122.7 (CH, C-5"), 121.1 (CH, C-4'), 120.3 (CH, C-5'), 116.9 (CH, C-5), 112.6 (q_c, C-3"), 112.4 (CH, C-7"), 111.6 (CH, C-7'), 110.3 (q_c, C-3') ppm; ESMS *m/z* (rel. int.) 235 $[M+H]^+$ (15), 200 (100), 175 (73), 150 (22), 140 (10), 129 (4), 124 (4), 114 (3); HRESMS *m/z* 412.0069 (calcd for $C_{20}H_{12}N_3OSCl_2^{35}$ $[M+H]^+$ 412.0078).

6"-Bromo-1*H*"-indol-3-yl[4-(6'-bromo-1*H*'-indol-3-yl)-thiazole-2-yl]-methanone (**1.65**): yellow amorphous solid (51% yield); IR (film) ν_{max} cm^{-1} 3253 2916 2161 1576 1447 1110; ^1H NMR (DMSO-d_6, 600 MHz) δ 12.32 (1H, s, NH-1"), 11.68 (1H, s, NH-1'), 9.26 (1H, d, *J* = 3.1 Hz, H-2"), 8.28 (1H, d, *J* = 8.5 Hz, H-4"), 8.25 (1H, s, H-5), 8.15 (1H, d, *J* = 2.5 Hz, H-2'), 8.11 (1H, d, *J* = 8.5 Hz, H-4'), 7.80 (1H, d, *J* = 1.4 Hz, H-7"), 7.70 (1H, d, *J* = 1.4 Hz, H-7'), 7.44 (2H, dd, *J* = 8.5, 1.6 Hz, H-5"), 7.29 (1H, dd, *J* = 8.5, 1.6 Hz, H-5'); ^{13}C NMR (DMSO-d_6, 150 MHz) δ 177.2 (q_c, C-8"), 168.1 (q_c, C-2), 152.2 (q_c, C-4), 138.5 (CH, C-2"), 137.5 (q_c, C-7a'), 137.3 (q_c, C-7a"), 126.5 (CH, C-2'), 125.6 (q_c, C-3a"), 125.3 (CH, C-5"), 123.6 (q_c, C-3a'), 123.1 (CH, C-4"), 122.8 (CH, C-5'), 121.5 (CH, C-4'), 116.9 (CH, C-5), 115.9 (q_c, C-6"), 115.3 (CH, C-7"), 114.6 (CH, C-7'), 114.4 (q_c, C-6'), 112.6 (q_c, C-3"), 110.7 (q_c, C-3') ppm; ESMS *m/z* (rel. int.) 304 $[M+H]^+$ (5), 279 (4), 223 (30), 198 (100), 193 (7), 173 (6), 143 (9), 115 (6), 102 (2); HRESMS *m/z* 499.9080 (calcd for $C_{20}H_{12}N_3OSBr_2^{79}$ $[M+H]^+$ 499.9068).

6”-Fluoro-1*H*”-indol-3-yl[4-(6’-bromo-1*H*’-indol-3-yl)-thiazole-2-yl]-methanone (**1.66**): yellow amorphous solid (31% yield); IR (film) ν_{max} cm^{-1} 3210 2160 1738 1574 1425 1378 1133; ^{1}H NMR (DMSO-d_6, 600 MHz) δ 12.28 (1H, s, NH-1”), 11.68 (1H, s, NH-1’), 9.25 (1H, d, *J* = 3.0 Hz, H-2”), 8.33 (1H, dd, *J* = 8.6, 5.6 Hz, H-4”), 8.24 (1H, s, H-5), 8.15 (1H, d, *J* = 2.5 Hz, H- 2’), 8.11 (1H, d, *J* = 8.5 Hz, H-4’), 7.69 (1H, d, *J* = 1.7 Hz, H-7’), 7.40 (1H, dd, *J* = 9.5, 2.3 Hz, H-7”), 7.30 (1H, dd, *J* = 8.5, 1.7 Hz, H-5’), 7.15 (1H, m, H-5”); ^{13}C NMR (DMSO-d_6, 150 MHz) δ 177.2 (q_c, C-8”), 168.2 (q_c, C-2), 159.5 (q_c, d, $J_{F,C}$ = 237.5 Hz, C-6”), 152.2 (q_c, C-4), 138.4 (CH, C-2”), 137.5 (q_c, C-7a’), 136.5 (q_c, d, $J_{F,C}$ = 12.6 Hz, C-7a”), 126.5 (CH, C-2’), 123.6 (q_c, C-3a’), 123.2 (q_c, C-3a”), 122.8 (CH, C-5’), 122.6 (CH, d, $J_{F,C}$ = 9.7 Hz, C-4”), 121.5 (CH, C-4’), 116.8 (CH, C-5), 114.6 (CH, C-7’), 114.4 (q_c, C-3’), 112.5 (q_c, C-3”), 110.6 (q_c, C-6’), 110.6 (CH, d, $J_{F,C}$ = 23.8 Hz, C-5’), 98.9 (CH, d, $J_{F,C}$ = 26.2 Hz, C-7’) ppm; ESMS *m/z* (rel. int.) 304 $[M+H]^+$ (5), 276 (5), 220 (28), 192 (100), 173 (7), 162 (58), 134 (15), 107 (2); HRESMS *m/z* 439.9861 (calcd for $C_{20}H_{12}N_3OSFBr^{79}$ $[M+H]^+$ 439.9868).

6”-Bromo-1*H*”-indol-3-yl[4-(6’-fluoro-1*H*’-indol-3-yl)-thiazole-2-yl]-methanone (**1.67**): yellow amorphous solid (54% yield); IR (film) ν_{max} cm^{-1} 3162 2915 2159 1619 1455 1113; ^{1}H NMR (DMSO-d_6, 600 MHz) δ 12.33 (1H, s, NH-1”), 11.61 (1H, s, NH-1’), 9.27 (1H, d, *J* = 2.4 Hz, H-2”), 8.28 (1H, d, *J* = 8.4 Hz, H-4”), 8.24 (1H, s, H-5), 8.14 (1H, dd, *J* = 8.6, 5.6 Hz, H- 4’), 8.12 (1H, d, *J* = 2.5 Hz, H-2’), 7.80 (1H, d, *J* = 1.6 Hz, H-7”), 7.43 (1H, dd, *J* = 8.4, 1.7 Hz, H-5”), 7.28 (1H, dd, *J* = 9.9, 2.5 Hz, H-7’), 7.03 (1H, m, H-5’); ^{13}C NMR (DMSO-d_6, 150 MHz) δ 177.3 (q_c, C-8”), 168.0 (q_c, C-2), 158.9 (q_c, d, $J_{F,C}$ = 235.7 Hz, C-6’), 152.5 (q_c, C-4), 138.5 (CH, C-2”), 137.3 (q_c, C-7a”), 136.6 (q_c, d, $J_{F,C}$ = 12.0 Hz, C-7a’), 126.2 (CH, C-2’), 125.6 (q_c, C-3a”), 125.3 (CH, C-5”), 123.1 (CH, C-4”), 121.4 (q_c, C-3a’), 120.1 (CH, d, $J_{F,C}$ = 10.2 Hz, C-4’), 116.7 (CH, C-5), 115.9 (q_c, C-6”), 115.3 (CH, C-7”), 112.6 (q_c, C-3”), 110.6 (q_c, C-3’), 108.4 (CH, d, $J_{F,C}$ = 24.1 Hz, C-5’), 98.0 (CH, d, $J_{F,C}$ = 25.4 Hz, C-7’) ppm; EIMS *m/z* (rel. int.) 245 $[M+H]^+$ (5), 221 (51), 217 (47), 192 (20), 159 (100), 148 (15), 143 (10) 115 (5); HREIMS *m/z* 439.9868 (calcd for $C_{20}H_{12}N_3OSFBr^{79}$ $[M+H]^+$ 439.9868).

6"-Chloro-1*H*"-indol-3-yl[4-(6'-fluoro-1*H*'-indol-3-yl)-thiazole-2-yl]-methanone (**1.68**): yellow amorphous solid (53% yield); IR (film) ν_{max} cm^{-1} 3180 2916 2160 1710 1619 1566 1439 1113; ^{1}H NMR (DMSO-d_6, 600 MHz) δ 12.33 (1H, s, NH-1"), 11.61 (1H, s, NH-1'), 9.23 (1H, s, H-2"), 8.33 (1H, d, *J* = 8.5 Hz, H-4"), 8.24 (1H, s, H-5), 8.15 (1H, dd, *J* = 8.7, 5.5 Hz, H- 4'), 8.12 (1H, d, *J* = 2.5 Hz, H-2'), 7.66 (1H, d, *J* = 1.7 Hz, H-7"), 7.43 (1H, dd, *J* = 8.5, 1.8 Hz, H-5"), 7.28 (1H, dd, *J* = 9.9, 2.2 Hz, H-7'), 7.03 (1H, m, H-5'); ^{13}C NMR (DMSO-d_6, 150 MHz) δ 177.3 (q_c, C-8"), 168.0 (q_c, C-2), 158.9 (q_c, d, $J_{F,C}$ = 235.5 Hz, C-6'), 152.5 (q_c, C-4), 138.6 (CH, C-2"), 136.9 (q_c, C-7a"), 136.6 (q_c, d, $J_{F,C}$ = 12.4 Hz, C-7a'), 127.9 (q_c, C-6"), 126.2 (CH, C-2'), 125.3 (q_c, C-3a"), 122.8 (CH, C-4"), 122.7 (CH, C-5"), 121.4 (q_c, C-3a'), 120.8 (CH, d, $J_{F,C}$ = 10.0 Hz, C-4'), 116.7 (CH, C-5), 112.6 (q_c, C-3"), 112.4 (CH, C-7"), 110.6 (q_c, C-3'), 108.4 (CH, d, $J_{F,C}$ = 24.3 Hz, C-5'), 98.0 (CH, d, $J_{F,C}$ = 25.4 Hz, C-7') ppm; ESMS *m/z* (rel. int.) 245 $[M+H]^+$ (5), 219 (43), 192 (16), 178 (54), 159 (100), 148 (30), 132 (9) 122 (4); HRESMS *m/z* 396.0380 (calcd for $C_{20}H_{12}N_3OSFCl^{35}$ $[M+H]^+$ 396.0374).

5.3.16 Hantzsch thiazole synthesis from 2,2-dibromo-1-(1*H*-indol-3-yl)-ethanone **3.37** [172]

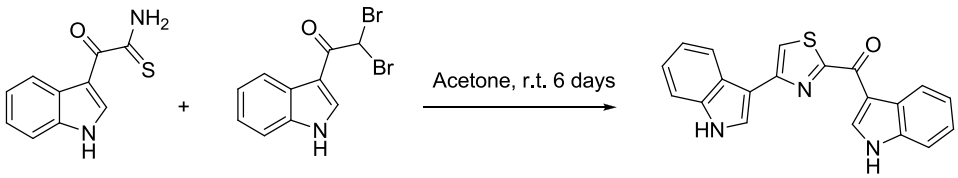

3.48 **3.37** **1.62**

Compounds **3.48** (7.1 mg, 0.034 mmol, 1 eq.) and **3.37** (11 mg, 1 eq.) were dissolved in acetone (1 ml) and allowed to stir for six days hours in the dark, whilst being monitored by TLC, forming a dark orange solution. Routine NP-HPLC (hexane: EtOAc) yielded **1.62** (1.3 mg, 0.0037 mmol, 11%) as a yellow solid.

5.3.17 Attempted oxazole synthesis

5.3.17.1 Synthesis of indolyl-3-α-oxoacetamide 3.32

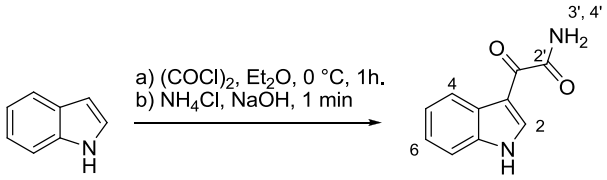

3.32

Oxalyl chloride (420 µl, 4.8 mmol, 1.13 eq.) was added dropwise to a stirring solution of indole (500 mg, 4.26 mmol, 1 eq.) in dry Et_2O (10 ml) at 0 °C under an inert atmosphere of dry argon gas, resulting in an instant colour change to yellow. After one hour an aq. solution of NH_4OAc and NaOH was added and stirred for one minute. The reaction mixture was acidified with dilute HCl, and washed with EtOAc, and finally neutralized with sat. $NaHCO_3$ and extracted with EtOAc. The organic fraction was dried over anhydrous $MgSO_4$ and concentrated *in vacuo* to yield **3.32** as a beige powder (800 mg, 4.8 mmol, 100%).

Indolyl-3-α-oxoacetamide (**3.32**): beige powder (100% yield); IR (film) ν_{max} cm^{-1} 3201 2160 1664 1578 1403 1155; ^1H NMR (DMSO-d_6, 600 MHz) δ 12.29 (1H, s, NH-1), 8.57 (1H, s, H-2), 8.22 (1H, d, *J* = 7.3 Hz, H-4), 8.05 (1H, s, NH-3'), 7.69 (1H, s, NH-4'), 7.53 (1H, d, *J* = 7.4 Hz, H-7), 7.25 (2H, m, H-5, H-6); ^{13}C NMR (DMSO-d_6, 150 MHz) δ 182.9 (q_c, C-2'), 166.0 (q_c, C-1'), 138.2 (CH, C-2), 136.3 (q_c, C-7a), 126.1 (q_c, C-3a), 123.3 (CH, C-6), 122.2 (CH, C-5), 121.2 (CH, C-4), 112.5 (CH, C-7), 112.0 (q_c, C-3) ppm; ESMS *m/z* (rel. int.) 144 $[M+H]^+$ (65), 116 (25), 89 (35); HRESMS *m/z* 189.0653 (calcd for $C_{10}H_9N_2O_2$ $[M+H]^+$ 189.0664).

5.3.17.2 Attempted oxazole synthesis and subsequent formation of 2-ethoxy-1-(1*H*-Indol-3-yl)-ethanone 3.59[201]

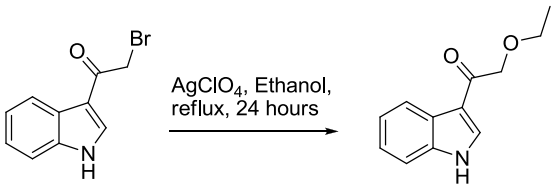

2.2 **3.59**

Silver perchlorate (70.4 mg, 2 eq.) was added to a stirring solution of **3.32** (31.8 mg, 0.17 mmol, 1 eq.) and **2.2** (40 mg, 1 eq.) in acetone (4 ml). The reaction was heated to reflux and allowed to react for 24 hours in the dark forming a black precipitate. The reaction mixture was diluted with water (1 x 10 ml) and extracted with EtOAc (3 x 5 ml). The combined organic fractions were washed with sat. brine (1x 10 ml) and concentrated *in vacuo*. Flash chromatography (100% DCM) yielded compound **3.59** (27.6 mg, 0.136 mmol, 80%) as a white amorphous solid.

2-Ethoxy-1-(1*H*-Indol-3-yl)-ethanone (3.59): white amorphous solid; IR (film) ν_{max} cm^{-1} 2864 2160 1643 1532 1423 1309; ^{1}H NMR (DMSO-d_6, 600 MHz) δ 11.96 (1H, s, NH-1), 8.35 (1H, d, *J* = 2.27 Hz, H-2), 8.17 (1H, d, *J* = 7.3 Hz, H-4), 7.48 (1H, d, *J* = 7.7 Hz, H-7), 7.20 (2H, m, H-5, H-6), 4.53 (2H, s, H-3'), 3.56 (2H, q, *J* = 7.0 Hz H-4'), 1.12 (3H, t, *J* = 7.0 Hz, H-5') ; ^{13}C NMR (DMSO-d_6, 150 MHz) δ 192.2 (q_c, C-1'), 136.2 (q_c, C-7a), 133.6 (CH, C-2), 125.5 (q_c, C-3a), 122.8 (CH, C-6), 121.8 (CH, C-5) 121.2 (CH, C-4), 113.8 (q_c, C-3) 112.1 (CH, C-7), 65.9 (CH_2, C-4'), 15.1 (CH_3, C-5') ppm; HRESMS *m/z* 204.1024 (calcd for $C_{12}H_{14}NO_2$ $[M+H]^+$ 204.1023).

5.3.18 Attempted synthesis of indolyl-3-α-oxocarboxamidine 3.58 and subsequent synthesis of 1*H* Indole-3-carboxylic acid methyl ester 3.60[180]

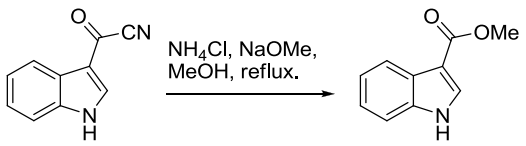

2.13 **3.60**

Sodium methoxide (1.56 mg, 0.029 mmol, 0.1 eq.) and NH_4Cl (31 mg, 2 eq.) was added to a methanolic (2 ml) solution of **2.13** (50 mg, 0.29 mmol, 1 eq.) and heated to reflux. After 30 minutes the reaction mixture was diluted with water (10 ml) and extracted with EtOAc (3 x 15 ml). The combined organic fractions were washed with sat. brine (1x 10 ml) and concentrated *in vacuo* to yield **3.60** (51 mg, 0.29 mmol, 100%) as a yellow solid.

1*H* Indole-3-carboxylic acid methyl ester[232] (**3.60**): yellow crystalline solid; mp 147—149 °C, lit 146—148 °C;[232] IR (film) ν_{max} cm^{-1} 2945 2161 1663 1527 1443 1371; ^1H NMR (DMSO-d_6, 600 MHz) δ 11.90 (1H, s, NH-1'), 8.09 (1H, s, H-2), 7.99 (1H, d, *J* = 7.3 Hz, H-4), 7.47 (1H, d, *J* = 7.9 Hz, H-7), 7.19 (2H, m, H-5, H-6), 3.80 (3H, s, H-3'); ^{13}C NMR (DMSO-d_6, 150 MHz) δ 164.8 (q_c, C-1'), 136.4 (q_c, C-7a), 132.5 (CH, C-2), 125.6 (q_c, C-3a), 122.4 (CH, C-6), 121.3 (CH, C-5) 120.4 (CH, C-4), 112.2 (CH, C-7), 106.3 (q_c, C-3), 50.6 (CH_3, C-3') ppm; ESMS *m/z* (rel. int.) 144 $[M+H]^+$ (41), 116 (100), 89 (46); HRESMS *m/z* 176.0706 (calcd for $C_{10}H_{10}NO_2$ $[M+H]^+$ 176.0712).

References

(1) Lyont, B. R.; Skurray, R. O. N. *Microbiol. Mol. Biol. R.* **1987**, *51*, 88–134.

(2) Otero, L. H.; Rojas-altuve, A.; Llarrull, L. I.; Carrasco-López, C.; Kumarasiri, M.; Lastochkin, E.; Fishowitz, J.; Dawley, M.; Hesek, D.; Lee, M.; Johnson, J. W.; Fisher, J. F.; Chang, M.; Mobashery, S.; Hermoso, J. A. *PNAS* **2013**, *110*, 16808–16813.

(3) Georgopapadakou, N. H. *Antimicrob. Agents Chemother.* **1993**, *37*, 2045–2053.

(4) Boneca, I. G. *Curr. Opinion Microbiol.* **2005**, *8*, 46–53.

(5) Livermore, D. M. *J. Antimicrob. Chemother.* **1998**, *41 Suppl D*, 25–41.

(6) Ubukata, K.; Nonoguchi, R.; Matsuhashi, M.; Konno, M. *J. Bacteriol.* **1989**, *171*, 2882–2885.

(7) Sakoulas, G.; Moellering, R. C.; Eliopoulos, G. M. *Clin. Infect. Dis.* **2006**, *42 Suppl 1*, S40–50.

(8) Robert, J.; Bismuth, R.; Jarlier, V. *J. Antimicrob. Chemoth.* **2006**, *57*, 506–510.

(9) Nagarajan, R. *Antimicrob. Agents Chemother.* **1991**, *35*, 605–609.

(10) Courvalin, P. *Clin. Infect. Dis.* **2006**, *42 Suppl 1*, S25–34.

(11) Micek, S. T. *Clin. Infect. Dis.* **2007**, *45 Suppl 3*, S184–90.

(12) Zoraghi, R.; See, R. H.; Axerio-Cilies, P.; Kumar, N. S.; Gong, H.; Moreau, A.; Hsing, M.; Kaur, S.; Swayze, R. D.; Worrall, L.; Amandoron, E.; Lian, T.; Jackson, L.; Jiang, J.; Thorson, L.; Labriere, C.; Foster, L.; Brunham, R. C.; McMaster, W. R.; Finlay, B. B.; Strynadka, N. C.; Cherkasov, A.; Young, R. N.; Reiner, N. E. *Antimicrob. Agents Chemother.* **2011**, *55*, 2042–2053.

(13) Kumar, N. S.; Amandoron, E. A.; Cherkasov, A.; Finlay, B. B.; Gong, H.; Jackson, L.; Kaur, S.; Lian, T.; Moreau, A.; Labrière, C.; Reiner, N. E.; See, R. H.; Strynadka, N. C.; Thorson, L.; Wong, E. W. Y.; Worrall, L.; Zoraghi, R.; Young, R. N. *Bioorg. Med. Chem.* **2012**, *20*, 7069–7082.

(14) Zoraghi, R.; Reiner, N. E. *Curr. Opinion Microbiol.* **2013**, *16*, 1–7.

(15) Cherkasov, A.; Hsing, M.; Zoraghi, R.; Foster, L. J.; See, R. H.; Stoynov, N.; Jiang, J.; Kaur, S.; Lian, T.; Jackson, L.; Gong, H.; Swayze, R.; Amandoron, E.; Hormozdiari, F.; Dao, P.; Sahinalp, C.; Santos-Filho, O.; Axerio-Cilies, P.; Byler, K.; McMaster, W. R.; Brunham, R. C.; Finlay, B. B.; Reiner, N. E. *J. Proteome. Res.* **2011**, *10*, 1139–1150.

(16) Zoraghi, R.; Worrall, L.; See, R. H.; Strangman, W.; Popplewell, W. L.; Gong, H.; Samaai, T.; Swayze, R. D.; Kaur, S.; Vuckovic, M.; Finlay, B. B.; Brunham, R. C.; McMaster, W. R.; Davies-Coleman, M. T.; Strynadka, N. C.; Andersen, R. J.; Reiner, N. E. *J. Biol. Chem.* **2011**, *286*, 44716–44725.

(17) Bauer, R. a; Wurst, J. M.; Tan, D. S. *Curr. Opin. Chem. Biol.* **2010**, *14*, 308–314.

(18) Jurica, M. S.; Mesecar, A.; Heath, P. J.; Shi, W.; Nowak, T.; Stoddard, B. L. *Structure* **1998**, *6*, 195–210.

(19) Morgan, H. P.; O'Reilly, F. J.; Wear, M. A.; O'Neill, J. R.; Fothergill-Gilmore, L. A.; Hupp, T.; Walkinshaw, M. D. *PNAS* **2013**, *110*, 5881–5886.

(20) Sievers, F.; Wilm, A.; Dineen, D.; Gibson, T. J.; Karplus, K.; Li, W.; Lopez, R.; McWilliam, H.; Remmert, M.; Söding, J.; Thompson, J. D.; Higgins, D. G. *Mol. Syst. Biol.* **2011**, *7*, 539.

(21) Accelrys Software Inc., Discovery Studio Modeling Environment, Release 4.0, San Diego: Accelrys Software Inc., 2013.

(22) Strangman, W.; Zoraghi, R.; See, R. H.; Gong, H.; Popplewell, W. L.; Davies-Coleman, M. T.; Reiner, N. E.; Andersen, R. J. *Poster presentation: 52nd American Society for Pharmacognosy meeting San Diego*; 2011.

(23) Wilcken, R.; Zimmermann, M. O.; Lange, A.; Joerger, A. C.; Boeckler, F. M. *J. Med. Chem.* **2013**, *56*, 1363–1388.

(24) Feher, M.; Schmidt, J. M. *J. Chem. Inf. Comput. Sci.* **2003**, *43*, 218–227.

(25) Cragg, G. M.; Newman, D. J. *Biochim. Biophys. Acta* **2013**, *1830*, 3670–3695.

(26) Lachance, H.; Wetzel, S.; Kumar, K.; Waldmann, H. *J. Med. Chem.* **2012**, *55*, 5989–6001.

(27) Haefner, B. *Drug Discov. Today* **2003**, *8*, 536–544.

(28) Pauletti, P. M.; Cintra, L. S.; Braguine, C. G.; da Silva Filho, A. A.; Silva, M. L. A. E.; Cunha, W. R.; Januário, A. H. *Mar. Drugs* **2010**, *8*, 1526–1549.

(29) Rosén, J.; Gottfries, J.; Muresan, S.; Backlund, A.; Oprea, T. I. *J. Med. Chem.* **2009**, *52*, 1953–1962.

(30) Overington, J. P.; Al-Lazikani, B.; Hopkins, A. L. *Nat. Rev. Drug. Discov.* **2006**, *5*, 993–996.

(31) Molinski, T. F.; Dalisay, D. S.; Lievens, S. L.; Saludes, J. P. *Nat. Rev. Drug. Discov.* **2009**, *8*, 69–85.

(32) Li, J. W.-H.; Vederas, J. C. *Science* **2009**, *325*, 161–165.

(33) Gerwick, W. H.; Moore, B. S. *Chem. Biol.* **2012**, *19*, 85–98.

(34) Querellou, J.; Børresen, T.; Boyen, C.; Dobson, A.; Höfle, M.; Ianora, A.; Jaspars, M.; Kijjoa, A.; Olafsen, J.; Rigos, G.; Wijffels, R. *Marine Biotechnology: A New Vision and Strategy for Europe 15*, 37–59.

(35) Proksch, P.; Edrada-Ebel, R.; Ebel, R. *Mar. Drugs* **2003**, *1*, 5–17.

(36) Munro, M. H.; Blunt, J. W.; Dumdei, E. J.; Hickford, S. J.; Lill, R. E.; Li, S.; Battershill, C. N.; Duckworth, A. R. *J. Biotechnol.* **1999**, *70*, 15–25.

(37) Cuevas, C.; Francesch, A. *Nat. Prod. Rep.* **2009**, *26*, 322–337.

(38) Ongley, S. E.; Bian, X.; Zhang, Y.; Chau, R.; Gerwick, W. H.; Müller, R.; Neilan, B. A. *ACS Chem. Biol.* **2013**, *8*, 1888–1893.

(39) Li, T.; Du, Y.; Cui, Q.; Zhang, J.; Zhu, W.; Hong, K.; Li, W. *Mar. Drugs* **2013**, *11*, 466–88.

(40) Veale, C. G. L.; Davies-Coleman, M. T. *The Alkaloids* **2014**, *74*, 1–64.

(41) Zehr, J. P.; Kudela, R. M. *Annu. Rev. Mar. Sci.* **2011**, *3*, 197–225.

(42) Norton, R. S.; Wells, R. J. *J. Am. Chem. Soc.* **1982**, *104*, 3628–3635.

(43) Palermo, J. A.; Flower, P. B.; Seldes, A. M. *Tetrahedron Lett.* **1992**, *33*, 3097–3100.

(44) Davyt, D.; Entz, W.; Fernandez, R.; Mariezcurrena, R.; Mombrú, A. W.; Saldaña, J.; Domínguez, L.; Coll, J.; Manta, E. *J. Nat. Prod.* **1998**, *61*, 1560–1563.

(45) Yang, C.-G.; Huang, H.; Jiang, B. *Curr. Org. Chem.* **2004**, *8*, 1691–1720.

(46) Kohmoto, S.; Kashman, Y.; McConnell, O. J.; Rinehart, K. L. J.; Wright, A.; Koehn, F. *J. Org. Chem.* **1988**, *53*, 3116–3118.

(47) Capon, R. J.; Rooney, F.; Murray, L. M.; Collins, E.; Sim, A. T. R.; Rostas, J. A. P.; Butler, M. S.; Carroll, A. R. *J. Nat. Prod.* **1998**, *61*, 660–662.

(48) Wright, A. E.; Pomponi, S. A.; Cross, S. S.; McCarthy, P. *J. Org. Chem.* **1992**, *57*, 4772–4775.

(49) Gunasekera, S. P.; McCarthy, P. J.; Kelly-Borges, M. *J. Nat. Prod.* **1994**, *57*, 1437–1441.

(50) Cutignano, A.; Bifulco, G.; Bruno, I.; Casapullo, A.; Gomez-Paloma, L.; Riccio, R. *Tetrahedron* **2000**, *56*, 3743–3748.

(51) Bao, B.; Sun, Q.; Yao, X.; Hong, J.; Lee, C.-O.; Sim, C. J.; Im, K. S.; Jung, J. H. *J. Nat. Prod.* **2005**, *68*, 711–715.

(52) Bao, B.; Sun, Q.; Yao, X.; Hong, J.; Lee, C.-O.; Cho, H. Y.; Jung, J. H. *J. Nat. Prod.* **2007**, *70*, 2–8.

(53) Oh, K.-B.; Mar, W.; Kim, S.; Kim, J.-Y.; Lee, T.-H.; Kim, J.-G.; Shin, D.; Sim, C. J.; Shin, J. *Biol. Pharm. Bull.* **2006**, *29*, 570–573.

(54) Alvarado, S.; Roberts, B. F.; Wright, A. E.; Chakrabarti, D. *Antimicrob. Agents Chemother.* **2013**, *57*, 2362–2364.

(55) Oh, K. B.; Mar, W.; Kim, S.; Kim, J.-Y.; Oh, M.-N.; Kim, J.-G.; Shin, D.; Sim, C. J.; Shin, J. *Bioorg. Med. Chem. Lett.* **2005**, *15*, 4927–4931.

(56) Endo, T.; Tsuda, M.; Fromont, J.; Kobayashi, J. *J. Nat. Prod.* **2007**, *70*, 423–424.

(57) Tasch, B. O. A. .; Merkul, E.; Müller, T. J. J. *Eur. J. Org. Chem.* **2011**, 4532–4535.

(58) Swersey, J. C.; Ireland, C. M.; Cornell, L. M.; Peterson, R. W. *J. Nat. Prod.* **1994**, *57*, 842–845.

(59) Tapiolas, D. M.; Bowden, B. F.; Abou-Mansour, E.; Willis, R. H.; Doyle, J. R.; Muirhead, A. N.; Liptrot, C.; Llewellyn, L. E.; Wolff, C. W. W.; Wright, A. D.; Motti, C. *J. Nat. Prod.* **2009**, *72*, 1115–1120.

(60) Tadesse, M.; Tabudravu, J. N.; Jaspars, M.; Strøm, M. B.; Hansen, E.; Andersen, J. H.; Kristiansen, P. E.; Haug, T. *J. Nat. Prod.* **2011**, *74*, 837–841.

(61) Maiti, B. C.; Thomson, R. H.; Mahendran, M. *J. Chem. Res., Synop.* **1978**, *4*, 126–127.

(62) Lu, Y.; Lu, D.; Zheng, Q-T.; Lian, B.; Su, J-Y.; Cen, Y.-Z. *Jiegou Huaxue.* **1994**, *13*, 472–476.

(63) Mancini, I.; Guella, G.; Zibrowius, H.; Pietra, F. *Tetrahedron* **2003**, *59*, 8757–8762.

(64) Dai, J.; Jiménez, J. I.; Kelly, M.; Barnes, S.; Lorenzo, P.; Williams, P. *J. Nat. Prod.* **2008**, *71*, 1287–1290.

(65) Dai, J.; Jiménez, J. I.; Kelly, M.; Williams, P. G. *J. Org. Chem.* **2010**, *75*, 2399–2402.

(66) Bartik, K.; Braekman, J.; Daloze, D.; Stoller, C.; Huysecom, J.; Vandevyver, G.; Ottinger, R. *Can. J. Chem.* **1987**, *65*, 2118–2121.

(67) Tsujii, S.; Rinehart, K. L.; Gunasekera, S. P.; Kashman, Y.; Cross, S. S.; Lui, M. S.; Pomponi, S. A.; Diaz, M. C. *J. Org. Chem.* **1988**, *53*, 5446–5453.

(68) Phife, D. W.; Ramos, R. A.; Feng, M.; King, I.; Gunasekera, S. P.; Wright, A.; Patel, M.; Pachter, J. A.; Coval, S. J. *Bioorg. Med. Chem. Lett.* **1996**, *6*, 2103–2106.

(69) Murray, L. M.; Lim, T. K.; Hooper, J. N. A.; Capon, R. J. *Aust. J. Chem.* **1995**, *48*, 2053–2058.

(70) Shin, J.; Seo, Y.; Cho, K. W.; Rho, J. R.; Sim, C. J. *J. Nat. Prod.* **1999**, *62*, 647–649.

(71) Morris, S. A.; Andersen, R. J. *Can. J. Chem.* **1989**, *67*, 677–681.

(72) Morris, S. A.; Andersen, R. J. *Tetrahedron* **1990**, *46*, 715–720.

(73) Casapullo, A.; Bifulco, G.; Bruno, I.; Riccio, R. *J. Nat. Prod.* **2000**, *63*, 447–451.

(74) Jung, J. H.; Shinde, P. B.; Hong, J.; Liu, Y.; Sim, C. J. *Biochem. Syst. Ecol.* **2007**, *35*, 48–51.

(75) Braekman, J.; Daloze, D.; Moussiaux, C.; Stoller, C.; Deneubourg, F. *Pure Appl. Chem.* **1989**, *61*, 509–512.

(76) Sakemi, S.; Sun, H. H. *J. Org. Chem.* **1991**, *56*, 4304–4307.

(77) Sun, H.; Sakemi, S.; Gunasekera, S.; Kashman, Y.; Lui, M.; Burres, N.; McCarthy, P. *US Patent 4,970,226 Chem. Abstr.* **1991**. *115*, 35701z.

(78) Mancini, I.; Guella, G.; Debitus, C.; Waikedre, J.; Pietra, F. *Helv. Chim. Acta.* **1996**, *79*, 2075–2082.

(79) Tilvi, S.; Moriou, C.; Martin, M.-T.; Gallard, J.-F.; Sorres, J.; Patel, K.; Petek, S.; Debitus, C.; Ermolenko, L.; Al-Mourabit, A. *J. Nat. Prod.* **2010**, *73*, 720–723.

(80) Sato, H.; Tsuda, M.; Watanabe, K.; Kobayashi, J. *Tetrahedron* **1998**, *54*, 8687–8690.

(81) Burres, N. S.; Barber, D. A.; Gunasekera, S. P.; Shen, L. L.; Clement, J. J. *Biochem. Pharmcol.* **1991**, *42*, 745–751.

(82) Braekman, J. C.; Daloze, D.; Stoller, C. *Bull. Soc. Chim. Belg.* **1987**, *96*, 809–812.

(83) Kawasaki, I.; Yamashita, M.; Ohta, S. *J. Chem. Soc., Chem. Commun.* **1994**, *4*, 2085–2086.

(84) Kawasaki, I.; Yamashita, M.; Ohta, S. *Chem. Pharm. Bull.* **1996**, *44*, 1831–1839.

(85) Achab, S. *Tetrahedron Lett.* **1996**, *37*, 5503–5506.

(86) Mal, S. K.; Bohé, L.; Achab, S. *Tetrahedron* **2008**, *64*, 5904–5914.

(87) Miyake, F. Y.; Yakushijin, K.; Horne, D. A. *Org. Lett.* **2000**, *2*, 2121–2123.

(88) Hogan, I. T.; Sainsbury, M. *Tetrahedron* **1984**, *40*, 681–682.

(89) Moody, C. J.; Roffey, J. R. A. *Arkivoc* **2000**, *iii*, 393–401.

(90) Fresneda, P.; Molina, P.; Sanz, M. A. *Synlett* **2001**, 218.

(91) Guinchard, X.; Vallée, Y.; Denis, J.-N. *J. Org. Chem.* **2007**, *72*, 3972–3975.

(92) Guinchard, X.; Vallée, Y.; Denis, J.-N. *Org. Lett.* **2007**, *9*, 3761–3764.

(93) Khalili, B.; Tondro, T.; Hashemi, M. M. *Tetrahedron* **2009**, *65*, 6882–6887.

(94) Young, R. M. *PhD Thesis, Rhodes University* **2011**.

(95) Laval, S.; Dayoub, W.; Favre-Reguillon, A.; Berthod, M.; Demonchaux, P.; Mignani, G.; Lemaire, M. *Tetrahedron Lett.* **2009**, *50*, 7005–7007.

(96) Kumar, D.; Sundaree, S.; Patel, G.; Rao, V. S. *Tetrahedron Lett.* **2008**, *49*, 867–869.

(97) Kamila, S.; Ankati, H.; Biehl, E. R. *Arkivoc* **2011**, *ix*, 94–104.

(98) Kamila, S.; Ankati, H.; Biehl, E. R. *Tetrahedron Lett.* **2011**, *52*, 4375–4377.

(99) Garg, N. K.; Sarpong, R.; Stoltz, B. M. *J. Am. Chem. Soc.* **2002**, *124*, 13179–13184.

(100) Marchand, N. J.; Grée, D. M.; Martelli, J. T.; Grée, L. *J. Org. Chem.* **1996**, *32*, 5063–5072.

(101) Young, R. M.; Davies-Coleman, M. T. *Tetrahedron Lett.* **2011**, *52*, 4036–4038.

(102) Kornblum, N.; Powers, J. W.; Anderson, G. J.; Jones, W. J.; Larson, H. O.; Levand, O.; Wraver, W. M. *J. Am. Chem. Soc.* **1957**, *79*, 6562.

(103) Kornblum, N.; Jones, W. J.; Anderson, G. J. *J. Am. Chem. Soc.* **1959**, *81*, 4113–4114.

(104) Ottoni, O.; Neder, A. de V. F.; Dias, A.; Cruz, R. P. A.; Aquino, L. B. *Org. Lett* **2001**, *3*, 1005–1007.

(105) Nagarajan, R.; Perumal, P. T. *Tetrahedron* **2002**, *58*, 1229–1232.

(106) Barreca, M. L.; Ferro, S.; Rao, A.; Luca, L. De; Zappalà, M.; Monforte, A.-M.; Debyser, Z.; Witvrouw, M.; Chimirri, A. *J. Med. Chem.* **2005**, *48*, 7084–7088.

(107) Simon, G.; Couthon-Gourves, H.; Haelters, J.-P.; Corbel, B.; Kervarec, N.; Michaud, F.; Meijer, L. *J. Heterocyclic Chem.* **2007**, *44*, 793–801.

(108) De Luca, L.; Barreca, M. L.; Ferro, S.; Iraci, N.; Michiels, M.; Christ, F.; Debyser, Z.; Witvrouw, M.; Chimirri, A. *Bioorg. Med. Chem. Lett.* **2008**, *18*, 2891–2895.

(109) Guchhait, S. K.; Kashyap, M.; Kamble, H. *J. Org. Chem.* **2011**, *76*, 4753–4758.

(110) Jiang, T.-S.; Wang, G.-W. *Org. Lett.* **2013**, *15*, 788–791.

(111) Taylor, J. E.; Jones, M. D.; Williams, J. M. J.; Bull, S. D. *Org. Lett.* **2010**, *12*, 5740–5743.

(112) Janosik, T.; Johnson, A.-L.; Bergman, J. *Tetrahedron* **2002**, *58*, 2813–2819.

(113) Sunassee, S. N.; Veale, C. G. L.; Shunmoogam-Gounden, N.; Osoniyi, O.; Hendricks, D. T.; Caira, M. R.; de la Mare, J.-A.; Edkins, A. L.; Pinto, A. V; da Silva Júnior, E. N.; Davies-Coleman, M. T. *Eur. J. Med. Chem.* **2013**, *62*, 98–110.

(114) Aupoix, A.; Bournaud, C.; Vo-Thanh, G. *Eur. J. Org. Chem.* **2011**, 2772–2776.

(115) Szmuszkovicz, J. *J. Org. Chem.* **1962**, *27*, 511–514.

(116) Wang, L.; Shao, Y.; Liu, Y. *Org. Lett.* **2012**, *14*, 3978–3981.

(117) Matsukawa, S.; Funabashi, Y.; Imamoto, T. *Tetrahedron Lett.* **2003**, *44*, 1007–1010.

(118) Dimitrov, V.; Kostova, K.; Genov, M. *Tetrahedron Lett.* **1996**, *37*, 6787–6790.

(119) Imamoto, T. *Pure. Appl. Chem.* **1990**, *62*, 747–752.

(120) Imamoto, T.; Takiyama, N.; Nakamura, K.; Hatajima, T.; Kamiya, Y. *J. Am. Chem. Soc.* **1989**, *111*, 4392–4398.

(121) Schmitz-Dumont, O.; Motzkus, E. *Chem. Ber.* **1929**, *62*, 466.

(122) Lista, L.; Pezzella, A.; Napolitano, A.; d'Ischia, M. *Tetrahedron* **2008**, *64*, 234–239.

(123) Castanet, A.-S.; Colobert, F.; Broutin, P.-E. *Tetrahedron Lett.* **2002**, *43*, 5047–5048.

(124) Ganguly, N.; Barik, S.; Dutta, S. *Synthesis* **2010**, 1467–1472.

(125) L'Helgoual'ch, J.-M.; Seggio, A.; Chevallier, F.; Yonehara, M.; Jeanneau, E.; Uchiyama, M.; Mongin, F. *J. Org. Chem.* **2008**, *73*, 177–183.

(126) Deng, H.; Gifford, A. N.; Zvonok, A. M.; Cui, G.; Li, X.; Fan, P.; Deschamps, J. R.; Flippen-Anderson, J. L.; Gatley, S. J.; Makriyannis, A. *J. Med. Chem.* **2005**, *48*, 6386–6392.

(127) Irie, K.; Iguchi, M.; Oda, T.; Suzuki, Y.; Okuno, S.; Ohigashi, H.; Koshimizu, K. *Tetrahedron* **1995**, *51*, 6255–6266.

(128) Moskalev, N.; Makosza, M. *Tetrahedron Lett.* **1999**, *40*, 5395–5398.

(129) Feldman, K. S.; Ngernmeesri, P. *Org. Lett.* **2011**, *13*, 5704–5707.

(130) Dobbs, A. P.; Voyle, M.; Whittall, N. *Synlett* **1999**, 1594–1596.

(131) Hodgkinson, R. C.; Schulz, J.; Willis, M. C. *Org. Biomol. Chem.* **2009**, *7*, 432–434.

(132) McAusland, D.; Seo, S.; Pintori, D. G.; Finlayson, J.; Greaney, M. F. *Org. Lett.* **2011**, *13*, 3667–3669.

(133) Gu, X.; Wan, X.; Jiang, B. *Bioorg. Med. Chem. Lett.* **1999**, *9*, 569–572.

(134) Ottoni, O.; Cruz, R.; Krammer, N. H. *Tetrahedron Lett.* **1999**, *40*, 1117–1120.

(135) Yamada, Y.; Akiba, A.; Arima, S.; Okada, C.; Yoshida, K.; Itou, F.; Kai, T.; Satou, T.; Takeda, K.; Harigaya, Y. *Chem. Pharm. Bull.* **2005**, *53*, 1277–1290.

(136) Willem, R.; Jans, A.; Hoogzand, C.; Gielen, M.; van Binst, G.; Pepermans, H. *J. Am. Chem. Soc.* **1985**, *107*, 28–32.

(137) Pons, M.; Millet, O. *Prog. Nucl. Magn. Reson. Spectrosc.* **2001**, *38*, 267–324.

(138) Gordon, W. E.; Cupery, M. E. *Ind. Eng. Chem.* **1939**, *31*, 1237–1238.

(139) Cupery, M. E.; Gordon, W. E. *Ind. Eng. Chem.* **1942**, *34*, 792–797.

(140) Bozell, J. J.; Hames, B. R. *J. Org. Chem.* **1995**, *60*, 2398–2404.

(141) Eftekhari-Sis, B.; Khajeh, S. V.; Büyükgüngör, O. *Synlett* **2013**, *24*, 977–980.

(142) Dandepally, S. R.; Williams, A. L. *Tetrahedron Lett.* **2009**, *50*, 1071–1074.

(143) Tom, N. J.; Simon, W. M.; Frost, H. N.; Ewing, M. *Tetrahedron Lett.* **2004**, *45*, 905–906.

(144) El Kazzouli, S.; Koubachi, J.; Berteina-Raboin, S.; Mouaddib, A.; Guillaumet, G. *Tetrahedron Lett.* **2006**, *47*, 8575–8577.

(145) Rawal, V. H.; Cava, M. P. *Tetrahedron Lett.* **1985**, *26*, 6141–6142.

(146) Wang, G.; Li, C.; Li, J.; Jia, X. *Tetrahedron Lett.* **2009**, *50*, 1438–1440.

(147) Umbreit, M. A.; Sharpless, K. B. *J. Am. Chem. Soc.* **1977**, *99*, 5526 – 5528.

(148) Burange, A. S.; Kale, S. R.; Jayaram, R. V. *Tetrahedron Lett.* **2012**.

(149) Wójtowicz, H.; Brzaszcz, M.; Kloc, K.; Młochowski, J. *Tetrahedron* **2001**, *57*, 9743–9748.

(150) Sharpless, K. B.; Gordon, K. M. *J. Am. Chem. Soc.* **1976**, *98*, 300–301.

(151) Patiny, L.; Borel, A. *J. Chem. Inf. Model* **2013**, *53*, 1223–1228.

(152) Jiang, B.; Gu, X. H. *Bioorg. Med. Chem.* **2000**, *8*, 363–371.

(153) Just-Baringo, X.; Bruno, P.; Ottesen, L. K.; Cañedo, L. M.; Albericio, F.; Álvarez, M. *Angew. Chem. Int. Ed.* **2013**, *52*, 7818–7821.

(154) Just-Baringo, X.; Bruno, P.; Albericio, F.; Álvarez, M. *Tetrahedron Lett.* **2011**, *52*, 5435–5437.

(155) Davyt, D.; Serra, G. *Mar. Drugs* **2010**, *8*, 2755–2780.

(156) Hughes, R. A.; Moody, C. J. *Angew. Chem. Int. Ed.* **2007**, *46*, 7930–7954.

(157) Li, C.; Kelly, W. L. *Nat. Prod. Rep.* **2010**, *27*, 153–164.

(158) Nicolaou, K. C.; Chen, D. Y.-K.; Huang, X.; Ling, T.; Bella, M.; Snyder, S. A. *J. Am. Chem. Soc.* **2004**, *126*, 12888–12896.

(159) Nicolaou, K. C.; Hao, J.; Reddy, M. V; Rao, P. B.; Rassias, G.; Snyder, S. a; Huang, X.; Chen, D. Y.-K.; Brenzovich, W. E.; Giuseppone, N.; O'Brate, A.; Giannakakou, P. *J. Am. Chem. Soc.* **2004**, *126*, 12897–12906.

(160) Lindquist, N.; Fenical, W.; van Duyne, G. D.; Clardy, J. *J. Am. Chem. Soc.* **1991**, *113*, 2303–2304.

(161) Moody, C. J.; Swann, E. *J. Chem. Soc. Perkin Trans. 1* **1993**, 2561–2565.

(162) Miyake, F.; Hashimoto, M.; Tonsiengsom, S.; Yakushijin, K.; Horne, D. A. *Tetrahedron* **2010**, *66*, 4888–4893.

(163) Faulkner, D. J. *Nat. Prod. Rep.* **1998**, *15*, 113–158.

(164) Blunt, J. W.; Copp, B. R.; Hu, W.-P.; Munro, M. H. G.; Northcote, P. T.; Prinsep, M. R. *Nat. Prod. Rep.* **2009**, *26*, 170–244.

(165) Reigo, E. *Synthesis* **2005**, 1907–1922.

(166) Lau, R. C. M.; Rinehart, K. L. *J. Am. Chem. Soc.* **1995**, *1146*, 7606–7610.

(167) Rauhut, T.; Spiteller, P.; Eisenreich, W.; Spiteller, M.; Glawischnig, E. *J. Org. Chem.* **2008**, *73*, 5279–5286.

(168) Fu, P.; Zhuang, Y.; Wang, Y.; Liu, P.; Qi, X.; Gu, K.; Zhang, D.; Zhu, W. *Org. Lett.* **2012**, *14*, 6194–61977.

(169) Zhang, F.; Greaney, M. F. *Org. Lett.* **2010**, *12*, 4745–4747.

(170) Moody, C. J.; Swann, E.; Houlbrook, S.; Stephens, M. A.; Stratford, I. J. *J. Med. Chem.* **1995**, *38*, 1039–1043.

(171) Oka, K.; Hara, S. *Tetrahedron Lett.* **1976**, *32*, 2783–2786.

(172) LaMattina, J. L.; Mularski, C. J. *J. Org. Chem.* **1986**, *51*, 413–415.

(173) Benner, S. A. *Tetrahedron Lett.* **1981**, *22*, 1851–1854.

(174) Coleman, C. M.; Macelroy, J. M. D.; Gallagher, J. F.; Shea, D. F. O. *J. Comb. Chem.* **2002**, *4*, 87–93.

(175) Taylor, E. C.; Zoltewicz, J. A. *J. Am. Chem. Soc.* **1960**, *82*, 2656–2657.

(176) Chihiro, M.; Nagamoto, H.; Takemura, I.; Kitano, K.; Komatsu, H.; Sekiguchi, K.; Tabusa, F.; Mori, T.; Tominaga, M.; Yabuuchi, Y. *J. Med. Chem.* **1995**, *38*, 353–358.

(177) Rosenthal, D.; Taylor, T. I. *J. Am. Chem. Soc.* **1957**, *79*, 2684–2690.

(178) Ferro, S.; De Grazia, S.; De Luca, L.; Letizia Barreca, M.; Debyser, Z.; Chimirri, A. *Heterocycles* **2009**, *78*, 947–959.

(179) Schaefer, F. C.; Krapcho, A. P. *J. Org. Chem.* **1962**, *27*, 1255–1258.

(180) Cheng, D.; Han, D.; Gao, W.; Jing, Q.; Jiang, J.; Wan, Y.; Englund, N. P.; Tuntland, T.; Wu, X.; Pan, S. *Bioorg. Med. Chem. Lett.* **2012**, *22*, 6573–6576.

(181) Frutos, R.; Wei, X.; Patel, N. *J. Org. Chem.* **2013**, *79*, 5800–5803.

(182) Bergman, J.; Bäckvall, J.; Lindström, J. *Tetrahedron* **1973**, *29*, 971–976.

(183) King, L. C.; Ostrum, G. K. *J. Org. Chem.* **1964**, *29*, 3459–3461.

(184) Fort, W. A. *J. Org. Chem.* **1961**, *26*, 765–767.

(185) Johnson, A.-L.; Bergman, J. *Tetrahedron* **2006**, *62*, 10815–10820.

(186) Miyake, F. Y.; Yakushijin, K.; Horne, D. A. *Org. Lett.* **2000**, *2*, 3185–3187.

(187) Miyake, F. Y.; Yakushijin, K.; Horne, D. A. *Angew. Chem. Int. Ed.* **2005**, *44*, 3280–3282.

(188) Miyake, F. Y.; Yakushijin, K.; Horne, D. A. *Org. Lett.* **2002**, *4*, 941–943.

(189) Ma, Y.; Yakushijin, K.; Miyake, F.; Horne, D. *Tetrahedron Lett.* **2009**, *50*, 4343–4345.

(190) Tonsiengsom, F.; Miyake, F. Y.; Yakushijin, K.; Horne, D. A. *Synthesis* **2006**, *1*, 49–54.

(191) Peterson, P.; Wolf III, J.; Nieman, C. *J. Org. Chem.* **1958**, *23*, 303–304.

(192) Zitt, H.; Dix, I.; Hopf, H.; Jones, P. G. *Eur. J. Org. Chem.* **2002**, 2298–2307.

(193) Duplais, C.; Bures, F.; Sapountzis, I.; Korn, T. J.; Cahiez, G.; Knochel, P. *Angew. Chem. Int. Ed.* **2004**, *41*, 2968–2970.

(194) Yu, S.; You, X.; Liu, Y. *Chem. Eur. J.* **2012**, *18*, 13939–13940.

(195) Kurnia, K.; Giles, D. E.; May, P. M.; Singh, P.; Hefter, G. T. *Talanta* **1996**, *43*, 2045–2051.

(196) Yeung, K.-S.; Qiu, Z.; Xue, Q.; Fang, H.; Yang, Z.; Zadjura, L.; D'Arienzo, C. J.; Eggers, B. J.; Riccardi, K.; Shi, P.-Y.; Gong, Y.-F.; Browning, M. R.; Gao, Q.; Hansel, S.; Santone, K.; Lin, P.-F.; Meanwell, N. a; Kadow, J. F. *Bioorg. Med. Chem. Lett.* **2013**, *23*, 198–202.

(197) Epple, R.; Cow, C.; Xie, Y.; Azimioara, M.; Russo, R.; Wang, X.; Wityak, J.; Karanewsky, D. S.; Tuntland, T.; Nguyên-Trân, V. T. B.; Cuc Ngo, C.; Huang, D.; Saez, E.; Spalding, T.; Gerken, A.; Iskandar, M.; Seidel, H. M.; Tian, S.-S. *J. Med. Chem.* **2010**, *53*, 77–105.

(198) Stephens, C. E.; Tanious, F.; Kim, S.; Wilson, W. D.; Schell, W. a; Perfect, J. R.; Franzblau, S. G.; Boykin, D. W. *J. Med. Chem.* **2001**, *44*, 1741–1748.

(199) Jakše, R.; Golič, L.; Meden, A.; Grošelj, U.; Svete, J.; Stanovnik, B. *Heterocycles* **2007**, *74*, 293–307.

(200) Kumar, P. S.; Kumar, G. S.; Kumar, R. A.; Reddy, N. V.; Reddy, K. R. *Eur. J. Org. Chem.* **2013**, 1218–1222.

(201) Ritson, D. J.; Spiteri, C.; Moses, J. E. *J. Org. Chem.* **2011**, *76*, 3519–3522.

(202) Yuriev, E.; Ramsland, P. A. *J. Mol. Recognit.* **2013**, *26*, 215–239.

(203) Trott, O.; Olson, A. J. *J. Comput. Chem.* **2010**, *31*, 455–461.

(204) Morris, G. M.; Goodsell, D. S.; Halliday, R. S.; Huey, R.; Hart, W. E.; Belew, R. K.; Olson, A. J. *J. Comput. Chem.* **1998**, *19*, 1639–1662.

(205) Yuriev, E.; Agostino, M.; Ramsland, P. A. *J. Mol. Recognit.* **2011**, *24*, 149–164.

(206) Ian, I.-F.; Luis, R.-T. J.; Pablo, C.-V. J.; Luis, V.-S. J.; Normande, C.-I.; Beatriz, Z.-L.; Sandino, R.-L. C. A.; Guadalupe, B.-C. C.; Jose, C.-B.; Absalom, Z.-C. *AJABS* **2013**, *8*, 89–106.

(207) Wiley, E. A.; Macdonald, M.; Lambropoulos, A.; Harriman, D. J.; Deslongchamps, G. *Can. J. Chem.* **2006**, *391*, 384–391.

(208) Hassam, M.; Basson, A. E.; Liotta, D. C.; Morris, L.; van Otterlo, W. A. L.; Pelly, S. C. *ACS Med. Chem. Lett.* **2012**, *3*, 470–475.

(209) Morris, G. M.; Huey, R.; Lindstrom, W.; Sanner, M. F.; Belew, R. K.; Goodsell, D. S.; Olson, A. J. *J. Comput. Chem.* **2009**, *38*, 2785–2791.

(210) Kolář, M.; Hobza, P. *J. Chem. Theory Comput.* **2012**, *8*, 1325–1333.

(211) Riley, K. E.; Hobza, P. *Cryst. Growth Des.* **2011**, *11*, 4272–4278.

(212) Clark, T.; Hennemann, M.; Murray, J. S.; Politzer, P. *J. Mol. Model* **2007**, *13*, 291–296.

(213) Murray, J. S.; Lane, P.; Politzer, P. *J. Mol. Model* **2009**, *15*, 723–729.

(214) Parisini, E.; Metrangolo, P.; Pilati, T.; Resnati, G.; Terraneo, G. *Chem. Soc. Rev.* **2011**, *40*, 2267–2278.

(215) Auffinger, P.; Hays, F. a; Westhof, E.; Ho, P. S. *PNAS.* **2004**, *101*, 16789–16794.

(216) Stumpfe, D.; Hu, Y.; Dimova, D. *J. Med. Chem.* **2013**.

(217) Gottlieb, H. E.; Kotlyar, V.; Nudelman, A. *J. Org. Chem.* **1997**, *62*, 7512–7515.

(218) Armarego, W. L. F.; Perrin, D. D. *Purification of Laboratory Chemicals*; 4th ed.; The Bath Press, 1998.

(219) Casey, M.; Leonard, J.; Lygo, B.; Procter, G. *Advanced Practical Organic Chemistry*; 2nd ed.; Blackie Academic & Professional, 1993; p. 36.

(220) GraphPad Software Inc., La Jolla, CA.

(221) Zhang, F.; Zhao, Y.; Sun, L.; Ding, L.; Gu, Y.; Gong, P. *Eur. J. Med. Chem.* **2011**, *46*, 3149–3157.

(222) Ferro, S.; Barreca, M. L.; De Luca, L.; Rao, A.; Monforte, A.-M.; Debyser, Z.; Witvrouw, M.; Chimirr *Arch. Pharm.* **2007**, *340*, 292–298.

(223) Fresneda, P. M.; Mollna, P.; Bleda, J. A. *Tetrahedron* **2001**, *57*, 2355–2363.

(224) Ohta, T.; Yoshinori, Y.; Hiriko, T.; Masanori, S. *Heterocycles* **1987**, *26*, 2817–2822.

(225) Zhang, L.; Wen, Q.; Jin, J.; Wang, C.; Lu, P.; Wang, Y. *Tetrahedron* **2013**, *69*, 4236–4240.

(226) Carmen de la Fuente, M.; Domínguez, D. *Tetrahedron* **2011**, *67*, 3997–4001.

(227) Zhang, P.; Sun, X.; Xu, B.; Bijian, K.; Wan, S.; Li, G.; Alaoui-Jamali, M.; Jiang, T. *Eur. J. Med. Chem.* **2011**, *46*, 6089–6097.

(228) Aubry, C.; Wilson, a J.; Emmerson, D.; Murphy, E.; Chan, Y. Y.; Dickens, M. P.; García, M. D.; Jenkins, P. R.; Mahale, S.; Chaudhuri, B. *Bioorg. Med. Chem.* **2009**, *17*, 6073–6084.

(229) Wang, Y.; Hämäläinen, A.; Tois, J.; Franzén, R. *Tetrahedron: Asymmetry* **2010**, *21*, 2376–2384.

(230) Harris, R. L. N. *Aust. J. Chem.* **1974**, *27*, 2635–2643.

(231) Bourdais, J.; Germain, C. *Tetrahedron Lett.* **1970**, 195–198.

(232) Oikawa, Y.; Yonemitsu, O. *J. Org. Chem.* **1977**, *42*, 1213–1216.